Asymptotic Analysis of Discrete Random Structures: Constrained Integer Partitions and Aggregating Particle Systems

Jean Charles Peyen

School of Mathematics

University of Leeds

Submitted in accordance with the requirements for the degree of

Doctor of Philosophy

October 2023

Acknowledgements

I would like to express my deepest gratitude to the Engineering and Physical Sciences Research Council (EPSRC) for their generous support during my research at the School of Mathematics of the University of Leeds.

I have had the privilege of crossing paths with many exceptional individuals throughout this journey. I regret that I cannot mention all of them in these acknowledgments.

Special thanks are owed to my supervisors, Leonid Bogachev and Paul Martin. They gave me the opportunity to pursue my passion and without their guidance there wouldn't be much of a thesis. I am grateful for the patience you have shown in supervising a stubborn student like me. My early reviewers, Konstantinos Dareiotis and Charles Taylor, deserve my appreciation for their insightful comments and suggestions. I also wish to express my gratitude to Yuri Yakubovich for our useful discussions. My thanks also go to all of my friends in the School of Mathematics.

I also want to thank my family. I wish I had been more present for you during these demanding years. I cannot thank you enough for your support and your unconditional love.

I extend my sincere thanks to the staff at Queen's University Belfast for their warm hospitality during the past two months and for providing an environment that greatly aided the completion of this thesis.

Finally, I wish to thank my very dear Victoria. Thank you for being there for this very stupid man.

Abstract

The unifying thrust of this thesis is to explore asymptotic properties of discrete random structures of large "size", focusing on their limit shapes. The first part (Chapters 2 and 3) is concerned with asymptotic analysis of the so-called Boltzmann distributions over the spaces of strict integer partitions (i.e. with distinct parts) into sums of perfect q-th powers (e.g. squares). The model is calibrated via the hyper-parameters $\langle N \rangle$ and $\langle M \rangle$ controlling the expected weight and length of partitions. In this framework, we obtain a variety of limit theorems for "short" partitions as $\langle N \rangle \to \infty$, while $\langle M \rangle$ is either fixed or grows slower than for unconstrained partitions. Our results include the asymptotics of the cumulative cardinality in the case of fixed $\langle M \rangle$ and the derivation of limit shape in the case of slow growth of $\langle M \rangle$.

Building on these and other results, we have also designed sampling algorithms for our models, and studied their complexity and performance. Boltzmann sampling is a topical area in computer science research, but we also argue that our algorithms can be used as exploratory tools in additive number theory.

In the second part (Chapter 4), we study the limit shape of integer partitions emerging in the classical occupancy problem, i.e. as a result of random allocation of a large number of independent "balls" with a given frequency distribution over infinitely many "boxes". To clarify the ideas and to streamline calculations, we focus on a specific model based on the Rayleigh frequency distribution (but generalising to a random number of balls). We also indicate a link with strict partitions, thereby offering an alternative method of sampling.

In the last part of the thesis (Chapter 5), we study the mass distribution in a stochastic system comprising particles of integer weight, which can either aggregate via diffusion or fragment by chipping off a single mass unit. For the model of pure aggregation on a one-dimensional cycle, analysed with a combination of computer simulations and analytical techniques. We observe that the Rayleigh distribution represents the limit shape for the spatial mass profile at intermediate times. In a model with linear dependence between the transition rates and the masses, we show that the role of the limit shape is played by the exponentiated Weibull distribution.

Contents

Chapter 1

Introduction

1.1. Aims and objectives

1.1.1. Background

A *partition* of a natural number is a decomposition of this number as a sum of natural parts, up to reordering (e.g., partitions of 5 given by 2 + 3 and 3 + 2 are not distinguished). We call the number that is decomposed the *weight* or the *size* of the partition. The number of parts is called the *length*. Partitions are combinatorial objects that are commonly used in many areas such as:

- Algebra, where partitions represent the size of blocks in a Jordan decomposition or the conjugacy classes of the symmetric group [35].
- Biology, notably via the Ewens sampling formula which is used to describe distribution of non-selective alleles in a population [29].
- Statistical physics, where partitions represent the distribution of energy in assemblies of indistinguishable particles [6].
- Analysis of citations, where partition models are used to model citation count data [65], [94].

In addition to their expression as sums they are represented in various ways according to the focus:

- Multiplicities/Occupancy: This consists in a sequential representation, indicating the number of times each natural number appears in a partition. This representation underlines the interpretation of integer partitions as *multisets*.

- Young diagram (French convention): This representation consists in stacking squares of unit size in the first corner of the plane so that each row contains a number of blocks corresponding to the parts in the decreasing order.

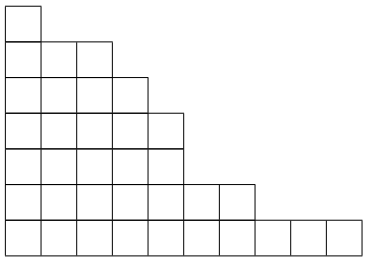

Figure 1.1: Young diagram of $35 = 10 + 7 + 5 + 5 + 4 + 3 + 1$

  This representation can be interpreted as a functional embedding by considering the step function defined by the upper boundary of the diagram.

Our aim is to study ensembles of partitions of large numbers. This involves combinatorial questions, typically consisting in the enumeration of partitions of such large numbers, either with or without structural constraints. Our research focuses specifically on partitions with a restriction on multiplicities (no repetitions of parts), on the nature of the parts (restricted to perfect q-th powers for a natural exponent), and on the number of parts (Chapters 2 and 3). From a statistical perspective, this is the equivalent to studying the family of uniform distributions over the level sets of the weight function.

The defining characteristic of uniform distributions is that they do not exhibit any bias towards particular features. This is equivalent to maximising the *Gibbs entropy*

$$S(p) = -\sum_{x\,\text{state}} p_x \log(p_x),$$

where $S(p)$ is the entropy associated with a probability distribution p, and the sum is taken over all possible outcomes. The entropy is a measurement of the average information, or of disorder, in a random system. This naturally suggests a connection with statistical mechanics, as it follows from the second law of thermodynamics that the equilibrium distribution of isolated thermodynamic systems must also maximise the entropy. However, these systems encompass potentially infinite sets of configurations, contrary to uniform distributions, and they are subject to a condition of mean energy. The *Boltzmann distribution* appears as the solution of this constrained maximisation problem. It is generically given by

$$\mathsf{P}_\beta(x) \propto \exp(-\beta E(x)), \qquad x \text{ state}.$$

Where $E(x)$ is the energy of the state x and β is the inverse temperature of the system. In the case of integer partitions, the energy function E is often taken as their weight. More generally, the energy function can include multiple extensive quantities, as long as the level sets are finite. In this thesis, we will consider the couple formed by the weight and the length. We observe that the Boltzmann distribution is *conditionally uniform*, meaning that it is constant across the level sets of E.

In addition, the Boltzmann distribution can be introduced for its mathematical convenience. It approximates the uniform distribution across configurations that have a specified energy. This is achieved by setting the mean energy of the Boltzmann distribution to match this specified energy. It possesses desirable independence properties, which are absent in a uniform distribution constrained by fixed energy. Typically, in the context of integer partitions, the multiplicities of parts are independent.

The Boltzmann distribution describes closed systems in thermodynamic equilibrium. Beyond these, numerous systems behave differently. Systems involving aggregation (Chapter 5), for instance as a result of chemical reactions may appear to order themselves, thus decreasing the entropy and violating the second law of thermodynamics. This apparent paradox arises from not taking into account that reactions of aggregation induce a release of components, such as energy or particles, which are not tracked. These systems are classified as non-equilibrium systems. In these, the concept of entropy must be applied more broadly, considering the interactions between the system and its surroundings. Fragmentation can be regarded as the reverse or dual process to aggregation. However, this relationship is non-trivial, as there is no direct one-to-one correspondence between the ways an aggregate can fragment and the ways multiple aggregates can merge into one. This is due to the loss of the spatial information of the individual fragments during the aggregation process. Systems involving fragmentation should also be understood through the lens of non-equilibrium thermodynamics, where reactions of fragmentation are triggered by an input of energy.

Integer partitions are a natural way to encode count data, assuming that the categories are indistinguishable. This motivates the construction of flexible partition distributions. In particular, occupancy models (Chapter 4) are a ubiquitous class of such distributions, obtained by the independent allocation of indistinguishable balls into bins according to a specified categorical distribution.

1.1.2. Combinatorial questions

Many results concerning integer partitions involve their enumeration [41, 90, 26, 48, 61, 43, 52]. The Hardy–Ramanujan formula [41], which gives an asymptotic expansion for the number of partitions, stands as a prime example of such a

result. Similar formulas are known for the (asymptotic) enumeration of integer partitions under various constraints, such as restrictions on the source of parts and/or their number, on the permitted repetitions of parts, etc. Such constraints echo in statistical physics where the energy levels of a particle are not necessarily uniformly spread and where two identical fermions cannot occupy the same state due to the *Pauli exclusion principle*.

One of our goals is to enumerate strict partitions (repetitions are not allowed), where the parts are q-th power and the number of parts is fixed despite the size approaching infinity. This can be seen as a variation of Waring's problem [83], which is concerned with determining the smallest number of parts $G(q)$ such that all large enough numbers can be partitioned into at least $G(q)$ numbers, each raised to the q-th power. This classical problem of additive number theory has several variants such as the anti-Waring problem, which consists in finding the number $N(q, m)$ such that every larger integer can be written as the sum of the q-th powers of at least $m \geq G(q)$ integers. Bounds for this problem have been given in [53].

While the aforementioned problems are concerned with determining whether numbers can be represented in a specific manner, our focus lies in determining the number of such representations. This proves to be a challenge due to the tight restriction of length, that prevents from finding a single closed form to estimate the counting sequence. In this research, we bypass this limitation by deriving a result of cumulative enumeration (Theorem 2.34). This cumulative result can be interpreted as a partial answer to a generalised m-dimensional Gauss circle problem under the q-norm (see Figure 2.2).

Further exploration is needed to address the irregularity and gaps in the counting sequence. This is why we provide preliminary computing tools, facilitating this exploration despite the absence of an analytical solution (Section 3.3). Incidentally, it is interesting to observe an analogy with multiplicative number theory, as the erratic behavior of the counting sequence, notably seen in Figure 3.4, bears a resemblance to the behavior of the divisor function. In both cases, adopting a cumulative approach is relevant in order to derive a normal order.

1.1.3. Asymptotic structure

What do partitions of large numbers look like? One approach to addressing this question involves examining their overall shape, specifically their Young diagrams. Temperley [81] initially provided an answer to this question (see Figure 1.2).

This result has been subsequently re-derived by Vershik [85]. To define a *limit shape*, we assume that partitions are endowed with a family of distributions. In this particular context, we consider the family of uniform distributions, which are parameterised by partition size. Vershik's approach, inspired by sta-

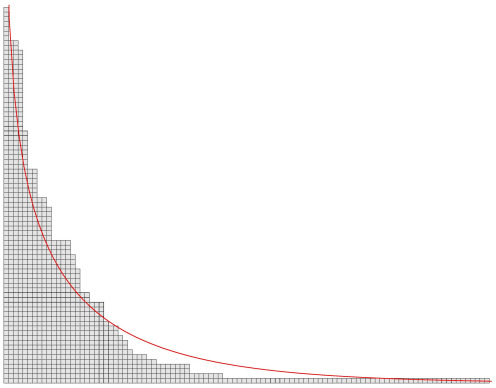

Figure 1.2: A uniformly sampled partition of $n = 1000$ along with the (scaled) Temperley curve ($\mathrm{e}^{-x\pi/\sqrt{6n}} + \mathrm{e}^{-y\pi/\sqrt{6n}} = 1$)

tistical physics, relies on the use of the *Boltzmann/multiplicative* distribution. It involves relaxing the constraint on the size of uniform distributions. Through what is known of the physicists as the *equivalence of ensembles*, insights from the Boltzmann distribution can be transferred to the uniform distribution.

The challenge of defining a limit shape lies in being able to implement an appropriate *scaling*. In loose terms, this implies that when observing the Young diagram from an adequate distance, a smooth curve should become discernible. This challenge is more apparent when considering asymptotic regimes that constrain other parameters (such as the length) when the size goes to infinity. In this thesis, we determine the limit shape for a family of Boltzmann distributions, $\mathsf{P}_{\boldsymbol{z}}$, over strict partitions into perfect q-th powers with a length that grows relatively slowly (Theorem 2.44).

Certain information cannot be extracted from scaled Young diagrams. Therefore, it becomes imperative to focus on some observables separately, specifically those that exhibit distinct scaling behaviors. This is the case, for instance, when considering the maximal part and length of uniform unrestricted partitions [26]. In this thesis we determine the asymptotic distribution of the extreme parts of $\mathsf{P}_{\boldsymbol{z}}$-distributed partitions when the number of parts is fixed as the size approaches infinity (Theorem 2.35) and when the number of parts is allowed to grow relatively slowly (Theorem 2.40).

Partitions can be conceptualised as the distribution of an extensive quantity across indistinguishable sites. Therefore, it becomes pertinent to examine physical processes through this framework, with the aim of identifying the partition distributions that emerge from these processes, assuming that we can meaningfully "forget" the spatial component. Temperley's derivation [81] was in fact motivated by modelling the growth of a crystal into a quadrant. This process

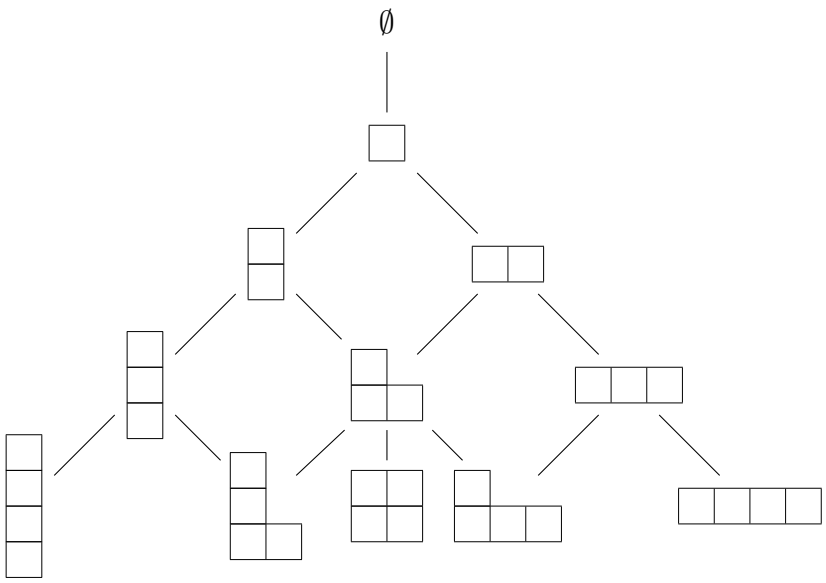

Figure 1.3: Young's lattice for partitions of integers from 0 to 4

is defined as the successive addition of blocks to a Young diagram, that can be interpreted as a downward random walk on the *Young's lattice* (Figure 1.3).

Processes of aggregation and fragmentation are also a source of partition distributions. These distributions can manifest either systematically, within the framework of mean-field processes, or as marginal distributions, when the spatial positioning of aggregates is ignored. Our research focuses on a specific process that originates from a model previously studied by Majumdar et al. [57, 58, 59]. In this model, massive particles undergo stochastic diffusion across a lattice. When a particle lands on an already occupied site, aggregation occurs. Additionally, units of mass may dissociate from particles. There are two approaches to obtaining limit shapes in this model:

- **Purely aggregating case**: In this scenario, the optimal time for observation falls between two extremes: the early phase, where the system's state is predominantly dictated by the initial distribution, and the late phase, where the system ultimately converges to a single aggregate. Observing the process at this opportune time allows for meaningful insights into the system's evolution. Assuming the lattice is a one-dimensional, periodic space (a *cycle*), the Rayleigh distribution emerges as the limit shape.

- **Equilibrium**: When fragmentation is introduced, the system has a non-trivial equilibrium distribution. In the mean-field setting, it has been shown

that a phase transition occurs, contingent on the rate of fragmentation relative to the rate of diffusion.

We have extended Majumdar's model by introducing mass-dependent transition rates, thereby broadening the model's applicability to a wider variety of physical systems. Our investigation targets three specific scenarios of the purely aggregating case on a cycle (Section 5.2). Our methods combine both simulation and analytic techniques to arrive at the following insights:

- **Diffusion rates independent of the mass:** When the diffusion rates are mass-independent, we demonstrate that the time to reach a state with a single particle grows quadratically with the system's size. Our simulations coincide with Majumdar's result and indicate that the Rayleigh distribution is the limit shape.
- **Diffusion rates proportional to the mass:** Our analysis indicates that in a system where diffusion rates scale with the mass, the time until the ultimate aggregation exhibits a logarithmic growth relative to the system size (equation (5.27)). We propose the exponentiated Weibull distribution as a likely candidate for the limit shape.
- **Diffusion rates inversely proportional to the mass:** Our observations remain inconclusive at this stage.

We also explored the equilibrium distribution in particular instances of the mean-field setting (Setting 5.3). The methods used here should be applied to other cases and extended to multispecies models.

1.1.4. Fitting

From a supply perspective, parametric partition models offer tools for fitting data, serving as a source of models for their analysis and interpretation. An example of such use can be found in bibliometrics [65, 14]. A range of parametric partition models can be defined using an infinite urn scheme that involves independently throwing balls into urns labelled by the natural numbers, according to a given distribution. One way to produce a partition in this manner is to consider the number of balls in each urn as the parts of the partition [36], thereby generating a partition of the total number of balls. Alternatively, the number of balls per urn can be interpreted as representing the multiplicities of the parts, thus providing a flexible model where the frequency distribution can be inferred from count data [65, 14]. In this research we only consider the latter construction.

Bogachev et al. [14] investigated the asymptotic behaviour of a model founded on the Generalised Inverse Gaussian-Poisson Distribution (GIGP). As a model

with three parameters, the determination of a limit shape necessitates the segregation of multiple asymptotic regimes. This situation is reminiscent of the situation we encounter in Chapter 2, with the Boltzmann distribution calibrated for both weight and length.

In the present study, we opt not to explore the complexities associated with the segregation of multiple asymptotic regimes, which are inherent in multi-parameter models. Instead, we present an elementary example based on the Rayleigh distribution to illustrate the core concepts involved in determining a limit shape for such models (Section 4.2). Unlike [14], where the number of balls is deterministic, we allow it to be random. Although occupancy/urn models discussed here are not specifically designed to fit data with structural constraints, we establish a link with strict partitions and utilise this connection to reproduce the Boltzmann distribution (Section 4.3).

1.1.5. Sampling

Random sampling serves as a tool for the exploration of combinatorial structures, including but not limited to integer partitions. This alternative approach can aid in obtaining empirically-driven conjectures where analytical methods fail. An additional practical aspect of random sampling lies in its application to the benchmarking of computational algorithms. Generated instances of combinatorial structures can serve as benchmarks to empirically evaluate the performance, robustness, and limitations of algorithms designed to process instances of these structures. The efficiency of the sampling algorithms is generally measured in terms of time complexity and memory requirements. Efficient sampling algorithms aim to generate a large number of large instances of the combinatorial structures in question, thereby providing a rich dataset for analysis.

In addition to their analytic properties, Boltzmann models provide a general framework for efficient sampling of a variety of combinatorial objects. This was demonstrated by Duchon [24], under the assumption that these objects can be symbolically specified in the language introduced by Flajolet [32]. Specifically, unrestricted partitions with a large expected size n can be generated in sub-linear time [31], with a time complexity of $O(n^{1/2})$. However, this comes at the cost of requiring an *oracle* to estimate the generating function of the partitions. By incorporating a rejection loop to achieve uniformly distributed partitions of n, the complexity remains sub-quadratic, $O(n^{5/4})$.

We leverage our analysis of the two-parametric Boltzmann distribution for strict partitions into m perfect q-th powers (Chapter 2) to design and analyse sampling algorithms (algorithms 1 and 2). We use a truncation approach, proved to be a good approximation of the Boltzmann distribution, instead of relying on an oracle. If an oracle is available, we propose an alternative approach that uses an

occupancy scheme (Section 4.3). A significant challenge in the rejection process is the potential emptiness of the classes of partitions to be sampled. Therefore, it is essential to detect such scenarios with high confidence to ensure the termination of the rejection scheme while avoiding the oversight of non-empty cases. Our design also has the benefit of providing computing tools to study analogues of Waring's problems, as mentioned earlier.

1.2. Layout of the thesis and contribution

The remainder of the thesis comprises five chapters, concluding with a summary and a review of some future research. It is accompanied by several appendices. Appendix A provides an expanded view on integer partitions. Appendices B and C contain supplementary material about combinatorics and Boltzmann sampling. Appendix D contains selected computer codes that have been used in this research. Chapters 2 and 3 involve material from the jointly authored paper [68] (submitted to *Advances in Applied Mathematics*).

Chapter 2. We perform a thorough analysis of the Boltzmann distribution over the class $\check{\Lambda}^q$ of strict partitions into perfect q-th powers, for a fixed natural number q under the assumption that the weight goes to infinity while the length growth is restricted (Assumption 2.1). The constraints considered here have not been examined collectively. They give an interesting case of structure with gaps in the sense that the support of the counting sequence may contain arbitrarily large gaps depending on q and further restriction of the length. It also has potential extensions to non-integral q values discussed in Chapter 6. Our analysis is divided into two distinct cases. Firstly, we consider the expected length to be fixed (Section 2.3). Then we allow it to go to infinity while keeping Assumption 2.1 satisfied (Section 2.4). We derive a calibration of the distribution valid in both cases (Theorem 2.21). In the case where the expected length is fixed the asymptotic distribution of length and weight (Theorem 2.26) as well as the extrema (Theorem 2.35) are derived. The distribution of length and weight is used to provide a cumulative enumeration result (Theorem 2.34). In the latter case we obtain analogous results for the distribution of length and weight (Theorem 2.40) and of the extrema (Theorem 2.48), we also derive the limit shape and the fluctuations of the Young diagram (Theorem 2.44 and Theorem 2.45).

Chapter 3. We propose an application of the previously developed tools and results in the context of random sampling. Based on Lemma 2.12, sampling from the Boltzmann distribution over $\check{\Lambda}^q$ is seemingly straightforward thanks to the intrinsic independence of the random multiplicities of parts. However, there

are issues with ensuring the finiteness of the sampling loops. A solution is to use a method based on deploying an *oracle* [24, 31, 11], which is a collective name for an external device that is capable of computing at request (exactly or approximately) the values of the corresponding generating function, serving as a normalising denominator in probability expressions. Oracles are frequently considered as granted primitives; however, an insightful discussion regarding their implementation can be found in [71, Chap. 2]. Instead, we pursue an approach based on a truncation of the sampling loop on the basis of high statistical confidence, thus adopting the methodology of hypotheses testing in statistics. Selection of the proper truncation thresholds is guided by our limit theorems for the partition weight and length. This approach is especially useful in the case of partition spaces $\check{\Lambda}^q(n,m)$ that are empty for some of the pairs (n,m) (which may not be known in advance). This statistical approach to sampling offers a practical method to effectively explore the hypothetical partitionability of large integers. Section 3.3 serves as a proof of concept for this method.

Chapter 4. We turn onto partitions generated through an occupancy model according to the scheme described in Section 4.1, whereas a random number of parts M are allocated independently to parts size with a common distribution (f_j). Section 4.2 serves as an illustration of a general approach to limit results for scaled Young diagrams. As previously mentioned, our approach is similar to that in [14], where a limit for a model based on the Generalised Inverse Gaussian-Poisson Distribution is established. However, we allow the number of parts to be random. For simplicity, the case presented here is based on the family of Rayleigh distributions, although it can easily be extended to other scale families, and does not require the distinction of multiple asymptotic regimes.

Section 4.3 provides a simple connection between a strict partition distribution obtained from an occupancy model and the Boltzmann distribution. This result can be used to design another alternative to the Boltzmann sampler for powersets presented in [31] and which also requires an oracle contrary to the sampler proposed in Chapter 3.

Chapter 5. In Section 5.1, we present a particular setup for processes of aggregation and fragmentation involving particles with discrete mass, located on an oriented graph (the *ambient space*). These particles are involved in interactions governed by a continuous time Markov process. A notable aspect of this work is that interaction rates vary based on the mass of the particles. Particles may either jump or transfer a single unit of mass to an adjacent site. This setup aims to generalise the model studied by Majumdar et al. [57, 58, 59]. The model parameters dictate the cohesion of these aggregates, that is how the overall mass attracts or repels individual units of mass, as well as their rate of diffusion. These

parameters can be seen as a proxy for the internal structure of the sites and of the particles.

In Section 5.2, we narrow our focus to a specific instance of the model where the ambient space forms a directed cycle and the system is purely aggregating, with particles only executing jumps to neighboring sites without any fragmentation. This non-reversible setup ends with the formation of a singular aggregate. To study this, we develop and apply a simulation algorithm, detailed in Section 5.2.1 and Appendix D.4. Our simulations reveal the following:

- When the jump rates are mass-independent, the mass distribution appears to converge to a Rayleigh distribution (Figure 5.5 and Figure 5.8). It is consistent with the limit found in [57].
- When the jump rates are proportional to particle mass, the mass distribution seems to tend toward an exponentiated Weibull distribution (Figure 5.6). It appears to be a discovery that warrants further exploration.

Additionally, we analytically determine the second-order moments when the rates are independent of the mass (Proposition 5.3). This analysis enables a rigorous determination of the time scale for the final coalescence (Corollary 5.3.1). In this case and when the jump rates are proportional to the mass, we provide heuristic estimates for the aggregation times (equations (5.18) and (5.27)).

In Section 5.3, we consider a mean-field setting that incorporates fragmentation, where individual units of mass can jump between sites. Using generating functions, we derive the equilibrium distributions in the following scenarios

- when units of mass chip at a rate independent of the mass of their aggregate, the equilibrium distribution is geometric (Theorem 5.7),
- when units of mass chip at a rate proportional to the mass of their aggregate, the equilibrium distribution is Poissonian (Theorem 5.9),
- when both diffusion and fragmentation occur at a rate that is independent of mass, using the radius of convergence transfer theorem, we re-derive a result that was initially proven by Majumdar [59] (Theorem 5.10).

This chapter serves as a foundational step for a larger project focused on aggregation and fragmentation models, especially multispecies models, such as the one briefly mentioned in Section 6.4.

Chapter 2

"Short" integer partitions with power parts: Limit laws

We focus on integer partitions under a conjunction of the following conditions:

(i) Firstly, the source of parts is limited to perfect q-th powers, with some $q \in \mathbb{N}$.

(ii) Secondly, partitions are assumed to be *strict*, in that all parts must be distinct.

(iii) Finally, we consider "short" partitions, where the length (i.e., the number of parts) is either fixed or grows slowly as compared to the "free", unrestricted regime.

We denote by $\check{\Lambda}^q$ the class of integer partitions satisfying the first two conditions.

Each of the constraints (i) to (iii) taken alone has been considered in prior research; for instance, power parts were considered in [90, 85, 39, 19, 75]; restricted growth of length was addressed in [26, 88]; and strict partitions are a classical subject (see, e.g., [45, 75, 33]). A juxtaposition of the first and third constraints is new. Notably, when the length is bounded by a sufficiently small number, it induces a structure with "gaps" that make enumerative questions challenging and is a source of number theoretical problems. The choice of strict rather than plain partitions is less significant. It facilitates the analysis without diminishing the interest of our discussion.

We endow the space $\check{\Lambda}^q$ with a variant of the Boltzmann distribution $\mathsf{P}_{\boldsymbol{z}}$ (as in Definition 2.1), with probability weights assigned to each partition $\lambda \in \check{\Lambda}^q$ proportional to $z_1^{N_\lambda} z_2^{M_\lambda}$, where N_λ and M_λ are the weight and length of λ, respectively. The couple of parameters $\boldsymbol{z} := (z_1, z_2)$ is calibrated through the

moment conditions $\mathsf{E}_{\boldsymbol{z}}(N_\lambda) = \langle N\rangle$, $\mathsf{E}_{\boldsymbol{z}}(M_\lambda) = \langle M\rangle$, where $\langle N\rangle$ and $\langle M\rangle$ are the external hyper-parameters that are used to control the distribution of the random weight and length. In this formalism, the condition (iii) specialises as $\kappa := \langle M\rangle^{q+1}/\langle N\rangle \to 0$ (Assumption 2.1) when $\langle N\rangle$ goes to infinity and the calibrations are solved by (Theorem 2.21)

$$z_1 \sim \exp\left(-\frac{\langle M\rangle}{q\,\langle N\rangle}\right), \qquad z_2 \sim \frac{\kappa^{1/q}}{q^{1/q}\,\Gamma(1+1/q)}.$$

We observe that z_1 goes to 1 while z_2 goes to zero. If we use thermodynamic variables, thus interpreting $-\log z_1$ as the *inverse temperature* $1/(k_B T)$ (where k_B is the Boltzmann constant and $T > 0$ is the absolute temperature), and z_2 as the *fugacity*, it implies that we describe a particle assembly in a high-temperature regime and at a low fugacity, which is explained by a constrained number of particles, insufficient to create a non-negligible pressure. In this ansatz, the calibration implies an analogue of the state equation of perfect gas,

$$n \times \frac{k_B}{q} \times T = E,$$

assuming that the expected weight $\langle N\rangle$ is identified to an energy E and the number of parts $\langle M\rangle$ corresponds to a number of particles n. The regime dictated by (iii) must be separated in two different cases depending if $\langle M\rangle$ is fixed or allowed to go to infinity. In particular, in the latter case, there is a meaningful *limit shape* for the Young diagram (Theorem 2.44)

$$\mathsf{P}_{\boldsymbol{z}}\left(\lambda \in \breve{\Lambda}^q\colon \sup_{x\geq 0}\left|\frac{Y_\lambda(q\,\langle N\rangle\, x/\,\langle M\rangle)}{\langle M\rangle} - \frac{1}{\Gamma(1/q)}\int_x^\infty u^{1/q-1}\,\mathrm{e}^{-u}\,\mathrm{d}u\right| > \varepsilon\right) \to 0,$$

while in the former case, the lack of parts reduces this to a limit in expectation.

The determination of the distribution of length and weight is an essential step towards proving enumeration results using the Boltzmann distribution. This is an immediate consequence of the conditional uniformity.

When $\langle M\rangle$ is fixed, we prove that the distribution of the length M_λ is asymptotically Poisson, while the conditional distribution of the weight N_λ subject to the condition $M_\lambda = m \geq 1$ is given by (Theorem 2.26)

$$\mathsf{P}_{\boldsymbol{z}}\big(\gamma N_\lambda \leq x \,\big|\, M_\lambda = m\big) \to G_{m/q}(x) = \frac{1}{\Gamma(m/q)}\int_0^x u^{m/q-1}\,\mathrm{e}^{-u}\,\mathrm{d}u, \qquad x \geq 0,$$

where $\gamma := -\log z_1$. When $\langle M\rangle$ is allowed to go to infinity, one can expect a Gaussian limit for the weight N_λ, noting that it is a sum of independent (although not identically distributed) terms. Indeed, this Gaussian limit is established in Theorem 2.40.

Using the conditional uniformity of the Boltzmann distribution the asymptotic law for length and weight can be utilised in order to identify the growth rate of the number of elements of $\check{\Lambda}^q$ with length m and weight smaller than x (Theorem 2.34). It gives the leading term in a generalised m-dimensional Gauss circle problem under the q-norm in $\mathbb{R}^m$,

$$L_m^q(x) \sim \frac{q\left(\Gamma(1+1/q)\right)^m x^{m/q}}{m!\, m\, \Gamma(m/q)}.$$

Asymptotics of extreme values in the partition spectrum (i.e., the smallest and largest parts) can also be analysed. Specifically, if $\langle M\rangle$ is fixed then all parts appear to grow on the same linear scale of order $\langle N\rangle / \langle M\rangle$ (Theorem 2.35). In the slow growth regime of $\langle M\rangle$, the extremal parts are on two different scales. The smallest part is of order $\kappa^{-1} = \langle N\rangle / \langle M\rangle^{q+1}$ and has a Weibull limit distribution, whereas the largest part scales as $q\,\langle N\rangle / \langle M\rangle$ and has the Gumbel double-exponential limit (Theorem 2.48).

The chapter is organised as follows. Section 2.1.1 introduces the main elements that we use throughout the chapter, including the definition of restricted classes of integer partitions and basic results about the Boltzmann distribution. In Section 2.2 we present foundational results for our analysis of the class $\check{\Lambda}^q$ under the asymptotic regime specified by Assumption 2.1. The main result of this section is Theorem 2.21 about the asymptotic calibration of the Boltzmann parameters. Section 2.3 focuses on partitions with fixed expected length, where the main Theorem 2.26 characterises the limit distribution of the random length and weight. This result can be used for enumeration purposes, at least in the cumulative sense (Theorem 2.34). We also obtain the joint limit distribution of the largest and smallest parts (Theorem 2.35). Section 2.4 extends the analysis to partitions with a slowly growing expected length (under Assumption 2.3), where we obtain asymptotic results for the length and weight (Theorem 2.40) as well as for the extreme parts (Theorem 2.48). In this regime it is also possible to derive the limit shape of appropriately scaled Young diagrams, which forms a family of curves indexed by q (Theorems 2.44 and 2.45).

2.1. Preliminaries

2.1.1. Integer partitions

For a given integer $n \in \mathbb{N}$, a *partition* of n is a decomposition of n into a sum of non-negative integers, disregarding the order of the terms; for example, $35 = 10+7+5+5+4+3+1$ is an integer partition of $n = 35$. To fix the notation, we adopt a convention of non-increasing ordering of terms; that is to say, a sequence

of integers $\lambda_1 \geq \lambda_2 \geq \cdots \geq 0$ with finitely many parts $\lambda_i > 0$ is a partition of $n \in \mathbb{N}$ if $n = \lambda_1 + \lambda_2 + \cdots$. This is expressed as $\lambda \vdash n$. We formally allow the case $n = 0$ represented by the "empty" partition $\lambda_\varnothing = (0, 0, \dots)$, with no parts. This is convenient when working with generating functions. The set of all partitions $\lambda \vdash n$ is denoted by $\mathit{\Lambda}(n)$, and the set $\mathit{\Lambda} := \bigcup_{n\in\mathbb{N}_0} \mathit{\Lambda}(n)$ is the collection of *all* integer partitions. The subset $\check{\mathit{\Lambda}} \subset \mathit{\Lambda}$ of *strict* partitions is defined by the property that all parts (λ_i) are different from one another, $\lambda_1 > \lambda_2 > \cdots$. Accordingly, the set of all strict partitions $\lambda \vdash n$ is denoted $\check{\mathit{\Lambda}}(n)$.

For a partition $\lambda = (\lambda_i) \in \mathit{\Lambda}$, the sum $N_\lambda := \lambda_1 + \lambda_2 + \cdots$ is referred to as its *weight* (i.e., $\lambda \vdash N_\lambda$), and the number of its parts $M_\lambda := \#\{\lambda_i \in \lambda\colon \lambda_i > 0\}$ is called the *length* of λ. Thus, for $\lambda \in \mathit{\Lambda}(n)$ we have $N_\lambda = n$ and $M_\lambda \leq n$. The largest and smallest parts of a partition $\lambda = (\lambda_i)$ are denoted $\lambda_{\max} = \lambda_1 = \max_{1\leq i\leq M_\lambda} \lambda_i$ and $\lambda_{\min} = \lambda_{M_\lambda} = \min_{1\leq i\leq M_\lambda} \lambda_i$, respectively. We make a convention that for the empty partition $\lambda_\varnothing$, its largest and smallest parts are defined[1] as $\lambda_{\max} = 0$ and $\lambda_{\min} = \infty$.

The alternative notation $\lambda = (1^{\nu_1}2^{\nu_2}\dots)$ refers to the *multiplicities* of the parts involved, $\nu_\ell := \#\{\lambda_i \in \lambda\colon \lambda_i = \ell\}$ $(\ell \in \mathbb{N})$, with zero multiplicities usually omitted from the notation. Thus, the partition $\lambda \vdash 35$ in the example above can be written as $\lambda = (1^1 3^1 4^1 5^2 7^1 10^1)$.

The weight and length of a partition $\lambda \in \mathit{\Lambda}$ can be expressed through its multiplicities (ν_ℓ) as follows,

$$N_\lambda = \sum_\ell \ell\,\nu_\ell, \qquad M_\lambda = \sum_\ell \nu_\ell. \tag{2.1}$$

In terms of multiplicities (ν_ℓ), the set of strict partitions $\check{\mathit{\Lambda}}$ is defined by the condition that any part ℓ can be used no more than once,

$$\check{\mathit{\Lambda}} := \{\lambda = (\ell^{\nu_\ell}) \in \mathit{\Lambda}\colon \nu_\ell \leq 1 \text{ for all } \ell\}.$$

2.1.2. Young diagrams and limit shape

A partition $\lambda = (\lambda_1, \lambda_2, \dots)$ is succinctly visualised by its Young diagram $\mathit{\Upsilon}_\lambda$ formed by (left- and bottom-aligned) row blocks with $\lambda_1, \lambda_2, \dots$ unit square cells (see Figure 2.1(a)). The upper boundary of $\mathit{\Upsilon}_\lambda$ is a piecewise constant, non-increasing function $Y_\lambda\colon [0, \infty) \to \mathbb{N}_0$ defined by

$$Y_\lambda(x) = \sum_{\ell\geq x} \nu_\ell \qquad (x \geq 0). \tag{2.2}$$

[1] The familiar paradox of such definitions, suggesting that the maximum is smaller than the minimum, is but a logical consequence of applying the operations sup and inf to the empty set $\varnothing$. Despite a counter-intuitive appearance, these definitions are perfectly consistent with our limiting results in Theorem 2.35.

In particular, $Y_\lambda(0) = M_\lambda$, while the area of the Young diagram Υ_λ is

$$\int_0^\infty Y_\lambda(x)\,\mathrm{d}x = \sum_\ell \ell\,\nu_\ell = N_\lambda.$$

According to the definition (2.2), the step function $Y_\lambda(x)$ is left-continuous and has right limits (and is also right-continuous at the origin).

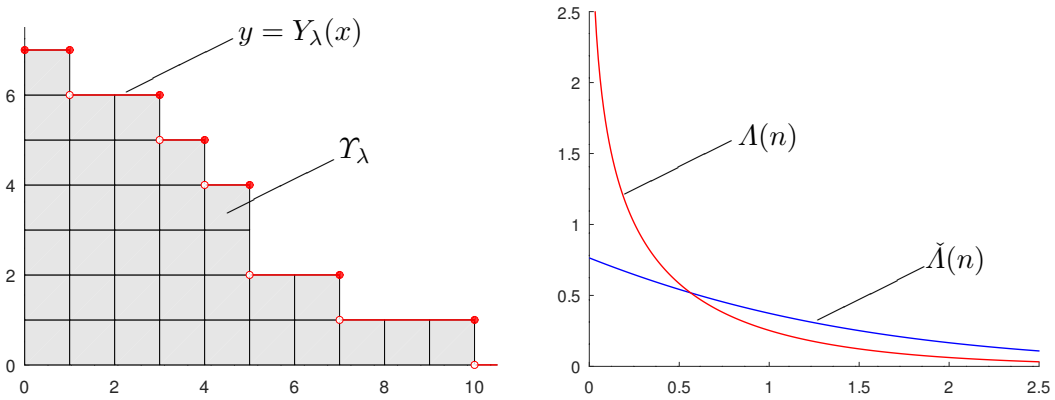

Figure 2.1: (a) The Young diagram Υ_λ (shaded) of partition $\lambda = (10, 7, 5, 5, 4, 3, 1)$, with weight $N_\lambda = 35$ and length $M_\lambda = 7$. The graph of the step function $x \mapsto Y_\lambda(x)$ defined in (2.2) depicts the upper boundary of Υ_λ (shown in red in the online version). (b) Two classical limit shapes, for plain partitions $\lambda \in \Lambda(n)$ (red) and strict partitions $\lambda \in \check{\Lambda}(n)$ (blue), determined by equations (2.4) and (2.5), respectively.

The geometric nature of Young diagrams naturally leads to the question of whether there is a typical behaviour of their boundaries as the "size" of partitions grows. This motivates the concept of *limit shape*, which may be thought of as such a curve to which the boundaries of the Young diagrams of the "bulk" of random partitions are asymptotically close upon a suitable scaling. More precisely, choosing some sequences $a_n \to \infty$, $b_n \to \infty$, define, the scaled Young boundary

$$\widetilde{Y}_\lambda^{(n)}(x) := b_n^{-1}\, Y_\lambda(a_n x), \qquad x \geq 0.$$

Then (the graph of) a function $y = \omega^*(x)$ is the *limit shape* for partitions $\lambda \in \Lambda(n)$ as $n \to \infty$ if, for all $x > 0$ and for any $\varepsilon > 0$,

$$\lim_{n\to\infty} \frac{\#\{\lambda \in \Lambda(n) \colon |\widetilde{Y}_\lambda^{(n)}(x) - \omega^*(x)| \leq \varepsilon\}}{\#\Lambda(n)} = 1. \tag{2.3}$$

If such function exists for some sequences a, b, it is unique. The limit shape ω^* exists under the scaling $a_n = b_n = \sqrt{n}$ and is determined by the equation

$$\mathrm{e}^{-x\pi/\sqrt{6}} + \mathrm{e}^{-y\pi/\sqrt{6}} = 1. \tag{2.4}$$

It was first identified by Temperley [81] in connection with the equilibrium shape of a growing crystal, with a much later mathematical derivation credited to Vershik [85] (see also Pittel [70]).

The form of the above scaling limit exhibits the invariance of the uniform distribution over unrestricted partitions under the operation of *conjugation* which consists in switching the parts size and multiplicities.

Note from (2.4) that $\omega^*(0) = \infty$, indicating that the number of parts, M_λ, grows faster than $\sqrt{n}$. Indeed, as was shown by Erdős and Lehner [26], $M_\lambda \sim (2\pi)^{-1}\sqrt{6n}\log n$ (in a sense similar to (2.3)).

For strict partitions $\lambda \in \check{\Lambda}(n)$, the limit shape (under the same scaling $a_n = b_n = \sqrt{n}$ and in the sense of definition (2.3) adapted to $\check{\Lambda}(n)$) is specified by the equation (see Vershik [85])

$$\mathrm{e}^{y\pi/\sqrt{12}} = 1 + \mathrm{e}^{-x\pi/\sqrt{12}}. \tag{2.5}$$

Note that here the value at the origin is finite, $\omega^*(0) = \pi^{-1}\sqrt{12}\log 2$, which implies that the number of parts M_λ in a typical strict partition $\lambda \in \check{\Lambda}(n)$ grows like $\pi^{-1}\log 2\sqrt{12n}$ [26]. The graphs of the limit shapes (2.4) and (2.5) are shown in Figure 2.1(b).

Remark 2.1. The limiting formula (2.3) and its version for strict partitions, as mentioned above, may be interpreted as convergence in probability, $\widetilde{Y}_\lambda^{(n)}(x) \xrightarrow{p} \omega^*(x)$, under the uniform probability measure on the corresponding partition spaces $\Lambda(n)$ or $\check{\Lambda}(n)$ (whereby all member partitions are assumed to be equally likely). A general question about limit shapes under alternative measures was pioneered by Vershik [84, 85]. In this chapter, we study the limit shape under the Boltzmann measure (see Sections 2.1.4 and 2.4.2).

2.1.3. Integer partitions with constraints

We focus on strict partitions with parts confined to be *q-th powers of integers* (for some $q \in \mathbb{N}$), which means that $\nu_\ell = 0$ unless $\ell \in \mathbb{N}^q$; we denote the corresponding set of partitions by Λ^q. Moreover, it is of interest to combine these two constraints by considering only strict partitions in Λ^q, leading to the subset that we naturally denote by $\check{\Lambda}^q$.

A general approach to introducing constraints in the partition spaces can be described as follows. Fix non-empty integer sets $\mathbb{A} \subseteq \mathbb{N}$ and $\mathbb{B}_\ell \subseteq \mathbb{N}_0$ ($\ell \in \mathbb{A}$),

assuming that $0 \in \mathbb{B}_\ell$ but $\mathbb{B}_\ell \neq \{0\}$, for each $\ell \in \mathbb{A}$. The set $\mathbb{A}$ specifies the source of permissible parts $\ell \in \mathbb{N}$. For example, if $\mathbb{A} = 2\mathbb{N}_0 + 1$ then all parts must be odd integers, or if $\mathbb{A} = \mathbb{N}^q$ with some $q \in \mathbb{N}$ then only perfect q-th powers can be used; if $\mathbb{A} = \mathbb{N}$ then any (positive) integer part is allowed. The sets $(\mathbb{B}_\ell)$ specify the allowed values of multiplicities $\nu_\ell \in \mathbb{B}_\ell$ for each part $\ell \in \mathbb{A}$. For example, if $\mathbb{B}_\ell = \{0, 1\}$ then part ℓ can be used no more than once; if $\mathbb{B}_\ell = \mathbb{N}_0$ then ν_ℓ is not constrained.

Given the sets $\mathbb{A}$ and $(\mathbb{B}_\ell, \ell \in \mathbb{A})$, we use a generic notation $\tilde{\Lambda}$ to denote the set of integer partitions satisfying the constraints imposed by $\mathbb{A}$ and $(\mathbb{B}_\ell)$ as described above,

$$\tilde{\Lambda} := \{\lambda = (\ell^{\nu_\ell}) \in \Lambda\colon\ \ell \in \mathbb{A},\ \nu_\ell \in \mathbb{B}_\ell\}. \tag{2.6}$$

In this loose notation we take the liberty to omit the explicit reference to $\mathbb{A}$ and $(\mathbb{B}_\ell)$, which should cause no confusion. When the specific choice of $\mathbb{A}$ and $(\mathbb{B}_\ell)$ becomes important (in Section 2.2 below), this will be clarified. For a partition $\lambda \in \tilde{\Lambda}$, we keep using the notation N_λ and M_λ for its weight and length, respectively, which are now given by (cf. (2.1))

$$N_\lambda = \sum_{\ell \in \mathbb{A}} \ell\, \nu_\ell, \qquad M_\lambda = \sum_{\ell \in \mathbb{A}} \nu_\ell. \tag{2.7}$$

.

2.1.4. Boltzmann distributions

The general idea of the *Boltzmann distribution* as a probability measure on a combinatorial structure $\mathcal{A} = \{a\}$ (such as the set of all integer partitions Λ or its constrained versions, e.g., the set of strict partitions $\check{\Lambda}$) is that it is defined by picking some additive structural features of the elements in $\mathcal{A}$ (such as weight and/or length of a partition) and making the probability of the element $a \in \mathcal{A}$ depend only on those features in a "geometric" fashion. Below, this idea is made precise for the class $\tilde{\Lambda}$ of integer partitions (see (2.6)) with constraints on the source of parts (via set $\mathbb{A}$) and their multiplicities (via sets $(\mathbb{B}_\ell)$). Background material about combinatorial structures and the Boltzmann distribution is provided in Appendix B.

Definition 2.1. Suppose that the constraining sets $\mathbb{A}$ and $(\mathbb{B}_\ell)$ are fixed, and consider the corresponding partition space $\tilde{\Lambda}$ defined in (2.6). Given a two-dimensional parameter $\boldsymbol{z} = (z_1, z_2)$, with $0 < z_1 < 1$ and $0 < z_2 < 1/z_1$, the *Boltzmann distribution* on $\tilde{\Lambda}$ is defined by the formula

$$\mathsf{P}_{\boldsymbol{z}}(\lambda) = \frac{z_1^{N_\lambda} z_2^{M_\lambda}}{F(\boldsymbol{z})}, \qquad \lambda \in \tilde{\Lambda}, \tag{2.8}$$

with the normalising factor

$$F(\boldsymbol{z}) = \sum_{\lambda \in \tilde{\Lambda}} z_1^{N_\lambda} z_2^{M_\lambda}. \tag{2.9}$$

Considering the constituent subspaces

$$\tilde{\Lambda}(n,m) := \{\lambda \in \tilde{\Lambda} \colon N_\lambda = n, M_\lambda = m\}, \tag{2.10}$$

and indeterminate $\boldsymbol{z}$, the *generating function* $F(\boldsymbol{z})$ can be expressed as a double power series,

$$F(\boldsymbol{z}) = \sum_{n,m} F_{n,m} z_1^n z_2^m, \tag{2.11}$$

where $F_{n,m} = \#\tilde{\Lambda}(n,m)$. In particular, the "initial" values with $n = 0$ are reduced to

$$F_{0,0} = 1, \qquad F_{0,m} = 0 \quad (m \geq 1). \tag{2.12}$$

Of course, $F_{n,m} > 0$ if and only if the condition $\{N_\lambda = n, M_\lambda = m\}$ is realisable, that is, if $\tilde{\Lambda}(n,m) \neq \varnothing$. If the focus is on the specific weight $N_\lambda = n$ or length $M_\lambda = m$ alone, this corresponds to the "marginal" subspaces

$$\tilde{\Lambda}(n,\cdot) := \bigcup_{m \leq n} \tilde{\Lambda}(n,m) = \{\lambda \in \tilde{\Lambda} \colon N_\lambda = n\}, \tag{2.13}$$

$$\tilde{\Lambda}(\cdot,m) := \bigcup_{n \geq m} \tilde{\Lambda}(n,m) = \{\lambda \in \tilde{\Lambda} \colon M_\lambda = m\}. \tag{2.14}$$

The joint distribution of N_λ and M_λ under the Boltzmann measure (2.8) is given by

$$\mathsf{P}_{\boldsymbol{z}}(N_\lambda = n, M_\lambda = m) = \mathsf{P}_{\boldsymbol{z}}(\tilde{\Lambda}(n,m)) = \frac{F_{n,m} z_1^n z_2^m}{F(\boldsymbol{z})}, \tag{2.15}$$

with the marginals

$$\mathsf{P}_{\boldsymbol{z}}(N_\lambda = n) = \mathsf{P}_{\boldsymbol{z}}(\tilde{\Lambda}(n,\cdot)) = \frac{z_1^n}{F(\boldsymbol{z})} \sum_{m \leq n} F_{n,m} z_2^m, \tag{2.16}$$

$$\mathsf{P}_{\boldsymbol{z}}(M_\lambda = m) = \mathsf{P}_{\boldsymbol{z}}(\tilde{\Lambda}(\cdot,m)) = \frac{z_2^m}{F(\boldsymbol{z})} \sum_{n \geq m} F_{n,m} z_1^n. \tag{2.17}$$

Remark 2.2. For the empty partition $\lambda_\varnothing \vdash 0$ formally associated with the null configuration $\nu_\ell \equiv 0$, formula (2.8) yields $\mathsf{P}_{\boldsymbol{z}}(\lambda_\varnothing) = 1/F(\boldsymbol{z}) > 0$. On the other hand, $\mathsf{P}_{\boldsymbol{z}}(\lambda_\varnothing) < 1$, since $F(\boldsymbol{z}) > F(0,0) = 1$.

The following result describes the Boltzmann distribution (2.8) in terms of the joint distribution of the multiplicities (ν_ℓ). As a by-product, it provides a multiplicative representation of the generating function $F(\boldsymbol{z})$.

Lemma 2.3. *Fix $\boldsymbol{z} \in \mathbb{R}^2$ as in Definition 2.1 above. Under the Boltzmann measure $\mathsf{P}_{\boldsymbol{z}}$ on the generic partition space $\tilde{\Lambda}$ defined in (2.6), the random multiplicities $(\nu_\ell,\ \ell \in \mathbb{A})$ are mutually independent, with marginal distributions*

$$\mathsf{P}_{\boldsymbol{z}}(\nu_\ell = k) = \frac{z_1^{\ell k} z_2^k}{F_\ell(\boldsymbol{z})}, \qquad k \in \mathbb{B}_\ell, \tag{2.18}$$

where

$$F_\ell(\boldsymbol{z}) = \sum_{k \in \mathbb{B}_\ell} z_1^{\ell k} z_2^k, \qquad \ell \in \mathbb{A}. \tag{2.19}$$

In particular, the generating function $F(\boldsymbol{z})$ admits the following product representation,

$$F(\boldsymbol{z}) = \prod_{\ell \in \mathbb{A}} F_\ell(\boldsymbol{z}). \tag{2.20}$$

Proof. It suffices to verify that the product measure $\tilde{\mathsf{P}}_{\boldsymbol{z}}$ on $\tilde{\Lambda}$ with marginals (2.18) is consistent with the definition (2.8). Let a partition $\lambda \in \tilde{\Lambda}$ be specified by the sequence of multiplicities $k_\ell \in \mathbb{B}_\ell$ $(\ell \in \mathbb{A})$. Due to independence of (ν_ℓ) under $\tilde{\mathsf{P}}_{\boldsymbol{z}}$ and formula (2.18), we have on account of expressions (2.7),

$$\begin{aligned} \tilde{\mathsf{P}}_{\boldsymbol{z}}(\lambda) = \prod_{\ell \in \mathbb{A}} \tilde{\mathsf{P}}_{\boldsymbol{z}}(\nu_\ell = k_\ell) &= \prod_{\ell \in \mathbb{A}} \frac{z_1^{\ell k_\ell} z_2^{k_\ell}}{F_\ell(\boldsymbol{z})} \\ &= \frac{z_1^{\sum_{\ell \in \mathbb{A}} \ell k_\ell} z_2^{\sum_{\ell \in \mathbb{A}} k_\ell}}{\prod_{\ell \in \mathbb{A}} F_\ell(\boldsymbol{z})} = \frac{z_1^{N_\lambda} z_2^{M_\lambda}}{\widetilde{F}(\boldsymbol{z})}, \end{aligned} \tag{2.21}$$

where $\widetilde{F}(\boldsymbol{z}) := \prod_{\ell \in \mathbb{A}} F_\ell(\boldsymbol{z})$. Since the probability distributions (2.8) and (2.21) on the same space $\tilde{\Lambda}$ appear to be proportional to one another, it follows that the normalisation factors $F(\boldsymbol{z})$ and $\widetilde{F}(\boldsymbol{z})$ coincide, which proves the product representation (2.20). □

Remark 2.4. Since $0 \in \mathbb{B}_\ell$, we have a lower bound

$$F_\ell(\boldsymbol{z}) = \sum_{k \in \mathbb{B}_\ell} z_1^{\ell k} z_2^k \geq 1, \qquad \ell \in \mathbb{A}. \tag{2.22}$$

The next lemma ensures that a random partition generated according to the Boltzmann distribution $\mathsf{P}_{\boldsymbol{z}}$ is almost surely (a.s.) finite, so that $\mathsf{P}_{\boldsymbol{z}}(M_\lambda < \infty) = 1$.

Lemma 2.5. *Fix $\boldsymbol{z} \in \mathbb{R}^2$ as in Definition 2.1 above. Under the probability measure $\mathsf{P}_{\boldsymbol{z}}$, the number of nonzero terms in the sequence of multiplicities (ν_ℓ) is a.s. finite.*

Proof. By the Borel–Cantelli lemma (see, e.g., [78, Sec. II.10, p. 255]), it suffices to check that

$$\sum_{\ell\in\mathbb{A}} \mathsf{P}_{\boldsymbol{z}}(\nu_\ell > 0) < \infty.$$

Noting that $z_1^\ell z_2 \le z_1 z_2 < 1$ (see Definition 2.1), we have

$$F_\ell(\boldsymbol{z}) = \sum_{k\in\mathbb{B}_\ell} z_1^{\ell k} z_2^k \le \sum_{k=0}^{\infty} (z_1^\ell z_2)^k = \frac{1}{1 - z_1^\ell z_2}.$$

Hence, from the distribution formula (2.18) we get

$$\mathsf{P}_{\boldsymbol{z}}(\nu_\ell > 0) = 1 - \frac{1}{F_\ell(\boldsymbol{z})} \le 1 - \left(1 - z_1^\ell z_2\right) = z_1^\ell z_2,$$

and therefore

$$\sum_{\ell\in\mathbb{A}} \mathsf{P}_{\boldsymbol{z}}(\nu_\ell > 0) \le z_2 \sum_{\ell\in\mathbb{A}} z_1^\ell \le z_2 \sum_{\ell=1}^{\infty} z_1^\ell = \frac{z_1 z_2}{1 - z_1} < \infty,$$

as required. □

Remark 2.6. While the constraining sets $\mathbb{A}$ and $(\mathbb{B}_\ell)$ are pre-determined they can be relaxed by introducing supplementary free variables thus giving the following contribution for each $\ell \in \mathbb{N}$

$$\mathsf{P}_{\boldsymbol{z}}(\nu_\ell = k) = \frac{z_{\mathbb{A}}^{1-\mathbf{1}_{\mathbb{A}}(\ell)} z_{\mathbb{B}_\ell}^{1-\mathbf{1}_{\mathbb{B}_\ell}(k)} z_1^{k\ell} z_2^k}{F_\ell(\boldsymbol{z})}. \tag{2.23}$$

If it is re-expressed in terms of thermodynamic-like variables this gives

$$\mathsf{P}_{\boldsymbol{z}}(\nu_\ell = k) = \frac{\exp\left(-\beta_{\mathbb{A}}(1 - \mathbf{1}_{\mathbb{A}}(\ell)) - \beta_{\mathbb{B}_\ell}(1 - \mathbf{1}_{\mathbb{B}_\ell}(k)) - \beta_1 k\ell - \beta_2 k\right)}{F_\ell(\boldsymbol{z})}. \tag{2.24}$$

The Boltzmann distribution studied in this chapter can be interpreted as an ordered version where $\beta_{\mathbb{A}}$ and $\beta_{\mathbb{B}_\ell}$ are sent to infinity so the "temperature" goes to zero. More generally when studying complex systems the energy can be represented by a composite Hamiltonian that incorporates the contributions of the components of the system, adding or removing contributions allows to merge and interpolate models. Here, allowing finite values of $\beta_{\mathbb{A}}$ and $\beta_{\mathbb{B}_\ell}$ "erase" the gaps in the structure. Though this is not discussed here, the analysis of the transition to infinite values may provide valuable insights.

2.1.5. Conditional Boltzmann distributions

Recall that the Boltzmann distribution $\mathsf{P}_{\boldsymbol{z}}$ (see (2.8)) is defined on the partition space $\tilde{\Lambda}$ subject to the tacit constraints determined by the sets $\mathbb{A}$ and $(\mathbb{B}_\ell, \ell \in \mathbb{A})$, as described in Section 2.1.1. It is sometimes useful to impose further constraints on permissible partitions and consider the arising conditional projections of the original measure $\mathsf{P}_{\boldsymbol{z}}$ onto the corresponding partition subspaces. To be specific, let $\tilde{\Lambda}^\dagger \subseteq \tilde{\Lambda}$ and consider the conditional measure supported on the space $\tilde{\Lambda}^\dagger$,

$$\mathsf{P}^\dagger_{\boldsymbol{z}}(\lambda) := \mathsf{P}_{\boldsymbol{z}}(\lambda \,|\, \tilde{\Lambda}^\dagger) = \frac{\mathsf{P}_{\boldsymbol{z}}(\lambda)}{\mathsf{P}_{\boldsymbol{z}}(\tilde{\Lambda}^\dagger)}, \qquad \lambda \in \tilde{\Lambda}^\dagger. \tag{2.25}$$

Lemma 2.7. *The measure (2.25) coincides with the Boltzmann measure on the partition space $\tilde{\Lambda}^\dagger$.*

Proof. By the definition (2.8), for any partition $\lambda \in \tilde{\Lambda}^\dagger$ we have

$$\mathsf{P}_{\boldsymbol{z}}(\lambda \,|\, \tilde{\Lambda}^\dagger) = \frac{z_1^{N_\lambda} z_2^{M_\lambda}/F(\boldsymbol{z})}{F^\dagger(\boldsymbol{z})/F(\boldsymbol{z})} = \frac{z_1^{N_\lambda} z_2^{M_\lambda}}{F^\dagger(\boldsymbol{z})}, \qquad \lambda \in \tilde{\Lambda}^\dagger, \tag{2.26}$$

where

$$F^\dagger(\boldsymbol{z}) = \sum_{\lambda \in \tilde{\Lambda}^\dagger} z_1^{N_\lambda} z_2^{M_\lambda}.$$

Again referring to (2.8) together with (2.9), we see that formula (2.26) defines the Boltzmann distribution on $\tilde{\Lambda}^\dagger$ with the same parameters $\boldsymbol{z} = (z_1, z_2)$. □

In fact, the Boltzmann measure (2.8) on the partition space $\tilde{\Lambda}$ constrained by means of the sets $\mathbb{A}$ and $(\mathbb{B}_\ell)$ as described in Definition 2.1, can itself be identified with the conditional Boltzmann measure projected from the full partition space Λ via conditioning on $\lambda \in \tilde{\Lambda}$. The following particular cases of further constraints on the space $\tilde{\Lambda}$ are also of interest:

$$\begin{aligned}
\tilde{\Lambda}_K &:= \{\lambda \in \tilde{\Lambda}\colon\ \max \nu_\ell \le K\} && \text{(multiplicities bounded by } K\text{)};\\
\tilde{\Lambda}_L &:= \{\lambda \in \tilde{\Lambda}\colon\ \max \lambda_i \le L\} && \text{(parts bounded by } L\text{)};\\
\tilde{\Lambda}_M &:= \{\lambda \in \tilde{\Lambda}\colon\ \textstyle\sum_\ell \nu_\ell = M\} && \text{(fixed length } M_\lambda = M\text{)};\\
\tilde{\Lambda}_N &:= \{\lambda \in \tilde{\Lambda}\colon\ \textstyle\sum_\ell \ell\nu_\ell = N\} && \text{(fixed weight } N_\lambda = N\text{)}.
\end{aligned}$$

Note that the result of Lemma 2.3 about mutual independence and marginal distributions of the multiplicities (ν_ℓ) remains true for the first two examples, $\tilde{\Lambda}_K$ and $\tilde{\Lambda}_L$, simply because they follow our basic Definition 2.1 with the constraining sets $\mathbb{B}_\ell$ or $\mathbb{A}$ replaced by $\mathbb{B}_{\ell,K} = \{k \in \mathbb{B}_\ell\colon k \le K\}$ or $\mathbb{A}_L = \{\ell \in \mathbb{A}\colon \ell \le L\}$, respectively. However, this result does not apply to the Boltzmann measures on

the spaces $\tilde{\Lambda}_M = \tilde{\Lambda}(\cdot, M)$ or $\tilde{\Lambda}_N = \tilde{\Lambda}(N, \cdot)$ (see (2.13) and (2.14)), which take a reduced form by "burning out" the parameters z_1 or z_2, respectively:

$$\mathsf{P}_{\boldsymbol{z}}(\lambda \,|\, \tilde{\Lambda}_M) = \frac{z_1^{N_\lambda}}{\sum_{n \geq M} F(n, M)\, z_1^n}, \qquad \lambda \in \tilde{\Lambda}_M, \tag{2.27}$$

$$\mathsf{P}_{\boldsymbol{z}}(\lambda \,|\, \tilde{\Lambda}_N) = \frac{z_2^{M_\lambda}}{\sum_{m \leq N} F(N, m)\, z_2^m}, \qquad \lambda \in \tilde{\Lambda}_N. \tag{2.28}$$

Individual constraints such as listed above can be combined. An important example is considered in the next lemma, stating that the Boltzmann distribution conditioned on both N_λ and M_λ is reduced to a uniform measure on the corresponding partition subspace.

Lemma 2.8. *Let $n, m \in \mathbb{N}_0$ be such that the conditions $N_\lambda = n$ and $M_\lambda = m$ are compatible with the constraining sets $\mathbb{A}$ and $(\mathbb{B}_\ell)$, that is, $\tilde{\Lambda}(n, m) \neq \varnothing$. Then*

$$\mathsf{P}_{\boldsymbol{z}}\big(\lambda \,|\, \tilde{\Lambda}(n, m)\big) = \frac{1}{\#\tilde{\Lambda}(n, m)}, \qquad \lambda \in \tilde{\Lambda}(n, m). \tag{2.29}$$

Proof. By virtue of Lemma 2.7, it suffices to observe that the Boltzmann distribution on $\tilde{\Lambda}(n, m)$ is uniform, because $\mathsf{P}_{\boldsymbol{z}}(\lambda) \propto z_1^n z_2^m = \text{const}$ for all $\lambda \in \tilde{\Lambda}(n, m)$. □

Thanks to Lemma 2.8, the Boltzmann distribution can be used for enumeration purposes.

Corollary 2.8.1. *The following representation holds with any $\boldsymbol{z} = (z_1, z_2)$ such that $0 < z_1 < 1$ and $z_2 < 1/z_1$,*

$$F_{n,m} \equiv \#\tilde{\Lambda}(n, m) = \frac{F(\boldsymbol{z})\, \mathsf{P}_{\boldsymbol{z}}(N_\lambda = n, M_\lambda = m)}{z_1^n z_2^m}. \tag{2.30}$$

To use formula (2.30) in practice, the parameters z_1, z_2 are usually calibrated so as to make the events $\{N_\lambda = n, M_\lambda = m\}$ "likely" under the Boltzmann distribution $\mathsf{P}_{\boldsymbol{z}}$ when n and m are close to some target values $\langle N \rangle$ and $\langle M \rangle$, respectively (treated as *hyper-parameters*). We pursue the standard approach (see, e.g., [13], [34], [87] [88]) based on making the *expected values* of N_λ and M_λ consistent with the prescribed values $\langle N \rangle$ and $\langle M \rangle$, respectively,

$$\mathsf{E}_{\boldsymbol{z}}(N_\lambda) = \langle N \rangle\,, \qquad \mathsf{E}_{\boldsymbol{z}}(M_\lambda) = \langle M \rangle\,. \tag{2.31}$$

Using (2.18), conditions (2.31) are rewritten more explicitly as a system of equations for the parameters z_1 and z_2,

$$\begin{cases} \displaystyle\sum_{\ell \in \mathbb{A}} \ell \sum_{k \in \mathbb{B}_\ell} \frac{k\, z_1^{\ell k} z_2^k}{F_\ell(\boldsymbol{z})} = \langle N \rangle, \\[2ex] \displaystyle\sum_{\ell \in \mathbb{A}} \sum_{k \in \mathbb{B}_\ell} \frac{k\, z_1^{\ell k} z_2^k}{F_\ell(\boldsymbol{z})} = \langle M \rangle. \end{cases} \tag{2.32}$$

Solving such a system exactly is beyond reach but an asymptotic analysis may be feasible when one or both of the hyper-parameters $\langle N\rangle$ and $\langle M\rangle$ are large (see Section 2.2.3 below).

Truncation of the source of parts, thus reducing the partition space to $\tilde{\Lambda}_L$ may be useful in the design of Boltzmann samplers with the aim to avoid indefinite computation (see Chapter 3). Clearly, if $L < \max \mathbb{A}$ then the truncation leads to a distortion of the original Boltzmann distribution $\mathsf{P}_{\boldsymbol{z}}$; in particular, it will cause a negative bias between the target hyper-parameters $\langle N\rangle$ and $\langle M\rangle$ used for calibration of $\mathsf{P}_{\boldsymbol{z}}$ (see (2.32)) and the truncated expected values,

$$\mathsf{E}^L_{\boldsymbol{z}}(N_\lambda) = \sum_{\ell\in\mathbb{A}_L} \ell \sum_{k\in\mathbb{B}_\ell} \frac{k\, z_1^{\ell k} z_2^k}{F_\ell(\boldsymbol{z})} < \sum_{\ell\in\mathbb{A}} \ell \sum_{k\in\mathbb{B}_\ell} \frac{k\, z_1^{\ell k} z_2^k}{F_\ell(\boldsymbol{z})} = \mathsf{E}_{\boldsymbol{z}}(N_\lambda) = \langle N\rangle, \tag{2.33}$$

$$\mathsf{E}^L_{\boldsymbol{z}}(M_\lambda) = \sum_{\ell\in\mathbb{A}_L} \sum_{k\in\mathbb{B}_\ell} \frac{k\, z_1^{\ell k} z_2^k}{F_\ell(\boldsymbol{z})} < \sum_{\ell\in\mathbb{A}} \sum_{k\in\mathbb{B}_\ell} \frac{k\, z_1^{\ell k} z_2^k}{F_\ell(\boldsymbol{z})} = \mathsf{E}_{\boldsymbol{z}}(M_\lambda) = \langle M\rangle. \tag{2.34}$$

However, if the probability of the condition $\{\lambda \in \tilde{\Lambda}_L\}$ is large enough, then the two distributions are close to one another in total variation, which is justified by the following elementary estimate.

Lemma 2.9. *Let $(\Omega, \mathcal{F}, \mathsf{P})$ be a probability space, and let an event $A \in \mathcal{F}$ be such that $\mathsf{P}(A) \geq 1-\delta$ for some (small) $\delta > 0$. Then for any event $B \in \mathcal{F}$,*

$$|\mathsf{P}(B\,|\,A) - \mathsf{P}(B)| \leq \frac{2\delta}{1-\delta}.$$

Proof. Denoting $A^c = \Omega \setminus A$, we have

$$\begin{aligned} |\mathsf{P}(B\,|\,A) - \mathsf{P}(B)| &= \frac{|\mathsf{P}(B\cap A) - \mathsf{P}(B)\,\mathsf{P}(A)|}{\mathsf{P}(A)} \\ &= \frac{|\mathsf{P}(B\cap A)\,\mathsf{P}(A^c) - \mathsf{P}(B\cap A^c)\,\mathsf{P}(A)|}{1-\mathsf{P}(A^c)} \\ &\leq \frac{2\,\mathsf{P}(A^c)}{1-\mathsf{P}(A^c)} \leq \frac{2\delta}{1-\delta}, \end{aligned}$$

noting that $\mathsf{P}(A^c) \leq \delta$. □

A simple but useful version of the truncation idea adapted to the spaces $\tilde{\Lambda}(n,m)$ states that if the truncation threshold L is high enough then the additional condition $\ell \leq L$ does not affect the conditional uniformity stated in Lemma 2.8.

Definition 2.2. Assuming that the partition space $\tilde{\Lambda}(n,m)$ is non-empty, denote by $L^* = L^*(n,m)$ any *majorant* of parts involved in partitions λ belonging to this space, that is,

$$L^* \geq \max\{\lambda_1 \colon \lambda = (\lambda_i) \in \tilde{\Lambda}(n,m)\}. \tag{2.35}$$

In terms of multiplicities (ν_ℓ) encoding partitions $\lambda \in \tilde{\Lambda}(n,m)$, condition (2.35) is equivalent to saying that $\nu_\ell \equiv 0$ for all $\ell > L^*$.

For example, a loose majorant is provided by $L^* = n$; this is actually sharp if $m = 1$. In general, a sharp majorant is given by

$$L^* = \max\{\ell \in \mathbb{A} \colon \tilde{\Lambda}(n-\ell, m-1) \neq \varnothing\}. \tag{2.36}$$

Note that formula (2.36) holds in the boundary case $m = 1$ due to our convention in Section 2.1.1, effectively stating that the set $\tilde{\Lambda}(0,0)$ is not empty by containing a (single) partition $\lambda_\varnothing = (0,0,\dots)$.

The following fact is self-evident by observing that $\tilde{\Lambda}(n,m) \cap \tilde{\Lambda}_{L^*} = \tilde{\Lambda}(n,m)$ and in view of Lemma 2.8.

Lemma 2.10. *Suppose that $\tilde{\Lambda}(n,m) \neq \varnothing$ and let L^* be a majorant as in Definition 2.2. Then*

$$\mathsf{P}_{\boldsymbol{z}}(\lambda \,|\, \tilde{\Lambda}(n,m) \cap \tilde{\Lambda}_{L^*}) = \frac{1}{\#\tilde{\Lambda}(n,m)}, \qquad \lambda \in \tilde{\Lambda}(n,m). \tag{2.37}$$

This lemma can be utilised in random sampling of integer partitions based on the Boltzmann distribution. Indeed, choosing a suitable majorant L^* and building a random partition in $\tilde{\Lambda}(n,m)$ by iteratively sampling the multiplicities ν_ℓ with $\ell \in \mathbb{A}_{L^*}$ until the target conditions (2.10) are satisfied, the resulting partition $\lambda = (\ell^{\nu_\ell})$ will be uniformly sampled from $\tilde{\Lambda}(n,m)$, according to (2.37). We will return to these issues in Chapter 3.

2.1.6. Second-order moments of the partition weight and length

Consider the covariance matrix of the vector (N_λ, M_λ) under the Boltzmann measure $\mathsf{P}_{\boldsymbol{z}}$,

$$\boldsymbol{K}(\boldsymbol{z}) := \begin{pmatrix} \mathsf{Var}_{\boldsymbol{z}}(N_\lambda) & \mathsf{Cov}_{\boldsymbol{z}}(N_\lambda, M_\lambda) \\ \mathsf{Cov}_{\boldsymbol{z}}(N_\lambda, M_\lambda) & \mathsf{Var}_{\boldsymbol{z}}(M_\lambda) \end{pmatrix}, \qquad \boldsymbol{z} = (z_1, z_2). \tag{2.38}$$

As such, the matrix $\boldsymbol{K}(\boldsymbol{z})$ is automatically positive semi-definite; moreover, it is *positive definite* provided that the set $\mathbb{A}$ of permissible parts contains at least two elements, $\#\mathbb{A} \geq 2$. To this effect, since both $\mathsf{Var}_{\boldsymbol{z}}(N_\lambda) > 0$ and $\mathsf{Var}_{\boldsymbol{z}}(M_\lambda) > 0$, we

only need to check that $\det \boldsymbol{K}(\boldsymbol{z}) > 0$, that is, the underlying Cauchy inequality is strict, $\bigl|\mathsf{Cov}_{\boldsymbol{z}}(N_\lambda, M_\lambda)\bigr| < \sqrt{\mathsf{Var}_{\boldsymbol{z}}(N_\lambda)\,\mathsf{Var}_{\boldsymbol{z}}(M_\lambda)}$. Indeed, otherwise the random variables N_λ and M_λ would be linearly dependent, that is, with some deterministic constants $c_1, c_2 \in \mathbb{R}$

$$c_1 N_\lambda + c_2 M_\lambda = \sum_{\ell \in \mathbb{A}} (c_1 \ell + c_2)\, \nu_\ell \equiv \text{const} \qquad (\mathsf{P}_{\boldsymbol{z}}\text{-a.s.}).$$

But this is impossible if $\#\mathbb{A} \geq 2$, since (ν_ℓ) are mutually independent and $\nu_\ell \not\equiv$ const ($\mathsf{P}_{\boldsymbol{z}}$-a.s.).

A single-parameter version of the next lemma is well known (see, e.g., [24, Proposition 2.1] or [11, formula (2.2), p. 110]). An extension to the general multi-parametric case is stated, with a sketch proof, in [10, Proposition 7, pp. 772–773]. For convenience, we give a direct proof in the general case of a constrained partition space $\tilde{\Lambda}$ described in Definition 2.1.

Lemma 2.11. *For $\boldsymbol{s} = (s_1, s_2)$, denote $\mathrm{e}^{\boldsymbol{s}} := (\mathrm{e}^{s_1}, \mathrm{e}^{s_2})$. Define the function*

$$\Phi(\boldsymbol{s}) := \log F(\mathrm{e}^{\boldsymbol{s}}), \qquad s_1, s_2 < 0, \tag{2.39}$$

where $F(\boldsymbol{z})$ is introduced in (2.9). Then

$$\frac{\partial \Phi}{\partial s_1} = \mathsf{E}_{\boldsymbol{z}}(N_\lambda)\big|_{\boldsymbol{z}=\mathrm{e}^{\boldsymbol{s}}}, \qquad \frac{\partial \Phi}{\partial s_2} = \mathsf{E}_{\boldsymbol{z}}(M_\lambda)\big|_{\boldsymbol{z}=\mathrm{e}^{\boldsymbol{s}}}, \tag{2.40}$$

Moreover, the Hessian of $\Phi(\boldsymbol{s})$ is expressed as follows,

$$\left(\frac{\partial^2 \Phi}{\partial s_i \partial s_j}\right) = \boldsymbol{K}(\boldsymbol{z})\big|_{\boldsymbol{z}=\mathrm{e}^{\boldsymbol{s}}}, \tag{2.41}$$

where $\boldsymbol{K}(\boldsymbol{z})$ is the covariance matrix defined in (2.38).

Proof. Differentiating (2.11) and using formula (2.16), we get

$$\begin{aligned} z_1 \frac{\partial F}{\partial z_1} &= z_1 \sum_{n=0}^{\infty} n\, z_1^{n-1} \sum_{m=0}^{n} F_{n,m} z_2^m \\ &= F(\boldsymbol{z}) \sum_{n=0}^{\infty} n\, \mathsf{P}_{\boldsymbol{z}}(N_\lambda = n) = F(\boldsymbol{z})\, \mathsf{E}_{\boldsymbol{z}}(N_\lambda). \end{aligned}$$

Similarly, using (2.17),

$$\begin{aligned} z_2 \frac{\partial F}{\partial z_2} &= z_2 \sum_{m=0}^{\infty} m\, z_2^{m-1} \sum_{n=m}^{\infty} F_{n,m} z_1^n \\ &= F(\boldsymbol{z}) \sum_{m=0}^{\infty} m\, \mathsf{P}_{\boldsymbol{z}}(M_\lambda = m) = F(\boldsymbol{z})\, \mathsf{E}_{\boldsymbol{z}}(M_\lambda). \end{aligned}$$

Hence, the chain rule applied to (2.39) yields

$$\frac{\partial \Phi}{\partial s_1} = \mathrm{e}^{s_1} \frac{\partial F/\partial z_1}{F(\boldsymbol{z})}\bigg|_{\boldsymbol{z}=\mathrm{e}^{\boldsymbol{s}}} = \mathsf{E}_{\boldsymbol{z}}(N_\lambda)\big|_{\boldsymbol{z}=\mathrm{e}^{\boldsymbol{s}}},$$
$$\frac{\partial \Phi}{\partial s_2} = \mathrm{e}^{s_2} \frac{\partial F/\partial z_2}{F(\boldsymbol{z})}\bigg|_{\boldsymbol{z}=\mathrm{e}^{\boldsymbol{s}}} = \mathsf{E}_{\boldsymbol{z}}(M_\lambda)\big|_{\boldsymbol{z}=\mathrm{e}^{\boldsymbol{s}}},$$

which proves formulas (2.40).

Likewise, considering second-order partial derivatives, we obtain

$$\begin{aligned} z_1^2 \frac{\partial^2 F}{\partial z_1^2} &= z_1^2 \sum_{n=0}^{\infty} n(n-1) z_1^{n-2} \sum_{m=0}^{n} F_{n,m} z_2^m \\ &= F(\boldsymbol{z}) \sum_{n=0}^{\infty} n(n-1)\, \mathsf{P}_{\boldsymbol{z}}(N_\lambda = n) \\ &= F(\boldsymbol{z})\, \mathsf{E}_{\boldsymbol{z}}\big(N_\lambda^2 - N_\lambda\big). \end{aligned}$$

Therefore,

$$\begin{aligned} \frac{\partial^2 \Phi}{\partial s_1^2} &= \frac{\partial}{\partial s_1}\left(\mathrm{e}^{s_1} \frac{\partial F/\partial z_1}{F(\boldsymbol{z})}\bigg|_{\boldsymbol{z}=\mathrm{e}^{\boldsymbol{s}}} \right) \\ &= \mathrm{e}^{s_1} \frac{\partial F/\partial z_1}{F(\boldsymbol{z})}\bigg|_{\boldsymbol{z}=\mathrm{e}^{\boldsymbol{s}}} + \mathrm{e}^{2s_1} \frac{\partial^2 F/\partial z_1^2}{F(\boldsymbol{z})}\bigg|_{\boldsymbol{z}=\mathrm{e}^{\boldsymbol{s}}} - \mathrm{e}^{2s_1} \left(\frac{\partial F/\partial z_1}{F(\boldsymbol{z})}\bigg|_{\boldsymbol{z}=\mathrm{e}^{\boldsymbol{s}}} \right)^2 \\ &= \Big(\mathsf{E}_{\boldsymbol{z}}(N_\lambda) + \mathsf{E}_{\boldsymbol{z}}\big(N_\lambda^2 - N_\lambda\big) - \big(\mathsf{E}_{\boldsymbol{z}}(N_\lambda)\big)^2 \Big)_{\boldsymbol{z}=\mathrm{e}^{\boldsymbol{s}}} \\ &= \mathsf{Var}_{\boldsymbol{z}}(N_\lambda)\big|_{\boldsymbol{z}=\mathrm{e}^{\boldsymbol{s}}}. \end{aligned} \tag{2.42}$$

Similarly, one can show that

$$\frac{\partial^2 \Phi}{\partial s_2^2} = \mathsf{Var}_{\boldsymbol{z}}(M_\lambda)\big|_{\boldsymbol{z}=\mathrm{e}^{\boldsymbol{s}}}. \tag{2.43}$$

Furthermore, considering the mixed partial derivative, by means of formula (2.15) we have

$$\begin{aligned} z_1 z_2 \frac{\partial^2 F}{\partial z_1 \partial z_2} &= z_1 z_2 \sum_{n=0}^{\infty} \sum_{m=0}^{n} F_{n,m}\, n z_1^{n-1} m z_2^{m-1} \\ &= F(\boldsymbol{z}) \sum_{n=0}^{\infty} \sum_{m=0}^{n} nm\, \mathsf{P}_{\boldsymbol{z}}(N_\lambda = n, M_\lambda = m) = F(\boldsymbol{z})\, \mathsf{E}_{\boldsymbol{z}}\big(N_\lambda M_\lambda\big). \end{aligned}$$

Hence,

$$\begin{aligned}\frac{\partial^2\Phi}{\partial s_1\partial s_2} &= \frac{\partial}{\partial s_2}\left(\mathrm{e}^{s_1}\,\frac{\partial F/\partial z_1}{F(\boldsymbol{z})}\bigg|_{\boldsymbol{z}=\mathrm{e}^{\boldsymbol{s}}}\right)\\ &= \mathrm{e}^{s_1}\mathrm{e}^{s_2}\,\frac{\partial^2 F/\partial z_1^2}{F(\boldsymbol{z})}\bigg|_{\boldsymbol{z}=\mathrm{e}^{\boldsymbol{s}}} - \mathrm{e}^{s_1}\mathrm{e}^{s_2}\left(\frac{\partial F/\partial z_1}{F(\boldsymbol{z})}\cdot\frac{\partial F/\partial z_2}{F(\boldsymbol{z})}\right)\bigg|_{\boldsymbol{z}=\mathrm{e}^{\boldsymbol{s}}}\\ &= \Big(\mathsf{E}_{\boldsymbol{z}}(N_\lambda M_\lambda) - \mathsf{E}_{\boldsymbol{z}}(N_\lambda)\,\mathsf{E}_{\boldsymbol{z}}(M_\lambda)\Big)_{\boldsymbol{z}=\mathrm{e}^{\boldsymbol{s}}} = \mathsf{Cov}_{\boldsymbol{z}}(N_\lambda, M_\lambda)\big|_{\boldsymbol{z}=\mathrm{e}^{\boldsymbol{s}}}. \qquad (2.44)\end{aligned}$$

Finally, it remains to notice that, collectively, formulas (2.42), (2.43) and (2.44) prove the claim (2.41), which completes the proof of Lemma 2.11. □

Corollary 2.11.1. *Suppose that $\#\mathbb{A} \geq 2$ (see a comment after definition (2.38)). Then the function $\Phi(\boldsymbol{s})$ defined in (2.39) is strictly convex. Consequently, any system of equations in variables $\boldsymbol{z} = (z_1, z_2)$ of the form (2.31) has at most one solution.*

Proof. Convexity of $\Phi(\boldsymbol{s})$ follows from the representation (2.41) and the fact that the covariance matrix $\boldsymbol{K}(\boldsymbol{z})$ is positive definite. □

2.2. Strict power partitions

2.2.1. Basic formulas

From now on, we consider the case $\mathbb{A} = \mathbb{N}^q$, with a fixed $q \in \mathbb{N}$, and $\mathbb{B}_\ell \equiv \{0, 1\}$ for all $\ell \in \mathbb{N}^q$. This specification corresponds to strict integer partitions (i.e., with unequal parts) into perfect q-th powers. To highlight the choice of this model, in what follows we switch from the generic notation $\tilde{\Lambda}$ and $\tilde{\Lambda}(n, m)$ to a more adapted notation $\check{\Lambda}^q$ and $\check{\Lambda}^q(n, m)$, where the super-index ^{q} indicates that parts are q-th powers, while the "check" symbol $\check{}$ stands as a reminder that partitions are strict. To conform with the conventional notation, for $q = 1$ we will omit the super-index by writing $\check{\Lambda}$, $\check{\Lambda}(n, m)$, etc.

The next key lemma is but a specialisation of the general Proposition 2.3 to the case $\check{\Lambda}^q$.

Lemma 2.12. *Under the Boltzmann distribution on the space $\check{\Lambda}^q$, the random multiplicities $(\nu_\ell,\ \ell \in \mathbb{N}^q)$ are mutually independent and have a Bernoulli distribution with the corresponding parameter $z_1^\ell z_2\,(1 + z_1^\ell z_2)^{-1}$,*

$$\mathsf{P}_{\boldsymbol{z}}(\nu_\ell = 0) = \frac{1}{1 + z_1^\ell z_2}, \qquad \mathsf{P}_{\boldsymbol{z}}(\nu_\ell = 1) = \frac{z_1^\ell z_2}{1 + z_1^\ell z_2} \qquad (\ell \in \mathbb{N}^q). \qquad (2.45)$$

Furthermore, the corresponding generating function is given by

$$F(\boldsymbol{z}) = \prod_{\ell\in\mathbb{N}^q}(1+z_1^{\ell}z_2) = \prod_{j=1}^{\infty}(1+z_1^{j^q}z_2). \tag{2.46}$$

Remark 2.13. Here the Borel–Cantelli condition $\sum_\ell \mathsf{P}_{\boldsymbol{z}}(\nu_\ell > 0) < \infty$ (see the proof of Lemma 2.5) specialises to

$$\sum_{\ell\in\mathbb{N}^q}\frac{z_1^{\ell}z_2}{1+z_1^{\ell}z_2} \le z_2\sum_{\ell=1}^{\infty}z_1^{\ell} = \frac{z_1z_2}{1-z_1}.$$

Thus, we need $0 < z_1 < 1$ but no condition on $z_2 > 0$.

2.2.2. Sums asymptotics

We will be frequently using asymptotic formulas for certain sums over the integer set $\mathbb{N}^q$. Of course, such results are well known for $q = 1$. The analysis is greatly facilitated by the classic (first-order) *Euler–Maclaurin summation formula* (see, e.g., [22, §12.2]), conveniently written in the form

$$\sum_{j=1}^{\infty}f(j) = \int_0^{\infty}f(x)\,\mathrm{d}x + \int_0^{\infty}\widetilde{B}_1(x)\,f'(x)\,\mathrm{d}x, \tag{2.47}$$

where $\widetilde{B}_1(x) := \{x\} \equiv x - \lfloor x\rfloor$ $(x\in\mathbb{R})$, and both the series $\sum_{j=1}^{\infty}f(j)$ and the integral $\int_0^{\infty}f(x)\,\mathrm{d}x$ are assumed to converge. In particular, formula (2.47) gives a simple bound for the error arising from replacing the sum with the integral,

$$\sum_{j=1}^{\infty}f(j) = \int_0^{\infty}f(x)\,\mathrm{d}x + O(1)\int_0^{\infty}|f'(x)|\,\mathrm{d}x.$$

A more general "indented" version of the Euler–Maclaurin formula reads

$$\sum_{j>j_*}f(j) = \int_{j_*}^{\infty}f(x)\,\mathrm{d}x + \int_{j_*}^{\infty}\widetilde{B}_1(x)\,f'(x)\,\mathrm{d}x, \tag{2.48}$$

leading to the estimate

$$\sum_{j>j_*}^{\infty}f(j) = \int_{j_*}^{\infty}f(x)\,\mathrm{d}x + O(1)\int_{j_*}^{\infty}|f'(x)|\,\mathrm{d}x.$$

For most of our purposes, the first-order formulas will suffice. If needed, a refined estimate of the remainder term can be obtained with a second-order Euler–Maclaurin formula [66, #2.10.1, p. 63],

$$\sum_{j=1}^{\infty} f(j) = \int_0^{\infty} f(x)\,\mathrm{d}x - \frac{f(0)}{2} + \frac{1}{2}\int_0^{\infty} \widetilde{B}_2(x)\, f''(x)\,\mathrm{d}x, \tag{2.49}$$

where $\widetilde{B}_2(x) := \{x\} - \{x\}^2$ $(x \in \mathbb{R})$.

Lemma 2.14. *Let $s \geq 0$ be fixed. Then, as $\gamma \to 0+$,*

$$\sum_{\ell \in \mathbb{N}^q} \ell^s \mathrm{e}^{-\gamma \ell} = \frac{\Gamma(s+1/q)}{q\,\gamma^{s+1/q}} \left(1 + O\big(\gamma^{1/q}\big)\right). \tag{2.50}$$

Proof. Setting $f(x) := \ell^s \mathrm{e}^{-\gamma\ell}|_{\ell = x^q}$, we have

$$f'(x) = \left.\frac{\mathrm{d}(\ell^s \mathrm{e}^{-\gamma\ell})}{\mathrm{d}\ell}\right|_{\ell = x^q} \cdot (x^q)' = (s - \gamma\ell)\,\ell^{s-1}\mathrm{e}^{-\gamma\ell}|_{\ell = x^q} \cdot q\,x^{q-1}. \tag{2.51}$$

Hence, the Euler–Maclaurin formula (2.47) yields

$$\sum_{\ell \in \mathbb{N}^q} \ell^s \mathrm{e}^{-\gamma\ell} = \sum_{j=1}^{\infty} j^{qs} \mathrm{e}^{-\gamma j^q} = \int_0^{\infty} x^{qs}\,\mathrm{e}^{-\gamma x^q}\mathrm{d}x + \Delta_s(\gamma), \tag{2.52}$$

where the error term is given by

$$\Delta_s(\gamma) = q\int_0^{\infty} \widetilde{B}_1(x)\,(s - \gamma x^q)\,x^{qs-1}\,\mathrm{e}^{-\gamma x^q}\,\mathrm{d}x. \tag{2.53}$$

The integral in (2.52) is easily computed by the substitution $u = \gamma x^q$,

$$\int_0^{\infty} x^{qs}\,\mathrm{e}^{-\gamma x^q}\mathrm{d}x = \frac{1}{q\,\gamma^{s+1/q}} \int_0^{\infty} u^{s+1/q-1}\,\mathrm{e}^{-u}\,\mathrm{d}u = \frac{\Gamma(s+1/q)}{q\,\gamma^{s+1/q}}. \tag{2.54}$$

To estimate the error term $\Delta_s(\gamma)$, we have to consider the cases $s = 0$ and $s > 0$ separately. Using that $0 \leq \widetilde{B}_1(x) \leq 1$, from (2.53) we obtain, via the same substitution $u = \gamma x^q$,

$$0 < -\Delta_0(\gamma) < q\gamma \int_0^{\infty} x^{q-1}\mathrm{e}^{-\gamma x^q}\mathrm{d}x = \int_0^{\infty} \mathrm{e}^{-u}\mathrm{d}u = 1. \tag{2.55}$$

If $s > 0$ then expression (2.53) implies a two-sided inequality,

$$-q\gamma \int_0^{\infty} x^{q(s+1)-1}\mathrm{e}^{-\gamma x^q}\mathrm{d}x < \Delta_s(\gamma) < qs \int_0^{\infty} x^{qs-1}\mathrm{e}^{-\gamma x^q}\mathrm{d}x. \tag{2.56}$$

Computing the integrals as before, the bounds (2.56) specialise as follows,

$$-\frac{\Gamma(s+1)}{\gamma^s} < \Delta_s(\gamma) < \frac{s\,\Gamma(s)}{\gamma^s} = \frac{\Gamma(s+1)}{\gamma^s}. \tag{2.57}$$

In fact, the estimate (2.55) for $s = 0$ can be included in (2.57).

Finally, the claim (2.48) follows from (2.52), (2.54) and (2.57). □

Refined asymptotics of sums of the form (2.50) can be obtained with the help of the second-order Euler–Maclaurin formula (2.49). Keeping the same notation $f(x) = \ell^s \mathrm{e}^{-\gamma\ell}|_{\ell=x^q}$ and using that $\widetilde{B}_2(x)$ is bounded, we obtain

$$\sum_{\ell\in\mathbb{N}^q} \ell^s \mathrm{e}^{-\gamma\ell} = \int_0^\infty f(x)\,\mathrm{d}x - \frac{f(0)}{2} + O(1)\int_0^\infty |f''(x)|\,\mathrm{d}x, \tag{2.58}$$

where $f(0) = 0$ for $s > 0$ and $f(0) = 1$ for $s = 0$. Similarly as in (2.51), we have

$$f''(x) = \frac{\mathrm{d}^2(\ell^s \mathrm{e}^{-\gamma\ell})}{\mathrm{d}\ell^2}\bigg|_{\ell=x^q} \cdot (x^q)'^2 + \frac{\mathrm{d}(\ell^s \mathrm{e}^{-\gamma\ell})}{\mathrm{d}\ell}\bigg|_{\ell=x^q} \cdot (x^q)''. \tag{2.59}$$

Recalling from (2.51) that $\frac{\mathrm{d}}{\mathrm{d}\ell}(\ell^s \mathrm{e}^{-\gamma\ell}) = (s-\gamma\ell)\,\ell^{s-1}\mathrm{e}^{-\gamma\ell}$, we further compute

$$\frac{\mathrm{d}^2(\ell^s \mathrm{e}^{-\gamma\ell})}{\mathrm{d}\ell^2} = \frac{\mathrm{d}}{\mathrm{d}\ell}\big((s-\gamma\ell)\,\ell^{s-1}\mathrm{e}^{-\gamma\ell}\big) = \big((s-1)s - 2s\gamma\ell + \gamma^2\ell^2\big)\,\ell^{s-2}\mathrm{e}^{-\gamma\ell}.$$

Returning to (2.59) and (2.58), one can check that each of the arising integrals in the remainder term is estimated by $O(\gamma^{-s+1/q})$. As a result, this leads to an improved asymptotic formula (cf. (2.50))

$$\sum_{\ell\in\mathbb{N}^q} \ell^s \mathrm{e}^{-\gamma\ell} = \begin{cases} \dfrac{\Gamma(1/q)}{q\,\gamma^{1/q}} - \dfrac{1}{2} + O\big(\gamma^{1/q}\big), & s = 0, \\ \dfrac{\Gamma(s+1/q)}{q\,\gamma^{s+1/q}}\,\big(1 + O\big(\gamma^{2/q}\big)\big), & s > 0. \end{cases} \tag{2.60}$$

The refined estimate (2.60) with $s = 1$ will be useful in the discussion of a numerical implementation of the Boltzmann sampler in Chapter 3.

Lemma 2.15. *As $\eta \to 0$ and $\gamma \to 0+$,*

$$\sum_{\ell\in\mathbb{N}^q} \log\big(1 + \eta\,\mathrm{e}^{-\gamma\ell}\big) = \frac{\eta\,\Gamma(1/q)}{q\,\gamma^{1/q}}\,\big(1 + O(\eta) + O\big(\gamma^{1/q}\big)\big). \tag{2.61}$$

Proof. By the elementary inequalities

$$x - \tfrac{1}{2}x^2 \le \log(1+x) \le x \qquad (0 < x < 1),$$

applied to each term in the sum, we obtain

$$\begin{aligned}\sum_{\ell\in\mathbb{N}^q} \log\bigl(1+\eta\,\mathrm{e}^{-\gamma\ell}\bigr) &= \eta \sum_{\ell\in\mathbb{N}^q} \mathrm{e}^{-\gamma\ell} + O(\eta^2) \sum_{\ell\in\mathbb{N}^q} \mathrm{e}^{-2\gamma\ell} \\ &= \eta \sum_{\ell\in\mathbb{N}^q} \mathrm{e}^{-\gamma\ell} \left(1 + O(\eta)\,\frac{\sum_{\ell\in\mathbb{N}^q} \mathrm{e}^{-2\gamma\ell}}{\sum_{\ell\in\mathbb{N}^q} \mathrm{e}^{-\gamma\ell}}\right),\end{aligned}$$

and the claim follows due to Lemma 2.14 (with $s = 0$). □

We will also need a more general version of Lemmas 2.14 and 2.15, which can be proved in a similar manner using the indented Euler–Maclaurin formula (2.48). In what follows, the summation range $\{\ell \ge \ell_*\}$ is a shorthand for $\{\ell \in \mathbb{N}^q \colon \ell \ge \ell_*\}$. We also use the notation

$$\Gamma(a,x) := \int_x^\infty u^{a-1}\,\mathrm{e}^{-u}\,\mathrm{d}u \qquad (a > 0,\ x \ge 0) \tag{2.62}$$

for the *(upper) incomplete gamma function* [66, 8.2.2, p. 174].

Lemma 2.16. *As $\gamma \to 0+$,*

$$\sum_{\ell\ge\ell_*} \ell^s \mathrm{e}^{-\gamma\ell} = \frac{\Gamma(s+1/q, \gamma\ell_*)}{q\,\gamma^{s+1/q}}\,\bigl(1 + O\bigl(\gamma^{1/q}\bigr)\bigr). \tag{2.63}$$

Lemma 2.17. *As $\eta \to 0$ and $\gamma \to 0+$,*

$$\sum_{\ell\ge\ell_*} \log\bigl(1+\eta\,\mathrm{e}^{-\gamma\ell}\bigr) = \frac{\eta\,\Gamma(1/q, \gamma\ell_*)}{q\,\gamma^{1/q}}\,\bigl(1 + O(\eta) + O\bigl(\gamma^{1/q}\bigr)\bigr). \tag{2.64}$$

For ease of future reference, we state a variant of Dini's theorem. Similar criteria for uniform convergence of monotone functions can be found in literature (see, e.g. [74, Sec. 0.1] and [3, App. A.6])

Lemma 2.18. *Let $(f_n)_{n\ge1}$ be a sequence of all decreasing (or all increasing) functions from $\overline{\mathbb{R}}_+ := \mathbb{R}_+ \cup \{\infty\}$ to $\mathbb{R}$, converging pointwise to a continuous (decreasing, or increasing) function $f : \overline{\mathbb{R}}_+ \to \mathbb{R}$. Then, this convergence is uniform.*

Remark 2.19. By defining f as a continuous function from $\overline{\mathbb{R}}_+$ to $\mathbb{R}$ we mean that $f(\infty)$ is well-defined and finite. Specifically, it is the limit of $f(x)$ when x goes to ∞.

Proof. In this proof we assume that the functions are all decreasing (the increasing case is nearly identical). We remark that the image of $\overline{\mathbb{R}}_+$ is the interval $[a, b] := [f(\infty), f(0)]$. Let $\varepsilon > 0$, and $q \in \mathbb{N}$ such that $1/q < \varepsilon/(b-a)$ and define

$$\beta_k := a + k \cdot \frac{b-a}{q}, \qquad k \in [\![0, q]\!].$$

By virtue of the intermediate value theorem there exists

$$\infty = x_0 > x_1 > \cdots > x_{q-1} > x_q = 0$$

such that $f(x_k) = \beta_k$. The pointwise convergence of the sequence $(f_n)_{n\geq 1}$ guarantees that there exists $N \in \mathbb{N}$ such that for all $n \geq N$,

$$|f_n(x_k) - f(x_k)| \leq \varepsilon,$$

independently of $k \in [\![0, q]\!]$, that is because N can be chosen as the maximum of a finite number of N_k, each corresponding to the convergence at x_k. Since f and the functions f_n are decreasing, for all $x \in [x_{k+1}, x_k]$

$$\begin{aligned} |f(x) - f_n(x)| &\leq |f(x) - f(x_k)| + |f(x_k) - f_n(x)| \\ &\leq |f(x_{k+1}) - f(x_k)| + |f(x_k) - f_n(x)| \leq \varepsilon + |f(x_k) - f_n(x)| \end{aligned}$$

we also have

$$f(x_k) - \varepsilon \leq f_n(x_k) \leq f_n(x) \leq f_n(x_{k+1}) \leq f(x_{k+1}) + \varepsilon \leq f(x_k) + 2\varepsilon$$

thus we can conclude

$$|f(x) - f_n(x)| \leq 3\varepsilon$$

independently of x. □

2.2.3. Calibration of the parameters

To analyse the Boltzmann distribution under various limit regimes, it is convenient to re-parameterise it via the *hyper-parameters*

$$\langle N \rangle = \mathsf{E}_{\boldsymbol{z}}(N_\lambda), \qquad \langle M \rangle = \mathsf{E}_{\boldsymbol{z}}(M_\lambda). \tag{2.65}$$

The conditions (2.65) can be viewed as a set of equations on the parameters z_1 and z_2 (cf. (2.31)). According to Corollary 2.11.1, solution to (2.65) is unique, if it exists. The following lemma gives an asymptotic representation of the roots z_1 and z_2 in terms of $\langle N \rangle$ and $\langle M \rangle$ as $\langle N \rangle \to \infty$ and under a suitable growth condition on $\langle M \rangle$.

Assumption 2.1. Suppose that $\langle M\rangle^{-1} = O(1)$ (that is, $\langle M\rangle$ is bounded away from zero) and

$$\kappa := \frac{\langle M\rangle^{q+1}}{\langle N\rangle} \to 0. \tag{2.66}$$

Remark 2.20. The meaning of Assumption 2.1 is elucidated by a comparison with the case of *all* strict partitions $\check{\Lambda}^q$, that is, *without controlling the number of parts*. Here, the parameter z_2 would become obsolete (we can formally set $z_2 = 1$ in the Boltzmann distribution formula (2.8)), while the parameter $z_1 \in (0,1)$, calibrated from the weight condition in (2.65), can be shown (using the Euler–Maclaurin sum formula (2.73), similarly as in the proof of Theorem 2.21 below) to satisfy the asymptotics $-\log z_1 \sim c_q \langle N\rangle^{-q/(q+1)}$, with

$$c_q^{1+1/q} = \frac{1}{q}\int_0^\infty u^{1/q}\frac{\mathrm{e}^{-u}}{1+\mathrm{e}^{-u}}\,\mathrm{d}u. \tag{2.67}$$

In turn, the expected length has the asymptotics $\mathsf{E}_{\boldsymbol{z}}(M_\lambda) \sim C_q \langle N\rangle^{1/(q+1)}$, where

$$C_q = \frac{1}{q\, c_q^{1/q}}\int_0^\infty u^{1/q-1}\frac{\mathrm{e}^{-u}}{1+\mathrm{e}^{-u}}\,\mathrm{d}u. \tag{2.68}$$

For example, for $q = 1$ the integrals in (2.67) and (2.68) can be evaluated to yield $c_1 = \pi/\sqrt{12}$ and $C_1 = \big(\sqrt{12}\log 2\big)/\pi$ (cf. [26]). Thus, the restriction that we put on the growth of $\langle M\rangle$ in Assumption 2.1 means that the number of parts is asymptotically smaller than what is expected from typical partitions in $\check{\Lambda}^q$ of large expected weight $\langle N\rangle$.

Theorem 2.21. *Under Assumption 2.1, the roots z_1 and z_2 of the equations (2.65) are asymptotically given by*

$$z_1 = \exp\left(-\frac{\langle M\rangle}{q\,\langle N\rangle}\big(1+O\big(\kappa^{1/q}\big)\big)\right), \tag{2.69}$$

$$z_2 = \frac{\kappa^{1/q}}{q^{1/q}\,\Gamma(1+1/q)}\big(1+O\big(\kappa^{1/q}\big)\big). \tag{2.70}$$

Proof. Denote for short $\gamma := -\log z_1$. In view of Lemma 2.12 (see (2.45)), we have

$$\mathsf{E}_{\boldsymbol{z}}(M_\lambda) = \sum_{\ell\in\mathbb{N}^q}\mathsf{E}_{\boldsymbol{z}}(\nu_\ell) = \sum_{\ell\in\mathbb{N}^q}\frac{z_1^\ell z_2}{1+z_1^\ell z_2} = z_2\sum_{\ell\in\mathbb{N}^q} z_1^\ell - R_1(\boldsymbol{z}), \tag{2.71}$$

where

$$0 < R_1(\boldsymbol{z}) = \sum_{\ell\in\mathbb{N}^q}\frac{z_1^{2\ell}z_2^2}{1+z_1^\ell z_2} < z_2^2\sum_{\ell\in\mathbb{N}^q} z_1^{2\ell}. \tag{2.72}$$

Then Lemma 2.14 (with $s = 0$) applied to the sums on the right-hand side of (2.71) and (2.72) yields

$$\mathsf{E}_{\boldsymbol{z}}(M_\lambda) = \frac{z_2\,\Gamma(1/q)}{q\,\gamma^{1/q}}\,\bigl(1 + O\bigl(\gamma^{1/q}\bigr) + O(z_2)\bigr). \tag{2.73}$$

Similarly,

$$\mathsf{E}_{\boldsymbol{z}}(N_\lambda) = \sum_{\ell\in\mathbb{N}^q} \ell\,\mathsf{E}_{\boldsymbol{z}}(\nu_\ell) = \sum_{\ell\in\mathbb{N}^q} \frac{\ell\, z_1^\ell z_2}{1 + z_1^\ell z_2} = z_2 \sum_{\ell\in\mathbb{N}^q} \ell\, z_1^\ell - R_2(\boldsymbol{z}), \tag{2.74}$$

where

$$0 < R_2(\boldsymbol{z}) = \sum_{\ell\in\mathbb{N}^q} \frac{\ell\, z_1^{2\ell} z_2^2}{1 + z_1^\ell z_2} < z_2^2 \sum_{\ell\in\mathbb{N}^q} \ell\, z_1^{2\ell}. \tag{2.75}$$

Again applying Lemma 2.14 (now with $s = 1$), we get

$$\mathsf{E}_{\boldsymbol{z}}(N_\lambda) = \frac{z_2\,\Gamma(1 + 1/q)}{q\,\gamma^{1+1/q}}\,\bigl(1 + O\bigl(\gamma^{1/q}\bigr) + O(z_2)\bigr). \tag{2.76}$$

Returning to the calibrating conditions (2.65) and substituting the asymptotic expressions (2.73) and (2.76), we obtain the following system of asymptotic equations,

$$\begin{cases} \langle M\rangle = \dfrac{z_2\,\Gamma(1/q)}{q\,\gamma^{1/q}}\,\bigl(1 + O\bigl(\gamma^{1/q}\bigr) + O(z_2)\bigr), \\[2ex] \langle N\rangle = \dfrac{z_2\,\Gamma(1 + 1/q)}{q\,\gamma^{1+1/q}}\,\bigl(1 + O\bigl(\gamma^{1/q}\bigr) + O(z_2)\bigr). \end{cases} \tag{2.77}$$

Since $\langle M\rangle$ is bounded away from zero, the first of these equations implies that $\gamma^{1/q} = O(z_2)$, so that the error terms $O(\gamma^{1/q})$ in (2.77) are superfluous.

A further simple analysis of the system (2.77) shows that z_2 is of order of $\kappa^{1/q}$; specifically, using that $\Gamma(1 + 1/q) = (1/q)\,\Gamma(1/q)$, we find

$$\begin{aligned} \gamma &= \frac{\langle M\rangle}{q\,\langle N\rangle}\,\bigl(1 + O\bigl(\kappa^{1/q}\bigr)\bigr), \\ z_2 &= \frac{\langle M\rangle\,\gamma^{1/q}}{\Gamma(1 + 1/q)}\,\bigl(1 + O\bigl(\kappa^{1/q}\bigr)\bigr) = \frac{\kappa^{1/q}}{q^{1/q}\,\Gamma(1 + 1/q)}\,\bigl(1 + O\bigl(\kappa^{1/q}\bigr)\bigr), \end{aligned}$$

in line with formulas (2.69) and (2.70). □

Assumption 2.2. Throughout the rest of the chapter, we assume that the parameters z_1 and z_2 are chosen according to formulas (2.69) and (2.70), respectively. In particular, the Boltzmann measure $\mathsf{P}_{\boldsymbol{z}}$ becomes dependent on the hyperparameters $\langle N\rangle$ and $\langle M\rangle$, as well as the $\mathsf{P}_{\boldsymbol{z}}$-probabilities and the corresponding expected values.

For the sake of future reference and to fix the notation already used in the proof of Theorem 2.21, the asymptotic formula (2.69) can be written as

$$\gamma := -\log z_1 = \frac{\langle M\rangle}{q\,\langle N\rangle}\,\big(1+O\big(\kappa^{1/q}\big)\big). \tag{2.78}$$

It is also useful to record a simple consequence of the relations (2.69) and (2.70) (on account of the notation (2.66) and (2.78)),

$$\frac{z_2}{\gamma^{1/q}} = \frac{\langle M\rangle}{\Gamma(1+1/q)}\,\big(1+O\big(\kappa^{1/q}\big)\big). \tag{2.79}$$

Lemma 2.22. *Under Assumptions 2.1 and 2.2,*

$$\log F(\boldsymbol{z}) \sim \langle M\rangle\,. \tag{2.80}$$

Proof. Using formula (2.46) and applying Lemma 2.15 with $\gamma = -\log z_1$ and $\eta = z_2$, we have

$$\log F(\boldsymbol{z}) = \sum_{\ell\in\mathbb{N}^q} \log\big(1+z_1^{\ell}z_2\big) \sim \frac{z_2\,\Gamma(1+1/q)}{\gamma^{1/q}} \sim \langle M\rangle\,,$$

according to formula (2.79). □

Remark 2.23. The result (2.80) provides the asymptotics of the probability of the empty partition $\lambda_\varnothing$ (cf. Remark 2.2); indeed, by formula (2.8)

$$\mathsf{P}_{\boldsymbol{z}}(\lambda_\varnothing) = \frac{1}{F(\boldsymbol{z})} = \mathrm{e}^{-\langle M\rangle\,(1+o(1))}. \tag{2.81}$$

2.2.4. Asymptotics of the covariance matrix

Theorem 2.24. *Under Assumptions 2.1 and 2.2, we have*

$$\mathsf{Var}_{\boldsymbol{z}}(M_\lambda) \sim \langle M\rangle\,, \qquad \mathsf{Var}_{\boldsymbol{z}}(N_\lambda) \sim \frac{(q+1)\,\langle N\rangle^2}{\langle M\rangle}, \qquad \mathsf{Cov}_{\boldsymbol{z}}(M_\lambda, N_\lambda) \sim \langle N\rangle\,. \tag{2.82}$$

Proof. Using formulas (2.1), mutual independence of the multiplicities (ν_ℓ) and the Bernoulli marginals (2.45), we have

$$\mathsf{Var}_{\boldsymbol{z}}(M_\lambda) = \sum_{\ell\in\mathbb{N}^q} \mathsf{Var}_{\boldsymbol{z}}(\nu_\ell) = \sum_{\ell\in\mathbb{N}^q} \frac{z_1^{\ell}z_2}{(1+z_1^{\ell}z_2)^2} = z_2\sum_{\ell\in\mathbb{N}^q} z_1^{\ell} - R_3(\boldsymbol{z}), \tag{2.83}$$

where (cf. the proof of Theorem 2.21)

$$0 < R_3(\boldsymbol{z}) = \sum_{\ell\in\mathbb{N}^q} \frac{z_1^{2\ell} z_2^2 \left(2 + z_1^\ell z_2\right)}{(1 + z_1^\ell z_2)^2} < 2z_2^2 \sum_{\ell\in\mathbb{N}^q} z_1^{2\ell} + z_2^3 \sum_{\ell\in\mathbb{N}^q} z_1^{3\ell}. \tag{2.84}$$

By Lemma 2.14 we obtain, for any $r > 0$,

$$z_2 \sum_{\ell\in\mathbb{N}^q} z_1^{r\ell} \sim \frac{z_2 \Gamma(1/q)}{q\,(r\gamma)^{1/q}} \sim \frac{\langle M\rangle}{r^{1/q}}, \tag{2.85}$$

according to (2.79). Recalling that $z_2 = o(1)$ (see (2.70)), it follows from (2.84) and (2.85) that

$$R_3(\boldsymbol{z}) = O\left(z_2 \langle M\rangle\right) = o(\langle M\rangle). \tag{2.86}$$

Hence, returning to (2.83) and using (2.85), (2.86) and formulas (2.69) and (2.70), we get

$$\mathsf{Var}_{\boldsymbol{z}}(M_\lambda) \sim z_2 \sum_{\ell\in\mathbb{N}^q} z_1^\ell \sim \langle M\rangle\,, \tag{2.87}$$

in accord with the first formula in (2.82).

Similarly (omitting technical details), we obtain

$$\begin{aligned}\mathsf{Var}_{\boldsymbol{z}}(N_\lambda) = \sum_{\ell\in\mathbb{N}^q} \ell^2\, \mathsf{Var}_{\boldsymbol{z}}(\nu_\ell) &= \sum_{\ell\in\mathbb{N}^q} \frac{\ell^2 z_1^\ell z_2}{(1 + z_1^\ell z_2)^2} \\ &\sim z_2 \sum_{\ell\in\mathbb{N}^q} \ell^2 z_1^\ell \sim \frac{z_2\,\Gamma(2 + 1/q)}{q\,\gamma^{2+1/q}} \sim \frac{(q+1)\,\langle N\rangle^2}{\langle M\rangle},\end{aligned} \tag{2.88}$$

and

$$\begin{aligned}\mathsf{Cov}_{\boldsymbol{z}}(M_\lambda, N_\lambda) = \sum_{\ell\in\mathbb{N}^q} \ell\, \mathsf{Var}_{\boldsymbol{z}}(\nu_\ell) &= \sum_{\ell\in\mathbb{N}^q} \frac{\ell z_1^\ell z_2}{(1 + z_1^\ell z_2)^2} \\ &\sim z_2 \sum_{\ell\in\mathbb{N}^q} \ell z_1^\ell \sim \frac{z_2\,\Gamma(1 + 1/q)}{q\,\gamma^{1+1/q}} \sim \langle N\rangle\,,\end{aligned} \tag{2.89}$$

as claimed in (2.82). □

Corollary 2.24.1. *The correlation coefficient between M_λ and N_λ is asymptotically given by*

$$\varrho(M_\lambda, N_\lambda) \sim \frac{1}{\sqrt{q+1}}.$$

Remark 2.25. Corollary 2.24.1 shows that the dependence between M_λ and N_λ does not vanish, and also that the magnitude of this dependence is decreasing with the growth of the power index q.

2.3. Fixed expected length

2.3.1. Limit theorems for the partition length and weight

In what follows, we use the notation

$$G_\alpha(x) := \frac{1}{\Gamma(\alpha)} \int_0^x u^{\alpha-1} \mathrm{e}^{-u} \, \mathrm{d}u, \qquad x \geq 0, \tag{2.90}$$

for the distribution function of the gamma distribution $\mathrm{Gamma}(\alpha)$ with shape parameter $\alpha > 0$ (and unit scale parameter). We are now in a position to obtain our main result in this section.

Theorem 2.26. *Under Assumptions 2.1 and 2.2, consider the regime where $\mathsf{E}_{\boldsymbol{z}}(M_\lambda) = \langle M \rangle > 0$ is fixed, while $\mathsf{E}_{\boldsymbol{z}}(N_\lambda) = \langle N \rangle \to \infty$. Then the following distributional asymptotics hold under the Boltzmann distribution $\mathsf{P}_{\boldsymbol{z}}$ on the space $\check{\Lambda}^q$.*

(a) *The distribution of the length M_λ converges to a Poisson distribution with parameter $\langle M \rangle$,*

$$\mathsf{P}_{\boldsymbol{z}}(M_\lambda = m) \to \pi_m := \frac{\langle M \rangle^m \, \mathrm{e}^{-\langle M \rangle}}{m!}, \qquad m \in \mathbb{N}_0. \tag{2.91}$$

(b) *The conditional distribution of the weight N_λ given $M_\lambda = m \geq 1$ converges to the gamma distribution with shape parameter $\alpha_m = m/q$,*

$$\mathsf{P}_{\boldsymbol{z}}\big(\gamma N_\lambda \leq x \,\big|\, M_\lambda = m\big) \to G_{m/q}(x) = \frac{1}{\Gamma(m/q)} \int_0^x u^{m/q-1} \mathrm{e}^{-u} \, \mathrm{d}u, \qquad x \geq 0, \tag{2.92}$$

where γ is defined in (2.78), Moreover, convergence (2.92) is uniform in $x \geq 0$.

(c) *The marginal (unconditional) distribution function $G(x) = \lim_{\langle N \rangle \to \infty} \mathsf{P}_{\boldsymbol{z}}(\gamma N_\lambda \leq x)$, with atom $G(0) = \pi_0$ at zero, is determined by its Laplace transform*

$$\phi(s) = \exp\big\{ - \langle M \rangle \big(1 - (1+s)^{-1/q} \big) \big\}, \qquad s \geq 0. \tag{2.93}$$

Furthermore, conditioned on $M_\lambda > 0$, the Laplace transform becomes

$$\tilde{\phi}(s) = \frac{\mathrm{e}^{-\langle M \rangle}}{1 - \mathrm{e}^{-\langle M \rangle}} \left(\exp\left\{ \frac{\langle M \rangle}{(1+s)^{1/q}} \right\} - 1 \right), \qquad s \geq 0. \tag{2.94}$$

Remark 2.27. Part (a) is a particular case of a well-known Poisson approximation for the distribution of the total number of successes in a sequence of independent Bernoulli trials with success probabilities (p_i), which is valid as long as $\sum_i p_i \to \text{const} > 0$ and $\sum_i p_i^2 \to 0$ [8, 64]. Indeed, here we deal with the Bernoulli sequence (ν_ℓ), where $M_\lambda = \sum_\ell \nu_\ell$ and $p_\ell = \mathsf{E}_{\boldsymbol{z}}(\nu_\ell) = z_1^\ell z_2/(1+z_1^\ell z_2)$. According to (2.65), $\sum_\ell p_\ell = \langle M\rangle$. Furthermore, noting that (p_ℓ) is monotone decreasing, we obtain

$$\sum_{\ell\in\mathbb{N}^q} p_\ell^2 \le p_1 \sum_{\ell\in\mathbb{N}^q} p_\ell = \frac{z_1 z_2}{1+z_1 z_2}\,\langle M\rangle \le z_2\,\langle M\rangle = O\big(\langle N\rangle^{-1/q}\big) = o(1), \qquad (2.95)$$

on account of formula (2.70). Alternatively, the asymptotic estimate (2.95) follows with the help of formula (2.85) (with $r=2$).

Remark 2.28. The normalising constant γ in parts (b) and (c) can be replaced by its asymptotic equivalent $\gamma_0 = \langle M\rangle/(q\,\langle N\rangle)$ (see (2.78)).

Remark 2.29. The case $m=0$ excluded in Theorem 2.26(b) corresponds to the empty partition $\lambda_\varnothing$,

$$\mathsf{P}_{\boldsymbol{z}}\big(\gamma N_\lambda \le x \,\big|\, M_\lambda = 0\big) = \mathsf{P}_{\boldsymbol{z}}(N_\lambda = 0\,|\,M_\lambda = 0) = 1, \qquad x \ge 0.$$

This is consistent with the gamma distribution (2.92) weakly converging to 0 as the parameter $\alpha_m = m/q$ is formally sent to zero. Indeed, using the Laplace transform, for any $s>0$ we have

$$\frac{1}{\Gamma(\alpha)}\int_0^\infty x^{\alpha-1}\mathrm{e}^{-sx-x}\,\mathrm{d}x = \frac{1}{(s+1)^\alpha} \to 1 \qquad (\alpha\to 0+).$$

Remark 2.30. Noting that $\mathrm{Gamma}\,(m/q)$ is the convolution of m copies of $\mathrm{Gamma}\,(1/q)$, the result of Theorem 2.26(b) may be interpreted by saying that, on the scale $\gamma^{-1} \sim q\,\langle N\rangle/\langle M\rangle$ and conditional on $M_\lambda = m$, the partition parts $\{\lambda_1,\dots,\lambda_m\}$ (considered without ordering) behave asymptotically as m independent random variables with distribution $\mathrm{Gamma}\,(1/q)$ each.

Proof of Theorem 2.26. Consider the Laplace transform of the pair (N_λ, M_λ),

$$\phi_{\boldsymbol{z}}(\boldsymbol{s}) := \mathsf{E}_{\boldsymbol{z}}\big[\exp\left(-s_1 N_\lambda - s_2 M_\lambda\right)\big], \qquad s_1, s_2 \ge 0. \qquad (2.96)$$

Using formulas (2.1), mutual independence of the multiplicities (ν_ℓ) and the Bernoulli marginals (2.45), the definition (2.96) is rewritten as

$$\begin{aligned}\phi_{\boldsymbol{z}}(\boldsymbol{s}) &= \mathsf{E}_{\boldsymbol{z}}\left[\exp\left(-\sum_{\ell\in\mathbb{N}^q}(s_1\ell+s_2)\,\nu_\ell\right)\right]\\ &= \prod_{\ell\in\mathbb{N}^q}\mathsf{E}_{\boldsymbol{z}}\big[\mathrm{e}^{-(s_1\ell+s_2)\nu_\ell}\big] = \prod_{\ell\in\mathbb{N}^q}\frac{1+z_1^\ell z_2\,\mathrm{e}^{-(s_1\ell+s_2)}}{1+z_1^\ell z_2}.\end{aligned}$$

The normalisation γN_λ corresponds to replacing the argument s_1 in (2.96) by γs_1. Hence,

$$\begin{aligned}\log \phi_{\boldsymbol{z}}(\gamma s_1, s_2) &= \log \mathsf{E}_{\boldsymbol{z}}\left[\exp\left(-\gamma s_1 N_\lambda - s_2 M_\lambda\right)\right] \\ &= \sum_{\ell \in \mathbb{N}^q} \log \frac{1 + z_1^\ell z_2 \, \mathrm{e}^{-(\gamma s_1 \ell + s_2)}}{1 + z_1^\ell z_2} \\ &= \sum_{\ell \in \mathbb{N}^q} \log\bigl(1 + z_1^\ell z_2 \, \mathrm{e}^{-(\gamma s_1 \ell + s_2)}\bigr) - \sum_{\ell \in \mathbb{N}^q} \log\bigl(1 + z_1^\ell z_2\bigr). \end{aligned} \tag{2.97}$$

Starting with the last sum in (2.97), Lemma 2.22 immediately gives

$$\sum_{\ell \in \mathbb{N}^q} \log\bigl(1 + z_1^\ell z_2\bigr) = \log F(\boldsymbol{z}) \to \langle M \rangle \,. \tag{2.98}$$

Similarly, applying Lemma 2.15 we obtain

$$\sum_{\ell \in \mathbb{N}^q} \log\bigl(1 + z_1^\ell z_2 \, \mathrm{e}^{-(\gamma s_1 \ell + s_2)}\bigr) \sim \frac{z_2 \, \mathrm{e}^{-s_2} \, \Gamma(1/q)}{q \, \gamma^{1/q} (1 + s_1)^{1/q}} \sim \frac{\mathrm{e}^{-s_2} \, \langle M \rangle}{(1 + s_1)^{1/q}}, \tag{2.99}$$

according to the asymptotic relation (2.79).

As a result, combining (2.98) and (2.99) yields

$$\phi_{\boldsymbol{z}}(\gamma s_1, s_2) \to \exp\left\{ - \langle M \rangle \left(1 - \frac{\mathrm{e}^{-s_2}}{(1 + s_1)^{1/q}} \right) \right\}. \tag{2.100}$$

In particular, setting $s_1 = 0$ we get the limiting Laplace transform of M_λ,

$$\phi_{\boldsymbol{z}}(0, s_2) \to \exp\bigl(- \langle M \rangle \, (1 - \mathrm{e}^{-s_2}) \bigr) = \sum_{m=0}^{\infty} \pi_m \, \mathrm{e}^{-s_2 m},$$

which corresponds to the Poisson distribution (π_m) (see (2.91)), thus proving the claim of part (a).

Furthermore, by Taylor expanding the exponential in the formula (2.100), we obtain

$$\mathrm{e}^{-\langle M \rangle} \exp\left(\frac{\langle M \rangle \, \mathrm{e}^{-s_2}}{(1 + s_1)^{1/q}} \right) = \sum_{m=0}^{\infty} \frac{\pi_m \, \mathrm{e}^{-m s_2}}{(1 + s_1)^{m/q}}. \tag{2.101}$$

This can be interpreted as follows: by the total expectation formula, we have

$$\begin{aligned}\phi_{\boldsymbol{z}}(\gamma s_1, s_2) &= \mathsf{E}_{\boldsymbol{z}}\left[\mathsf{E}_{\boldsymbol{z}}\bigl(\mathrm{e}^{-\gamma s_1 N_\lambda - s_2 M_\lambda} \bigm| M_\lambda = m \bigr) \right] \\ &= \sum_{m=0}^{\infty} \mathsf{P}_{\boldsymbol{z}}(M_\lambda = m) \, \phi_{\boldsymbol{z}}(\gamma s_1 \,|\, m) \, \mathrm{e}^{-m s_2}, \end{aligned} \tag{2.102}$$

where $\phi_{\boldsymbol{z}}(s\,|\,m) := \mathsf{E}_{\boldsymbol{z}}\big(\mathrm{e}^{-sN_\lambda}\,|\,M_\lambda = m\big)$. Comparing (2.101) and (2.102), we conclude that

$$\phi_{\boldsymbol{z}}(\gamma s_1\,|\,m) \to \frac{1}{(1+s_1)^{m/q}}. \tag{2.103}$$

To be more precise, by the continuity theorem for Laplace transforms [30, Sec. XIII.1, Theorem 2, p. 431] applied to the measure with atoms $a_{\boldsymbol{z}}(m; s_1) := \mathsf{P}_{\boldsymbol{z}}(M_\lambda = m)\,\phi_{\boldsymbol{z}}(\gamma s_1\,|\,m)$ (with $s_1 \geq 0$ fixed), it follows from (2.101) and (2.102) that

$$a_{\boldsymbol{z}}(m; s_1) \to \frac{\pi_m}{(1+s_1)^{m/q}}, \qquad m \in \mathbb{N}_0.$$

But since the convergence (2.91) has already been established, this implies (2.103), and it remains to observe that the right-hand side is the Laplace transform of $\mathrm{Gamma}\,(m/q)$, as claimed in part (b). Finally, the uniform convergence in (2.92) readily follows by application of Lemma 2.18.

As for part (c), the first claim follows immediately by setting $s_2 = 0$ in the limit (2.100). The atom at zero is identified as $\lim_{s\to\infty} \phi(s) = \mathrm{e}^{-\langle M\rangle} = \pi_0$, and the conditional Laplace transform is expressed as $\tilde{\phi}(s) = (\phi(s) - \mathrm{e}^{-\langle M\rangle})/(1 - \mathrm{e}^{-\langle M\rangle})$. This completes the proof of Theorem 2.26. □

The limiting marginal distribution defined in (2.93) is a mixture of a discrete family of gamma distributions indexed by the shape parameter $\alpha_m = m/q$ ($m \in \mathbb{N}_0$), subject to a Poisson mixing distribution with parameter $\langle M\rangle$,

$$G(x) = \pi_0 + \sum_{m=1}^{\infty} \pi_m\, G_{m/q}(x), \qquad x \geq 0. \tag{2.104}$$

Formula (2.104) defines the compound Poisson-Gamma distribution of a random variable

$$Y = Z_1 + \cdots + Z_M, \tag{2.105}$$

where (Z_i) are independent random variables with gamma distribution $\mathrm{Gamma}\,(1/q)$ and M is an independent random variable with a Poisson distribution (π_m). In line with Remark 2.29, the case $m = 0$ is represented in (2.104) by a point mass $\pi_0 = \mathrm{e}^{-\langle M\rangle}$ at zero. The absolutely continuous part of this distribution has density

$$\begin{aligned} g(x) &= \sum_{m=1}^{\infty} \pi_m\, G'_{m/q}(x) = \sum_{m=1}^{\infty} \pi_m\, \frac{x^{m/q-1}\,\mathrm{e}^{-x}}{\Gamma(m/q)} \\ &= \frac{\mathrm{e}^{-\langle M\rangle - x}}{x}\, W_{1/q}\big(\langle M\rangle\, x^{1/q}\big), \end{aligned} \tag{2.106}$$

where $W_\varrho(x) = \sum_{m=1}^{\infty} \dfrac{x^m}{m!\,\Gamma(m\varrho)}$ is a special case of the *Wright function* [91]. Noting that Gamma(α) has mean α, the expected value of the distribution (2.104) is given by

$$\sum_{m=1}^{\infty} \pi_m \int_0^{\infty} x \,\mathrm{d}G_{m/q}(x) = \sum_{m=1}^{\infty} \pi_m \frac{m}{q} = \frac{\langle M \rangle}{q},$$

which is consistent with the calibration $\mathsf{E}_z(N_\lambda) = \langle N \rangle$ (see (2.65)) in view of the asymptotic formula $\gamma \sim \gamma_0 = \langle M \rangle / (q \langle N \rangle)$ (see (2.78)). Of course, the same result can be obtained by differentiating the Laplace transform (2.93) at $s = 0$.

The principal term in the asymptotics of the density $g(x)$ as $x \to +\infty$ can be recovered from the known asymptotic expansion of the Wright function [91, Theorem 2, p. 258], yielding

$$g(x) = \frac{\mathrm{e}^{-\langle M \rangle}}{2\pi\,(q+1)} \left(\frac{q}{x}\right)^{\frac{q+2}{2(q+1)}} \exp\left((q+1) \left(\frac{x}{q}\right)^{\frac{q}{q+1}} - x \right) \left(1 + O\big(x^{-\frac{q}{q+1}}\big)\right).$$

Turning to the behaviour of $g(x)$ near zero, from the expansion (2.106) it is clear that this is determined by the lowest-order terms with $m \le q$, that is,

$$g(x) = \sum_{m=1}^{q} \pi_m \frac{x^{m/q-1}}{\Gamma(m/q)} + O(x^{1/q}) \qquad (x \to 0+). \tag{2.107}$$

Observe that if $q > 1$ then the density of the absolutely continuous part of $G(x)$ has singularity at the origin, thus causing an "excess" of partitions with an anomalously small weight on the scale $\gamma^{-1} \sim \gamma_0^{-1} = q \,\langle N \rangle / \langle M \rangle$. On the other hand, the contribution of this singularity is exponentially vanishing as $\langle M \rangle \to \infty$. These effects will be verified empirically using the output of the Boltzmann sampler considered below in Section 3.1.3 (see Figure 3.1). The exact distribution (2.104) will also be contrasted there with a crude approximation via replacing the Poisson mixing parameter by its expected value $\langle M \rangle$, yielding the gamma distribution with shape parameter $\langle M \rangle / q$. Of course, such an approximation cannot capture the aforementioned singularity at zero, but it works reasonably well for larger values of $\langle M \rangle$, whereby singularity becomes immaterial.

For the benefit of the Boltzmann sampling considered below in Section 3, we conclude this section by stating a "truncated" version of Theorem 2.26 with a reduced source of parts. We write $G_\alpha(x \,|\, a) := G_\alpha(x)/G_\alpha(a)$ $(0 \le x \le a)$ for the distribution function of the Gamma(α)-distribution truncated by threshold $a > 0$. The symbol $\star$ stands for the convolution of probability distributions.

Theorem 2.31. *Under the hypotheses of Theorem 2.26, let $L \sim \theta \langle N \rangle$ with $\theta > 0$, and denote $a_\theta := \theta \langle M \rangle / q$. Then the following distributional asymptotics hold subject to the constraint $\lambda_{\max} \le L$.*

(a) *The conditional distribution of the length M_λ converges to a Poisson law,*

$$\mathsf{P}_{\boldsymbol{z}}(M_\lambda = m \,|\, \lambda_{\max} \le L) \to \pi_m^\theta := \frac{\mu_\theta^m \, \mathrm{e}^{-\mu_\theta}}{m!}, \qquad m \in \mathbb{N}_0, \tag{2.108}$$

with mean

$$\mu_\theta := \langle M \rangle \; G_{1/q}(a_\theta) = \frac{\langle M \rangle}{\Gamma(1/q)} \int_0^{a_\theta} u^{1/q-1} \, \mathrm{e}^{-u} \, \mathrm{d}u. \tag{2.109}$$

(b) *The conditional distribution of the weight N_λ given $M_\lambda = m \ge 1$ converges to the convolution of m copies of an a_θ-truncated gamma distribution with shape $1/q$,*

$$\mathsf{P}_{\boldsymbol{z}}(\gamma N_\lambda \le x \,\big|\, M_\lambda = m, \lambda_{\max} \le L) \to \big(\underbrace{G_{1/q}(\cdot \,|\, a_\theta) \star \cdots \star G_{1/q}(\cdot \,|\, a_\theta)}_{m}\big)(x), \tag{2.110}$$

for $0 < x \le m a_\theta$.

Like in (2.92), convergence (2.110) is uniform in $0 \le x \le m a_\theta$.

(c) *The marginal distribution function $G(x;\theta) := \lim_{\langle N \rangle \to \infty} \mathsf{P}_{\boldsymbol{z}}(\gamma N_\lambda \le x \,|\, \lambda_{\max} \le L)$, with atom $G(0;\theta) = \pi_0^\theta = \exp\big\{-\langle M \rangle \, G_{1/q}(a_\theta)\big\}$ at zero, is determined by its Laplace transform*

$$\phi(s;\theta) = \exp\left\{-\langle M \rangle \left(G_{1/q}(a_\theta) - \frac{G_{1/q}\big(a_\theta(1+s)\big)}{(1+s)^{1/q}} \right) \right\}, \quad s \ge 0. \tag{2.111}$$

Furthermore, conditioned on $M_\lambda > 0$, the Laplace transform becomes

$$\tilde{\phi}(s;\theta) = \frac{\mathrm{e}^{-\mu_\theta}}{1 - \mathrm{e}^{-\mu_\theta}} \left(\exp\left\{ \frac{\langle M \rangle \, G_{1/q}\big(a_\theta(1+s)\big)}{(1+s)^{1/q}} \right\} - 1 \right), \quad s \ge 0. \tag{2.112}$$

This theorem can be proved by adapting the proof of Theorem 2.26, whereby the (finite) sums of logarithmic expressions are analysed with the help of Lemma 2.17 in place of Lemma 2.15.

Remark 2.32. Comparing Theorems 2.26 and 2.31, a reduction of the Poisson parameter (mean) in part (a) from $\langle M \rangle$ to $\mu_\theta = \langle M \rangle \, G_{1/q}(a_\theta) < \langle M \rangle$ (see (2.109)), as well as the replacement of the gamma distribution $G_{1/q}(x)$ in part (b) with a truncated version $G_{1/q}(x \,|\, a_\theta)$ (see (2.110)) is clearly due to a reduced source of parts, $\ell \le L \sim \theta \, \langle N \rangle$.

Remark 2.33. As a sanity check of formula (2.111), the expected value of γN_λ conditional on $\lambda_{\max} \le L$ is asymptotically evaluated (using Lemma 2.16 and formula (2.79)) as

$$\mathsf{E}_{\boldsymbol{z}}(\gamma N_\lambda \,|\, \lambda_{\max} \le L) = \gamma \sum_{\ell \le L} \frac{\ell\, z_1^\ell z_2}{1 + z_1^\ell z_2} \sim \frac{\langle M \rangle}{\Gamma(1/q)} \int_0^{a_\theta} u^{1/q} \mathrm{e}^{-u}\, \mathrm{d}u. \tag{2.113}$$

On the other hand, by differentiating the Laplace transform (2.111) at $s = 0$ we obtain

$$\mathsf{E}_{\boldsymbol{z}}(\gamma N_\lambda \,|\, \lambda_{\max} \le L) \sim \langle M \rangle \left(\frac{1}{q}\, G_{1/q}(a_\theta) - \frac{a_\theta^{1/q} \mathrm{e}^{-a_\theta}}{\Gamma(1/q)} \right).$$

These two expressions are reconciled by integration of parts in (2.113) and in view of notation (2.90).

2.3.2. Cumulative cardinality of strict power partitions

For fixed $q, m \in \mathbb{N}$ and for any $x > 0$, consider a sub-level partition set

$$\check{\Lambda}^q_m(x) := \bigcup_{n \le x} \check{\Lambda}^q(n, m), \tag{2.114}$$

and denote its cardinality

$$L^q_m(x) := \#\check{\Lambda}^q_m(x) = \sum_{n \le x} \#\check{\Lambda}^q(n, m). \tag{2.115}$$

That is to say, $L^q_m(x)$ denotes the number of integral solutions to the inequality $j_1^q + \cdots + j_m^q \le x$ such that $j_1 > \cdots > j_m > 0$.

Theorem 2.34. *The following asymptotics hold as* $x \to \infty$,

$$L^q_m(x) \sim \frac{q \left(\Gamma(1 + 1/q)\right)^m x^{m/q}}{m!\, m\, \Gamma(m/q)}. \tag{2.116}$$

In particular, for $q = 1$ *and* $q = 2$

$$L_m(x) \sim \frac{x^m}{m!\, m!}, \qquad L^2_m(x) \sim \frac{\pi^{m/2} x^{m/2}}{2^{m-1} m!\, m\, \Gamma(m/2)}. \tag{2.117}$$

Proof. Without loss of generality, we may and will assume that x is an integer. Set the hyper-parameters in the Boltzmann distribution $\mathsf{P}_{\boldsymbol{z}}$ to be $\langle M \rangle = m$ and $\langle N \rangle = x$. By Corollary 2.8,

$$\#\check{\Lambda}^q(n, m) = \frac{F(\boldsymbol{z})\, \mathsf{P}_{\boldsymbol{z}}(M_\lambda = m)\, \mathsf{P}_{\boldsymbol{z}}(N_\lambda = n \,|\, M_\lambda = m)}{z_1^n z_2^m}. \tag{2.118}$$

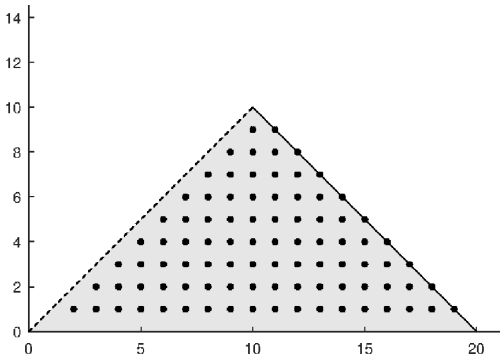

(a) Sub-level set $\check{\Lambda}_m^q(x)$ with $q = 1$, $m = 2$, $x = 20$.

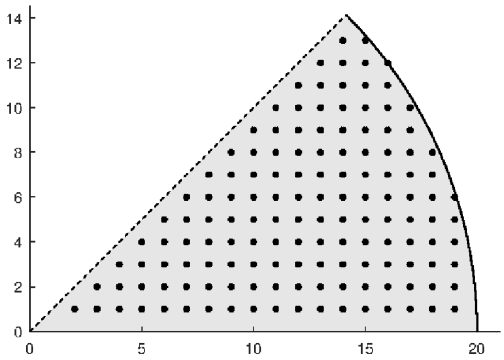

(b) Sub-level set $\check{\Lambda}_m^q(x)$ with $q = 2$, $m = 2$, $x = 400$.

Figure 2.2: Geometric illustration of the sub-level partition sets $\check{\Lambda}_m^q(x)$ (defined in (2.114)) with $m = 2$ and (a) $q = 1$ or (b) $q = 2$, represented as the sets of integer points $(j_1, j_2) \in \mathbb{Z}^2$ such that $0 < j_2 < j_1$ and $j_1 + j_2 \le x$ or $j_1^2 + j_2^2 \le x$, respectively. In line with Theorem 2.34, their cardinalities have the asymptotics $L_2(x) \sim \frac{1}{4}x^2$ and $L_2^2(x) \sim \frac{1}{8}\pi x$, corresponding to the area of the shaded domains.

Hence, according to (2.115),

$$L_m^q(x) = \frac{F(\boldsymbol{z})\,\mathsf{P}_{\boldsymbol{z}}(M_\lambda = m)}{z_2^m} \sum_{n \le x} \frac{\mathsf{P}_{\boldsymbol{z}}\left(N_\lambda = n \,|\, M_\lambda = m\right)}{z_1^n}. \tag{2.119}$$

First of all, by Lemma 2.22, Theorem 2.26(a) and formula (2.70), we get

$$\begin{aligned} \frac{F(\boldsymbol{z})\,\mathsf{P}_{\boldsymbol{z}}(M_\lambda = m)}{z_2^m} &\sim \mathrm{e}^m\, \frac{m^m\,\mathrm{e}^{-m}}{m!} \left(\frac{m^{1+1/q}}{q^{1/q}\,\Gamma(1+1/q)}\, x^{-1/q} \right)^{-m} \\ &= \frac{q^{m/q} \big(\Gamma(1+1/q)\big)^m\, x^{m/q}}{m!\, m^{m/q}}. \end{aligned} \tag{2.120}$$

To handle the sum in (2.119), define the cumulative probabilities

$$T_n := \mathsf{P}_{\boldsymbol{z}}(N_\lambda \le n \,|\, M_\lambda = m), \qquad T_0 := 0. \tag{2.121}$$

Then by Abel's summation-by-parts formula (see, e.g., [78, p. 390]) we can write

$$\begin{aligned} \sum_{n \le x} \frac{\mathsf{P}_{\boldsymbol{z}}\left(N_\lambda = n \,|\, M_\lambda = m\right)}{z_1^n} &= \sum_{n \le x} \big(T_n - T_{n-1}\big)\, \frac{1}{z_1^n} \\ &= \frac{T_x}{z_1^{x+1}} - \frac{T_0}{z_1} - \sum_{n \le x} T_n \left(\frac{1}{z_1^{n+1}} - \frac{1}{z_1^n} \right) \\ &= \frac{T_x}{z_1^{x-1}} - \frac{1 - z_1}{z_1} \sum_{n \le x} \frac{T_n}{z_1^n}. \end{aligned} \tag{2.122}$$

To shorten the notation, denote $\alpha := m/q$. By the asymptotic formula (2.69), we have $1 - z_1 \sim \alpha/x$; moreover, uniformly in $n \le x$

$$z_1^{-n} = \mathrm{e}^{\alpha n/x}\left(1 + O\big(x^{-1/q}\big)\right), \tag{2.123}$$

since $\kappa = m^{q+1}/x = O(x^{-1})$ (see (2.66)). Furthermore, using Theorem 2.26(b) and Remark 2.28 we get for the first term in (2.122),

$$\frac{T_x}{z_1^{x-1}} \to \mathrm{e}^{\alpha}\, G_\alpha(\alpha) = \frac{\mathrm{e}^{\alpha}}{\Gamma(\alpha)} \int_0^{\alpha} u^{\alpha-1}\, \mathrm{e}^{-u}\, \mathrm{d}u. \tag{2.124}$$

Generalising, observe that $T_n \approx G_\alpha(\alpha n/x)$ for $n \le x$. More precisely, taking advantage of the uniform convergence in (2.92), for any $\varepsilon > 0$ and all large enough $\langle N \rangle$ we have, uniformly in $n \le x$,

$$|T_n - G_\alpha(\alpha n/x)| < \varepsilon.$$

Hence, the total approximation error arising from the sum in (2.122) is estimated as follows,

$$\begin{aligned}(1 - z_1) \sum_{n \le x} \frac{|T_n - G_\alpha(\alpha n/x)|}{z_1^n} &\le \varepsilon\,(1 - z_1) \sum_{n=0}^{x} z_1^{-n} \\ &= \varepsilon\left(z_1^{-x} - z_1\right) = O(\varepsilon).\end{aligned} \tag{2.125}$$

Therefore, replacing T_n with $G_\alpha(\alpha n/x)$ in the sum (2.124) and also using (2.123), we obtain

$$\frac{1 - z_1}{z_1} \sum_{n \le x} z_1^{-n}\, G_\alpha(\alpha n/x) \sim \frac{\alpha}{x} \sum_{n=1}^{x} \mathrm{e}^{\alpha n/x}\, G_\alpha(\alpha n/x) \to \int_0^{\alpha} \mathrm{e}^{u}\, G_\alpha(u)\, \mathrm{d}u. \tag{2.126}$$

Furthermore, the integral in (2.126) is evaluated by integration by parts,

$$\int_0^{\alpha} G_\alpha(u)\, \mathrm{d}(\mathrm{e}^u) = \mathrm{e}^{\alpha} G_\alpha(\alpha) - \frac{1}{\Gamma(\alpha)} \int_0^{\alpha} u^{\alpha-1}\, \mathrm{d}u = \mathrm{e}^{\alpha}\, G_\alpha(\alpha) - \frac{\alpha^{\alpha-1}}{\Gamma(\alpha)}. \tag{2.127}$$

Thus, collecting (2.124), (2.125), (2.126) and (2.127), from (2.122) we obtain

$$\lim_{x \to \infty} \sum_{n \le x} \frac{\mathsf{P}_{\boldsymbol{z}}(N_\lambda = n \,|\, M_\lambda = m)}{z_1^n} = \frac{\alpha^{\alpha-1}}{\Gamma(\alpha)} + O(\varepsilon) \equiv \frac{\alpha^{\alpha-1}}{\Gamma(\alpha)}, \tag{2.128}$$

since $\varepsilon > 0$ is arbitrary.

Finally, returning to (2.119) and substituting the limits (2.120) and (2.128) (the latter with $\alpha = m/q$), we obtain the asymptotic formula (2.116). □

Continuing an illustration of Theorem 2.34 for $q = 1$ and $q = 2$ started in Figure 2.2 with $m = 2$, it is well known [26, Theorem 4.1, p. 341][1] (see also [2, Theorem 4.3, p. 56]) that, with $m \geq 2$ fixed (or even $m = o(n^{1/3})$),

$$\#\check{\Lambda}(n, m) \sim \frac{1}{m!}\binom{n-1}{m-1} \sim \frac{n^{m-1}}{m!\,(m-1)!} \qquad (n \to \infty). \tag{2.129}$$

This is consistent with our cumulative formula (2.117) for $q = 1$, noting that

$$\sum_{n \leq x} n^{m-1} \sim \frac{x^m}{m} \qquad (x \to \infty).$$

With regards to the case $q = 2$, it is interesting that in their famous paper of 1918 on an "exact" enumeration of plain integer partitions, Hardy and Ramanujan [41, Eq. (7.21), p. 110] stated without proof an asymptotic formula for the number of representations of a large $n \in \mathbb{N}$ as the sum of $m > 4$ squares,

$$\begin{aligned} r_m(n) &:= \#\{(j_1, \ldots, j_m) \in \mathbb{Z}^m \colon j_1^2 + \cdots + j_m^2 = n\} \\ &= \frac{C_m\, \pi^{m/2}\, n^{m/2-1}}{\Gamma(m/2)} + O(n^{m/4}), \end{aligned} \tag{2.130}$$

where the constant $C_m > 0$ is defined through a series $\sum_{k \geq 1} c_k\, k^{-m/2}$ with computable coefficients $c_k = O(k)$. Using a geometric embedding of such representations into the space $\mathbb{Z}^m$, it is easy to see that their enumeration is asymptotically reduced to strict partitions with m positive parts,

$$r_m(n) \sim 2^m m!\, \#\check{\Lambda}^2(n, m),$$

and in view of (2.130) it follows

$$\#\check{\Lambda}^2(n, m) \sim \frac{C_m\, \pi^{m/2}\, n^{m/2-1}}{2^m m!\, \Gamma(m/2)}. \tag{2.131}$$

By the order of growth, this formula matches our cumulative asymptotic result (2.117) (for $q = 2$), and moreover, the constant is explicitly recovered from this comparison, $C_m = 1$.

2.3.3. A joint limit theorem for the extreme parts (fixed expected length)

In this section, we address the limiting distribution of the largest and smallest parts of a random partition, $\lambda_{\max}$ and $\lambda_{\min}$. Recall the notation $\gamma = -\log z_1 \sim \gamma_0 = \langle M \rangle / (q \langle N \rangle)$ (see (2.78)).

[1] To be precise, Theorem 4.1 of [26] is stated for partitions with at most m parts, but due to Corollary 4.3 [26, p. 343] the same result also holds for partitions into exactly m distinct parts.

Theorem 2.35. *Assume that $\langle M\rangle > 0$ is fixed. Then $\lambda_{\max}$ and $\lambda_{\min}$ are asymptotically independent as $\langle N\rangle \to \infty$, with the marginal limiting laws given by (for any $x \geq 0$)*

$$\mathsf{P}_{\boldsymbol{z}}(\gamma\lambda_{\max} \leq x) \to G_{\max}(x) := \mathrm{e}^{-\langle M\rangle\left(1-G_{1/q}(x)\right)}, \tag{2.132}$$

$$\mathsf{P}_{\boldsymbol{z}}(\gamma\lambda_{\min} > x) \to G^{c}_{\min}(x) := \mathrm{e}^{-\langle M\rangle\, G_{1/q}(x)}. \tag{2.133}$$

Moreover, conditionally on non-empty partition,

$$\mathsf{P}_{\boldsymbol{z}}(\gamma\lambda_{\max} \leq x \,|\, \lambda_{\max} > 0) \to \widetilde{G}_{\max}(x) := \frac{G_{\max}(x) - \mathrm{e}^{-\langle M\rangle}}{1 - \mathrm{e}^{-\langle M\rangle}}, \tag{2.134}$$

$$\mathsf{P}_{\boldsymbol{z}}(\gamma\lambda_{\min} > x \,|\, \lambda_{\min} < \infty) \to \widetilde{G}^{c}_{\min}(x) := \frac{G^{c}_{\min}(x) - \mathrm{e}^{-\langle M\rangle}}{1 - \mathrm{e}^{-\langle M\rangle}}. \tag{2.135}$$

Remark 2.36. Clearly, the normalisation γ in Theorem 2.35 can be replaced by its asymptotic equivalent, $\gamma_0 = \langle M\rangle / (q\,\langle N\rangle)$ (see (2.78)).

Remark 2.37. Note that the distribution function $G_{\max}(x)$ has a jump at zero with mass $G_{\max}(0) = \mathrm{e}^{-\langle M\rangle}$. This is in line with our convention for $\lambda_{\max} = 0$, which corresponds to the empty partition $\lambda_{\varnothing}$ (cf. Remark 2.23 and formula (2.81)). On the other hand, $\widetilde{G}_{\max}(0) = 0$, and so the distribution function $\widetilde{G}_{\max}(x)$ is continuous at zero. Likewise, the tail distribution function $G^{c}_{\min}(x)$ is improper, with defect mass $G^{c}_{\min}(\infty) = \mathrm{e}^{-\langle M\rangle}$, which again matches our convention for $\lambda_{\min} = \infty$. But $\widetilde{G}^{c}_{\min}(\infty) = 0$, so $\widetilde{G}^{c}_{\min}(x)$ defines a proper distribution.

Proof of Theorem 2.35. For $x \geq 0$, set $\ell_*(x) := \min\{\ell \in \mathbb{N}^q \colon \ell > \gamma^{-1}x\}$, and note that $\gamma\ell_*(x) \to x$. By virtue of Lemma 2.12,

$$\begin{aligned}
\mathsf{P}_{\boldsymbol{z}}(\gamma\lambda_{\min} > x_1, \gamma\lambda_{\max} \leq x_2) &= \mathsf{P}_{\boldsymbol{z}}\big(\nu_\ell \equiv 0 \text{ for all } \ell < \ell_*(x_1) \text{ and } \ell \geq \ell_*(x_2)\big) \\
&= \prod_{\ell < \ell_*(x_1),\, \ell \geq \ell_*(x_2)} \frac{1}{1 + z_1^{\ell} z_2} \\
&= \exp\left\{ -\left(\sum_{\ell \in \mathbb{N}^q}^{\infty} - \sum_{\ell \geq \ell_*(x_1)}^{\infty} + \sum_{\ell \geq \ell_*(x_2)}^{\infty} \right) \log\big(1 + z_1^{\ell} z_2\big) \right\}.
\end{aligned} \tag{2.136}$$

Hence, applying Lemma 2.17 (with $\gamma = -\log z_1$ and $\eta = z_2$) and using the asymptotic relation (2.79), we get

$$\begin{aligned}
-\log \mathsf{P}_{\boldsymbol{z}}(\gamma\lambda_{\min} > x_1, \gamma\lambda_{\max} \leq x_2) &\sim \frac{z_2}{q\,\gamma^{1/q}} \left(\int_0^{\infty} - \int_{\gamma\ell_*(x_1)}^{\infty} + \int_{\gamma\ell_*(x_2)}^{\infty} \right) u^{1/q-1}\, \mathrm{e}^{-u}\, \mathrm{d}u \\
&\sim \frac{\langle M\rangle}{\Gamma(1/q)} \big(\Gamma(1/q) - \Gamma(1/q, x_1) + \Gamma(1/q, x_2) \big) \\
&= -\log G^{c}_{\min}(x_1) - \log G_{\max}(x_2),
\end{aligned}$$

which proves asymptotic independence and the marginal laws (2.132) and (2.133).

The conditional versions (2.134) and (2.135) easily follow using that $G_{\max}(0) = G^c_{\min}(\infty) = \mathrm{e}^{-\langle M\rangle}$ (see Remark 2.37),

$$\begin{aligned}\mathsf{P}_{\boldsymbol{z}}(\gamma\lambda_{\max} \le x \,|\, \lambda_{\max} > 0) &= \frac{\mathsf{P}_{\boldsymbol{z}}(\gamma\lambda_{\max} \le x) - \mathsf{P}_{\boldsymbol{z}}(\lambda_{\max} = 0)}{1 - \mathsf{P}_{\boldsymbol{z}}(\lambda_{\max} = 0)} \\ &\to \frac{G_{\max}(x) - \mathrm{e}^{-\langle M\rangle}}{1 - \mathrm{e}^{-\langle M\rangle}} = \widetilde{G}_{\max}(x),\end{aligned}$$

and similarly

$$\begin{aligned}\mathsf{P}_{\boldsymbol{z}}(\gamma\lambda_{\min} > x \,|\, \lambda_{\min} < \infty) &= \frac{\mathsf{P}_{\boldsymbol{z}}(\gamma\lambda_{\min} > x) - \mathsf{P}_{\boldsymbol{z}}(\lambda_{\min} = \infty)}{1 - \mathsf{P}_{\boldsymbol{z}}(\lambda_{\min} = \infty)} \\ &\to \frac{G^c_{\min}(x) - \mathrm{e}^{-\langle M\rangle}}{1 - \mathrm{e}^{-\langle M\rangle}} = \widetilde{G}^c_{\min}(x),\end{aligned}$$

as claimed. □

Remark 2.38. The result of Theorem 2.35 indicates that all parts (λ_i) of a $\mathsf{P}_{\boldsymbol{z}}$-typical partition $\lambda \in \breve{\Lambda}^q$ 'live" on the universal scale $A = \gamma^{-1} \sim q\,\langle N\rangle / \langle M\rangle$. Clearly, this is a manifestation of keeping the expected number of parts $\langle M\rangle$ fixed. The situation is different when the parameter $\langle M\rangle$ is allowed to grow with $\langle N\rangle$, as will be shown below in Theorem 2.48.

Remark 2.39. The interpretation of the limiting distribution of parts given in Remark 2.30 can be used for a heuristic derivation of Theorem 2.35. Indeed, using independence and the Gamma$(1/q)$-distribution of the independent limiting parts (Z_i) (see (2.105)), the distribution function of $Z_{\max} = \max\{Z_1, \dots, Z_M\}$ is given by

$$\begin{aligned}G_{\max}(x) &= \sum_{m=0}^{\infty} \pi_m \big(G_{1/q}(x)\big)^m = \exp\big\{-\langle M\rangle\,\big(1 - G_{1/q}(x)\big)\big\} \\ &= \exp\left\{-\frac{\langle M\rangle\,\Gamma(1/q, x)}{\Gamma(1/q)}\right\},\end{aligned}$$

which conforms with claim (2.132). Derivation of (2.133) is similar.

2.4. Slow growth of the expected length

Throughout this section, we impose the following condition on the growth of the hyper-parameters $\langle N\rangle$ and $\langle M\rangle$ (cf. Theorem 2.21).

Assumption 2.3. In addition to Assumption 2.1 stating that $\kappa = \langle M\rangle^{q+1} / \langle N\rangle \to 0$ as $\langle N\rangle \to \infty$, it is assumed that $\langle M\rangle \to \infty$.

Recall that the vector parameter $\boldsymbol{z} = (z_1, z_2)$ of the Boltzmann measure $\mathsf{P}_{\boldsymbol{z}}$ is calibrated according to Assumption 2.2. We use our standard notation $\gamma = -\log z_1 \sim \langle M\rangle / (q \langle N\rangle)$ (see (2.78)).

2.4.1. A joint limit theorem for the weight and length

Theorem 2.40. *Under Assumptions 2.2 and 2.3, define the normalised versions of N_λ and M_λ,*

$$N_\lambda^* := \frac{\sqrt{\langle M\rangle}}{\sqrt{q+1}} \left(\frac{N_\lambda - \langle N\rangle}{\langle N\rangle} \right), \qquad M_\lambda^* := \frac{M_\lambda - \langle M\rangle}{\sqrt{\langle M\rangle}}. \tag{2.137}$$

Then both N_λ^* and M_λ^* are asymptotically standard normal,

$$N_\lambda^* \xrightarrow{\mathrm{d}} \mathcal{N}(0,1), \qquad M_\lambda^* \xrightarrow{\mathrm{d}} \mathcal{N}(0,1).$$

Moreover, the joint limiting distribution of N_λ^* and M_λ^* is bivariate normal with zero mean and covariance matrix

$$\boldsymbol{K}_q = \begin{pmatrix} 1 & \dfrac{1}{\sqrt{q+1}} \\ \dfrac{1}{\sqrt{q+1}} & 1 \end{pmatrix}. \tag{2.138}$$

Proof. Consider the characteristic function of the pair $(N_\lambda^*, M_\lambda^*)$,

$$\varphi(t_1, t_2) := \mathsf{E}_{\boldsymbol{z}}\left[\exp\left(\mathrm{i} t_1 N_\lambda^* + \mathrm{i} t_2 M_\lambda^* \right) \right], \qquad t_1, t_2 \in \mathbb{R}. \tag{2.139}$$

Substituting (2.137), this is transformed as

$$\varphi(t_1, t_2) = \exp\left(-\mathrm{i}\tilde{t}_1 \langle N\rangle - \mathrm{i}\tilde{t}_2 \langle M\rangle \right) \mathsf{E}_{\boldsymbol{z}}\left[\exp\left(\mathrm{i}\tilde{t}_1 N_\lambda + \mathrm{i}\tilde{t}_2 M_\lambda \right) \right], \tag{2.140}$$

where

$$\tilde{t}_1 = \frac{t_1 \sqrt{\langle M\rangle}}{\sqrt{q+1}\, \langle N\rangle}, \qquad \tilde{t}_2 = \frac{t_2}{\sqrt{\langle M\rangle}}. \tag{2.141}$$

Furthermore, using formulas (2.1), mutual independence of the multiplicities (ν_ℓ) and the Bernoulli marginals (2.45), the expectation in (2.139) is rewritten as

$$\begin{aligned} \mathsf{E}_{\boldsymbol{z}}\left[\exp\left(\sum_{\ell \in \mathbb{N}^q} \mathrm{i} \left(\tilde{t}_1 \ell + \tilde{t}_2 \right) \nu_\ell \right) \right] &= \prod_{\ell \in \mathbb{N}^q} \mathsf{E}_{\boldsymbol{z}}\left[\mathrm{e}^{\mathrm{i}(\tilde{t}_1 \ell + \tilde{t}_2)\nu_\ell} \right] \\ &= \prod_{\ell \in \mathbb{N}^q} \frac{1 + z_1^\ell z_2\, \mathrm{e}^{\mathrm{i}(\tilde{t}_1 \ell + \tilde{t}_2)}}{1 + z_1^\ell z_2}. \end{aligned} \tag{2.142}$$

Choosing the principal branch of the logarithm function $\mathbb{C}\setminus\{0\}\ni\xi\mapsto\log\xi\in\mathbb{C}$ (i.e., such that $\log 1=0$), we can rewrite (2.140) and (2.142) as

$$\log\varphi(t_1,t_2)=-\mathrm{i}\tilde{t}_1\,\langle N\rangle-\mathrm{i}\tilde{t}_2\,\langle M\rangle+\sum_{\ell\in\mathbb{N}^q}\log\left(1+w_\ell\right),\tag{2.143}$$

where

$$w_\ell\equiv w_\ell(\tilde{t}_1,\tilde{t}_2):=\frac{z_1^\ell z_2}{1+z_1^\ell z_2}\left(\mathrm{e}^{\mathrm{i}(\tilde{t}_1\ell+\tilde{t}_2)}-1\right).\tag{2.144}$$

Remembering that $0<z_1<1$ and $z_2\to 0$ (see (2.69) and (2.70)), note that, uniformly for $\ell\in\mathbb{N}^q$,

$$|w_\ell|\le\frac{2z_1^\ell z_2}{1+z_1^\ell z_2}\le\frac{2z_2}{1+z_2}\le\frac{1}{2}=:R_0,$$

provided that $\kappa=\langle M\rangle^{q+1}/\langle N\rangle$ is small enough (cf. Assumption 2.3).

By Taylor's formula for complex-analytic functions (see, e.g., [89, Sec. 5.4, p. 93]) applied to the function $g(w)=\log(1+w)$ with $|w|\le R_0<1$, we have

$$g(w)=g(0)+g'(0)\,w+\frac{w^2}{2\pi\mathrm{i}}\oint_{\Gamma_R}\frac{g(\xi)}{\xi^2(\xi-w)}\,\mathrm{d}\xi,\tag{2.145}$$

where Γ_R is the circle of radius $R\in(R_0,1)$ about the origin, positively oriented (i.e., anti-clockwise). Noting that $|\xi-w|\ge R-R_0$ for all $\xi\in\Gamma_R$ and $|w|\le R_0$, the remainder term in (2.145) is bounded in modulus as follows,

$$\left|\frac{w^2}{2\pi\mathrm{i}}\oint_{\Gamma_R}\frac{g(\xi)}{\xi^2(\xi-w)}\,\mathrm{d}\xi\right|\le\frac{2\pi R}{2\pi}\left(\frac{|w|}{R}\right)^2\frac{C_R}{R-R_0}=\frac{|w|^2C_R}{R(R-R_0)},$$

where

$$C_R:=\max\bigl\{|g(\xi)|,\,\xi\in\Gamma_R\bigr\}<\infty.$$

Thus, the expansion (2.145) specialises to

$$\log(1+w)=w+O(|w|^2),\tag{2.146}$$

where the O-term is uniform in the disk $|w|\le R_0=\frac{1}{2}$.

We will also use Taylor's expansion for the complex exponent in (2.144) with a uniform bound on the error term for any $k\in\mathbb{N}$ and all $t\in\mathbb{R}$ (see, e.g., [30, Sec. XV.4, Lemma 1, p. 512]),

$$\left|\mathrm{e}^{\mathrm{i}t}-\sum_{j=0}^{k-1}\frac{(\mathrm{i}t)^j}{j!}\right|\le\frac{|t|^k}{k!}.\tag{2.147}$$

Now, combining the uniform expansions (2.146) and (2.147) (the latter with $k=2$ or $k=1$ as appropriate) and returning to (2.143), we obtain

$$\begin{aligned}\sum_{\ell\in\mathbb{N}^q}\log\left(1+w_\ell\right) &= \sum_{\ell\in\mathbb{N}^q}\frac{z_1^\ell z_2}{1+z_1^\ell z_2}\left(\mathrm{i}\left(\tilde{t}_1\ell+\tilde{t}_2\right)-\frac{1}{2}\left(\tilde{t}_1\ell+\tilde{t}_2\right)^2+O(1)\left(\tilde{t}_1\ell+\tilde{t}_2\right)^3\right)\\ &\quad+O(1)\sum_{\ell\in\mathbb{N}^q}\frac{z_1^{2\ell}z_2^2}{(1+z_1^\ell z_2)^2}\left(\tilde{t}_1\ell+\tilde{t}_2\right)^2\\ &=\mathrm{i}\tilde{t}_1\sum_{\ell\in\mathbb{N}^q}\frac{\ell z_1^\ell z_2}{1+z_1^\ell z_2}+\mathrm{i}\tilde{t}_2\sum_{\ell\in\mathbb{N}^q}\frac{z_1^\ell z_2}{1+z_1^\ell z_2}-\frac{1}{2}\sum_{\ell\in\mathbb{N}^q}\frac{z_1^\ell z_2}{1+z_1^\ell z_2}\left(\tilde{t}_1\ell+\tilde{t}_2\right)^2\\ &\quad+O(1)\sum_{\ell\in\mathbb{N}^q}z_1^\ell z_2\left(\tilde{t}_1\ell+\tilde{t}_2\right)^3+O(1)\sum_{\ell\in\mathbb{N}^q}z_1^{2\ell}z_2^2\left(\tilde{t}_1\ell+\tilde{t}_2\right)^2\\ &=:\mathrm{i}\tilde{t}_1\Sigma_1+\mathrm{i}\tilde{t}_2\Sigma_2-\tfrac{1}{2}\Sigma_3+O(1)\Sigma_4+O(1)\Sigma_5. \end{aligned}\tag{2.148}$$

According to the calibration equations (see (2.71) and (2.74)), the first two sums in (2.148) are known exactly,

$$\Sigma_1=\langle N\rangle\,,\qquad \Sigma_2=\langle M\rangle\,.\tag{2.149}$$

Next, the error sums Σ_4 and Σ_5 can be shown to asymptotically vanish. Indeed, using the elementary inequality $(a+b)^r\le 2^{r-1}\left(a^r+b^r\right)$ $(r\ge 1)$ and combining Lemma 2.14 with formulas (2.69), (2.70) and (2.79) gives upon simple calculations the estimate

$$\begin{aligned}0\le\Sigma_4&\le 4\tilde{t}_1^3\sum_{\ell\in\mathbb{N}^q}\ell^3 z_1^\ell z_2+4\tilde{t}_2^3\sum_{\ell\in\mathbb{N}^q}z_1^\ell z_2\\ &=\frac{O(1)\,\langle M\rangle^{3/2}\,z_2}{\langle N\rangle^3\,\gamma^{3+1/q}}+\frac{O(1)\,z_2}{\langle M\rangle^{3/2}\,\gamma^{1/q}}=\frac{O(1)}{\langle M\rangle^{1/2}}=o(1).\end{aligned}\tag{2.150}$$

Similarly,

$$\begin{aligned}0\le\Sigma_5&\le 2\tilde{t}_1^2\sum_{\ell\in\mathbb{N}^q}\ell^2 z_1^{2\ell}z_2^2+2\tilde{t}_2^2\sum_{\ell\in\mathbb{N}^q}z_1^{2\ell}z_2^2\\ &=\frac{O(1)\,\langle M\rangle\,z_2^2}{\langle N\rangle^2\,\gamma^{2+1/q}}+\frac{O(1)\,z_2^2}{\langle M\rangle\,\gamma^{1/q}}=O(\kappa^{1/q})=o(1).\end{aligned}\tag{2.151}$$

Finally, consider the sum Σ_3 in (2.148) which, as we will see, provides the main contribution to (2.143). To this end, observe (cf. (2.71)) that

$$\begin{aligned}0\le\sum_{\ell\in\mathbb{N}^q}z_1^\ell z_2\left(\tilde{t}_1\ell+\tilde{t}_2\right)^2-\Sigma_3&=\sum_{\ell\in\mathbb{N}^q}\frac{z_1^{2\ell}z_2^2}{1+z_1^\ell z_2}\left(\tilde{t}_1\ell+\tilde{t}_2\right)^2\\ &\le\sum_{\ell\in\mathbb{N}^q}z_1^{2\ell}z_2^2\left(\tilde{t}_1\ell+\tilde{t}_2\right)^2=\Sigma_5=o(1),\end{aligned}\tag{2.152}$$

as shown in (2.151). In turn, using the asymptotic results (2.87), (2.88) and (2.89), and recalling the rescaling expressions (2.141), we obtain the limit

$$\sum_{\ell\in\mathbb{N}^q} z_1^\ell z_2 \left(\tilde{t}_1\ell + \tilde{t}_2\right)^2 = \tilde{t}_1^2 \sum_{\ell\in\mathbb{N}^q} \ell^2 z_1^\ell z_2 + 2\tilde{t}_1\tilde{t}_2 \sum_{\ell\in\mathbb{N}^q} \ell z_1^\ell z_2 + \tilde{t}_2^2 \sum_{\ell\in\mathbb{N}^q} z_1^\ell z_2$$
$$\to t_1^2 + \frac{2t_1t_2}{\sqrt{q+1}} + t_2^2, \tag{2.153}$$

which is a quadratic form with matrix (2.138).

Thus, substituting the estimates (2.149), (2.150), (2.151), (2.152) and (2.153) into (2.148) and returning to (2.143), we obtain

$$\varphi(t_1,t_2) \to \exp\left\{-\frac{1}{2}\left(t_1^2 + \frac{2t_1t_2}{\sqrt{q+1}} + t_2^2\right)\right\},$$

and the proof of Theorem 2.40 is complete. □

Corollary 2.40.1. *Under the hypotheses of Theorem 2.40, the following laws of large numbers hold under the Boltzmann measure* $\mathsf{P}_{\boldsymbol{z}}$*,*

$$\frac{M_\lambda}{\langle M\rangle} \xrightarrow{\mathrm{p}} 1, \qquad \frac{N_\lambda}{\langle N\rangle} \xrightarrow{\mathrm{p}} 1. \tag{2.154}$$

Remark 2.41. As a curiosity, we observe that the limiting distribution in Theorem 2.26 formally conforms to Theorem 2.40 under the additional limit as $\langle M\rangle \to \infty$. Indeed, start with the intermediate limit (2.100) (with $\langle M\rangle$ fixed) and switch from Laplace transform to characteristic function by formally changing (s_1, s_2) $(s_i \geq 0)$ to $-\mathrm{i}(t_1, t_2)$ $(t_i \in \mathbb{R})$. Then, bearing in mind the normalisation (2.137), we obtain

$$-\langle M\rangle\left(1 - \mathrm{e}^{\mathrm{i}t_2/\sqrt{\langle M\rangle}}\left(1 - \frac{\mathrm{i}t_1 q}{\sqrt{\langle M\rangle}}\right)^{-1/q}\right) + \frac{\mathrm{i}t_1\sqrt{\langle M\rangle}}{\sqrt{q+1}} \to -\frac{1}{2}\left(t_1^2 + \frac{2t_1t_2}{\sqrt{q+1}} + t_2^2\right), \tag{2.155}$$

by Taylor expanding the left-hand side of (2.155) up to the second order in parameter $\langle M\rangle^{-1/2} = o(1)$.

2.4.2. Limit shape of Young diagrams

In this section we show that, under the slow growth condition on $\langle M\rangle$, properly scaled Young diagrams of random partitions $\lambda \in \check{\Lambda}^q$ have a limit shape given by the tail of the gamma integral,

$$\omega_q^*(x) := \frac{1}{\Gamma(1/q)}\int_x^\infty u^{1/q-1}\,\mathrm{e}^{-u}\,\mathrm{d}u = 1 - G_{1/q}(x), \qquad x \geq 0, \tag{2.156}$$

where $G_{1/q}(x)$ is the distribution function of Gamma$(1/q)$ (see (2.90)). In particular, for $q = 1$ the definition (2.156) is reduced to

$$\omega_1^*(x) = \mathrm{e}^{-x}, \qquad x \geq 0.$$

Specifically, set

$$A := q\,\langle N\rangle\,/\,\langle M\rangle\,, \qquad B = \langle M\rangle\,, \tag{2.157}$$

and consider a scaled Young diagram with upper boundary

$$\widetilde{Y}_\lambda(x) = B^{-1}\,Y_\lambda(Ax), \qquad x \geq 0, \tag{2.158}$$

where (see (2.2))

$$Y_\lambda(x) = \sum_{\ell \geq x} \nu_\ell, \qquad x \geq 0. \tag{2.159}$$

Remark 2.42. The area under the scaled Young diagram is given by

$$\int_0^\infty \widetilde{Y}_\lambda(x)\,\mathrm{d}x = B^{-1}\int_0^\infty Y_\lambda(Ax)\,\mathrm{d}x = \frac{\langle N\rangle}{AB} = \frac{1}{q}.$$

Naturally, this condition is preserved by the limit shape; indeed, integrating by parts we get

$$\int_0^\infty \omega_q^*(x)\,\mathrm{d}x = \frac{1}{\Gamma(1/q)}\int_0^\infty x^{1/q}\,\mathrm{e}^{-x}\,\mathrm{d}x = \frac{\Gamma(1+1/q)}{\Gamma(1/q)} = \frac{1}{q}.$$

First, we obtain the *expected limit shape* result.

Theorem 2.43. *Under Assumptions 2.2 and 2.3, uniformly in $x \geq 0$*

$$\mathsf{E}_{\boldsymbol{z}}\big(\widetilde{Y}_\lambda(x)\big) \to \omega_q^*(x), \tag{2.160}$$

where the limit shape $x \mapsto \omega_q^*(x)$ is defined in (2.156).

Proof. We first show that for each $x \geq 0$, the convergence (2.160) holds. By Lemma 2.12,

$$\mathsf{E}_{\boldsymbol{z}}\big(Y_\lambda(Ax)\big) = \sum_{\ell \geq Ax} \mathsf{E}_{\boldsymbol{z}}(\nu_\ell) = \sum_{\ell \geq Ax} \frac{z_1^\ell z_2}{1 + z_1^\ell z_2} = \sum_{\ell \geq Ax} z_1^\ell z_2 - \widetilde{R}_1(\boldsymbol{z}), \tag{2.161}$$

where (cf. (2.71) and (2.72))

$$0 \leq \widetilde{R}_1(\boldsymbol{z}) = \sum_{\ell \geq Ax} \frac{z_1^{2\ell} z_2^2}{1 + z_1^\ell z_2} \leq \sum_{\ell \in \mathbb{N}^q} z_1^{2\ell} z_2^2 = \langle M\rangle\, O(\kappa^{1/q}), \tag{2.162}$$

by virtue of (2.85) (with $r = 2$). Furthermore, applying Lemma 2.16 (with $\gamma = -\log z_1$ and $s = 0$) and noting that $\gamma A \to 1$, we obtain

$$\sum_{\ell \ge Ax} z_1^\ell z_2 \sim \frac{z_2}{q\,\gamma^{1/q}} \int_{\gamma Ax}^\infty u^{1/q-1}\,\mathrm{e}^{-u}\,\mathrm{d}u \sim \frac{\langle M\rangle}{\Gamma(1/q)} \int_x^\infty u^{1/q-1}\,\mathrm{e}^{-u}\,\mathrm{d}u, \tag{2.163}$$

using the asymptotic formula (2.79), Thus, substituting (2.162) and (2.163) into (2.161) gives

$$\mathsf{E}_{\boldsymbol{z}}\big(\widetilde{Y}_\lambda(x)\big) = \frac{1}{\langle M\rangle}\,\mathsf{E}_{\boldsymbol{z}}\big(Y_\lambda(Ax)\big) \sim \frac{1}{\Gamma(1/q)} \int_x^\infty u^{1/q-1}\,\mathrm{e}^{-u}\,\mathrm{d}u = \omega_q^*(x),$$

as claimed. Finally, the uniform convergence in formula (2.160) follows by Lemma 2.18, noting that the function $x \mapsto \omega_q^*(x)$ is continuous, bounded, and decreasing on $[0, \infty)$. □

Now, we are ready to state and prove the main result of this section.

Theorem 2.44. *Under Assumptions 2.2 and 2.3, the rescaled Young diagrams converge to the limit shape $y = \omega_q^*(x)$ in $\mathsf{P}_{\boldsymbol{z}}$-probability uniformly for $x \ge 0$, that is,*

$$\mathsf{P}_{\boldsymbol{z}}\left(\lambda \in \check{\Lambda}^q\colon \sup_{x\ge 0}\big|\widetilde{Y}_\lambda(x) - \omega_q^*(x)\big| > \varepsilon\right) \to 0.$$

Proof. By virtue of Theorem 2.43, letting $Y_\lambda^0(x) := Y_\lambda(x) - \mathsf{E}_{\boldsymbol{z}}\big(Y_\lambda(x)\big)$ it suffices to check that

$$\mathsf{P}_{\boldsymbol{z}}\left(\sup_{x\ge 0}\big|Y_\lambda^0(Ax)\big| > B\varepsilon\right) \to 0. \tag{2.164}$$

Put $Z_\lambda(x) := Y_\lambda(x^{-1})$ for $0 \le x \le \infty$; in particular, $Z_\lambda(0) = Y_\lambda(\infty) = 0$, $Z_\lambda(\infty) = Y_\lambda(0) = M_\lambda$. By the definition (2.2), for any $0 < s < t \le \infty$ we have

$$Z_\lambda(t) - Z_\lambda(s) = Y_\lambda(t^{-1}) - Y_\lambda(s^{-1}) = \sum_{t^{-1} \le \ell < s^{-1}} \nu_\ell\,,$$

which implies that the random process $Z_\lambda(x)$ $(x \ge 0)$ has independent increments. Hence, $Z_\lambda^0(x) := Z_\lambda(x) - \mathsf{E}_{\boldsymbol{z}}\big(Z_\lambda(x)\big)$ is a martingale with respect to the filtration $\mathcal{F}_x = \sigma\{\nu_\ell,\, \ell \ge x^{-1}\}$. From (2.2) it is also evident that $Z_\lambda^0(x)$ is *càdlàg* (i.e., its paths are everywhere right-continuous and have left limits, cf. Figure 2.3). Therefore, by the Doob–Kolmogorov submartingale inequality (see, e.g., [93, Theorem 6.16, p. 101]) we obtain

$$\begin{aligned}\mathsf{P}_{\boldsymbol{z}}\left(\sup_{x\ge 0}\big|Y_\lambda^0(Ax)\big| > B\varepsilon\right) &\equiv \mathsf{P}_{\boldsymbol{z}}\left(\sup_{y\le\infty}|Z_\lambda^0(yA^{-1})| > B\varepsilon\right)\\ &\le \frac{\mathsf{Var}_{\boldsymbol{z}}\big(Z_\lambda(\infty)\big)}{B^2\varepsilon^2} = \frac{\mathsf{Var}_{\boldsymbol{z}}\big(Y_\lambda(0)\big)}{B^2\varepsilon^2}.\end{aligned} \tag{2.165}$$

Recalling that $Y_\lambda(0) = M_\lambda$ and using Theorem 2.24, the right-hand side of (2.165) is estimated by $O(\langle M\rangle^{-1})$. Thus, the claim (2.164) follows and the proof of Theorem 2.44 is complete. □

Convergence of normalised Young diagrams to their limits shape is illustrated in Figure 2.3 for $q = 1$ and $q = 2$. Random partitions were simulated using a suitable Boltzmann sampler implemented as Algorithm 1 (see Section 3.1).

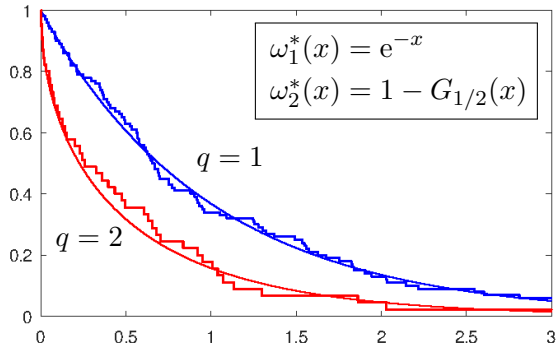

Figure 2.3: Illustration of convergence to the limit shape for $q = 1$ and $q = 2$ (in the online version shown in blue and red, respectively). The step plots depict the upper boundary of the scaled Young diagrams (see (2.158)), while the smooth lines represent the limit shape $\omega_q^*(x) = 1 - G_{1/q}(x)$ (see (2.156)). The corresponding partitions $\lambda \in \check{\Lambda}^q$ were sampled using Algorithm 1 with hyper-parameters $\langle M\rangle = 50$ and $\langle N\rangle = 2.5 \cdot 10^5$ ($q = 1$) or $\langle N\rangle = 1.25 \cdot 10^7$ ($q = 2$); in both cases, $\kappa = 0.01$ (cf. Assumption 2.2). The respective sample weight and length are $N_\lambda = 236{,}369$, $M_\lambda = 52$ ($q = 1$) and $N_\lambda = 12{,}733{,}323$, $M_\lambda = 45$ ($q = 2$).

Finally, we can analyse asymptotic fluctuations of scaled Young diagrams.

Theorem 2.45. *Under Assumptions 2.2 and 2.3, for any $x > 0$ the random value $\widetilde{Y}_\lambda(x)$ is asymptotically normal with variance $\omega_q^*(x)/\langle M\rangle$, that is,*

$$\widetilde{Y}_\lambda^*(x) := \frac{\sqrt{\langle M\rangle}\left(\widetilde{Y}_\lambda(x) - \mathsf{E}_{\boldsymbol{z}}\big(\widetilde{Y}_\lambda(x)\big)\right)}{\sqrt{\omega_q^*(x)}} \xrightarrow{\mathrm{d}} \mathcal{N}(0,1). \tag{2.166}$$

Proof. Consider the characteristic function of $\widetilde{Y}_\lambda^*(x)$,

$$\varphi_{\boldsymbol{z}}(t;x) := \mathsf{E}_{\boldsymbol{z}}\big[\exp\big(\mathrm{i}t\widetilde{Y}_\lambda^*(x)\big)\big] \qquad (t \in \mathbb{R}). \tag{2.167}$$

Substituting the definition (2.166) and using (2.157), (2.158) and (2.159), this is transformed as

$$\varphi_{\boldsymbol{z}}(t;x) = \exp\big\{-\mathrm{i}\tilde{t}\,\mathsf{E}_{\boldsymbol{z}}\big(Y_\lambda(Ax)\big)\big\}\,\mathsf{E}_{\boldsymbol{z}}\big[\exp\big(\mathrm{i}\tilde{t}\,Y_\lambda(Ax)\big)\big], \qquad \tilde{t} := \frac{t}{\sqrt{\langle M\rangle\,\omega_q^*(x)}}, \tag{2.168}$$

and furthermore (see (2.161))

$$\mathsf{E}_{\boldsymbol{z}}\big(Y_\lambda(Ax)\big) = \sum_{\ell\ge Ax} \frac{z_1^\ell z_2}{1+z_1^\ell z_2}. \tag{2.169}$$

Next, similarly to (2.142) and (2.143) the last expectation in (2.168) is expressed as

$$\mathsf{E}_{\boldsymbol{z}}\left[\exp\left(\mathrm{i}\tilde{t}\sum_{\ell\ge Ax}\nu_\ell\right)\right] = \prod_{\ell\ge Ax}\frac{1+z_1^\ell z_2\,\mathrm{e}^{\mathrm{i}\tilde{t}}}{1+z_1^\ell z_2} = \prod_{\ell\ge Ax}\big(1+w_\ell(\tilde{t})\big), \tag{2.170}$$

where

$$w_\ell(t) := \frac{z_1^\ell z_2}{1+z_1^\ell z_2}\,(\mathrm{e}^{\mathrm{i}t}-1). \tag{2.171}$$

Choosing the principal branch of the logarithm and using (2.169) and (2.170), from (2.168) we get

$$\log\varphi_{\boldsymbol{z}}(t;x) = -\mathrm{i}\tilde{t}\sum_{\ell\ge Ax}\frac{z_1^\ell z_2}{1+z_1^\ell z_2} + \sum_{\ell\ge Ax}\log\big(1+w_\ell(\tilde{t})\big). \tag{2.172}$$

In turn, similarly to (2.148) we obtain

$$\sum_{\ell\ge Ax}\log\big(1+w_\ell(\tilde{t})\big) = \Big(\mathrm{i}\tilde{t} - \tfrac{1}{2}\tilde{t}^2 + O(\tilde{t}^3)\Big)\sum_{\ell\ge Ax}\frac{z_1^\ell z_2}{1+z_1^\ell z_2} + O(\tilde{t}^2)\sum_{\ell\ge Ax}\frac{z_1^{2\ell} z_2^2}{(1+z_1^\ell z_2)^2}. \tag{2.173}$$

As was shown in the proof of Theorem 2.43 (see (2.161), (2.162)) and (2.163)),

$$\sum_{\ell\ge Ax}\frac{z_1^\ell z_2}{1+z_1^\ell z_2} \sim \langle M\rangle\,\omega_q^*(x), \qquad \sum_{\ell\ge Ax}\frac{z_1^{2\ell} z_2^2}{(1+z_1^\ell z_2)^2} = \langle M\rangle\,O(\kappa^{1/q}) = \langle M\rangle\,o(1). \tag{2.174}$$

Using (2.174) and recalling the notation of $\tilde{t}$ in (2.168), from (2.173) we get

$$\sum_{\ell\ge Ax}\log\big(1+w_\ell(\tilde{t})\big) = \mathrm{i}\tilde{t}\sum_{\ell\ge Ax}\frac{z_1^\ell z_2}{1+z_1^\ell z_2} - \tfrac{1}{2}t^2 + o(1).$$

Finally, returning to (2.172), we see that $\varphi_{\boldsymbol{z}}(t;x) \to -\frac{1}{2}t^2$, which proves the theorem. □

Remark 2.46. The reason for using in (2.166) the intrinsic centering $\mathsf{E}_{\boldsymbol{z}}\big(\widetilde{Y}_\lambda(x)\big)$ rather than the limit shape value $\omega_q^*(x)$ is that the error terms in the asymptotic estimates (2.174) are of order $\langle M\rangle\,\kappa^{1/q}$, where $\kappa = \langle M\rangle^{q+1}/\langle N\rangle = o(1)$ (see Assumption 2.3). Combined with the factor $\tilde{t} = O\big(\langle M\rangle^{-1/2}\big)$, this produces the error bound of order $\langle M\rangle^{1/2}\,\kappa^{1/q}$, which is not guaranteed to be small. Thus, a stronger assumption to this end is $\langle M\rangle^{1/2}\,\kappa^{1/q} = o(1)$, that is, $\langle M\rangle^{1+3q/2}/\langle N\rangle = o(1)$. On the other hand, lifting any control over the length may restore the limit-shape centering; for example, for $q = 1$ (ordinary strict partitions), a central theorem of that kind was proved in [33].

Remark 2.47. In [23], the authors have proven that Young diagrams confined to a rectangular box converge to the Ornstein–Uhlenbeck bridge. Extending our result in order to obtain to a similar functional theorem would be interesting. We observe that Theorem 2.45 could be expressed alternatively using a scaled variant of the martingale introduced in the proof of Theorem 2.44

$$\sqrt{\langle M\rangle}\,\Big(\widetilde{Y}_\lambda(x^{-1}) - \mathsf{E}_{\boldsymbol{z}}\big(\widetilde{Y}_\lambda(x^{-1})\big)\Big) \xrightarrow{\mathrm{d}} \mathcal{N}(0, \omega_q^*(x^{-1})),$$

which has independent increments. This suggests that further research might yield a theorem of convergence to a time-changed Brownian motion.

2.4.3. A joint limit theorem for the extreme parts (growing expected length)

We use the notation $\lambda_{\min}$ and $\lambda_{\max}$ (cf. Section 2.3.3).

Theorem 2.48. *Under Assumptions 2.2 and 2.3, set*

$$b_q := \left(\frac{q\,\langle M\rangle}{\Gamma(1/q)}\right)^q, \qquad B_q := \log\langle M\rangle - \big(1-\tfrac{1}{q}\big)\log\log\langle M\rangle - \log\Gamma(1/q), \tag{2.175}$$

and consider the normalised versions of $\lambda_{\min}$ and $\lambda_{\max}$ defined as follows,

$$\lambda^*_{\min} := \gamma\, b_q\, \lambda_{\min}, \qquad \lambda^*_{\max} := \gamma\,\lambda_{\max} - B_q\,. \tag{2.176}$$

Then $\lambda^*_{\min}$ and $\lambda^*_{\max}$ are asymptotically independent under the measure $\mathsf{P}_{\boldsymbol{z}}$ as $\langle N\rangle \to \infty$ and their marginal limiting laws are given, respectively, by a Weibull distribution with shape parameter $1/q$ and the standard double-exponential (Gumbel) distribution,

$$\mathsf{P}_{\boldsymbol{z}}(\lambda^*_{\min} > x_1) \to \exp\big(-x_1^{1/q}\big), \qquad x_1 \geq 0, \tag{2.177}$$

$$\mathsf{P}_{\boldsymbol{z}}(\lambda^*_{\max} \leq x_2) \to \exp\big(-\mathrm{e}^{-x_2}\big), \qquad x_2 \in \mathbb{R}. \tag{2.178}$$

Proof. For $x_1 \geq 0$ and $x_2 \in \mathbb{R}$, set

$$\ell_1^*(x_1) := \min\{\ell \in \mathbb{N}^q \colon \ell > x_1/(\gamma\, b_q)\}, \qquad \ell_2^*(x_2) := \min\{\ell \in \mathbb{N}^q \colon \ell > (B_q + x_2)\,\gamma^{-1}\}.$$

Recalling the asymptotic relations (2.69) and (2.66), observe that

$$\gamma\,\ell_1^*(x_1) = \frac{x_1}{b_q} + O(\gamma) \sim x_1 \left(\frac{\Gamma(1/q)}{q\,\langle M\rangle}\right)^q, \tag{2.179}$$

$$\gamma\,\ell_2^*(x_2) = B_q + x_2 + O(\gamma) \sim \log\langle M\rangle. \tag{2.180}$$

Like in the proof of Theorem 2.35, we have

$$\mathsf{P}_{\boldsymbol{z}}(\lambda_{\min}^* > x_1,\, \lambda_{\max}^* \leq x_2) = \exp\left\{-\left(\sum_{\ell\in\mathbb{N}^q} - \sum_{\ell\geq\ell_1^*(x_1)} + \sum_{\ell\geq\ell_2^*(x_2)}\right) \log\bigl(1 + z_1^\ell z_2\bigr)\right\}.$$

Applying Lemmas 2.15 and 2.17 (with $\gamma = -\log z_1$ and $\eta = z_2$) and using the asymptotic relation (2.79), we obtain

$$-\log \mathsf{P}_{\boldsymbol{z}}(\lambda_{\min}^* > x_1,\, \lambda_{\max}^* \leq x_2) \sim \frac{\langle M\rangle}{\Gamma(1/q)} \left(\int_0^{\gamma\ell_1^*(x_1)} + \int_{\gamma\ell_2^*(x_2)}^\infty\right) u^{1/q-1}\,\mathrm{e}^{-u}\,\mathrm{d}u. \tag{2.181}$$

Integrating by parts and using the asymptotic relation (2.179), we obtain

$$\int_0^{\gamma\ell_1^*(x_1)} u^{1/q-1}\,\mathrm{e}^{-u}\,\mathrm{d}u = q\int_0^{\gamma\ell_1^*(x_1)} \mathrm{e}^{-u}\,\mathrm{d}(u^{1/q}) \sim q\,\bigl(\gamma\,\ell_1^*(x_1)\bigr)^{1/q} \sim \frac{\Gamma(1/q)\,x_1^{1/q}}{\langle M\rangle}. \tag{2.182}$$

Next, using (2.180) we get

$$\begin{aligned}\int_{\gamma\ell_2^*(x_2)}^\infty u^{1/q-1}\,\mathrm{e}^{u}\,\mathrm{d}u &\sim \bigl(\gamma\,\ell_2^*(x_2)\bigr)^{1/q-1}\,\mathrm{e}^{-\gamma\ell_2^*(x_2)} \\ &\sim B_q^{1/q-1}\,\mathrm{e}^{-(B_q+x_2)} \sim \frac{\Gamma(1/q)\,\mathrm{e}^{-x_2}}{\langle M\rangle}.\end{aligned} \tag{2.183}$$

Hence, substituting (2.182) and (2.183) into (2.181) yields

$$-\log \mathsf{P}_{\boldsymbol{z}}(\lambda_{\min}^* > x_1,\, \lambda_{\max}^* \leq x_2) \sim x_1^{1/q} + \mathrm{e}^{-x_2},$$

which completes the proof of the theorem. □

Remark 2.49. The necessary use of the intrinsic calibration parameter $\gamma = -\log z_1$ in Theorem 2.48 may be a little disappointing. This can be easily improved under a slightly stronger condition on slow growth of $\langle M\rangle$ than in Assumption 2.3; namely, $\kappa^{1/q}\log\langle M\rangle = o(1)$, that is, $\langle M\rangle^{q+1}\,(\log\langle M\rangle)^q/\langle N\rangle = o(1)$. In this case, the normalisation (2.176) can be written more explicitly by replacing γ with $\gamma_0 = \langle M\rangle/(q\,\langle N\rangle)$ (see (2.78)).

Corollary 2.49.1. *Under the hypotheses of Theorem 2.48, the following law of large numbers holds,*

$$\frac{\langle M\rangle\,\lambda_{\max}}{q\,\langle N\rangle\log\langle M\rangle}\xrightarrow{\mathrm{p}}1, \tag{2.184}$$

where the symbol $\xrightarrow{\mathrm{p}}$ *indicates convergence in* $\mathsf{P}_{\boldsymbol{z}}$*-probability.*

Proof. Theorem 2.48 implies that $\gamma\lambda_{\max}/B_q \xrightarrow{\mathrm{p}} 1$, and the claim (2.184) follows by noting that $\gamma\sim\gamma_0=\langle M\rangle/(q\,\langle N\rangle)$ and $B_q\sim\log\langle M\rangle$. □

Remark 2.50. Theorem 2.48 indicates that, under the condition of slow growth of $\langle M\rangle$, the smallest part $\lambda_{\min}$ of a $\mathsf{P}_{\boldsymbol{z}}$-typical partition $\lambda\in\check{\Lambda}^q$ "lives" on the scale $A_*=(\gamma\,b_q)^{-1}\propto\langle N\rangle/\langle M\rangle^{q+1}=\kappa^{-1}$. On the other hand, Corollary 2.49.1 shows that the scale of variation of the largest part $\lambda_{\max}$ is given by $A^*=B_q\,\gamma^{-1}\propto\langle N\rangle\log\langle M\rangle/\langle M\rangle$. This is to be compared with the typical behaviour in the bulk of the partition "spectrum", where the scale of variation is given by $A\sim\gamma^{-1}\propto\langle N\rangle/\langle M\rangle$.

Remark 2.51. Continuing an asymptotic linkage between the cases of fixed or slowly growing parameter $\langle M\rangle$, observed above in Remark 2.41, the limiting distributions of Theorem 2.35 formally conform to Theorem 2.48 in the limit as $\langle M\rangle\to\infty$. Indeed, using (2.132) we have

$$\begin{aligned}-\log G_{\max}(x+B_q)&=\frac{\langle M\rangle\,\Gamma(1/q,x+B_q)}{\Gamma(1/q)}\\&\sim\frac{\langle M\rangle}{\Gamma(1/q)}\,(x+B_q)^{1/q-1}\,\mathrm{e}^{-x-B_q}\\&\sim\frac{\langle M\rangle}{\Gamma(1/q)}\,(\log\langle M\rangle)^{1-1/q}\,\mathrm{e}^{-x}\cdot\mathrm{e}^{-B_q}=\mathrm{e}^{-x},\end{aligned}$$

according to the definition of B_q in (2.175). Similarly, using (2.133) and (2.182) we have

$$\begin{aligned}-\log G^c_{\min}(x/b_q)&=\langle M\rangle\left(1-\frac{\Gamma(1/q,x/b_q)}{\Gamma(1/q)}\right)\\&\sim\frac{\langle M\rangle\,q}{\Gamma(1/q)}\left(\frac{x}{b_q}\right)^{1/q}=x^{1/q},\end{aligned}$$

by the definition of b_q in (2.175).

Chapter 3

"Short" integer partitions with power parts: Random sampling and applications

Boltzmann sampling is a powerful technique conceptualised, streamlined and popularised by Duchon et al. [24] in the context of single-parameter combinatorial structures (for multi-parametric extensions, see Bendkowski et al. [10] and the references therein). Random integer partitions with controlled expected weight and length provide an "exactly soluble" instance of a two-parametric combinatorial structure, where the issues of Boltzmann sampling implementation and efficiency can be analysed in some depth.

Specifically, in this chapter we discuss sampling from the Boltzmann distribution on partition spaces $\check{\Lambda}^q$ (i.e., into distinct q-power parts), calibrated under the predefined hyper-parameters $\langle N \rangle$ and $\langle M \rangle$, which have the meaning of the expected weight and length, respectively. The two controlling parameters in question are z_1 and z_2, which are amenable to asymptotic analysis as was shown in Section 2.2.3. Once these parameters are fixed, due to the mutual independence of the multiplicities (ν_ℓ) (see Proposition 2.3 and Lemma 2.12), the Boltzmann sampling is essentially reduced to an iterated independent testing of potential parts $\ell = j^q$ via dichotomous (Bernoulli) random trials with success probabilities $\mathsf{P}_{\boldsymbol{z}}(\nu_\ell = 1) = z_1^\ell z_2 (1 + z_1^\ell z_2)^{-1}$. The practical implementation of such sampling algorithms thus relies on a random number generator $\texttt{Ber}(p)$, in each call producing an independent pseudo-random value 1 or 0 with probabilities p and $1 - p$, respectively.

It is convenient to distinguish between the *free samplers* and the *rejection samplers*, with the former just producing independent random realisations of partitions under the said Boltzmann distribution, and the latter comprising one or more rejection loops that iterate a free Boltzmann sampler until the desired

targets are met. We discuss these two versions in Sections 3.1 and 3.2, respectively.

The pseudo-codes in Section 3.1 and 3.2 were implemented using the programming language C and Intel® `oneAPI DPC++` compiler, and run on a desktop CPU Intel® Core™ i5-10600 (processor base frequency 3.30 GHz, turbo boost frequency 4.80 GHz). Numerical calculations were carried out using Maple® (Release 2022.1, licensed to the University of Leeds).

3.1. Free sampler

In this subsection, we delineate a free Boltzmann sampler (see Algorithm 1 below) under the calibration through the hyper-parameters $\langle N \rangle$ and $\langle M \rangle$. It should be noted that, despite an intuitive appeal of iterated Bernoulli-type tests, there are some implementation concern that have to be addressed. We discuss them below before presenting the algorithm.

3.1.1. Correcting the bias

The first issue to consider is that of choosing the control parameters z_1 and z_2 to ensure that the sampler is unbiased, that is, $\mathsf{E}_{\boldsymbol{z}}(N_\lambda) = \langle N \rangle$ and $\mathsf{E}_{\boldsymbol{z}}(M_\lambda) = \langle M \rangle$. Unfortunately, we can solve this set of equations only asymptotically (see Lemma 2.12). In a "crude" version of Algorithm 1, we use the leading terms in the asymptotics by setting (cf. (2.69) and (2.70))

$$z_1 = \mathrm{e}^{-\gamma_0}, \qquad z_2 = \frac{\langle M \rangle \, \gamma_0^{1/q}}{\Gamma(1 + 1/q)}, \tag{3.1}$$

where $\gamma_0 = \langle M \rangle / (q \, \langle N \rangle)$. Inevitably, this causes a bias in the resulting expectations. More precisely, the first source of this bias clearly comes from dropping the (positive) remainder terms $R_1(\boldsymbol{z})$ and $R_2(\boldsymbol{z})$ in the approximate series representations of the aforementioned expected values (see equations (2.71) and (2.74)). A further error occurs when replacing the resulting series with the corresponding integrals, using Lemma 2.14. In fact, one can show that the overall bias due to (3.1) is always negative. Indeed, recalling that $\Delta_0(\gamma) < 0$ (see (2.55)[1]), we have

$$\begin{aligned} \mathsf{E}_{\boldsymbol{z}}(M_\lambda) = \sum_{\ell \in \mathbb{N}^q} \frac{z_1^\ell z_2}{1 + z_1^\ell z_2} < z_2 \sum_{\ell \in \mathbb{N}^q} z_1^\ell = z_2 \sum_{j=1}^{\infty} \mathrm{e}^{-\gamma_0 j^q} \\ < z_2 \int_0^\infty \mathrm{e}^{-\gamma_0 x^q} \mathrm{d}x = \frac{z_2 \, \Gamma(1/q)}{q \, \gamma_0^{1/q}} = \langle M \rangle , \end{aligned}$$

[1] The inequality $\Delta_0(\gamma) < 0$ can also be seen directly by monotonicity of the function $x \mapsto \mathrm{e}^{-\gamma x^q}$.

according to the parameter choice (3.1). Turning to $\mathsf{E}_{\boldsymbol{z}}(N_\lambda)$, recall from (2.75) that the error term $-R_2(\boldsymbol{z})$ is negative, and furthermore,

$$R_2(\boldsymbol{z}) \sim z_2^2 \sum_{\ell \in \mathbb{N}^q} \ell\, z_1^{2\ell} \sim \frac{z_2\, q\, \langle M \rangle\, \gamma_0^{1/q}}{\Gamma(1/q)} \cdot \frac{\Gamma(1+1/q)}{q\, \gamma_0^{1+1/q}} = \frac{z_2\, \langle M \rangle}{q\, \gamma_0}. \tag{3.2}$$

On the other hand, the error due to replacing the sum $\sum_\ell \ell z_1^\ell$ in (2.74) by the corresponding integral is bounded, according to (2.60), by $z_2\, O\big(\gamma_0^{-1+1/q}\big)$. Since $\langle M \rangle$ is bounded away from zero, it follows that the R_2-term (3.2) is dominant and, therefore, the overall bias in targeting $\langle N \rangle$ is negative.

A practical recipe towards correcting the bias may be to move the error terms $R_1(\boldsymbol{z})$ and $R_2(\boldsymbol{z})$ to the left-hand side of equations in (2.71) and (2.74), for simplicity using their integral approximations. Effectively, this amounts to redefining the hyper-parameters,

$$\langle \tilde{N} \rangle := \langle N \rangle + z_2^2 \sum_{\ell \in \mathbb{N}^q} \ell\, z_1^{2\ell} \approx \langle N \rangle + z_2^2 \int_0^\infty x^q\, \mathrm{e}^{-2\gamma_0 x^q}\, \mathrm{d}x = \langle N \rangle + \frac{\langle M \rangle^2\, \gamma_0^{1/q}}{2^{1/q}\, \Gamma(1/q)},$$

$$\langle \tilde{M} \rangle := \langle M \rangle + z_2^2 \sum_{\ell \in \mathbb{N}^q} z_1^{2\ell} \approx \langle M \rangle + z_2^2 \int_0^\infty \mathrm{e}^{-2\gamma_0 x^q}\, \mathrm{d}x = \langle N \rangle + \frac{q\, \langle M \rangle^2\, \gamma_0^{1/q}}{2^{1/q}\, \Gamma(1/q)}.$$

Accordingly, we redefine $\tilde{\gamma}_0 = \langle \tilde{M} \rangle / (q\, \langle \tilde{N} \rangle)$ and (cf. (3.1))

$$\tilde{z}_1 = \mathrm{e}^{-\tilde{\gamma}_0}, \qquad \tilde{z}_2 = \frac{q\, \langle \tilde{M} \rangle\, \tilde{\gamma}_0^{1/q}}{\Gamma(1/q)}. \tag{3.3}$$

A numerical illustration of the proposed modification is presented in Table 3.1, showing a significant reduction of bias. The expected values were computed from the exact series expansions (2.71) and (2.74) using Maple.

If the remaining (small) bias is still an issue, a further recalibration can be carried out by a suitable refinement of the solution $\boldsymbol{z} = (z_1, z_2)$ to the equations (2.71) and (2.74), for instance, by using a two-dimensional Newton–Raphson method. For a general approach to the multidimensional tuning of parameters based on convex optimisation, see Bendkowski et al. [10].

Table 3.1: Expected values of N_λ and M_λ for $q = 1$ and $q = 2$ under two choices of the calibrating parameters: using the leading asymptotic terms (3.1) and after a heuristic correction (3.3).

$q = 1$	
$\langle N \rangle = 10^6$	$\langle \tilde{N} \rangle \doteq 1{,}002{,}499.50$
$\langle M \rangle = 100$	$\langle \tilde{M} \rangle \doteq 100.4999$
$z_1 \doteq 0.9999000$	$\tilde{z}_1 = 0.9998998$
$z_2 \doteq 0.010000$	$\tilde{z}_2 \doteq 0.0100750$
$\mathsf{E}_{\boldsymbol{z}}(N_\lambda) \doteq 997{,}510.70$	$\mathsf{E}_{\tilde{z}}(N_\lambda) \doteq 999{,}985.73$
$\mathsf{E}_{\boldsymbol{z}}(M_\lambda) \doteq 99.498326$	$\mathsf{E}_{\tilde{z}}(M_\lambda) \doteq 99.992019$

$q = 2$	
$\langle N \rangle = 10^7$	$\langle \tilde{N} \rangle \doteq 10{,}315{,}391.57$
$\langle M \rangle = 50$	$\langle \tilde{M} \rangle \doteq 53.1539$
$z_1 \doteq 0.9999975$	$\tilde{z}_1 \doteq 0.9999974$
$z_2 \doteq 0.0892062$	$\tilde{z}_2 \doteq 0.0962720$
$\mathsf{E}_{\boldsymbol{z}}(N_\lambda) \doteq 9{,}699{,}070.63$	$\mathsf{E}_{\tilde{z}}(N_\lambda) \doteq 9{,}981{,}802.71$
$\mathsf{E}_{\boldsymbol{z}}(M_\lambda) \doteq 47.018388$	$\mathsf{E}_{\tilde{z}}(M_\lambda) \doteq 49.754495$

3.1.2. Truncation of the parts pipeline

We deal with a finitary computation, so should rule out the risk of indefinite processing. That is to say, the algorithm must have a well-defined stopping rule that would guarantee a finite-time termination. In a free sampler, the sequence of productive outcomes in successive Bernoulli trials (i.e., with sample multiplicities $\nu_\ell = 1$ corresponding to non-zero parts) is $\mathsf{P}_{\boldsymbol{z}}$-a.s. finite (see Lemma 2.5). More precisely, the last successful trial selects the largest part $\lambda_{\max}$, after which the testing settles down to pure idling. The $\mathsf{P}_{\boldsymbol{z}}$-distribution of $\lambda_{\max}$ is given by (cf. Sections 2.3.3 and 2.4.3)

$$\begin{aligned} \mathsf{P}_{\boldsymbol{z}}(\lambda_{\max} \le L) &= \mathsf{P}_{\boldsymbol{z}}(\nu_\ell \equiv 0 \text{ for all } \ell > L) \\ &= \prod_{\ell > L} \frac{1}{1 + z_1^\ell z_2} = \frac{1}{F(\boldsymbol{z})} \prod_{\ell \le L} (1 + z_1^\ell z_2), \end{aligned} \tag{3.4}$$

where $F(\boldsymbol{z}) = \prod_{\ell \in \mathbb{N}^q} (1 + z_1^\ell z_2)$ is the generating function of the partition space $\check{\Lambda}^p$ (see (2.46)). It is also easy to see that conditioning on $\lambda_{\max} = j_0^q$ does not change the distribution of the preceding multiplicities $\{\nu_{j^q}, 1 \le j \le j_0 - 1\}$, that is, they remain mutually independent and with Bernoulli distributions (2.45). Thus, if the numerical value of $F(\boldsymbol{z})$ can be calculated in advance, which is a common

convention in computing known as an *oracle* (see, e.g., [24, 31, 10]), then we can sample the random value $\lambda_{\max}$ using formula (3.4) and then sample independently the preceding candidate parts via the respective Bernoulli trials. Unfortunately, this approach embeds a computational error through the numerical calculation of $F(\boldsymbol{z})$, so it is not quite "exact"; besides, convergence of the infinite product may not be fast, given that the parameter z_1 is close to 1 (see (2.69)). Specifically, using Lemma 2.17 one can check that the truncation error arising from a partial product up to ℓ_* is of order $\langle M\rangle\,(\gamma\ell_*)^{1/q-1}\mathrm{e}^{-\gamma\ell_*}$, which dictates that ℓ_* be chosen much bigger than $\gamma^{-1} \sim q\,\langle N\rangle\,/\,\langle M\rangle$.

An alternative idea is to truncate the pipeline of potential parts $\ell \in \mathbb{N}^q$ subject to testing at an appropriate threshold L (see Section 2.1.5), so that the Bernoulli testing only runs over $\ell \le L$. A simple pragmatic solution is to choose the threshold L so that the probability of exceeding it in an indefinite free sampler is small enough, that is,

$$\mathsf{P}_{\boldsymbol{z}}(\lambda_{\max} > L) \le \delta, \tag{3.5}$$

where the confidence tolerance $\delta > 0$ can be chosen in advance to be as small as desired. Then the corresponding threshold $L = L(\delta)$ can be determined from a suitable limit theorem for the largest part, namely, Theorem 2.35 if $\langle M\rangle > 0$ is fixed, or Theorem 2.48 for slow growth of $\langle M\rangle$. In the former case, threshold L is determined by the asymptotic equation (see (2.132))

$$\Gamma(1/q, \gamma_0 L) = \frac{\Gamma(1/q)}{\langle M\rangle} \cdot \log\frac{1}{1-\delta}, \tag{3.6}$$

where, as before, $\gamma_0 = \langle M\rangle/(q\,\langle N\rangle)$. In the latter case, we obtain from (2.178)

$$L = \frac{1}{\gamma_0}\left(B_q - \log\log\frac{1}{1-\delta}\right), \tag{3.7}$$

where (see (2.175))

$$B_q = \log\langle M\rangle - \left(1 - \tfrac{1}{q}\right)\log\log\langle M\rangle - \log\Gamma(1/q).$$

Note that for $q = 1$ the bounds (3.6) and (3.7) coincide, reducing to

$$L = \frac{1}{\gamma_0}\left(\log\langle M\rangle - \log\log\frac{1}{1-\delta}\right). \tag{3.8}$$

An illustration of evaluation of the threshold L is presented in Table 3.2 for $q = 1$ and $q = 2$. The equation (3.6) was solved numerically using Maple. One can observe from the table that while the value $\delta = 10^{-k}$ $(k = 1, 2, \dots)$ is decreasing geometrically, the growth of threshold L is only about linear. Intuitively, this is

explained by the fact that the confidence probability $1-\delta$ enters expressions (3.6) and (3.7) under the logarithm, that is, as $\log(1-\delta)$. More precisely, it readily follows from (3.7) that

$$L - \frac{B_q}{\gamma_0} \sim \frac{1}{\gamma_0} \log \frac{1}{\delta} \qquad (\delta \to 0+).$$

Likewise, equation (3.6) asymptotically solves to yield

$$L - \frac{\log \langle M \rangle}{\gamma_0 \, \Gamma(1/q)} \sim \frac{1}{\gamma_0} \log \frac{1}{\delta} \qquad (\delta \to 0+).$$

Table 3.2: Threshold L for the largest part $\lambda_{\max}$ with confidence probability $1-\delta$, calculated from expressions (3.8) ($q = 1$) and (3.6) or (3.7) ($q = 2$) and rounded down to the nearest q-th power.

$q = 1$, $\langle N \rangle = 10^6$, $\langle M \rangle = 100$		$q = 2$, $\langle N \rangle = 10^7$, $\langle M \rangle = 50$		
δ	L (3.8)	δ	L (3.6)	L (3.7)
0.1	68,555	0.1	$1{,}890{,}625 = 1375^2$	$1{,}962{,}801 = 1401^2$
0.01	92,053	0.01	$2{,}762{,}244 = 1662^2$	$2{,}900{,}209 = 1703^2$
0.001	115,124	0.001	$3{,}636{,}649 = 1907^2$	$3{,}825{,}936 = 1956^2$
0.0001	138,154	0.0001	$4{,}515{,}625 = 2125^2$	$4{,}743{,}684 = 2178^2$

According to Lemma 2.7 (with $\tilde{\Lambda}^\dagger = \check{\Lambda}_L$), the output of a truncated sampling algorithm follows the Boltzmann distribution with a smaller source set $\mathbb{A}_L = \{\ell \in \mathbb{N}^q \colon \ell \le L\}$, which nonetheless approximates well the target Boltzmann distribution $\mathsf{P}_{\boldsymbol{z}}$ (see Lemma 2.9). One should be wary though that truncation contributes to the negative bias (see (2.33) and (2.34)), which may require a refined calibration through the parameters z_1 and z_2.

Note that the confidence guarantee $1-\delta$ as discussed above is valid only in the case of a single output instance. If the purpose of the free algorithm is to produce an independent sample of, say, k random Boltzmann partitions, then the overall confidence probability is approximately given by $(1-\delta)^k$, which may be exponentially small if k is large while δ stays fixed. A simple upper bound for the error probability is based on the Bernoulli inequality, yielding $1-(1-\delta)^k \le k\delta$. This motivates the well-known Bonferroni correction, which amounts to choosing the individual error probability $\delta_0 = \delta/k$ in order to ensure the overall error probability not exceeding δ. As an example, if $k = 1000$ and we would like to guarantee the overall error probability bound $\delta = 0.1$, then the individual error probability should be taken as $\delta_0 = 0.0001$. The approximation is quite accurate

here, as the exact solution is $\delta_0 \doteq 0.000105355$. Clearly, switching from δ to δ_0 leads to a higher threshold L. For instance, Table 3.2 shows that in the case $q = 1$ the suitable threshold L needs to double. In general, the increase of L due to multiple errors is not really dramatic because of the logarithmic dependence on δ mentioned above.

Another unwelcome outcome of the Bernoulli testing is that it may not return any parts at all, which has a positive $\mathsf{P}_{\boldsymbol{z}}$-probability even in the infinite sequence of tests (see Remark 2.23). This is not critical, as the sampling cycle can be repeated if necessary. However, it may be wasteful and can be easily rectified by adopting a similar approach based on confidence. Specifically, one can set a lower cutoff L_0 such that the run of the sampler is terminated, and the cycle is repeated, if the Bernoulli tests fail to select at least one (non-zero) part $\ell \le L_0$. To this end, we choose L_0 in such a way that $\mathsf{P}_{\boldsymbol{z}}(\lambda_{\min} > L_0) \le \delta$, where $\delta > 0$ is small enough (cf. (3.5)). Again referring to the limit theorems regarding the smallest part, we obtain from Theorem 2.35 (cf. (3.6))

$$\Gamma(1/q) - \Gamma(1/q, \gamma_0 L_0) = \frac{\Gamma(1/q)}{\langle M \rangle} \log \frac{1}{\delta}, \tag{3.9}$$

and from Theorem 2.48 (cf. (3.7))

$$L_0 = \frac{1}{\gamma_0} \left(\frac{\Gamma(1/q)}{q \langle M \rangle} \log \frac{1}{\delta} \right)^q. \tag{3.10}$$

A numerical illustration of the confident lower threshold L_0 is presented in Table 3.3 for $q = 1$ and $q = 2$. The equation (3.9) was solved numerically using Maple. The match between the results produced via equations (3.9) and (3.10) is quite close, especially for $q = 2$. One should also observe a significant difference between the thresholds L_0 and L, which underpins a considerable computational saving due to the lower cutoff, activated whenever the sampler fails to produce at least one positive part up to L_0.

Table 3.3: Asymptotic threshold L_0 for the smallest part $\lambda_{\min}$ with confidence probability $1 - \delta$, calculated from expressions (3.9) or (3.10), and rounded down to the nearest q-th power.

$q = 1$, $\langle N \rangle = 10^6$, $\langle M \rangle = 100$			$q = 2$, $\langle N \rangle = 10^7$, $\langle M \rangle = 50$		
δ	L_0 (3.9)	L_0 (3.10)	δ	L_0 (3.9)	L_0 (3.10)
0.1	232	230	0.1	$625 = 25^2$	$625 = 25^2$
0.01	471	460	0.01	$2{,}601 = 51^2$	$2{,}601 = 51^2$
0.001	715	690	0.001	$5{,}929 = 77^2$	$5{,}929 = 77^2$
0.0001	966	921	0.0001	$10{,}816 = 104^2$	$10{,}609 = 103^2$

Finally, if both cutoffs L and L_0 are exercised as described above then, due to the asymptotic independence of $\lambda_{\max}$ and $\lambda_{\min}$, the overall confidence probability is (asymptotically) given by $(1-\delta)^2 = 1 - 2\delta + \delta^2$, hence the resulting error probability is bounded by 2δ.

3.1.3. Free sampling algorithm

A free Boltzmann sampler is presented below in pseudocode as Algorithm 1. For simplicity, the algorithm incorporates only the upper threshold L selected in advance for a given confidence probability $1-\delta$. As discussed in Section 3.1.2, this is essential to ensure termination of the code, but for the sake of optimisation a lower cutoff L_0 can also be included without difficulty. As explained above, the confidence probability should be chosen carefully to match a possibly multiple output.

Algorithm 1: `FreeSampler`$(q, \langle N\rangle, \langle M\rangle, L)$

Input: integer q, real $\langle N\rangle, \langle M\rangle, L$
Output: partition $\lambda \in \check{\Lambda}^q_L$, weight N_λ, length M_λ

integer array $\lambda_{[\,]}$;
real z_1, z_2, γ_0, q;
$\gamma_0 \leftarrow \langle M\rangle/(q\langle N\rangle)$;
$z_1 \leftarrow \mathrm{e}^{-\gamma_0}$, $z_2 \leftarrow q\langle M\rangle \gamma_0^{1/q}/\Gamma(1/q)$;
integer j^*, j, N, M;
$j^* \leftarrow \lfloor L^{1/q} \rfloor$;
$N \leftarrow 0$, $M \leftarrow 0$;
for j *from* j^* *to* 1 *by* -1 **do**
  $p \leftarrow z_1^{j^q} z_2 (1 + z_1^{j^q} z_2)^{-1}$;
  if $\mathtt{Ber}(p) = 1$ **then**
    $N \leftarrow N + j^q$;
    $M \leftarrow M + 1$;
    $\lambda_M \leftarrow j^q$;
  end
end
$N_\lambda \leftarrow N$, $M_\lambda \leftarrow M$;
return $(\lambda, N_\lambda, M_\lambda)$

The code structure is fairly straightforward and consists in a single cycle of sequential Bernoulli tests over potential parts $\ell \in \mathbb{N}^q$. It is convenient to do this via downward scoping in view of our convention to enumerate the partition parts in decreasing order. Because the resulting length of the output partition $\lambda = (\lambda_i)$

is unknown in advance, the space for the corresponding integer array is defined in the code as $\lambda_{[\,]}$, that is, through a dynamically allocated memory. Finally, the calibration parameters z_1 and z_2 are specified using the leading-term formulas (3.1); if desired, these can be replaced by the bias-correcting values (3.3) or by any other, more refined choices.

By design, the output of Algorithm 1 is a random partition $\lambda \in \check{\Lambda}^q_L = \check{\Lambda}^q \cap \{(\lambda_i)\colon \lambda_{\max} \leq L\}$. It has a Boltzmann distribution on the space $\check{\Lambda}^q_L$, with expected values of weight N_λ and length M_λ close to the predefined hyper-parameters $\langle N\rangle$ and $\langle M\rangle$, respectively. As discussed in Section 2.1.5, this distribution approximates (in total variation) the Boltzmann distribution on the infinite partition space $\check{\Lambda}^q$, which may suffice for the sampling purposes at hand.

3.1.4. Validation

The output performance of the code in Algorithm 1 was visually monitored via the marginal histograms for the sample weight N_λ and length M_λ (Figure 3.1), as well as by the bivariate histograms and frequency level plots of the sample pairs (N_λ, M_λ) (Figure 3.2). The numerical illustration was carried out in the case of square parts, $q = 2$ (selected for computational convenience in order to reduce the completion time), and in two different regimes with regard to the hyper-parameter $\langle M\rangle$, that is, "fixed" and "slow growth", illustrated by $\langle M\rangle = 5$ ($\langle N\rangle = 12{,}500$) and $\langle M\rangle = 50$ ($\langle N\rangle = 10^7$), yielding for the parameter $\kappa = \langle M\rangle^3 / \langle N\rangle$ values $\kappa = 0.01$ and $\kappa = 0.0125$, respectively (cf. Assumption 2.3). The algorithm was run at a very low confidence tolerance (error probability) $\delta = 10^{-8}$ and with the corresponding truncation value L calculated using formulas (3.6) or (3.7) according to the regime at hand, yielding $L = 299^2 = 89{,}401$ and $L = 2{,}903^2 = 8{,}427{,}409$, respectively (cf. Table 3.2).

The empirical results (with 10^5 output partitions in both cases) were compared with the theoretical predictions from Theorems 2.26 and 2.40. The marginal histogram plots for N_λ and M_λ shown in Figure 3.1 depict bell-shaped unimodal empirical distributions with the sample modes noticeably shifted to the left of the calibration hyper-parameters $\langle N\rangle$ and $\langle M\rangle$, respectively. The discrepancy between the modes and the means is observed especially well in the weight plots (the more so for smaller $\langle M\rangle$), which is essentially due to the fact that the underlying gamma and Poisson distributions are right-skewed; for example, the mode of $\mathrm{Gamma}(\alpha)$ is given by $\max\{\alpha - 1, 0\}$ whereas the mean is α. Another (minor) reason for a negative bias is due to a certain miscalibration, as was pointed out in Section 3.1.1. In line with theoretical predictions, this mismatch is vanishing with the growth of the hyper-parameters $\langle N\rangle$ and $\langle M\rangle$, together with the improving accuracy of the normal approximations, both for N_λ and M_λ.

It is also interesting to note that the mean-gamma approximation $\mathrm{Gamma}(\langle M\rangle)$

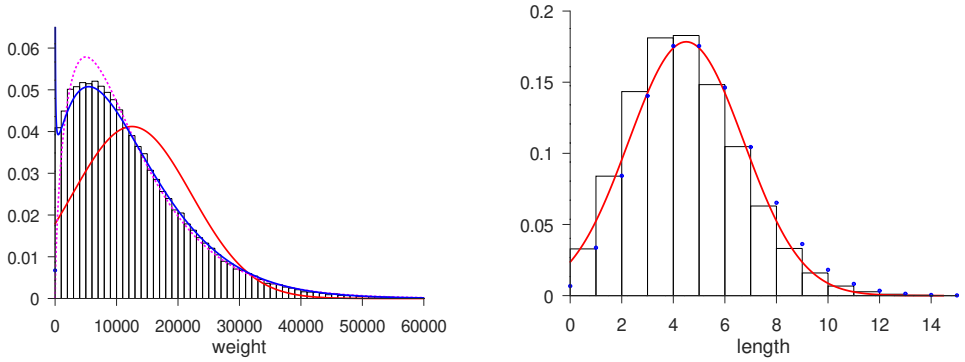

(a) $\langle M\rangle = 5$, $\langle N\rangle = 12{,}500$ ($\kappa = 0.01$). A dot at the origin on the left panel shows a discrete atom $\pi_0 = \mathrm{e}^{-\langle M\rangle} \doteq 0.00674$ (see (2.104)).

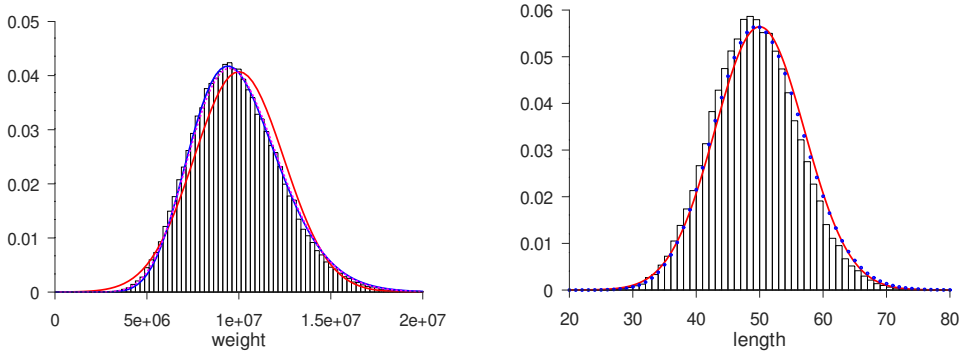

(b) $\langle M\rangle = 50$, $\langle N\rangle = 10^7$ ($\kappa = 0.0125$). The atom $\pi_0 = \mathrm{e}^{-\langle M\rangle} \doteq 2 \cdot 10^{-22}$ is too small to be visible.

Figure 3.1: Marginal histograms for the weight N_λ (left) and length M_λ (right) for random samples (of size 10^5 each) from the partition space $\check{\Lambda}^q$ ($q = 2$), simulated using a free Boltzmann sampler as set out in Algorithm 1. Colour coding: *blue* designates the limiting distributions under the "fixed" regime, that is, compound Poisson-Gamma (left) and Poisson (right); *red* indicates a normal approximation; *magenta* depicts a mean-gamma approximation (see Section 2.3.1).

(see Section 2.3.1) nearly perfectly matches the exact compound Poisson-Gamma distribution for $\langle M\rangle = 50$ (see Figure 3.1(b), left); for smaller values of $\langle M\rangle$, this approximates is rather crude, however it still captures well the mode of the Poisson-Gamma distribution and also its right shoulder (see Figure 3.1(a), left).

A remarkable exception to the unimodality of the plots in Figure 3.1 is the compound Poisson-Gamma plot for the weight N_λ, with a relatively small value of $\langle M\rangle = 5$ (see Figure 3.1(a), left), where one can clearly see a singularity at zero (cf. Section 2.3.1). This theoretical prediction is supported by the empirical results, with an obvious excess of smaller weights. With $\langle M\rangle = 5$ and

$\langle N \rangle = 12{,}500$, the local minimum of the theoretical density $g(x)$ defined in (2.106) occurs at $x_0 \doteq 0.10340$ with value[1] $g(x_0) \doteq 0.19632$, which corresponds to weight $n_0 = \lceil x_0/\gamma_0 \rceil = 517$. If the density $g(x)$ continued to decay to the left of x_0, this would predict the (asymptotic) probability of getting weights smaller than n_0 (together with an empty partition) loosely bounded by $x_0\, g(x_0) + \pi_0 \doteq 0.02704$. But the actual compound Poisson-Gamma probability is higher, $G(x_0) \doteq 0.03120$ (see (2.104)). The excess of "small" partitions is reminiscent of a partition interpretation of the Bose–Einstein condensation (see [86]). As already mentioned in Section 2.3.1, this is a truly finite-length phenomenon, which vanishes as $\langle M \rangle \to \infty$ (cf. Figure 3.1(b), where $\langle M \rangle = 50$).

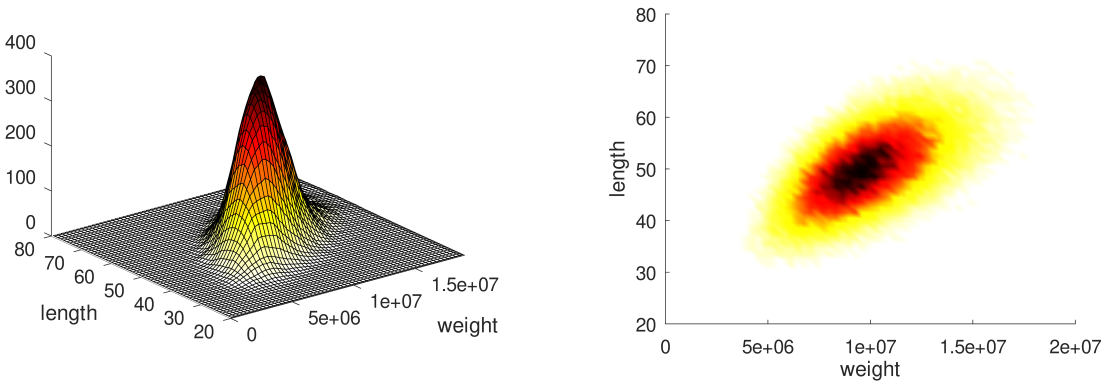

(a) Bivariate frequency plot.

(b) Frequency level sets.

Figure 3.2: Joint sampling distribution of weight N_λ and length M_λ for $q = 2$, $\langle M \rangle = 50$ and $\langle N \rangle = 10^7$ (cf. marginal plots in Figure 3.1(b)). A random Boltzmann sample of partitions $\lambda \in \check{\Lambda}^q$ (of size 10^5) was simulated using Algorithm 1.

The bivariate plots in Figure 3.2 (for $\langle M \rangle = 50$) appear to be approximately consistent with the asymptotically predicted (standardised) confidence ellipses of the form

$$\mathcal{L}_\alpha = \{\boldsymbol{x} \in \mathbb{R}^2 \colon \boldsymbol{x} \boldsymbol{K}_q^{-1} \boldsymbol{x}^\top \le \chi_2^2(1-\alpha)\}, \tag{3.11}$$

where $\boldsymbol{K}_q^{-1}$ is the inverse covariance matrix (2.138), and $\chi_2^2(1-\alpha)$ is the quantile of the chi-squared distribution with two degrees of freedom, corresponding to confidence probability $1-\alpha$. The latter distribution simplifies to an exponential distribution with mean 2, hence $\chi_2^2(1-\alpha) = 2\log(1/\alpha)$. According to Theorem 2.40, a sample point $(N_\lambda^*, M_\lambda^*)$ belongs to the ellipse (3.11) approximately with probability $1-\alpha$, where the standardised values N_λ^*, M_λ^* are defined in (2.137).

[1] Note that the asymptotic formula (2.107) gives a pretty accurate approximation $g(x_0) \approx 0.14334$.

The inverse of $\boldsymbol{K}_q$ is easily computed,

$$\boldsymbol{K}_q^{-1} = \frac{q+1}{q} \begin{pmatrix} 1 & \dfrac{-1}{\sqrt{q+1}} \\ \dfrac{-1}{\sqrt{q+1}} & 1 \end{pmatrix},$$

and the confidence ellipse (3.11) specialises as follows,

$$N_\lambda^{*2} - \frac{2N_\lambda^* M_\lambda^*}{\sqrt{q+1}} + M_\lambda^{*2} \le \frac{2q}{q+1} \log \frac{1}{\alpha}.$$

A closer inspection of the level plots in Figure 3.2(b) reveals some elongation of the frequency level sets towards bigger values of the weight N_λ, thus indicating a bit of discrepancy with the predicted elliptical shape. This observation is confirmed by comparison of the marginal histograms of N_λ and M_λ in Figure 3.1, where the latter is reasonably symmetric while the former is noticeably skewed to the right. A heuristic explanation of such an effect may be based on noticing from formulas (2.7) that, while the length M_λ is built by summation of multiplicities ν_ℓ, the weight N_λ involves size-biased terms $\ell\nu_\ell$, which pinpoint skewing the distribution to the right.

A well-localised unimodal nature of the distributions behind the outputs N_λ and M_λ is sometimes referred to as a *bumpy type* [24], characterised by an asymptotically large signal-to-noise ratio (SNR) in response to a large signal,[1]

$$\mathrm{SNR}(X) := \frac{[\mathsf{E}(X)]^2}{\mathsf{Var}(X)} \to \infty, \qquad \mathsf{E}(X) \to \infty. \tag{3.12}$$

Here, the notation X designates a random output in question (such as the size), which has a large expected value. Following definition (3.12) and applying Theorem 2.24, we readily get

$$\mathrm{SNR}(N_\lambda) \sim \frac{\langle N \rangle^2}{(q+1)\langle N \rangle^2 / \langle M \rangle} = \frac{\langle M \rangle}{q+1}, \qquad \mathrm{SNR}(M_\lambda) \sim \frac{\langle M \rangle^2}{\langle M \rangle} = \langle M \rangle,$$

so that under Assumption 2.3 (slow growth of $\langle M \rangle$) each of the marginal SNRs tends to infinity.

In the multivariate case, the SNR is usually defined in the literature as a scalar value,

$$\mathrm{SNR}(\boldsymbol{X}) := \boldsymbol{\mu}\boldsymbol{K}^{-1}\boldsymbol{\mu}^\top, \qquad \boldsymbol{\mu} := \mathsf{E}(\boldsymbol{X}), \quad \boldsymbol{K} := \mathsf{Cov}(\boldsymbol{X}, \boldsymbol{X}) \tag{3.13}$$

[1] The "bumpy" property is especially helpful for sampling with rejection designed to achieve certain targets for weight and length, due to a guaranteed asymptotically fast delivery of the output (see Section 3.2).

(see, e.g., [72, Eq. (1), p. 511]). Again using Theorem 2.24, we find the asymptotic inverse of the covariance matrix,

$$\boldsymbol{K}^{-1}(\boldsymbol{z}) \sim \frac{1}{q\langle N\rangle^2}\begin{pmatrix} \langle M\rangle & -\langle N\rangle \\ -\langle N\rangle & \dfrac{(q+1)\langle N\rangle^2}{\langle M\rangle}\end{pmatrix},$$

and hence

$$\mathrm{SNR}(N_\lambda, M_\lambda) \sim \frac{(\langle N\rangle, \langle M\rangle)}{q\langle N\rangle^2}\begin{pmatrix} \langle M\rangle & -\langle N\rangle \\ -\langle N\rangle & \dfrac{(q+1)\langle N\rangle^2}{\langle M\rangle}\end{pmatrix}\begin{pmatrix}\langle N\rangle \\ \langle M\rangle\end{pmatrix} = \langle M\rangle \to \infty.$$

However, a scalar definition (3.13) is not entirely satisfactory — for instance, it cannot detect whether the individual components of $\boldsymbol{X}$ are of bumpy type. As an alternative, we propose the following matrix definition,

$$\mathbf{SNR}(\boldsymbol{X}) := (\boldsymbol{\mu}\boldsymbol{K}^{-1/2})^\top(\boldsymbol{\mu}\boldsymbol{K}^{-1/2}) = \boldsymbol{K}^{-1/2}(\boldsymbol{\mu}^\top\boldsymbol{\mu})\,\boldsymbol{K}^{-1/2}, \tag{3.14}$$

where $\boldsymbol{K}^{-1/2}$ is the (unique) positive definite square root of the inverse covariance matrix $\boldsymbol{K}^{-1}$, that is, $\boldsymbol{K}^{-1/2}\boldsymbol{K}^{-1/2} = \boldsymbol{K}^{-1}$ [44, Theorem 7.2.6, p. 439]. In our case, the exact expression for $\boldsymbol{K}^{-1/2}(\boldsymbol{z})$ is cumbersome (although available), but its asymptotic version under Assumption 2.3 simplifies to

$$\boldsymbol{K}^{-1/2}(\boldsymbol{z}) \sim \frac{\sqrt{\langle M\rangle}}{\sqrt{q\,(q+1)\,\langle N\rangle}}\begin{pmatrix} \sqrt{q} & -1 \\ -1 & \dfrac{(q+1)\,\langle N\rangle}{\langle M\rangle}\end{pmatrix}.$$

Hence, after straightforward calculations we obtain from (3.14)

$$\mathbf{SNR}(N_\lambda, M_\lambda) \sim \frac{\langle M\rangle}{q+1}\begin{pmatrix} 1 & \sqrt{q} \\ \sqrt{q} & q\end{pmatrix},$$

which tends to infinity in matrix sense.

3.2. Rejection sampler

The idea of a rejection sampler discussed in this section is to run a free sampler in a loop until a prescribed target is met. For example, if the target is set in terms of the required partition length as $M_\lambda = m$, with a fixed $m \in \mathbb{N}$, then the free sampler is iterated until a partition of exact length m is obtained. Likewise, if the target is set for the partition weight, $N_\lambda = n$, with a fixed $n \in \mathbb{N}$, then

the free sampling loop runs until a partition of exact weight n is found. These two targets can be imposed simultaneously, $M_\lambda = m$ and $N_\lambda = n$; here, it is natural to design the rejection algorithm as a juxtaposition of two loops of the free sampler, such that the internal loop runs until the length target is met and, every time this happens, the resulting partition is checked with regards to the weight target and is either rejected, whereby the internal loop starts afresh, or accepted, in which case the algorithm stops.

A more general approach, leading to the so-called approximate algorithms, is to relax the exact targets to suitable intervals (brackets). In Algorithm 2 presented below in Section 3.2.3, we give an example of a Boltzmann rejection sampler aiming to sample a partition $\lambda \in \check{\Lambda}^q$ satisfying two conditions, $M_\lambda = m$ and $n \leq N_\lambda \leq \theta n$, for some predefined tolerance factor $\theta \geq 1$. Of course, if $\theta = 1$, the approximate algorithm is reduced to an exact one. An approximate target can also be considered for length, $m \leq M_\lambda \leq \theta' m$, and furthermore, such approximate targets can be combined if desired.

Before delineating Algorithm 2, we discuss a few implementation issues arising therein.

3.2.1. Calibration and truncation of parts

To start with, the choice of the calibrating parameters z_1 and z_2 now follows a slightly different logic as compared to the case of a free sampler. If only one target is set, such as $M_\lambda = m$, then according to formula (2.27) the conditional Boltzmann measure $\mathsf{P}_{\boldsymbol{z}}(\cdot \,|\, \check{\Lambda}^q(\cdot, m))$ does not depend on the parameter z_2, whereas the other parameter, z_1, can be chosen with a view on a desired expected value $\langle N \rangle$ of the output weight N_λ, as was the case with the free sampler. Nonetheless, in order to maximise efficiency of the sampling algorithm, the "free" parameter z_2 should still be chosen in line with the mean conditions (2.65) subject to the specification $\langle M \rangle = m$, thus aiming to benefit from the bumpy nature of the distribution $\mathsf{P}_{\boldsymbol{z}}(\cdot \,|\, \check{\Lambda}^q(\cdot, m))$ (cf. Section 3.1.3). Similarly, if the condition $N_\lambda = n$ is targeted then the conditional Boltzmann measure $\mathsf{P}_{\boldsymbol{z}}(\cdot \,|\, \check{\Lambda}^q(n, \cdot))$ does not depend on z_1, however both parameters z_1 and z_2 are chosen to match the mean conditions (2.65) with $\langle N \rangle = n$. Furthermore, if both targets are imposed, $N_\lambda = n$ and $M_\lambda = m$, then by Lemma 2.8 the measure $\mathsf{P}_{\boldsymbol{z}}(\cdot \,|\, \check{\Lambda}^q(n, m))$ is reduced to the uniform distribution on $\check{\Lambda}^q(n, m)$ regardless of the parameters z_1 and z_2. But, as explained above, it is worthwhile to calibrate them in line with the mean conditions (2.65). With these targets in mind, in what follows (including Algorithm 2) we use the specific hyper-parameters $\langle N \rangle = n$ and $\langle M \rangle = m$. Moreover, since avoiding bias is no longer a concern (unlike in the case of the free sampler), using the leading-term expressions (3.1) is a perfectly satisfactory option. Of course, the same recipe applies to the approximate sampling.

Another issue to be addressed is whether any truncation of the source of parts is needed in the algorithm (cf. Section 3.1.2). As long as the weight target is involved, $N_\lambda = n$, one can use a natural majorant $L^* = n$ as a call parameter L in Algorithm 1 (see Section 3.1.3), which clearly causes no loss in confidence (i.e., $\delta = 0$, see (3.5)). The same is true in the case of an approximate target, $N_\lambda \in [n, \theta n]$, by choosing the majorant $L^* = \theta n$. However, if only the length target is in place then no such majorant is available and, therefore, confidence considerations must be deployed, as discussed in Section 3.1.2.

3.2.2. Censoring of iterations

As was pointed out in the Introduction, in contrast to the special value $q = 1$, in the general case with $q \geq 2$ and arbitrary $m \geq 1$ there is no guarantee for a given natural number $n \in \mathbb{N}$ to be partitionable into a required number m of q-power parts (unless it is covered by a solution of the Waring problem [83]). The requirement that the parts be distinct adds to the complexity of the question. Therefore, the space $\check{\Lambda}^q(n, m)$ may well be empty and, not knowing this in advance, the task of sampling from such a space may be "mission impossible".

To be specific, consider sampling subject to the joint targets $M_\lambda = m$ and $N_\lambda = n$. As already indicated at the beginning of Section 3, a general design of the corresponding sampling algorithm is based on the two nested loops according to the separated targets, internal for M_λ and external for N_λ. While the internal loop is certain to produce a random partition in $\check{\Lambda}^q$ with exactly m parts (see more about this below), the external loop contains an inherent loose end due to its potential failure to satisfy the weight requirement, simply because there may be no such partitions. That is to say, although the successful completion of the external loop will take some time by repeatedly querying the internal loop, it may be pointless to wait for too long as there is no certainty if that is not wasteful.

We propose to resolve this difficulty by an appropriate "censoring" of processing time, that is, by setting a limit t^* on the waiting time, chosen to ensure sufficiently high confidence in the algorithm's ability to deliver a successful completion within the allocated time limit, of course provided that the task is feasible (i.e., required partitions exist). More precisely, given a confidence tolerance (significance level) $\delta \in (0, 1)$, the threshold t^* should be such that, if the target space is non-empty, the probability that the algorithm would not succeed by time t^* does not exceed δ. Such an approach is akin to statistical testing of the null hypothesis "the target is non-empty". Under this hypothesis, the test (implemented as a sampling algorithm) fails to produce a required partition (Type I error) with rate bounded by δ.

The choice of threshold t^* is determined by the sampling task at hand. A few examples of interest are as follows (assuming the number of parts m to be fixed):

(T1) *Exact sampling:* For a given n, attempt to sample $\lambda \in \check{\Lambda}^q(n,m)$ (in other words, check partitionability of n).

(T2) *Multiple exact sampling:* For a given n and some $\theta > 1$, attempt to sample $\lambda \in \check{\Lambda}^q(k,m)$ for each integer k in the range $k \in [n, \theta n]$ (that is, test partitionability of each of these numbers).

(T3) *Approximate sampling:* Same as in task (T2) but attempting to sample $\lambda \in \bigcup_{n \le k \le \theta n} \check{\Lambda}^q(k,m)$ (that is, to find at least one partitionable number in the said range).

Remark 3.1. If required, tasks (T2) and (T3) could be modified to a two-sided version, such as $\theta^{-1} n \le k \le \theta n$ or, more generally, $\theta_1 n \le k \le \theta_2 n$, with some $0 < \theta_1 < 1 < \theta_2$.

First, let us look at how the internal loop performs towards its task of sampling a partition $\lambda \in \check{\Lambda}^q_L(\cdot, m) = \check{\Lambda}^q(\cdot, m) \cap \{\lambda\colon \lambda_{\max} \le L\}$ (i.e., the source of parts is truncated to $\{\ell \le L\}$, see Section 2.1.5). According to Theorem 2.31(a), if $\langle M \rangle > 0$ is fixed and $L \sim \theta \langle N \rangle$ then the distribution of M_λ conditional on $\lambda_{\max} \le L$ converges to a Poisson law with mean $\mu_\theta = \langle M \rangle G_{1/q}(a_\theta)$, where $a_\theta = \theta \langle M \rangle / q$. A stronger result concerns a Poisson approximation (cf. Remark 2.27) under a suitable metric, such as the total variation distance between distributions. Namely, the said conditional distribution of M_λ can be replaced by a Poisson distribution with mean

$$\mathsf{E}_{\boldsymbol{z}}(M_\lambda \,|\, \lambda_{\max} \le L) = \sum_{\ell \le L} \frac{z_1^\ell z_2}{1 + z_1^\ell z_2} \sim \mu_\theta, \tag{3.15}$$

with the error in total variation bounded by (see [7, Theorem 1, p. 474])

$$\frac{1}{\mu_\theta} \sum_{\ell \le L} \left(\frac{z_1^\ell z_2}{1 + z_1^\ell z_2} \right)^2 = O(z_2) = O(\kappa^{1/q}) \to 0, \tag{3.16}$$

according to (2.95). The advantage of such an approximation is that it holds true even if $\langle M \rangle$ is slowly growing, whereby the error estimate (3.16) is still valid.

Returning to the analysis of the internal loop, with $\langle N \rangle = n$ and $\langle M \rangle = m$ we have

$$\mathsf{P}_{\boldsymbol{z}}(M_\lambda = m \,|\, \lambda_{\max} \le \theta n) \sim \frac{\mu_\theta^m \, \mathrm{e}^{-\mu_\theta}}{m!}, \qquad \mu_\theta = m\, G_{1/q}(\theta m / q). \tag{3.17}$$

Hence, the probability (3.17) is bounded away from zero, and since the attempts within the internal loop are independent, the number of internal runs until success has geometric distribution, with the expected time to success being bounded by

a constant (depending on m). If $m \to \infty$ (with $\kappa = m^{q+1}/n = o(1)$), then $\mu_\theta \sim m$ and, according to (3.15) and (3.16), we have

$$\mathsf{P}_{\boldsymbol{z}}(M_\lambda = m \,|\, \lambda_{\max} \le \theta n) = \frac{\mu_\theta^m \, \mathrm{e}^{-\mu_\theta}}{m!} + O(\kappa^{1/q}) \sim \frac{m^m \, \mathrm{e}^{-m}}{m!} \sim \frac{1}{\sqrt{2\pi m}}, \tag{3.18}$$

with the help of the Stirling formula. In turn, formula (3.18) implies that the expected number of runs of the internal loop is of order $O\bigl(\sqrt{m}\bigr)$, which is not particularly large for practical implementation.

Let us now turn to tasks (T1)–(T3) and focus on probabilistic analysis of runs of the external loop, taking for granted that $M_\lambda = m$ and, automatically, $\lambda_{\max} \le L^*$, where $L^* = \theta n$ is a majorant in $\bigcup_{n \le k \le \theta n} \check{\Lambda}^q(k, m)$. As stipulated above, we use the hyper-parameters $\langle N \rangle = n$ and $\langle M \rangle = m$, and specify the calibrating parameters z_1 and z_2 according to the leading-term expressions (3.1). Denote for short

$$p_k^* := \mathsf{P}_{\boldsymbol{z}}(N_\lambda = k \,|\, M_\lambda = m, \lambda_{\max} \le \theta n), \qquad n \le k \le \theta n. \tag{3.19}$$

for simplicity omitting reference to n and m. Of course, if $\check{\Lambda}^q(k, m) = \varnothing$ then $p_k^* = 0$. The probability (3.19) can be interpreted as the probability of successfully sampling a partition of weight k in a single run of the external loop. Due to independence of successive runs, the number T_k of attempts until success for a targeted weight value k follows geometric distribution,

$$\mathsf{P}_{\boldsymbol{z}}(T_k > t \,|\, M_\lambda = m, \lambda_{\max} \le n) = (1 - p_k^*)^t, \qquad t \in \mathbb{N}_0. \tag{3.20}$$

This includes the case $p_k^* = 0$, whereby $T_k = \infty$ ($\mathsf{P}_{\boldsymbol{z}}$-a.s.). Also note that (T_k) are mutually independent for different k.

(T1) Here, $\theta = 1$, so $L^* = n$. Suppose that $\check{\Lambda}^q(n, m) \ne \varnothing$ and let $\lambda_* \in \check{\Lambda}^q(n, m)$, so that $N_{\lambda_*} = n$ and $M_{\lambda_*} = m$. Then we can write

$$\mathsf{P}_{\boldsymbol{z}}(\lambda_* \,|\, M_\lambda = m, \lambda_{\max} \le n) = \frac{\mathsf{P}_z(\lambda_* \,|\, \lambda_{\max} \le n)}{\mathsf{P}_z(M_\lambda = m \,|\, \lambda_{\max} \le n)}. \tag{3.21}$$

Starting with the numerator, we have

$$\mathsf{P}_z(\lambda_* \,|\, \lambda_{\max} \le n) = z_1^n z_2^m \prod_{\ell \le n} \frac{1}{1 + z_1^\ell z_2}.$$

Substituting formulas (3.1), we obtain

$$z_1^n z_2^m \sim \mathrm{e}^{-m/q} \, \frac{q^{2m} (m/q)^{m + m/q}}{\bigl(\Gamma(1/q)\bigr)^m \, n^{m/q}},$$

while Lemma 2.17, with the help of the asymptotic relation (2.79), yields

$$\prod_{\ell\le n}\frac{1}{1+z_1^\ell z_2}\sim\exp\bigl(-m\,G_{1/q}(m/q)\bigr).$$

Furthermore, by Theorem 2.31(a) the denominator in (3.21) is asymptotically given by

$$\mathsf{P}_z(M_\lambda=m\,|\,\lambda_{\max}\le n)\sim\frac{m^m\bigl(G_{1/q}(m/q)\bigr)^m\exp\bigl(-m\,G_{1/q}(m/q)\bigr)}{m!}. \tag{3.22}$$

Hence, returning to (3.21) we obtain

$$p_n^*\ge\mathsf{P}_{\boldsymbol{z}}(\lambda_*\,|\,M_\lambda=m,\lambda_{\max}\le n)\sim\frac{1}{C_1(m,q)\,n^{m/q}}, \tag{3.23}$$

where

$$C_1(m,q):=\frac{1}{m!}\left(\frac{\mathrm{e}^{1/q}\,\Gamma(1/q)\,G_{1/q}(m/q)}{q^{1-1/q}m^{1/q}}\right)^m. \tag{3.24}$$

Combining (3.20) and (3.23), we have, asymptotically,

$$\mathsf{P}_{\boldsymbol{z}}(T_n>t\,|\,M_\lambda=m,\lambda_{\max}\le n)=(1-p_n^*)^t\le\left(1-\frac{1+o(1)}{C_1(m,q)\,n^{m/q}}\right)^t. \tag{3.25}$$

Thus, for the probability (3.25) not to exceed a predefined (small) confidence tolerance $\delta>0$, it suffices to choose the threshold $t=t_n^*$ as follows,

$$t_n^*\simeq\frac{\log\delta}{\log\left(1-\dfrac{1+o(1)}{C_1(m,q)\,n^{m/q}}\right)}\sim C_1(m,q)\,n^{m/q}\log\frac{1}{\delta}. \tag{3.26}$$

Remark 3.2. The bound (3.26) is very conservative due to a crude estimate (3.23) leveraging just one instance $\lambda_*\in\check{\Lambda}^q(n,m)$. If more information was available about the size of the space $\check{\Lambda}^q(n,m)$, the bound (3.26) could be reduced accordingly. For example, if $q=1$ then it is known that $\#\check{\Lambda}(n,m)\sim n^{m-1}(m!\,(m-1)!)^{-1}$ (see (2.129)). Hence, formula (3.26) for the time threshold in the case $q=1$ is replaced by a much better and more realistic estimate,

$$\tilde{t}_n^*\simeq\frac{C_1(m,1)}{\#\check{\Lambda}(n,m)}\,n^m\log\frac{1}{\delta}\sim\frac{\mathrm{e}^m\,(1-\mathrm{e}^{-m})^m\,(m-1)!}{m^m}\,n\log\frac{1}{\delta}. \tag{3.27}$$

Likewise, for $q = 2$ we get, using (2.131) (with $C_m = 1$),

$$\tilde{t}_n^* \simeq \frac{C_1(m,2)}{\#\check{\Lambda}^2(n,m)}\, n^{m/2} \log\frac{1}{\delta} \sim \left(\frac{2\mathrm{e}}{m}\right)^{m/2} \Gamma(m/2)\, \big(G_{1/2}(m/2)\big)^m\, n \log\frac{1}{\delta}, \tag{3.28}$$

which again grows only linearly in n.

(T2) For the multiple exact sampling in the range $k \in [n, \theta n]$, we can just repeat the procedure in task (T1) for each k in that range. According to (3.20), the probability that the number of attempts until success, T_k, exceeds a threshold t_k^* is given by (cf. (3.20))

$$\mathsf{P}_{\boldsymbol{z}}\big(T_k > t_k^* \,|\, M_\lambda = m, \lambda_{\max} \le k\big) = (1 - p_k^*)^{t_k^*}, \qquad n \le k \le \theta n.$$

Taking into account only partitionable numbers $k \in [n, \theta n]$ (i.e., such that $\check{\Lambda}^q(k,m) \neq \varnothing$ and, therefore, $p_k^* > 0$) and using a Bonferroni-type inequality, the probability of Type I error for task (T2) (i.e., that the external loop fails for at least one such k) is bounded as follows,

$$\mathsf{P}_{\boldsymbol{z}}\left(\bigcup_{k=n}^{\lfloor \theta n \rfloor} \{t_k^* < T_k < \infty\} \,\middle|\, M_\lambda = m, \lambda_{\max} \le \theta n\right) \le \sum_{k\,:\,p_k^* > 0} (1 - p_k^*)^{t_k^*}. \tag{3.29}$$

Motivated by formula (3.26), we can look for the time limits t_k^* in the form

$$t_k^* \sim c\, k^{m/q}. \tag{3.30}$$

Then from (3.29) using (3.23) we get, asymptotically,

$$\begin{aligned}\sum_{k\,:\,p_k^* > 0} (1 - p_k^*)^{t_k^*} &\lesssim \sum_{k=n}^{\lfloor \theta n \rfloor} \left(1 - \frac{1}{C_1(m,q)\, k^{m/q}}\right)^{c k^{m/q}} \\ &\le (\theta - 1)\, n \exp\left(-\frac{c}{C_1(m,q)}\right) \le \delta.\end{aligned}$$

Solving this inequality for c and returning to (3.30) ultimately yields

$$t_k^* \simeq C_1(m,q)\, k^{m/q} \log\frac{(\theta - 1)n}{\delta}, \qquad n \le k \le \theta n. \tag{3.31}$$

Thus, the time bound (3.31) follows the same formula as in a single test (cf. (3.26)) but with a Bonferroni-type adjustment of the significance level in order to offset the multiple testing.

Remark 3.3. The same comment as in Remark 3.2 applies to task (T2). Specifically, for $q = 1$ and $q = 2$ the improved formulas for the thresholds t_k^* are given, respectively, by

$$\tilde{t}_k^* \simeq \frac{\mathrm{e}^m\,(1-\mathrm{e}^{-m})^m\,(m-1)!}{m^m}\,k\log\frac{(\theta-1)n}{\delta}, \tag{3.32}$$

$$\tilde{t}_k^* \simeq \left(\frac{2\mathrm{e}}{\pi m}\right)^{m/2}\Gamma(m/2)\left(\int_0^{m/2} u^{-1/2}\,\mathrm{e}^{-u}\,\mathrm{d}u\right)^m k\log\frac{(\theta-1)n}{\delta}. \tag{3.33}$$

(T3) In a single attempt, the external loop gets a partition $\lambda \in \bigcup_{n\le k\le\theta n}\check{\Lambda}^q(k,m)$ with probability

$$\mathsf{P}_{\boldsymbol{z}}\big(n\le N_\lambda\le\theta n\,|\,M_\lambda=m,\lambda_{\max}\le\theta n\big)=\sum_{k=n}^{\lfloor\theta n\rfloor}p_k^*\to G_{1/q}^{\star m}(a_\theta\,|\,a_\theta)-G_{1/q}^{\star m}(a_1|\,a_\theta). \tag{3.34}$$

The limit (3.34) is due to Theorem 2.31(b), where $a_\theta = \theta m/q$ and $G_{1/q}^{\star m}(x\,|\,a_\theta)$ stands for the m-convolution of the a_θ-truncated gamma distribution $G_{1/q}(x\,|\,a_\theta)$.

To circumvent the trouble of computing such a convolution, observe that in the range $0\le x\le a$ the distribution function $G_\alpha^{\star m}(x\,|\,a)$ coincides with $G_{m\alpha}(x)$ up to the normalisation factor $G_\alpha(a)^m$. This is obvious for $m=1$, and the general case can be seen by induction over m using the convolution formula. Indeed, denoting the corresponding densities by $g_\alpha^{\star m}(x\,|\,a)$ and $g_{m\alpha}(x)$, respectively, we have by definition $g_\alpha(x\,|\,a)=g_\alpha(x)/G_\alpha(a)$ $(0\le x\le a)$, and the induction step is carried out as follows,

$$\begin{aligned} g_\alpha^{\star m}(x\,|\,a) &= \int_0^x g_\alpha^{\star(m-1)}(u\,|\,a)\,g_\alpha(x-u\,|\,a)\,\mathrm{d}u \\ &= \frac{1}{G_\alpha(a)^m}\int_0^x g_{(m-1)\alpha}(u)\,g_\alpha(x-u)\,\mathrm{d}u = \frac{g_{m\alpha}(x)}{\big(G_\alpha(a)\big)^m}, \qquad 0\le x\le a, \end{aligned}$$

due to the convolution property of the gamma distribution. Thus, formula (3.34) simplifies to

$$\sum_{k=n}^{\lfloor\theta n\rfloor}p_k^*\to\frac{G_{m/q}(\theta m/q)-G_{m/q}(m/q)}{\big(G_{1/q}(\theta m/q)\big)^m}=:C_3(m,q,\theta). \tag{3.35}$$

Now, since individual runs of the external loop are independent, the probability that the number of attempts until success, T, exceeds a threshold t

is given by (cf. (3.20))

$$\mathsf{P}_{\boldsymbol{z}}(T > t \,|\, M_\lambda = m, \lambda_{\max} \le \theta n) = \left(1 - \sum_{k=n}^{\lfloor \theta n \rfloor} p_k^*\right)^t \simeq \big(1 - C_3(m,q,\theta)\big)^t, \tag{3.36}$$

on account of (3.35). Hence, in order that this probability be bounded by a confidence tolerance $\delta > 0$, we may choose the threshold $t = t^*$ as follows,

$$t^* \simeq \frac{\log \delta}{\log\big(1 - C_3(m,q,\theta)\big)}. \tag{3.37}$$

Remark 3.4. According to formula (3.37), the threshold t^* does not depend on n. It is of interest to look at how it depends on the growth of the power q. To this end, by a direct analysis of the gamma distribution (see (2.90)) one can verify that

$$G_\alpha(\theta\alpha) = (\theta\alpha)^\alpha\big(1 + O(\alpha)\big) \qquad (\alpha \to 0+).$$

Hence, from formula (3.35) we get

$$C_3(m,q,\theta) \sim 1 - \theta^{-m/q} \sim \frac{m \log \theta}{q} \qquad (q \to \infty),$$

and then (3.37) gives

$$t^* \simeq \frac{q \log(1/\delta)}{m \log \theta}.$$

3.2.3. Rejection sampling algorithm

A stylised example of rejection sampler is presented below in pseudocode as Algorithm 2. It is set out in a flexible way so as to be usable in exact and approximate sampling alike, as determined by the tasks (T1)–(T3) described in Section 3.2.2. In particular, the range parameter θ is allowed to take the value $\theta = 1$, in which case the algorithm would work towards the exact sampling task (T1) (i.e., with a specific weight target $N_\lambda = n$). As explained in Section 3.2.1, the hyper-parameters are adapted to the desired targets, $\langle N \rangle = n$ and $\langle M \rangle = m$, and the calibrating parameters z_1 and z_2 are set according to the simplified expressions (3.1). A predefined time bound t^* for the external loop is selected according to the task at hand, as discussed in Section 3.2.2, and on account of the required confidence probability $1 - \delta$.

As briefly indicated at the start of Section 3.2, Algorithm 2 comprises an external loop that iterates the free sampler in an internal loop (i.e., Algorithm 1,

with the majorant $L = \theta n$), which delivers, in each productive cycle, a partition λ that meets the length target $M_\lambda = m$. This continues until the trial partition λ meets the weight target (e.g., $N_\lambda = n$ in task (T1) or $n \leq N_\lambda \leq \theta n$ in task (T3)). However, if the limit of attempts t^* is reached with no success then the algorithm terminates, returning a message 'VOID'. It remains to add that for task (T2) involving multiple exact sampling, the algorithm should be run in an additional loop to scan all weight values in the range $k \in [n, \theta n]$.

Algorithm 2: `ReSampler`(q, n, m, θ, t^*)

Input: integer q, n, m, real $\theta \geq 1$, t^*
Output: partition $\lambda \in \check{\Lambda}^q(\cdot, m)$ with $N_\lambda \in [n, \theta n]$, otherwise 'VOID'

integer array $\lambda_{[\,]}$;
integer N, M, t;
real L;
$L \leftarrow \theta n$;
$N \leftarrow 0$, $M \leftarrow 0$, $t \leftarrow 0$;
while $N \notin [n, \theta n]$ *and* $t \leq t^*$ **do**
  while $M \neq m$ **do**
    $(\lambda, N, M) \leftarrow$ `FreeSampler`(q, n, m, L)
  end
  $t \leftarrow t + 1$;
end
if $t \leq t^*$ **then**
  $N_\lambda \leftarrow N$;
  return (λ, N_λ)
else
  return `'VOID'`
end

Algorithm 2 can be optimised in a number of ways. Since the weight of a valid output λ should not exceed θn, it is clear that the run of the internal loop can be terminated prior to collecting the required number of parts m if the next candidate part is too large, so that the incremented weight will certainly exceed the majorant. Furthermore, if the number of collected parts has already reached the target value m then there is no need to keep scanning the remaining values in the range $\ell \leq L$ and the current run of the internal loop may be stopped without any loss. However, to avoid bias and maintain the Boltzmann distribution of the output, the corresponding proposal $\lambda \in \check{\Lambda}^q_L(\cdot, m)$ must be accepted only if the remaining candidate parts in the range $\ell \leq L$ were to be rejected by the respective Bernoulli checks. Since individual such checks are

mutually independent, their multitude can be replaced by a single Bernoulli trial with the corresponding product probability of failure. An additional benefit of such an aggregated Bernoulli check is that this will reduce the number of calls of the random number generator and hence improve the efficiency of the sampler.

Another improvement of the code implementation in the multiple testing task (T2) proceeds from the observation that the sequential procedure based on separate testing of each target in the range $[n, \theta n]$ (see Section 3.2.2) is apparently wasteful, because a partition of some $k' \in [n, \theta n]$ obtained whilst looking for partitions of a different number k would be discarded in that cycle of the external loop, whereas keeping it would have helped to achieve success if an earlier search with target k' failed, or to save time on a duplicate job when the algorithm moves to the new target k'. In practice, all partitions (at least, the new ones) obtained in every run of the external loop should be stored as long as they fit into the range $[n, \theta n]$, thus leaving dynamically fewer targets to address.

For the sake of presentational clarity, Algorithm 2 embeds iterated calls of the free sampler (Algorithm 1), but this means that the calibrating parameters z_1 and z_2 are recalculated at every such call, which is of course wasteful. This drawback can be easily amended by writing out the code explicitly. Note, however, that such an improvement would have no significant bearing on the asymptotic estimation of the code complexity.

3.2.4. Complexity and performance

Building on the probabilistic analysis of the internal and external loops carried out in Section 3.2.2, it is straightforward to estimate the *time complexity* of Algorithm 2, understood as the *expected number of elementary runs to completion*.

Starting with the internal loop, in its crude (non-optimised) version each internal run comprises $\lfloor (\theta n)^{1/q} \rfloor$ checks of available parts $\ell \in \mathbb{N}^q$ not exceeding $L^* = \theta n$. Combined with the estimate (3.17) of the probability to collect m parts in a single run and the corresponding geometric distribution of the number of attempts, the complexity of the internal loop is bounded by

$$\mu_\theta^{-m} m!\, \mathrm{e}^{\mu_\theta} (\theta n)^{1/q}. \tag{3.38}$$

As for the external loop, its complexity depends on the task at hand. If $\theta = 1$ (which corresponds to task (T1) of exact sampling with the weight target $N_\lambda = n$), then the time to completion, T_n, has geometric distribution with parameter p_n^* (see (3.20)). For simplicity dropping a time bound t^* (but still assuming that the space $\check{\Lambda}^q(n, m)$ is non-empty, so that $p_n^* > 0$), the expected time to completion is given by $\mathsf{E}_{\boldsymbol{z}}(T_n) = 1/p_n^*$. With a time bound t^*, the expectation is modified as

follows,

$$\mathsf{E}_{\boldsymbol{z}}(T_n; T_n \le t^*) = \sum_{t=1}^{t^*} t\,(1-p_n^*)^{t-1}p_n^* + t^*(1-p_n^*)^{t^*} = \frac{1-(1-p_n^*)^{t^*}}{p_n^*} < \frac{1}{p_n^*}. \tag{3.39}$$

However, the reduction in (3.39) is not significant, because under our confidence-based choice of the time limit (see (3.23)), we always have $(1-p_n^*)^{t^*} \le \delta$. Thus, combining formulas (3.38) and (3.39), the total complexity guarantee for task (T1) is estimated by

$$\frac{m!\,\mathrm{e}^{\mu_1}}{\mu_1^m}\,O\big(n^{1/q}/p_n^*\big), \qquad \mu_1 = m\,G_{1/q}(m/q). \tag{3.40}$$

Further specification depends on the informative lower bound for the probability p_n^*. For example, a crude estimate (3.23) gives a more explicit estimate for the complexity,

$$\left(\frac{\exp\big(G_{1/q}(m/q)+1/q\big)\,\Gamma(1/q)}{q^{1-1/q}m^{1+1/q}}\right)^m O\big(n^{(m+1)/q}\big). \tag{3.41}$$

For $q=1$ and $q=2$, this estimate can be significantly improved by using asymptotically exact cardinalities (2.129) and (2.131), respectively, yielding the estimates

$$\frac{(m!)^2\,\mathrm{e}^{2m}}{m^{2m+1}}\,O(n^2) = O(n^2) \tag{3.42}$$

and

$$\frac{2^{m/2}m!\,\Gamma(m/2)\,\mathrm{e}^{3m/2}}{m^{3m/2}}\,O\big(n^{3/2}\big) = O(n^{3/2}). \tag{3.43}$$

Interestingly, the asymptotic bounds (3.42) and (3.43) do not depend on the number of parts m.

For task (T2) (with some $\theta > 1$), the above estimates just need to be multiplied by the number of targeted weights, $\lfloor(\theta-1)\,n\rfloor + 1 = O(n)$. Finally, for task (T3) we can use formula (3.40), but with μ_1 changed to μ_θ (see (3.38)) and with the probability p_n^* of success in a single attempt replaced by the (asymptotic) probability (3.35) of at least one success in the range $[n, \theta n]$, yielding

$$\frac{m!\,\exp\big(m\,G_{1/q}(\theta m/q)\big)}{m^m\,\big(G_{m/q}(\theta m/q) - G_{m/q}(m/q)\big)}\,O(n^{1/q}) = O\big(mn^{1/q}\big).$$

To evaluate real time performance of the rejection sampler, we first need to take a practical look at the censoring time limits t^* in tasks (T1)–(T3) proposed in Section 3.2.2. These are numerically illustrated in Table 3.4 for $q = 1$ and

Table 3.4: Confident time thresholds t^* for the external loop in tasks (T1), (T2) and (T3), calculated for $q = 1$ and $q = 2$ with various values of confidence tolerance δ using formulas (3.26), (3.31) and (3.37). In both cases, the chosen values of n and m yield $\kappa = m^{q+1}/n = 0.01$. For tasks (T2) and (T3), the testing range is set with the factor $\theta = 1.1$. For comparison, corrected values $\tilde{t}^*$ for tasks (T1) and (T2) are calculated from formulas (3.27), (3.28) and (3.32), (3.33), respectively.

$q = 1$, $n = 2{,}500$, $m = 5$					
δ	t_n^* (T1)	$\tilde{t}_n^*$ (T1)	t_n^* (T2)	$\tilde{t}_n^*$ (T2)	t^* (T3)
0.1	$8.603518 \cdot 10^{13}$	6,343.202	$2.923424 \cdot 10^{14}$	21,553.82	26.01955
0.01	$1.720704 \cdot 10^{14}$	12,686.40	$3.783776 \cdot 10^{14}$	27,897.02	52.03911
0.001	$2.581056 \cdot 10^{14}$	19,029.61	$4.644128 \cdot 10^{14}$	34,240.22	78.05866
0.0001	$3.441407 \cdot 10^{14}$	25,372.81	$5.504479 \cdot 10^{14}$	40,583.43	104.0782

$q = 2$, $n = 12{,}500$, $m = 5$					
δ	t_n^* (T1)	$\tilde{t}_n^*$ (T1)	t_n^* (T2)	$\tilde{t}_n^*$ (T2)	t^* (T3)
0.1	198,687,146	41,485.61	814,003,357	169,962.8	34.94282
0.01	397,374,292	82,971.22	1,012,690,503	211,448.4	69.88564
0.001	596,061,438	124,456.8	1,211,377,649	252,934.0	104.8285
0.0001	794,748,583	165,942.4	1,410,064,795	294,419.7	139.7713

$q = 2$, with various values of n and m. Observe that the crude bounds for tasks (T1) and (T2) calculated via formulas (3.26) and (3.31) appear to be very high, especially for $q = 1$ (of order 10^{14}), casting doubt on whether such limits are usable. In real terms, since each run of the external loop is a simple check if $N_\lambda = n$ (see line 6 in Algorithm 2), we can assume for simplicity that it needs a single tick of the CPU clock. If the algorithm is executed on a contemporary mid-range desktop PC (say, with processor base frequency 3.30 GHz, which we used) then, under the estimate (3.26) for task (T1) with $q = 1$ and a fairly low confidence tolerance $\delta = 0.001$, the external loop alone may require up to $2.581056 \cdot 10^{14}/(3.30 \cdot 10^9 \cdot 60 \cdot 60) \doteq 21.72606 \approx 22$ hours until completion, which is unpleasantly long but not entirely unrealistic. This estimate drops dramatically for $q = 2$ to less than 1 second. A steep decreasing trend continues with larger powers;[1] for example, for $q = 3$, $n = 62{,}500$, $m = 5$ and $\delta = 0.001$, formula (3.26) gives $t_n^* = 3{,}358{,}531$, leading to the maximum execution time of up to

[1] Keeping m and $\kappa = m^{q+1}/n$ fixed, from formulas (3.24) and (3.26) we find $\lim_{q\to\infty} t_n^* = (m^m/m!)\log(1/\delta)$. For example, for $m = 5$ as in Table 3.4 and $\delta = 0.001$, this limiting value specialises to 179.8895

0.001 second. Thus, the sampler becomes progressively more efficient for larger q, even under a crude time bound. On the other hand, as pointed out in Remarks 3.2 and 3.3, additional information about the size of the corresponding partition spaces would allow a significant reduction of the estimated bound as illustrated in Table 3.4 (by a factor 10^{10} for $q = 1$ and about 4,790 for $q = 2$).

Let us now look at the real time computational cost due to the internal loop. As mentioned before (cf. (3.38)), the expected numbers of internal runs until collecting exactly m parts is asymptotically given by $\mu_1^{-m} m!\, \mathrm{e}^{\mu_1}$ (with $\theta = 1$), where $\mu_1 = m\, G_{1/q}(m/q)$. Using for numerical illustration the same values of q, n and m as in Table 3.4, this formula yields 5.6993 ($q = 1$) and 5.7043 ($q = 2$). The average computing time for each of such attempts is inversely proportional to the CPU base frequency (such as 3.30 GHz), but it involves many other important aspects such as the operational efficiency of a random number generator, design of memory allocation and data storage, numerical precision, coding implementation and compiler used, and the overall architecture of the computer (e.g., the number of cores and whether or not parallel processing was utilised). Thus, it is impossible to estimate the actual computing time without real benchmarking.

To test the performance of the internal loop, we implemented the algorithm on a desktop CPU as described at the beginning of Section 3, for simplicity using a single core. Since internal runs are independent from each other and the computational costs due to the multi-core design are negligible, we can roughly divide the average execution time on a single core by the number of cores at disposal. Cores only require to communicate once a sampling attempt meet the target in order to stop the program.

With the same values of q, n and m used above and in Table 3.4 (and with $\theta = 1$), the average number of sampling attempts (starting at line 7 of Algorithm 2) was 5.6956 for $q = 1$ and 5.6404 for $q = 2$; note that these sample averages match the expected values calculated above. Furthermore, the program took on average $2.1036 \cdot 10^{-3}$ seconds ($q = 1$) and $0.9780 \cdot 10^{-4}$ seconds ($q = 2$) per single successful completion of the internal loop. The corresponding number of ticks of the CPU clock per elementary check of a candidate part $\ell \le n$ (see formula (3.38)) is evaluated as $(2.1036 \cdot 10^{-3}/(5.6956 \cdot 2\,500)) \cdot 3.30 \cdot 10^9 \doteq 487.5258$ ($q = 1$) and $(0.9780 \cdot 10^{-4}/(5.6404\,\sqrt{12\,500})) \cdot 3.30 \cdot 10^9 = 511.7854$, so it stays in the range about $450 \div 550$.

However, there is a problem: if we combine the physical times benchmarked for the internal loop with the time bounds t_n^* for the external loop given in Table 3.4 (say, with tolerance $\delta = 0.001$), then for $q = 1$ we obtain, by converting seconds to minutes, hours, days and years, $2.1036 \cdot 10^{-3} \cdot 2.581056 \cdot 10^{14}/(60 \cdot 60 \cdot 24 \cdot 365) \approx 17{,}217$ years (!), which is clearly impractical. For $q = 2$, a similar calculation gives a more reasonable estimate, $0.9780 \cdot 10^{-4} \cdot 596\,061\,438/(60 \cdot 60) \approx$ 16 hours. But with the improved time bounds $\tilde{t}_n^*$ (see Table 3.4), we obtain much

more satisfactory estimates, $2.1036 \cdot 10^{-3} \cdot 19\,029.61 \approx 40$ seconds ($q = 1$) and $0.9780 \cdot 10^{-4} \cdot 124\,456.8 \approx 12$ seconds ($q = 2$).

3.3. Statistical number theory

3.3.1. Test of partitionability

Having some control over the acceptance rate of sampling procedures based on the Boltzmann distribution, we can use such procedures to design statistical tests of the null hypothesis of the form $H_0 \colon \check{\Lambda}^p(n, m) \neq \varnothing$. This idea bears similarities with Monte Carlo primality tests such as the Miller–Rabin algorithm [62, 73] or the Solovay–Strassen algorithm [80]. In both of these algorithms, under the null hypothesis that the number being tested is multiplicatively composite (i.e., non-prime), a suitable algorithmic procedure attempts to confirm this hypothesis. with a "low" error probability. It involves,

- a null hypothesis: if H_0 is true, the tested number n is composite,
- a single test procedure: take a random number $b < n$, and perform a congruence test. Assuming H_0, there are two outcomes:
  - b is a *witness*: the test confirms the hypothesis H_0,
  - b is a *liar*: H_0 is true but the test cannot confirm it. This is a *Type I error*. The probability of this event is less than 50% for the Solovay–Strassen algorithm and less than 25% for the Miller–Rabin algorithm
- multiple tests : successive numbers $b_1, \cdots, b_k$ are sampled and the test procedure is applied to each number. It effectively reduces the probability of Type I error to less than 2^{-k} for the Solovay–Strassen algorithm and 4^{-k} for the Miller–Rabin algorithm. The value of k can be set to have a probability of Type I error below an arbitrary small threshold $\delta > 0$ by taking $k \geq \log(\delta)/\log(0.5)$ or $k \geq \log(\delta)/\log(0.25)$ respectively.

Since we have prior knowledge about the weight and length marginals for the Boltzmann distribution, we can test the hypothesis $H_0 \colon \check{\Lambda}^p(n, m) \neq \varnothing$ by iterating a Boltzmann sampler. Similarly to the primality tests that we have mentioned, assuming that H_0 is true, there are two possible outcomes. Either it is a *success*, in the sense that the sampler has produced an element of $\check{\Lambda}^p(n, m)$ or a *failure* (Type I error). The test can be optimised for our specific purpose as we do not need conditional uniformity of the Boltzmann distribution or to have a non-biased sampler. It is only required to provide a sampler with success probability

Algorithm 3: `TweakedSampler`

Input: z_1, z_2, ℓ^*, n, m, q
Output: Partition $\lambda \in \check{\Lambda}^q$.

integer array $\lambda_{[\,]}$;
$\ell \leftarrow 1$;
while $M_\lambda < m$ *and* $\ell^p \leq n - N_\lambda$ *and* $\ell \leq \ell^*$ **do**
  $\nu_{\ell^p} \leftarrow \mathtt{Ber}(z_1^{j^p} z_2/(1 + z_1^{\ell^p} z_2))$;
  $\ell \leftarrow \ell + 1$;
end
return λ;

bounded below by the Boltzmann distribution. This can be implemented e.g. using Algorithm 3.

We have integrated this sampler in a multithreaded code derived from procedure (T1) provided in Appendix D.3. The purpose of this code is, given numbers L, ℓ, q, m and δ to indicate which numbers between ℓ and L can be partitioned into m parts that are q-th powers with significance level δ. The main components of the code are:

- the sampler,
- the *single test* function. It tests if a given number is partitionable and, as a byproduct, produces a table indicating partitions of smaller numbers into m, q-th powers. To optimise the process, independent samples are realised in parallel with time limits t^* divided by the number of cores of the CPU. Each core produces a table and once all cores have executed their task the tables are combined into a single table returned by the function,
- the *multiple test* function. For k from L down to ℓ, if k has not been partitioned yet, the multiple test function calls instances of the single test function with targeted weight k.

This program can be used to tackle variants of the Gauss circle problem and of the Waring problem. It can be used to evaluate the first term of sequences of partitionable numbers or their density. In future work we plan to provide further optimisation of this approach. Notably, in the multiple test it appears to be inefficient to go down from L to l by steps of 1 as it will lead to almost identical calibration. It would increase the efficiency while maintaining an adequate significance level to have a variable step.

This design was implemented in Python. While it typically offers slower single core performances compared to C, it allows to easily implement functionalities

and simplifies the design of a scalable code via the multiprocessing package that ultimately allows to exceed the performance of a single core code in C. A sample code is given in Appendix D.3.

3.3.2. Number of partitions

As we have seen, checking the partitionability of a given – large – number n is a potential application of rejection sampling. Here we discuss how to use rejection sampling as a tool to obtain more information about the counting sequence through a heuristic approach. The formulas that we derive are not proven rigorously, this section should be treated as a proof of concept.

Let us fix q and m and consider that n goes to infinity. We denote by $(n_k)_{k\in\mathbb{N}}$ the sequence of numbers that can be partitioned into m distinct q-th powers. We assume that we can define a *normal order* ρ for the count of the partitionable numbers, i.e.

$$\rho : x \in \mathbb{R} \mapsto \rho(x) \sim \#\{k \ : \ n_k \leq x\}. \tag{3.44}$$

We also assume that ρ is C^1 and strictly increasing. We observe that the sequence $(y_k)_{k\in\mathbb{N}}$ defined $y_k = \rho(n_k)$ is uniformly spread in the following sense

$$\#\{k \ : \ y_k \leq x\} = \#\{k \ : \ n_k \leq \rho^{-1}(x)\} \sim \rho(\rho^{-1}(x)) = x. \tag{3.45}$$

For instance if $m = 1$, we have $n_k = k^2$ and we can take the normal order $\rho(x) = \sqrt{x}$. If $m = 2$ and $q = 2$, a result by Landau and Ramanujan [51] states that we can take the normal order $\rho(x) = Kx/\sqrt{\log x}$, where $K \doteq 0.764223653$.

Subsequently we will write $g(n) := \mathsf{P}_{\boldsymbol{z}}(N_\lambda = n \mid M_\lambda = m)$ and $\gamma_0 = m/(qn)$. For $0 < a < b$ we have

$$\begin{aligned}\mathsf{P}_{\boldsymbol{z}}(a/\gamma_0 \leq N_\lambda \leq b/\gamma_0 \mid M_\lambda = m) &= \sum_{a/\gamma_0 \leq n_k \leq b/\gamma_0} g(n_k) \sim \sum_{\rho(a/\gamma_0) \leq y_k \leq \rho(b/\gamma_0)} g(\rho^{-1}(y_k)) \\ &\sim \int_{\rho(a/\gamma_0)}^{\rho(b/\gamma_0)} g(\rho^{-1}(y))\ \mathrm{d}y = \int_{a/\gamma_0}^{b/\gamma_0} g(x)\rho'(x)\ \mathrm{d}x \\ &= \frac{1}{\gamma_0} \int_a^b g(u/\gamma_0)\rho'(u/\gamma_0)\ \mathrm{d}u.\end{aligned}$$

Moreover, according to Theorem 2.26, we have

$$\mathsf{P}_{\boldsymbol{z}}(a/\gamma_0 \leq N_\lambda \leq b/\gamma_0 \mid M_\lambda = m) \sim \frac{1}{\Gamma(\alpha)} \int_a^b u^{\alpha-1}\mathrm{e}^{-u}\,\mathrm{d}u.$$

As a first guess, we may identify

$$g(u/\gamma_0) \sim \frac{u^{\alpha-1}\mathrm{e}^{-u}}{\Gamma(\alpha)} \cdot \frac{\alpha}{n\rho'(u/\gamma_0)}, \tag{3.46}$$

so by taking $u = \alpha$, we obtain

$$\mathsf{P}_{\boldsymbol{z}}(N_\lambda = n \mid M_\lambda = m) \sim \frac{\alpha^\alpha \mathrm{e}^{-\alpha}}{\Gamma(\alpha)} \cdot \frac{1}{n\rho'(n)}, \tag{3.47}$$

this does not account for potential fluctuations as we observe a disparity in the number of partitions, even between numbers that are partitionable. This can be observed in the effective success rate of the Boltzmann sampler for reaching an exact target. While the density of partitionable numbers and the success rates are related, our observations suggest that we should we can distinguish more classes of "partitionability" (see the Landau–Ramanujan case in Figure 3.4). In general we may not know a normal order ρ, however we can assume that $0 \leq \rho' \leq 1$ since the count of partitionable number cannot increase by more than one between two successive integers. Thus, in the absence of further information about ρ we may use the following estimate

$$\mathsf{P}_{\boldsymbol{z}}(N_\lambda = n \mid M_\lambda = m) \gtrsim \frac{\alpha^\alpha \mathrm{e}^{-\alpha}}{n\Gamma(\alpha)}. \tag{3.48}$$

Figures 3.3 and 3.4 appear to be consistent with equations (3.47) and (3.48).

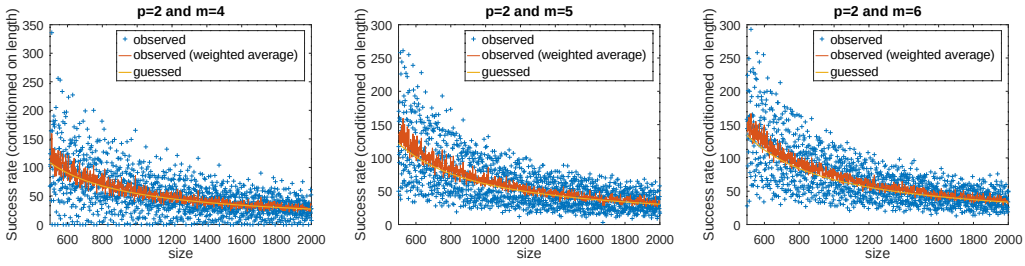

Figure 3.3: Observed size success rates per 10^5 samples in full density cases.

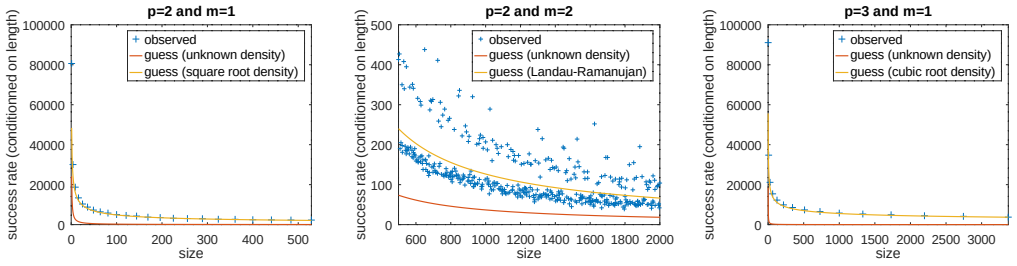

Figure 3.4: Comparison of observed size success rates per 10^5 samples in known density cases.

Chapter 4

Limit shape in occupancy models

It is common to classify data into multiple classes (or "boxes"), and to analyse the frequency of occurrence of each class in a given experiment. Assuming that the classes are countable and labelled by natural numbers we may provide a sequences of frequencies $(f_j, j \in \mathbb{N})$ (positive and normalised). For instance, here we are interested in parts size distribution. In Chapter 2, we observed that a part j is expected to occur with a geometric frequency.

In an occupancy model, a number of sources M are distributed independently among the classes according to the frequency distribution. One way to produce a partition using an occupancy model is presented in [36] and consist in ignoring the distinction between the classes and taking as parts the number of elements that fall into each boxes, thus giving a partition of M into a random number of parts. Alternately, if the classes are the natural numbers, a natural way to produce a partition is to take the result of each source as a part. This is the approach discussed in [14] under the name of "item production model" in the context of scientometrics. We will take the latter approach. Contrary to [14] where the number of parts is deterministic, we allow it to be random.

In Section 4.1, we describe formally the general framework to produce a partition with an occupancy model with a random number of sources. In Section 4.2 we detail how to obtain limit results for the Young diagram produced in this framework. While the Rayleigh distribution is used here, for illustration purposes and convenience, the results obtained in this section are generalisable to frequency distributions based on families of continuous distributions with a scale parameter.

The independence of sources in occupancy models means that there is no restriction of multiplicities; however, we can easily impose a restriction of the maximal multiplicity of a part by applying a projection. In particular, in Section 4.3 , we observe that we can reproduce the Boltzmann distribution over a class of strict partitions (or even more generally over a powerset) using this approach.

4.1. Occupancy models

Let M be a random variable with values in $\mathbb{N}_0$ and finite expectation $\langle M \rangle := \mathsf{E}(M)$. Independently of M, consider an infinite assembly of independent random variables (X_i) with common distribution $(f_j)_{j\in\mathbb{N}}$

$$f_j := \mathsf{P}(X_i = j) \qquad (j \in \mathbb{N}). \tag{4.1}$$

We assume that $\mathsf{E}(X_i) < \infty$. We can thus define a random variable in the partition space Λ with the following multiplicities

$$\nu_j := \sum_{i=1}^{M} \mathbf{1}_{\{X_i=j\}} = \#\{X_i = j,\, i = 1, \ldots, M\} \qquad (j \in \mathbb{N}). \tag{4.2}$$

The expected length of the said partition is $\langle M \rangle$ and its expected weight is

$$\mathsf{E}(N) = \langle M \rangle \, \mathsf{E}(X_i) \tag{4.3}$$

in accordance with Wald's identity (see [78, Sec. VII.3, Theorem 3, p. 488, and Sec. I.9, Problem 5, p. 83] for instance)).

Conditionally on M, the multiplicity ν_j follows the binomial distribution with M trials and success probability f_j,

$$\mathsf{P}(\nu_j = m \,|\, M) = \binom{M}{m} (f_j)^m (1 - f_j)^{M-m} \quad (m = 0, \ldots, M). \tag{4.4}$$

While it is clear that the multiplicities are not independent as in the Boltzmann model, we can still use the independence of the $\mathbf{1}_{\{X_i=j\}}$ across the i index. We can also use these variables to represent the Young diagram

$$Y(x) = \sum_{j\geq x} \nu_j = \sum_{j\geq x} \sum_{i=1}^{M} \mathbf{1}_{\{X_i=j\}} = \sum_{i=1}^{M} \mathbf{1}_{\{X_i\geq x\}}, \tag{4.5}$$

where the indicators $\mathbf{1}_{\{X_i\geq j\}}$ are independent identically distributed Bernoulli random variables with

$$\mathsf{P}(\mathbf{1}_{\{X_i\geq j\}} = 1) = \sum_{j\geq x} f_j =: \bar{F}(x), \qquad \mathsf{P}(\mathbf{1}_{\{X_i\geq j\}} = 0) = \sum_{j<x} f_j =: F(x) \tag{4.6}$$

In practice we may have to determine a frequency distribution based on a continuous density $f(x)$, for $x \in \mathbb{R}_+$. We can obtain a frequency distribution for the parts in the following way

$$f_j = \frac{f(j)}{\sum_{\ell\in\mathbb{N}} f(\ell)}, \qquad j \in \mathbb{N}. \tag{4.7}$$

4.2. Rayleigh distribution

In this section, we confine ourselves to a specific example based on the Rayleigh distribution, with the aim to illustrate how one can derive scaling limit results in such models. Consider the following continuous model,

$$f(x) = \frac{x}{\sigma^2}\, \mathrm{e}^{-x^2/(2\sigma^2)}, \qquad x \in \mathbb{R}_+, \tag{4.8}$$

where the scale parameter σ is strictly positive. Define the frequency distribution as in equation (4.7). For convenience, set

$$\gamma := \frac{1}{2\sigma^2}, \tag{4.9}$$

thus rewriting (4.8) in the form

$$f(x) = 2\gamma x\, \mathrm{e}^{-\gamma x^2}, \tag{4.10}$$

This makes it easier to use the sum asymptotics lemmas from Chapter 2.

We start by establishing a series of technical lemmas.

Lemma 4.1. *When σ goes to infinity, the expectation of the multiplicities is given by*

$$\mathsf{E}(\nu_j) = \langle M \rangle\, f(j)(1 + O(\gamma^{1/2})). \tag{4.11}$$

Proof. By definition, conditionally on M we have

$$\mathsf{E}(\nu_j \,|\, M) = M\, \frac{f(j)}{\sum_{j\in\mathbb{N}} 2\gamma j \mathrm{e}^{-\gamma j^2}}.$$

Using Lemma 2.14

$$\sum_{j\in\mathbb{N}} 2\gamma j \mathrm{e}^{-\gamma j^2} = 2\gamma \sum_{\ell\in\mathbb{N}^2} \ell^{1/2} \mathrm{e}^{-\gamma \ell} = 1 + O(\gamma^{1/2}), \tag{4.12}$$

thus

$$\mathsf{E}(\nu_j \,|\, M) = M f(j) \left(1 + O(\gamma^{1/2})\right). \tag{4.13}$$

By the total expectation rule, we have

$$\mathsf{E}(\nu_j) = \mathsf{E}\big(\mathsf{E}(\nu_j \,|\, M)\big) = \langle M \rangle\, f(j) \left(1 + O(\gamma^{1/2})\right), \tag{4.14}$$

and the claim follows. □

Lemma 4.2. *We define the following rescaled Young diagram*

$$\widetilde{Y}(x) = \frac{Y(\sigma x)}{\langle M \rangle}. \tag{4.15}$$

When σ goes to infinity, for all $x \geq 0$

$$\mathsf{E}(\widetilde{Y}(x)) = \mathrm{e}^{-x^2/2}(1 + O(\gamma^{1/2})) \tag{4.16}$$

Proof. Conditionally on M, we have

$$\mathsf{E}\big(\widetilde{Y}(x) \,|\, M\big) = \frac{1}{\langle M \rangle} \mathsf{E}(Y(\sigma x) \,|\, M) = \frac{1}{\langle M \rangle} \mathsf{E}\left(\sum_{j \geq \sigma x} \sum_{i=1}^{M} \mathbf{1}_{\{X_i = j\}} \,\middle|\, M \right).$$

Recall that (X_i) are i.i.d. and that $\mathbf{1}_{\{X_i \geq \sigma x\}}$ follows a Bernoulli distribution. According to Lemmas 2.14 and 2.16

$$\begin{aligned} \mathsf{P}(X_i \geq \sigma x) = \sum_{j \geq \sigma x} f_j &= \frac{\sum_{\ell \geq x^2/(2\gamma), \ell \in \mathbb{N}^2} \ell^{1/2} \mathrm{e}^{-\gamma \ell}}{\sum_{\ell \in \mathbb{N}^2} \ell^{1/2} \mathrm{e}^{-\gamma \ell}} \\ &= \frac{\Gamma(1, x^2/2)(1 + O(\gamma^{1/2}))}{1 + O(\gamma^{1/2})} = \mathrm{e}^{-x^2/2} \left(1 + O(\gamma^{1/2})\right), \end{aligned}$$

so we have

$$\mathsf{E}\big(\widetilde{Y}(x) \,|\, M\big) = \frac{M}{\langle M \rangle} \sum_{j \geq \sigma x} f_j.$$

The proof concludes by using the total expectation rule. □

Lemma 4.3. *When σ goes to infinity, for all $x \geq 0$, the variance of the scaled Young diagram is given by*

$$\mathsf{Var}\big(\widetilde{Y}(x)\big) = \left(\frac{1}{\langle M \rangle} \mathrm{e}^{-x^2/2} \big(1 - \mathrm{e}^{-x^2/2}\big) + \frac{\mathsf{Var}(M)}{\langle M \rangle^2} \mathrm{e}^{-x^2/2} \right) \big(1 + O(\gamma^{1/2})\big). \tag{4.17}$$

Proof. Using the representation of Young diagrams via the variables $\mathbf{1}_{\{X_i \geq \sigma x\}}$, and applying the total variance rule, we have

$$\begin{aligned} \mathsf{Var}(\widetilde{Y}(x)) &= \frac{1}{\langle M \rangle^2} \mathsf{Var}\left(\sum_{i=1}^{M} \mathbf{1}_{\{X_i \geq \sigma x\}} \right) \\ &= \frac{1}{\langle M \rangle^2} \left[\mathsf{E}\left(\mathsf{Var}\left(\sum_{i=1}^{M} \mathbf{1}_{\{X_i \geq \sigma x\}} \middle| M \right) \right) + \mathsf{Var}\left(\mathsf{E}\left(\sum_{i=1}^{M} \mathbf{1}_{\{X_i \geq \sigma x\}} \middle| M \right) \right) \right]. \end{aligned}$$

Again using independence of the random variables X_i and observing that

$$\mathsf{P}(\mathbf{1}_{\{X_i \geq \sigma x\}} = 1) = \mathrm{e}^{-x^2/2}(1 + O(\gamma^{1/2})),$$

we obtain

$$\begin{aligned}\mathsf{E}\left(\mathsf{Var}\left(\sum_{i=1}^{M} \mathbf{1}_{\{X_i \geq \sigma x\}} \,\middle|\, M\right)\right) &= \mathsf{E}\left(M\,\mathsf{Var}(\mathbf{1}_{\{X_i \geq \sigma x\}})\right) \\ &= \langle M \rangle\, \mathrm{e}^{-x/2}(1 - \mathrm{e}^{-x^2/2})\left(1 + O(\gamma^{1/2})\right)\end{aligned}$$

and, similarly,

$$\begin{aligned}\mathsf{Var}\left(\mathsf{E}\left(\sum_{i=1}^{M} \mathbf{1}_{\{X_i \geq \sigma x\}} \,\middle|\, M\right)\right) &= \mathsf{Var}(M\ \mathrm{e}^{-x^2/2})\left(1 + O(\gamma^{1/2})\right) \\ &= \mathsf{Var}(M)\ \mathrm{e}^{-x^2/2}\left(1 + O(\gamma^{1/2})\right),\end{aligned}$$

and the lemma is proved. □

Observe that the variance of the scaled Young diagram goes to zero uniformly in any asymptotic regime that satisfies the following

Assumption 4.1.

$$\langle M \rangle \to \infty, \quad \sigma \to \infty, \quad \mathsf{Var}(M) = o(\langle M \rangle^2). \tag{4.18}$$

Theorem 4.4. *Under Assumption 4.1, for any* $\varepsilon > 0$

$$\sup_{x \geq 0} \mathsf{P}\big(|\widetilde{Y}(x) - \mathrm{e}^{-x^2/2}| \geq \varepsilon\big) \to 0. \tag{4.19}$$

Proof. Due to equation (4.15), it suffices to show that

$$\sup_{x \geq 0} \mathsf{P}\left(|\widetilde{Y}(x) - \mathsf{E}(\widetilde{Y}(x))| \geq \varepsilon\right) \to 0.$$

Due to the Bienaymé–Chebyshev inequality and equation (4.17), we have, uniformly in $x \geq 0$,

$$\begin{aligned}\mathsf{P}\left(|\widetilde{Y}(x) - \mathsf{E}(\widetilde{Y}(x))| \geq \varepsilon\right) &\leq \frac{\mathsf{Var}(\widetilde{Y}(x))}{\varepsilon^2} \\ &\leq \frac{1}{\varepsilon^2}\left(\frac{1}{\langle M \rangle} + \frac{\mathsf{Var}(M)}{\langle M \rangle^2}\right)\left(1 + O(\gamma^{1/2})\right),\end{aligned}$$

and the claim follows by virtue of Assumption 4.1. □

Theorem 4.5. *Under Assumption 4.1, for all $\varepsilon > 0$,*

$$\mathsf{P}\left(\sup_{x\geq 0}\left|\widetilde{Y}(x) - \frac{M}{\langle M\rangle}\mathrm{e}^{-x^2/2}\right| \geq \varepsilon\right) \to 0. \tag{4.20}$$

Proof. We follow the proof scheme of [14, Theorem 4.1] introducing an auxiliary martingale W in order to apply the Doob–Kolmogorov inequality [93, Theorem 6.16]. This involves minor changes due to the randomness of M. This proof scheme bears similarities with the proof of Theorem 2.44. Instead of directly considering the Young diagram, we consider a process indexed by the inverse of its argument.

$$Z_i(t) := \frac{\mathbf{1}_{\{X_i<1/t\}}}{F(1/t)}, \qquad t \geq 0. \tag{4.21}$$

By definition, the expectation and the variance of the $Z_i(t)$ are given by

$$\mathsf{E}(Z_i(t)) = 1, \qquad \mathsf{Var}(Z_i(t)) = \frac{\bar{F}(1/t)}{F(1/t)}. \tag{4.22}$$

We define the following process

$$W(t) := \sum_{i=1}^{M}(Z_i(t) - 1). \tag{4.23}$$

Conditionally on M, the expectation and variance of $W(t)$ are given by

$$\mathsf{E}(W(t)\,|\,M) = 0, \qquad \mathsf{Var}(W(t)\,|\,M) = \frac{M\bar{F}(1/t)}{F(1/t)}, \tag{4.24}$$

hence

$$\mathsf{E}(W(t)) = 0, \qquad \mathsf{Var}(W(t)) = \frac{\langle M\rangle\,\bar{F}(1/t)}{F(1/t)}. \tag{4.25}$$

Claim. The process W is a martingale with respected to the natural filtration $\mathcal{F}$ generated by the processes $(Z_i)_{n\in\mathbb{N}}$ and M.

Let us check this claim. For $0 \leq s \leq t$ we have

$$\mathsf{E}(W(t)\,|\,\mathcal{F}(s)) = \mathsf{E}\left(\sum_{i=1}^{M}(Z_i(t) - 1)\,\middle|\,\mathcal{F}(s)\right) \tag{4.26}$$

$$= \left(\sum_{i=1}^{M}\mathsf{E}(Z_i(t)\,|\,\mathcal{F}_i(s))\right) - M, \tag{4.27}$$

where the $\mathcal{F}_i$, $i \in \mathbb{N}$, denote the natural filtration associated to the processes Z_i. In particular, in order to prove that W is a martingale, it is sufficient to that the Z_i are martingales i.e. we need to check the following

$$\mathsf{E}(Z_i(t) \,|\, \mathcal{F}(s)) = Z_i(s). \tag{4.28}$$

By definition $\mathcal{F}_i(s)$ indicates whether or not $X_i < 1/s$ so it suffices to compute the expectation of $Z_i(t)$ conditionally on the realisation or the non-realisation of this event.

$$\begin{aligned}
\mathsf{E}(Z_i(t) \,|\, X_i < 1/s) &= \mathsf{E}(\mathbf{1}_{\{X_i<1/t\}}/F(1/t) \,|\, X_i < 1/s) \\
&= \frac{\mathsf{P}(X_i < 1/t \,|\, X_i < 1/s)}{F(1/t)} = \frac{\mathsf{P}(X_i < 1/t)}{F(1/t)\mathsf{P}(X_i < 1/s)} \\
&= \frac{1}{F(1/s)} = Z_i(s),
\end{aligned}$$

and $\mathsf{E}(Z_i(t) \,|\, X_i \geq 1/s) = 0$ since the events $X_i < 1/t$ and $X_i \geq 1/s$ are mutually exclusive. This concludes the proof that W is a martingale with respect to the filtration $\mathcal{F}$. Now we have the elements to prove the theorem. First, note that it is equivalent to proving the following:

$$\mathsf{P}\left(\sup_{x\geq 0}\left|\widetilde{Y}(x) - \frac{M}{\langle M\rangle}\bar{F}(\sigma x)\right| \geq \varepsilon\right) \to 0.$$

We have

$$\begin{aligned}
\widetilde{Y}(x) - \frac{M}{\langle M\rangle}\,\bar{F}(\sigma x) &= \frac{1}{\langle M\rangle}\sum_{i=1}^{M}\big(\mathbf{1}_{\{X_i\geq\sigma x\}} - \bar{F}(\sigma x)\big) \\
&= \frac{1}{\langle M\rangle}\sum_{i=1}^{M}(-\mathbf{1}_{\{X_i<\sigma x\}} + F(\sigma x)) = -\frac{F(\sigma x)}{\langle M\rangle}\,W(1/(\sigma x)).
\end{aligned}$$

Let $\delta > 0$. Applying the Doob–Kolmogorov inequality to the martingale W yields

$$\begin{aligned}
\mathsf{P}\left(\sup_{x\geq\delta}\left|\widetilde{Y}(x) - \frac{M}{\langle M\rangle}\bar{F}(\sigma x)\right| \geq \varepsilon\right) &\leq \mathsf{P}\left(\sup_{t\leq 1/(\sigma\delta)}|W(t)| \geq \langle M\rangle\,\varepsilon\right) \\
&\leq \frac{\mathsf{Var}(W(1/(\sigma\delta)))}{\langle M\rangle^2\,\varepsilon^2} \\
&= \frac{\bar{F}(1/(\sigma\delta))}{\langle M\rangle\,F(1/(\sigma\delta))\varepsilon^2} \sim \frac{\mathrm{e}^{-\delta^2/2}}{\langle M\rangle\,\varepsilon^2} \leq \frac{1}{\langle M\rangle\,\varepsilon^2}.
\end{aligned}$$

This concludes the proof, since this bound is independent of δ. □

Remark 4.6. We did not state

$$\mathsf{P}\left(\sup_{x\geq 0}\left|\widetilde{Y}(x)-\mathrm{e}^{-x^2/2}\right|\geq\varepsilon\right)\to 0, \tag{4.29}$$

as it would involve the following less tractable decomposition

$$\widetilde{Y}(x)-\mathrm{e}^{-x^2/2}=\frac{1}{\langle M\rangle}\sum_{i=1}^{M}\left(\mathbf{1}_{\{X_i\leq x\}}-\frac{\langle M\rangle\,\bar{F}(x)}{M}\right).$$

Theorem 4.7. *Assume that M is deterministic. When M and σ go to infinity. We have the following convergence in law*

$$Y^*(x):=\frac{\sqrt{M}\left(\widetilde{Y}(x)-\mathsf{E}(\widetilde{Y}(x))\right)}{\sqrt{\mathrm{e}^{-x^2/2}(1-\mathrm{e}^{-x^2/2})}}\xrightarrow{d}\mathcal{N}(0,1). \tag{4.30}$$

Proof. The proof is similar to the proof of the classical central limit theorem. First of all, let us make the following decomposition

$$Y(\sigma x)-\mathsf{E}(Y(\sigma x))=\sum_{i=1}^{M}\left(\mathbf{1}_{\{X_i\geq\sigma x\}}-\bar{F}(\sigma x)\right).$$

This is a sum of M i.i.d. random variables with expectation equal to zero and with variance

$$F(\sigma x)\bar{F}(\sigma x)=\mathrm{e}^{-x^2/2}(1-\mathrm{e}^{-x^2/2})(1+O(\gamma^{1/2})).$$

The characteristic function of each term $\mathbf{1}_{\{X_i\geq\sigma x\}}-\bar{F}(\sigma x)$ is given by

$$\mathsf{E}\left(\exp \mathrm{i}t\left(\mathbf{1}_{\{X_i\geq\sigma x\}}-\bar{F}(\sigma x)\right)\right)=1-\frac{t^2}{2}\,\mathrm{e}^{-x^2/2}(1-\mathrm{e}^{-x^2/2})(1+O(\gamma^{1/2}))+o(t^2).$$

Thus, the characteristic function of $Y^*(x)$ is

$$\begin{aligned}\mathsf{E}(Y^*(x))&=\mathsf{E}\left(\exp\left[\frac{\mathrm{i}t(Y(\sigma x)-\mathsf{E}(Y(\sigma x)))}{\sqrt{M\mathrm{e}^{-x^2/2}(1-\mathrm{e}^{-x^2/2})}}\right]\right)\\&=\mathsf{E}\left(\exp\left[\frac{\mathrm{i}t\left(\mathbf{1}_{\{X_1\geq\sigma x\}}-\bar{F}(\sigma x)\right)}{\sqrt{M\mathrm{e}^{-x^2/2}(1-\mathrm{e}^{-x^2/2})}}\right]\right)^M\\&=\left(1-\frac{t^2}{2M}(1+O(\gamma^{1/2}))+o(t^2/M)\right)^M,\end{aligned}$$

which converges to $\exp(-t^2/2)$ when σ and M go to infinity. □

We can refine this result allowing M to be random, although it requires to center the Young diagram using the expectation conditionally on M in order to keep a similar proof scheme. While this proof is more tedious, it only differs from the previous one in that it requires to segregate rare events (M too small relatively to $\langle M\rangle$) in order to provide estimates.

Theorem 4.8. *Under Assumption 4.1, we have the following convergence in law*

$$Y^*(x) := \frac{\sqrt{M}\left(\widetilde{Y}(x) - \mathsf{E}(\widetilde{Y}(x)\,|\,M)\right)}{\sqrt{\mathrm{e}^{-x^2/2}(1-\mathrm{e}^{-x^2/2})}} \xrightarrow{d} \mathcal{N}(0,1). \tag{4.31}$$

Proof. Let us estimate the characteristic function of $Y^*(x)$

$$\begin{aligned}&\mathsf{E}\left(\exp\left(\mathrm{i}tY^*(x)\right)\right)\\ &\quad=\sum_{m=0}^{\infty}\mathsf{P}(M=m)\;\mathsf{E}\left(\exp(\mathrm{i}\tilde{t}(m)[Y(\sigma x)-\mathsf{E}(Y(\sigma x)\,|\,M=m)]\,|\,M=m\right)\end{aligned}$$

where

$$\tilde{t}(m) := \frac{\sqrt{m}}{\sqrt{\mathrm{e}^{-x^2/2}(1-\mathrm{e}^{-x^2/2})}}.$$

Thus we can write

$$\mathsf{E}\left(\exp(\mathrm{i}tY^*(x))\right) = \sum_{m=0}^{\infty}\mathsf{P}(M=m)\;\mathsf{E}\left(\exp\left(\mathrm{i}\tilde{t}\left[\mathbf{1}_{\{X_1\geq\sigma x\}} - \sum_{j\geq\sigma x} f_j\right]\right)\right)^m.$$

We separate this sum in two parts, with $m \leq \lfloor\langle M\rangle/2\rfloor$ and with $m > \lfloor\langle M\rangle/2\rfloor$. In the second part, we can argue as in the previous proof since $\lfloor\langle M\rangle/2\rfloor$ goes to infinity and we need to verify that the first part is asymptotically negligible.

For the first part, using the Bienaymé–Chebyshev inequality we obtain

$$\begin{aligned}&\left|\sum_{m=0}^{\lfloor\langle M\rangle/2\rfloor}\mathsf{P}(M=m)\;\mathsf{E}\left(\exp\left(i\tilde{t}\left[\mathbf{1}_{\{X^1\geq\sigma x\}} - \sum_{j\geq\sigma x} f_j\right]\right)\right)^m\right|\\ &\qquad\leq\sum_{m=0}^{\lfloor\langle M\rangle/2\rfloor}\mathsf{P}(M=m)\leq\mathsf{P}\left(|M-\langle M\rangle|\geq\frac{\langle M\rangle}{2}\right)\leq\frac{4\;\mathsf{Var}(M)}{\langle M\rangle^2}\to 0.\end{aligned}$$

For the second part, we can use the theorem for deterministic M as in each term m goes to infinity

$$\begin{aligned}&\sum_{m=\lfloor\langle M\rangle/2\rfloor+1}^{\infty}\mathsf{P}(M=m)\;\mathsf{E}\left(\exp\left(\mathrm{i}\tilde{t}\left[\mathbf{1}_{\{X_1\geq\sigma x\}} - \sum_{j\geq\sigma x} f_j\right]\right)\right)^m\\ &\qquad\sim\exp(-t^2/2)\sum_{m=\lfloor\langle M\rangle/2\rfloor+1}^{\infty}\mathsf{P}(M=m)\sim\exp(-t^2/2)\end{aligned}$$

□

4.3. Mapping to a strict partition model

The model discussed so far has the flexibility to produce any frequency distribution, but it is not suitable for classes of partitions with restricted multiplicities. In order to obtain strict partitions, we consider a modified model where we keep only one iteration of each part produced at least once in the initial occupancy model, thus defining the following multiplicities

$$\check{\nu}_\ell := \mathbf{1}_{\{\nu_\ell \geq 1\}}, \qquad \ell \in \mathbb{N}. \tag{4.32}$$

In this model, conditionally on M, the multiplicities $\check{\nu}_\ell$ follow the Bernoulli distribution with success probability

$$\mathsf{P}(\check{\nu}_\ell = 1 \,|\, M) = 1 - (1 - f_\ell)^M . \tag{4.33}$$

In particular, the unconditional success probability is related to the probability generating function of M,

$$\mathsf{P}(\check{\nu}_\ell = 1) = 1 - \sum_{m=0}^{\infty} \mathsf{P}(M = m)\,(1 - f_\ell)^m =: 1 - G_M(1 - f_\ell). \tag{4.34}$$

An interesting fact stated by the subsequent theorem is that we can reproduce the Boltzmann distribution over a class of strict partitions with this model.

Theorem 4.9. *Let $\mathbb{A}$ be a non-empty subset of $\mathbb{N}$. Let f be the frequency distribution*

$$f_\ell = \frac{\log(1 + z_1^\ell z_2)}{\log F(\boldsymbol{z})}, \qquad \ell \in \mathbb{A} \tag{4.35}$$

where F is the generating function of $PSet(\mathbb{A})$,

$$F(\boldsymbol{z}) = \prod_{\ell=1}^{\infty} (1 + z_1^\ell z_2) \tag{4.36}$$

and suppose that M follows the Poisson distribution with rate $\log(F)$. The strict partition defined by the multiplicities $(\check{\nu}_\ell)_{\ell \in \mathbb{A}}$ follows the Boltzmann distribution over $PSet(\mathbb{A})$.

Proof. Consider a subset $E = \{\ell_1, \ell_2, \dots\}$ of elements of $\mathbb{A}$. The probability that none of these are occupied is

$$\begin{aligned}\sum_{m=0}^{\infty} \mathsf{P}(M=m) \prod_{i=1}^{m} \mathsf{P}(X_i \notin E\}) &= \sum_{m=0}^{\infty} \mathsf{P}(M=m)\ \mathsf{P}(X_1 \notin E\})^m \\ &= G_M\left(1 - \sum_{k=1}^{\infty} f_\ell\right) = \exp\left[\log(F)\left(-\sum_{k=1}^{\infty} f_{\ell_k}\right)\right] \\ &= \prod_{k=1}^{\infty} \exp\left(-\log(1+z_1^{\ell_k} z_2)\right) = \prod_{k=1}^{\infty} \frac{1}{1+z_1^{\ell_k} z_2},\end{aligned}$$

which coincides with the Boltzmann distribution. Thus, the result follows thanks to the monotone class lemma. □

A consequence of this theorem is that we can design an alternative sampling scheme for the Boltzmann distribution over classes of strict partitions (or more general powersets). While it appears to provide an algorithm of complexity $O(\langle M \rangle)$, this requires to assume that we can sample each part X_i from the distribution f in a bounded time. In practice it may be necessary to approximate the generating function if $\mathbb{A}$ is infinite. More generally the multiplicities $\check{\nu}_\ell$ are still independent when M follows a Poisson distribution. For general length distribution, we can provide a simple expression of the covariance between the $\check{\nu}_\ell$ using the probability generating function of M.

Lemma 4.10. *The covariance of two multiplicities ℓ and ℓ' is given by*

$$\mathsf{Cov}(\check{\nu}_\ell, \check{\nu}_{\ell'}) = G_M(1-(f_\ell+f_{\ell'})) - G_M(1-f_\ell)\cdot G_M(1-f_{\ell'}). \tag{4.37}$$

Proof. We have

$$\mathsf{Cov}(\check{\nu}_\ell, \check{\nu}_{\ell'}) = \mathsf{E}(\check{\nu}_\ell\ \check{\nu}_{\ell'}) - \mathsf{E}(\check{\nu}_\ell)\ \mathsf{E}(\check{\nu}_{\ell'}) = \mathsf{P}(\check{\nu}_\ell = 1, \check{\nu}_{\ell'} = 1) - \mathsf{P}(\check{\nu}_\ell = 1)\ \mathsf{P}(\check{\nu}_{\ell'} = 1).$$

Furthermore,

$$\mathsf{P}(\check{\nu}_\ell = 1) = 1 - G_M(1-f_\ell), \qquad \mathsf{P}(\check{\nu}_{\ell'} = 1) = 1 - G_M(1-f_{\ell'})$$

and

$$\begin{aligned}\mathsf{P}(\check{\nu}_\ell = 1, \check{\nu}_{\ell'} = 1) &= \mathsf{P}(\check{\nu}_\ell = 1) + \mathsf{P}(\check{\nu}_{\ell'} = 1) - [1 - \mathsf{P}(\check{\nu}_\ell = 0, \check{\nu}_{\ell'} = 0)] \\ &= [1 - G_M(1-f_\ell)] + [1 - G_M(1-f_{\ell'})] \\ &\qquad - [1 - G_M(1-(f_\ell+f_{\ell'}))]\,.\end{aligned}$$

This proves the lemma. □

Chapter 5

Coalescing and fragmenting random walks of massive particles

In this chapter, we consider a continuous-time Markovian model where *particles* or *aggregates* move on an oriented graph (the *ambient space*). We assume that the aggregates are composed of *units of mass* and that the total mass (i.e., the total number of constituent units) is a constant $n \in \mathbb{N}$. The configurations of the system are the ways to distribute the mass n among the sites of the ambient space. In this model a given configuration can undergo two types of transitions:

- *Diffusion and aggregation*: at rate $\mu_x^{-\alpha}$, the total mass on site x moves and aggregates with the particle of a neighbouring site (as specified by the edges of the ambient space),
- *Chipping*: if $\mu_x > 0$, at rate $\omega\mu_x^{1+\beta}$, the site x gives a unit to a neighbouring site,

where $\alpha, \beta \in \mathbb{R}$ and $\omega \geq 0$. Models involving only diffusion and aggregation at rates independent of the mass are known as coalescing random walks. In these models the mass of the particles is usually not tracked [21]. The models involving only chipping are known as zero range processes [17]. A model involving these interactions has been considered in [58] and [59] with $\alpha = \beta = 0$. While the aggregates are simply treated as massive particles, the parameter β can be seen as a proxy for the microscopic structure of the sites and the aggregates (geometry and internal forces). Assuming that there are no internal forces bounding the units, we can take the following values of β:

- $\beta = -1$: the units stack into a linear aggregate, so only one unit at a time is subject to chipping,
- $\beta = 0$: the units can chip independently of size of the aggregate,

- $\beta = -1/d$: the units stack into a corner in d dimensions assuming that d is an integer larger than 1. For instance if $d = 2$ the aggregates can be identified to Young diagrams, if $d = 3$ they can be identified to a plane partition. If an aggregate contains a large number of units m, we may assume that the number of units at the boundary is proportional to $m^{(d-1)/d}$.

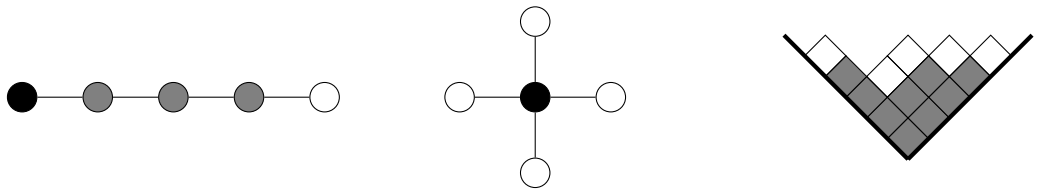

Figure 5.1: aggregate structures without internal forces with $\beta = -1; 0; 1/2$ respectively. The site is represented in black, the units that aren't subject to chipping are in grey and the units that can chip are in white.

Conversely, the parameter α accounts for a longer range interaction affecting all of the units of the sites together. We may consider a system where the sites accumulate energy at a fixed rate, the quantity μ_x^α is thus interpreted as the *activation energy* required in order to trigger a jump of the aggregate located on the site x.

The following types of problems are considered:

- *Analysis of the purely aggregating model:* in the purely aggregating case ($\alpha = 0$) the system eventually collapses to a single aggregate. We can study the times of aggregation (or equivalently, the number of aggregates as a function of time) as well as the distribution of mass between the aggregates at intermediate times. In order to find a suitable family to describe the distribution of mass as a function of the time, it is required to consider large systems in a time range that ensures that the number of aggregates is also large. We can distinguish two notions of asymptotics for the distribution of mass. A cumulative notion that arises when considering the Young diagram of an instance of the process and single aggregate mass distribution that can only be observed with many instances of the process.

- *Equilibrium distribution:* which is the distribution that balances out with the transition rates. It describes the long term behaviour of the system. It is trivial in the purely aggregating case and it becomes interesting when fragmentation is introduced, even in absence of diffusion and aggregation. This should not be confused with a thermodynamic equilibrium, which implies a state of minimal energy fluctuation and no net flow of energy, and which is described by the Boltzmann distribution. Here, interactions

may involve energy exchanges with an external environment, which are not accounted for. Therefore, even though in some cases the system may reach a ordered state, it does not contravene the second law of thermodynamics.

This chapter starts with a description of the general aggregation and fragmentation model considered here, it includes a brief review of some notions relative to continuous time Markov processes and interacting particle systems. Then in Section 5.2 we focus on the study of the purely aggregating case ($\omega = 0$) on a directed cycle of size $n \in \mathbb{N}$, assuming that the starting configuration of system contains one unit of mass per site. An essential tool for our study is a simulator which is discussed in Section 5.2.1. It has been implemented in C in Appendix D.4. We consider three particular values of α (0, -1 and 1). We observe the aggregate mass distribution when the process is stopped at a given number of aggregates. In particular, when $\alpha = 0$ the distribution of mass is well approximated by the Rayleigh distribution with parameter n/k, where n is the total mass of the system and k is the number of aggregates left (Figures 5.5 and 5.8). This is confirmed by statistical tests (Table 5.1 and Figure 5.11). It coincides with a result proven in [57] and indicates that this result may be strengthened. When $\alpha = -1$, the exponentiated Weibull distribution fitted with the maximum likelihood method appears to be a good fit (Figures 5.6 and 5.9). For $\alpha = 0$, we derive heuristically a formula for the aggregation times (equation (5.18)) which is further corroborated by the analysis of the second-order moments (Proposition 5.3). For $\alpha = -1$ we obtain an expression of the aggregation times with a similar argument (equation (5.27)). This argument is invalid when $\alpha > 0$ due to the singularity of the transition rates. In Section 5.3 we derive the equilibrium distribution in three different cases.

5.1. Mathematical set-up

5.1.1. Interacting particle systems

This section provides a succinct introduction to interacting particle systems starting by a discussion about continuous time homogeneous Markov processes. A more extensive and rigorous presentation can be found in [54].

A continuous time homogeneous Markov process over a *configuration space* Ω with *transition rates* $\{q_{\eta\eta'}\}_{\eta,\eta'\in\Omega}$ is a family a random variables $\{X(t)\}_{t\geq 0}$ such that the following *master equation* is verified for all functions $f\colon \Omega \to \mathbb{R}$

$$\frac{\mathrm{d}}{\mathrm{d}t}\mathsf{E}\left(f(X(t)) \mid X(0) = \eta\right) = \sum_{\eta'\in\Omega} q_{\eta\eta'}(f(\eta') - f(\eta)), \tag{5.1}$$

where $q_{\eta\eta'} \geq 0$ for $\eta \neq \eta'$ and $q_{\eta\eta} = -\sum_{\eta' \neq \eta} q_{\eta\eta'}$. For convenience, here we assume that Ω is finite but this discussion can be extended to countable configuration spaces. A useful way to interpret Markov processes is to consider that given a current state $X(t) = \eta$, an exponential clock with rate $q_{\eta\eta'}$ is associated to each transition $\eta \to \eta'$. Whenever one of the clocks "rings", the system undergoes the corresponding transition. An *interacting particle system* is a Markov process over a configuration space $\Omega \subset S^K$ where S is called the *ambient space* and K is the *particle state space*. The dynamic is defined via a set of *local transformations* Θ and their respective rates

$$\begin{aligned} r_T \colon \Omega &\longrightarrow \mathbb{R}_+ \\ \eta &\mapsto r_T(\eta) \end{aligned}$$

In this case the master equation takes the form

$$\frac{\mathrm{d}}{\mathrm{d}t}\mathsf{E}\left(f(X(t)) \mid X(0) = \eta\right) = \sum_{T \in \Theta} r_T(\eta)\left(f(T\eta) - f(\eta)\right). \tag{5.2}$$

As earlier, we can give an interpretation in terms of exponential clocks. When the system is in the configuration $\eta \in \Omega$ each local transformation $T \in \Theta$ is associated to an exponential clock with rate $r_T(\eta)$ and when a clock rings the corresponding transformation is applied.

5.1.2. Model of aggregation and fragmentation

Let $n \in \mathbb{N}$ (interpreted as the *size* of the system). The *ambient space* is an oriented connected graph $\mathcal{G} = (S, A)$ where S is the set of the vertices, $\#S = n$, and A is the set of edges. The *configuration space* is given by

$$\Omega := \left\{\mu = (\mu_x) \in \mathbb{N}_0^S \colon \sum\nolimits_{x \in S} \mu_x = n\right\}. \tag{5.3}$$

In addition, we define several parameters for our model $\alpha, \beta \in \mathbb{R}$ and $\omega \in \mathbb{R}_+$. A configuration μ can undergo the following transformations:

- **Diffusion and aggregation:** if $\mu_x \neq 0$, at rate $\mu_x^{-\alpha}$ the mass located on x moves to a neighbouring site y uniformly randomly selected in $A_x = \{y : (x, y) \in A\}$,
$$c_x \colon \mu \mapsto \mu + \mu_x(\delta_y - \delta_x), \tag{5.4}$$
where $\delta_x \colon S \mapsto \mathbb{R}$ such that $\delta_x(x) = 1$ and $\delta_x(y) = 0$ if $y \neq x$. In particular, if $\alpha = 0$ then every particle moves at the same rate, this is known as *coalescing random walks*; if $\alpha > 0$, more massive particles have more inertia; likewise, if $\alpha < 0$ then more massive particles are more mobile.

- **Chipping** if $\mu_x \neq 0$, at rate $\omega\mu_x^{1+\beta}$, the site x gives one unit of mass to a neighbouring site y uniformly randomly selected i.e.

$$f_x \colon \mu \mapsto \mu + (\delta_y - \delta_x). \tag{5.5}$$

  In particular when $\beta = 0$ units of mass follow independent random walks, when $\beta < 0$ there is an internal attraction that counterbalances the movement of the masses, when $\beta > 0$ there is a repulsion.

For the rest of the chapter, we denote by $\mu(t)$ the configuration of the system at time $t \geq 0$. We encounter multiple quantities that vary with time. In order to achieve more compact formulas, we have adopted a notational convention where the time variable is often omitted from these quantities. This omission is made under the assumption that the time-dependence of each variable is implicitly understood, unless a specific instance necessitates explicit mention of the time parameter for clarity or emphasis.

5.2. Aggregation model on a directed cycle

In this section $\mathcal{G}$ is a *directed cycle* with $n \in \mathbb{N}$ sites. We will take $S = \mathbb{Z}/n\mathbb{Z}$ and $A = \{(k, k-1) \mid k \in S\}$. We assume that at time $t = 0$ the configuration is deterministic with one unit of mass per site. This arbitrary choice is made to bypass a discussion on the selection of initial distribution. This is particularly convenient, as it allows to highlight the transition from a fully fragmented state to a fully aggregated state. In this model it is clear that the process will almost surely attain a distribution with a single particle of mass n located uniformly on S.

Definition 5.1. For $k = 1, \ldots, n$, we define the *coalescence time* T_k as first time such that there are k particles left in the system.

The second-order moments provide relevant information on the coalescence times. Since the initial state of the system is homogeneous, we can define them as follows.

Definition 5.2. For $d \in S$, define the corresponding *second-order moment* by

$$V(d) = \mathsf{E}[\mu_x(t)\mu_{x+d}(t)], \tag{5.6}$$

independently of the choice of site $x \in S$.

As we said, the system almost surely ends up with only one massive particle so the second-order moment must converge to the function $n\delta_0$ when the time goes

to infinity. The rate of convergence gives us information about the coalescence times.

It is also interesting to track the presence of particles on the sites independently of their mass.

Definition 5.3. For a site $x \in S$, we define the corresponding *particle indicator*:

$$s_x = \mathbf{1}_{\{\mu_x > 0\}}. \tag{5.7}$$

We also define the moments of orders 1 and 2 of the particle indicators by

$$G^{(1)} = \mathsf{E}[s_x], \qquad G^{(2)}(d) = \mathsf{E}[s_x s_{x+d}], \tag{5.8}$$

for $d \in S$, independently of the choice of x.

We can also consider the mass distribution independently of the location of the particles in order to determine if the model can be matched to non-spatial models.

Definition 5.4. We define the *distribution of mass per particle*

$$P(m;t) = \frac{\mathsf{P}(\mu_x(t) = m)}{G^{(1)}}, \tag{5.9}$$

independently of the choice of $x \in S$ such that $\mu_x \neq 0$.

Remark 5.1. To a given configuration μ, we associate an integer partition by only keeping the masses of the non-empty sites and ignoring the location of the particles.

Here we are interested in knowing the distribution of mass when a certain number of particles k are left in the system. One way to estimate this distribution is by replicating the process many times and estimating the distribution by averaging the counts of the different sizes of parts. This method requires a large number of samples to estimate the probability of rare parts. Alternatively, we may observe the Young diagram to select a model of distribution based its features. This approach provides valid observations with fewer realisations of the process as the expected Young diagram is the complementary cumulative distribution associated to the distribution of mass. For instance, if a mode exists, it should manifest as the steepest point on the expected Young diagram.

5.2.1. Simulation tool

The goal of our simulation program is to produce an instance of the aggregation process. It saves on the hard-drive the times of each event of aggregation and

the integer partition corresponding to the configuration of the system (that is the configuration when we forget the location of the particles). The integer partition representation is not only a convenient tool to represent the distribution of mass in a configuration but it also helps to identify adequate models of distributions to fit P.

In order to do so, the simulator keeps in memory the location and the mass of the particles in a table as well as the current time and iterates the following operations until only one particle is left. The validity of our simulator relies on the following lemma.

Lemma 5.2. *Let $X_1, \cdots, X_k$ be mutually independent exponential random variables with respective parameter $\lambda_i > 0$, $i \in [\![1, k]\!]$. The following statements hold true:*

1. *Their minimum is an exponential random variable with parameter $\sum_{i=1}^{k} \lambda_i$,*
2. *Independently of the value of their minimum, the probability that it is realised by X_i is given by*

$$\mathsf{P}\left(X_i = \min_{j\in[\![1,k]\!]} X_j \middle| \min_{j\in[\![1,k]\!]} X_j > t\right) = \frac{\lambda_i}{\sum_j \lambda_j}.$$

Proof. The proof of the first statement is elementary:

$$\mathsf{P}\left(\min_{j\in[\![1,k]\!]} X_j > t\right) = \mathsf{P}(X_i > x,\ \forall i \in [\![1,k]\!]) = \prod_{i=1}^{k} \mathsf{P}(X_i > t) = \mathrm{e}^{-\sum_i \lambda_i t}.$$

The second statement is proven by a similar computation. For convenience, assume without loss of generality that $i = 1$.

$$\begin{aligned}\mathsf{P}\left(X_1 = \min_{j\in[\![1,k]\!]} X_j \middle| \min_{j\in[\![1,k]\!]} X_j > t\right) &= \int_t^\infty \left(\prod_{j=2}^{k} \mathsf{P}(X_j > \tau)\right) \mathrm{d}\mathsf{P}(X_1 = \tau) \cdot \mathrm{e}^{\sum_{j=1}^k \lambda_i t} \\ &= \int_t^\infty \lambda_1 \mathrm{e}^{-\sum_{j=1}^k \lambda_j \tau} \mathrm{d}\tau \cdot \mathrm{e}^{\sum_{j=1}^k \lambda_j t} = \frac{\lambda_1}{\sum_{j=1}^k \lambda_j}.\end{aligned}$$

□

Simulation algorithm

1. Simulation of the next event: the time elapsed between two events is given by

$$E = \min_{\mu_x \neq 0} E_x, \tag{5.10}$$

where E_x are mutually independent random variables, following the exponential distribution with parameter $\mu_x^{-\alpha}$, respectively, for each $x \in S$ such that $\mu_x \neq 0$, therefore

$$E \sim Exp(\sum_{\mu_x \neq 0} \mu_x^{-\alpha}). \tag{5.11}$$

2. Determination of the moving aggregate: the probability that the particle located on an occupied site x moves at the next event is

$$\mu_x^{-\alpha} \cdot \left(\sum_{\mu_y \neq 0} \mu_y^{-\alpha} \right)^{-1}. \tag{5.12}$$

3. Update and save: the configuration is updated accordingly, the particles table is sorted so an integer partition can be produced an saved on a file.

A simulation code in C is presented in Appendix D.4.

5.2.2. Characterisation of the distribution of mass at intermediate times

The distribution at time zero is just the Dirac distribution in 1 (the system contains n particles of unit size). At T_1 the distribution is the Dirac distribution in n (the system contains one particle of mass n). We study the distribution of mass at the jump times T_k, which, unlike the analysis at predetermined times, ensures a fixed number of parts. We observed the system in three cases (independent rates, linear rates, inverse rates) and fitted multiple distributions (see the figures in Section 5.4). In all cases we observe that the distribution of mass at early times is strictly decreasing, then it transitions to an intermediate unimodal distribution. It is in this intermediate regime that we can expect to observe a limit shape.

Rates independent of the mass

Figure 5.5 has been produced through simulations for a system of size $n = 1000$. We observed the distribution of mass for different numbers of particles left in the system by computing the average over 100 simulations of the process. Initially there are only particles of mass one and through the beginning of the process the mass distribution is strictly decreasing. Subsequently, we observe a unimodal distribution. The Rayleigh distribution appears to be an adequate fit during this phase.

We compared the Rayleigh distribution with expectation equal to the size of the system divided by the number of particles that are left with the Gamma distribution with parameters computed via maximum likelihood estimation using

R. The χ^2 (Table 5.1) and the Kolmogorov–Smirnov tests (Figure 5.11) confirm our visual inspection. Interestingly, the Rayleigh distribution is used in the study of wave heights [55]. The behavior of mass in the system studied here bears similarity with the superposition of waves. This observation may be more than a mere analogy and should be investigated.

Table 5.1: χ^2 test p-values ($N = 1000$, $\alpha = 0$, data are pooled by 5% quantiles)

	Rayleigh	Gamma MLE
$k = 50$	1.31×10^{-2}	1.51×10^{-16}
$k = 40$	1.03×10^{-2}	3.96×10^{-16}
$k = 30$	2.53×10^{-1}	6.98×10^{-11}
$k = 20$	5.11×10^{-1}	3.08×10^{-3}
$k = 10$	8.44×10^{-1}	4.97×10^{-2}

Rates depending on the mass

We have simulated the aggregation process when $\alpha = -1$ (diffusion rate equal to the mass) and when $\alpha = 1$ (diffusion rate equal to the inverse of the mass) and reported the mass distribution in Figures 5.6 and 5.7. We can see that the Rayleigh distribution does not fit well, however we can use the family of the exponentiated Weibull distributions, which includes the Rayleigh distribution. Upon visual inspection, the exponentiated Weibull distribution is a good fit when $\alpha = -1$ (Figure 5.6). The results of the χ^2 test appear to confirm this observation (Table 5.2). When $\alpha = 1$ none of the distributions that we have tested provide satisfactory fit (Figure 5.7) and the p-values for the goodness of fit tests are negligible.

Table 5.2: χ^2 test p-values ($N = 1000$, $\alpha = -1$, data are pooled by 5% quantiles)

	Gamma MLE	Exponentiated Weibull MLE
$k = 40$	5.04×10^{-96}	3.08×10^{-5}
$k = 30$	1.31×10^{-71}	5.59×10^{-2}
$k = 20$	4.80×10^{-57}	3.86×10^{-2}
$k = 10$	7.47×10^{-27}	2.84×10^{-2}

5.2.3. Moments and aggregation events times

Through the process, the particles rarefy. At least when $\alpha \geq 0$ the time between two successive coalescence increases. Conversely, significantly negative values of α counteract this phenomenon. We observe this general trend in Figure 5.2.

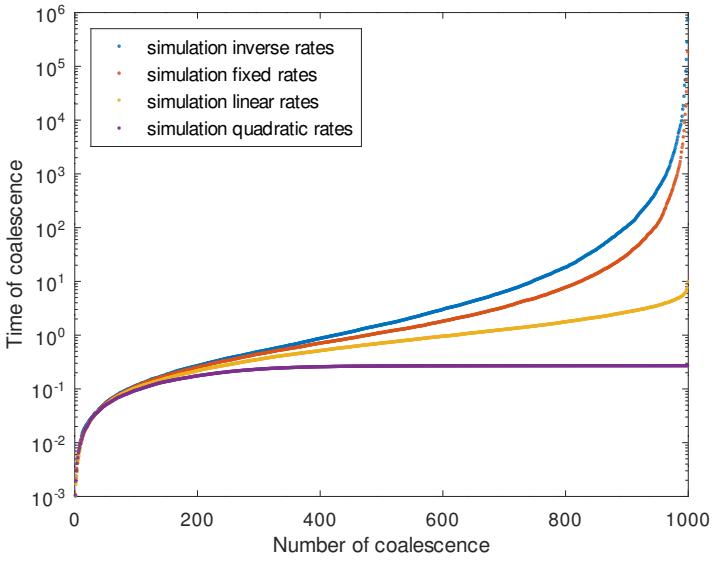

Figure 5.2: Comparison of the coalescence times for $\alpha = 1$, $\alpha = 0$ and $\alpha = -1$

Rates independent of the mass

Since the interaction rates don't depend on the mass, we can realise an analysis of the particles indicator independently of the mass distribution. This allows us to infer the behaviour of the coalescence times.

Given the configuration at a time t, after a small increment of time Δt the only events that can affect a site x are a movement of the particle located on x or a movement of the aggregate located on $x+1$. If the particle located on $x+1$ moves and x is already occupied, s_x does not change.

$$\mathsf{E}[s_x(t+\Delta t)|\mu(t)] = s_x(t) - \underbrace{\Delta t \cdot s_x(t)}_{x \text{ moves}} + \underbrace{\Delta t \cdot (1 - s_x(t)) s_{x+1}(t)}_{x+1 \text{ moves}} + o(\Delta t). \quad (5.13)$$

In particular, the probability of having a particle on a given site satisfies the following differential equation,

$$\frac{\mathrm{d}G^{(1)}(t)}{\mathrm{d}t} = -G^{(2)}(1,t). \quad (5.14)$$

If we could ignore the correlations we would simply have

$$G^{(2)}(d) = \left(G^{(1)}\right)^2 \tag{5.15}$$

Thus the solution would be

$$G^{(1)} = \frac{\mathbf{1}_{\{t<n-1\}}}{t+1} + \frac{\mathbf{1}_{\{t\geq n-1\}}}{n}. \tag{5.16}$$

In particular, when k is small and n goes to infinity, up to random fluctuations, we should expect that the coalescence time can be approximated in the following way,

$$T_k \simeq \frac{n-k}{k}. \tag{5.17}$$

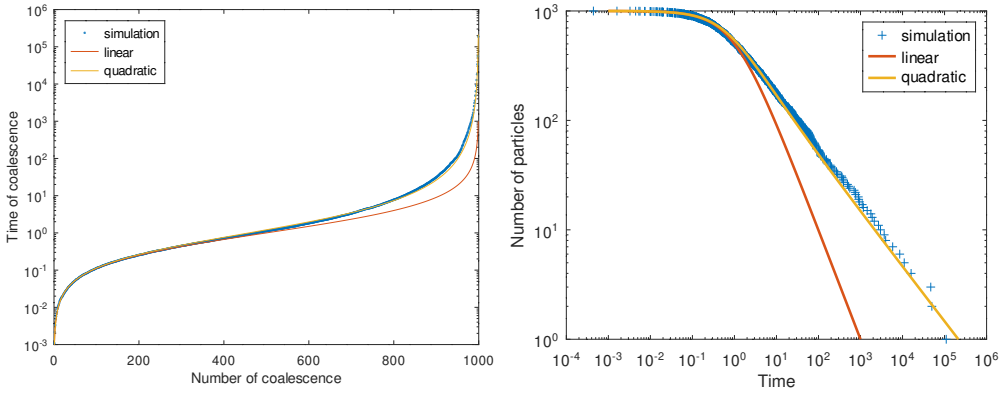

Figure 5.3: Times of coalescence with rates independent of the mass

According to the simulations (Figure 5.3), this non-correlated approximation is satisfactory in the beginning but a quadratic term needs to be added to fit subsequent times thus giving the following approximation and the corresponding expression f the number of particles as a function of the time

$$T_k \simeq \frac{2}{3\pi}\left(\frac{n-k}{k}\right)^2 + \frac{n-k}{k}, \qquad k(t) \simeq \frac{N(\sqrt{1+4t}-1)}{2t}. \tag{5.18}$$

This expression for the coalescence times is corroborated by an analysis of the convergence of the moments of order 2 of the mass.

Proposition 5.3.

1. *The second-order moments of the mass satisfy the following equation,*

$$\frac{\mathrm{d}}{\mathrm{d}t}\begin{pmatrix} V(0) \\ V(1) \\ V(2) \\ \vdots \\ V(n-1) \end{pmatrix} = \begin{pmatrix} 2V(1) \\ C \cdot \begin{pmatrix} V(1) \\ V(2) \\ \vdots \\ V(n-1) \end{pmatrix} \end{pmatrix} \tag{5.19}$$

where C is the tridiagonal Toeplitz matrix of size $(n-1)$ with -2 on the principal diagonal and 1 around the diagonal.

2. *The matrix C can be diagonalised and its eigenvalues are*

$$\lambda_k = -2\left(\cos\left(\frac{k\pi}{n}\right)+1\right), \qquad k = 1,\dots,n-1. \tag{5.20}$$

Proof. **1.** We have

$$\boxed{\frac{\mathbf{d}}{\mathbf{dt}}\mathbf{V}(\mathbf{0}) = \mathbf{2V}(\mathbf{1})}$$

In a small interval of time Δt the quantity $\mu_x(t)^2$ can be modified by the following local events at rate 1:

- The mass located on x moves: $\mu_x^2 \to 0$.
- The mass located on $x+1$ moves: $\mu_x^2 \to \mu_x^2 + (\mu_{x+1}^2 + 2\mu_x\mu_{x+1})$.

Using the homogeneity and the total expectation rule we get:

$$\begin{aligned} V(0,t+\Delta t) &= \mathsf{E}\left[\mathbb{E}[\mu_x(t+\Delta t)^2|\mu(t)]\right] \\ &= \mathsf{E}\left[\mu_x(t)^2 - \Delta t\cdot\mu_x(t)^2 + \Delta t\cdot\mu_{x+1}(t)^2 + 2\Delta t\cdot\mu_x(t)\mu_{x+1}(t) + o(\Delta t)\right] \\ &= V(0,t) + 2\Delta t\cdot V(1,t) + o(\Delta t). \end{aligned}$$

Thus we have verified the equation. The proof of the subsequent equations is nearly identical and we will simply indicate the local events that are involved.

$$\boxed{\frac{\mathbf{d}}{\mathbf{dt}}\mathbf{V}(\mathbf{1}) = -\mathbf{2V}(\mathbf{1}) + \mathbf{V}(\mathbf{2})}$$

- The mass located on x moves: $\mu_x\mu_{x+1} \to 0$.
- The mass located on $x+1$ moves: $\mu_x\mu_{x+1} \to 0$.
- The mass located on $x+2$ moves: $\mu_x\mu_{x+1} \to \mu_x\mu_{x+1} + \mu_x\mu_{x+2}$.

Now let $k \in \{2,\dots,n-2\}$, we have the equation:

$$\boxed{\frac{\mathbf{d}}{\mathbf{dt}}\mathbf{V}(\mathbf{k}) = -\mathbf{2V}(\mathbf{k}) + \mathbf{V}(\mathbf{k-1}) + \mathbf{V}(\mathbf{k+1})}$$

- The mass located on x moves: $\mu_x\mu_{x+k} \to 0$.
- The mass located on $x+1$ moves: $\mu_x\mu_{x+k} \to \mu_x\mu_{x+k} + \mu_{x+1}\mu_{x+k}$.

- The mass located on $x+k$ moves: $\mu_x\mu_{x+k} \to 0$.
- The mass located on $x+k+1$ moves: $\mu_x\mu_{x+k} \to \mu_x\mu_{x+k} + \mu_x\mu_{x+k+1}$.

$$\boxed{\frac{\mathbf{d}}{\mathbf{dt}}\mathbf{V}(\mathbf{n-1}) = \mathbf{V}(\mathbf{n-2}) - \mathbf{2V}(\mathbf{n-1})}$$

This equation is identical to the equation for $V(1)$.

2. This is a consequence of formula (2.7) from [38]. □

An immediate consequence of this, is that we can observe the full coalescence via the second-order moments at times of order n^2.

Corollary 5.3.1. *Let $t^*(n)$ be a sequence of times such that $n^2 = o(t^*)$ when n goes to infinity, then*

$$\frac{V(\cdot, t^*)}{n} \to \delta_0. \tag{5.21}$$

Proof. λ_{n-1} is the dominant eigenvalue of C and

$$\lambda_{n-1} \sim -\frac{\pi^2}{n^2}, \tag{5.22}$$

thus we can write

$$\begin{pmatrix} V(2,t^*) \\ \vdots \\ V(n-1,t^*) \end{pmatrix} = \exp(t^*C) \cdot \begin{pmatrix} 1 \\ \vdots \\ 1 \end{pmatrix} = O\left(\exp(-t^* \cdot \frac{\pi^2}{n^2})\right) \to 0. \tag{5.23}$$

□

Rates equal to the mass

Similarly to previously, we can give the equation for the moment of the particle indicator

$$\frac{\mathrm{d}}{\mathrm{d}t}G^{(1)} = -\mathsf{E}[s_x s_{x+1}\mu_{x+1}]. \tag{5.24}$$

If we neglect the correlations between the sites, then

$$\frac{\mathrm{d}}{\mathrm{d}t}G^{(1)} = -G^{(1)}\mathsf{E}[s_{x+1}\mu_{x+1}] = -G^{(1)}\mathsf{E}[\mu_{x+1}] = -G^{(1)} \tag{5.25}$$

using the fact that the initial configuration contains one unit of mass per site and that the mass is preserved. In particular this gives the solution

$$G^{(1)} = \frac{\mathbf{1}_{\{t<\log n\}}}{\exp(t)} + \frac{\mathbf{1}_{\{t\geq\log n\}}}{n}. \tag{5.26}$$

So we obtain the following approximation for the coalescence times,

$$T_k \simeq -\log\left(\frac{k}{n}\right), \qquad k(t) = n\ \exp(-t). \tag{5.27}$$

As we can see in Figure 5.4, the approximation given by equation (5.18) is still valid for early times but the approximation given by equation (5.27) is better overall.

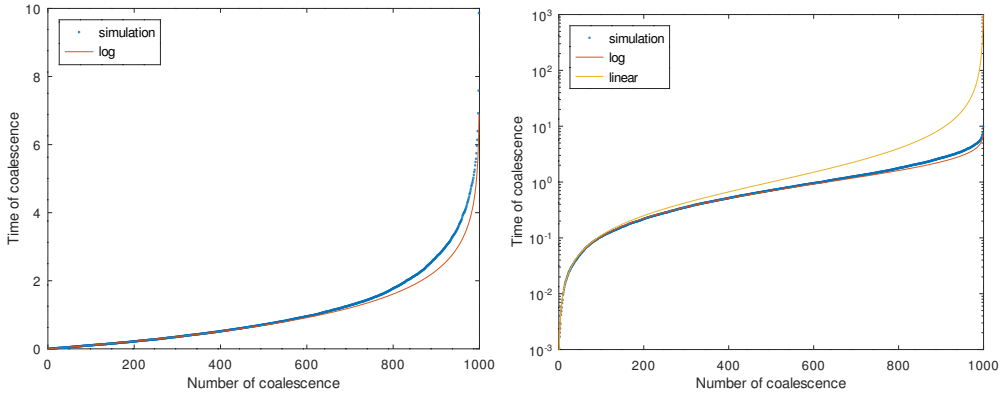

Figure 5.4: Times of coalescence with rates equal to the mass

5.3. Equilibrium distribution in mean-field

In this section, we assume that $\mathcal{G}$ is an infinite complete graph endowed with a time-dependent family of distributions $P(\cdot;t)\colon V \to \mathbb{R}$, such that

$$\mathsf{P}[\mu_x(t) = m] = P(m;t), \qquad \forall x \in V, m \in \mathbb{N}_0. \tag{5.28}$$

Proposition 5.4. *In this model the distribution of mass satisfies the following set of differential equations,*

$$\begin{aligned}\frac{\mathrm{d}}{\mathrm{d}t}P(m) = &- P(m)\left(m^{-\alpha} + \omega m^{1+\beta} + \sum_{k=1}^{\infty} P(k)(k^{-\alpha} + \omega k^{1+\beta})\right) \\ &+ P(m+1)\,\omega(m+1)^{1+\beta} + P(m-1)\sum_{k=1}^{\infty} P(k)(\omega k^{1+\beta}) \\ &+ \sum_{k=1}^{m} P(m-k)P(k)\,k^{-\alpha} \qquad (m \geq 1),\end{aligned} \tag{5.29}$$

$$\frac{\mathrm{d}}{\mathrm{d}t}P(0) = - P(0)\sum_{k=1}^{\infty} P(k)(k^{-\alpha} + \omega k^{1+\beta}) + \omega P(1) + \sum_{k=1}^{\infty} P(k)k^{-\alpha}.$$

Proof. We have to count the events that can affect the sites of mass m and the corresponding rates:

- Loss of sites of mass m can occur by diffusion of or chipping from sites of mass m and by diffusion or chipping to sites of mass m.
- Gain of sites of mass m can occur by chipping from sites of mass $m+1$, by chipping to sites of mass $m-1$ or by diffusion from a site of mass $m-k$ to a site of mass k.

□

In this section we are specifically interested in the equilibrium distribution, which is cancelled by the time derivative.

Definition 5.5. Denote by G the *probability generating function* of P

$$G(z) = \sum_{m=1}^{\infty} P(m) z^m. \tag{5.30}$$

We call the *equilibrium distribution*, and denote by $P_{eq} = (P_{eq}(m))$, the solution of the differential equation

$$\frac{\mathrm{d}}{\mathrm{d}t} P_{eq}(m) = 0, \qquad m \in \mathbb{N}_0. \tag{5.31}$$

Denote by G_{eq} the corresponding probability generating function.

Remark 5.5. As a consequence of the definition of the generating function, the *density of mass* in the system—that is, the average mass per site—is given by

$$\rho = \sum_{m=1}^{\infty} m P(m) = \partial_z G(z)|_{z=1}. \tag{5.32}$$

Since we consider an isolated system, this quantity is constant. Denote by s the probability that a site contains a non-zero mass,

$$s = 1 - P(0) = \sum_{m=1}^{\infty} P(m), \tag{5.33}$$

which can be interpreted as the density of particles.

If ω is not equal to zero, there is a non-trivial equilibrium distribution. In order to estimate it, it can be useful to estimate its probability generating function using the radius of convergence transfer theorem [77, Theorem 5.5].

Theorem 5.6 (Radius of convergence transfer)**.** *Let f be an analytic function with a radius of convergence larger than 1 such that $f(1) \neq 0$. For any real number $\alpha \notin \{0, -1, -2, \dots\}$, the coefficients of the Taylor expansion of f in the neighbourhood of 0 satisfy*

$$[z^n] \frac{f(z)}{(1-z)^\alpha} \sim \frac{f(1)}{\Gamma(\alpha)} n^{\alpha-1}. \tag{5.34}$$

5.3.1. No diffusion and chipping rate independent of the mass

In this case the evolution equations are

$$\begin{aligned} \frac{\mathrm{d}}{\mathrm{d}t} P(m) &= \omega \left[-(1+s)P(m) + P(m+1) + sP(m-1) \right], \\ \frac{\mathrm{d}}{\mathrm{d}t} P(0) &= \omega \left[P(1) - sP(0) \right], \end{aligned} \tag{5.35}$$

for $m \geq 1$.

Theorem 5.7. *The equilibrium distribution in this model is given by the geometric distribution with parameter $(1-s)$*

$$P_{eq}(m) = s^m - s^{m+1} \tag{5.36}$$

Proof. The equilibrium distribution solves the following second-order linear recurrence:

$$P_{eq}(m+1) = (1+s)P_{eq}(m) - sP_{eq}(m-1), \qquad P_{eq}(1) = s(1-s),$$

in particular, we have

$$P_{eq}(m) = \lambda s^m + \mu. \tag{5.37}$$

Since P_{eq} is a probability distribution it must add up to one, thus we can close the equations for λ and μ (given s)

$$\frac{\lambda}{1-s} + \mu = 1, \qquad \lambda s + \mu = s(1-s)$$

giving $\lambda = 1 - s$ and $\mu = 0$. □

Remark 5.8. In this particular case, we observe that the equilibrium distribution can be interpreted as the Boltzmann distribution over $\mathbb{N}$ where the inverse temperature would be $\beta = -\log s$. Unsurprisingly, this implies that the temperature is equal to zero when the density of particle reaches zero ($s = 0$).

5.3.2. No diffusion and chipping rate proportional to the mass

The evolution equations are

$$\begin{aligned}\frac{\mathrm{d}}{\mathrm{d}t}P(m) &= \omega\left[-mP(m) - \rho P(m) + (m+1)P(m+1) + \rho P(m-1)\right],\\ \frac{\mathrm{d}}{\mathrm{d}t}P(0) &= \omega\left[-\rho P(0) + P(1)\right].\end{aligned} \tag{5.38}$$

This model is known as the zero range process.

Theorem 5.9. *The equilibrium distribution is the Poisson law with parameter ρ,*

$$P_{eq}(m) = \frac{\mathrm{e}^{-\rho}\cdot\rho^m}{m!}. \tag{5.39}$$

Proof. The equilibrium distribution must satisfy the following balance equations

$$\begin{aligned}0 &= -m\,P_{eq}(m) - \rho\,P_{eq}(m) + (m+1)\,P_{eq}(m+1) + \rho\,P_{eq}(m-1),\\ 0 &= -\rho\,P_{eq}(0) + P_{eq}(1).\end{aligned}$$

By summing the terms we find that the generating function of the equilibrium distribution satisfies a homogeneous linear equation

$$0 = (1-z)\,G'_{eq} + \rho\,(z-1)\,G_{eq},$$

we can conclude by finding the general solution of this equation and again using the condition $\sum_m P(m) = 1$. □

5.3.3. Diffusion and chipping rates independent of the mass

When $\alpha = 0$ and $\beta = -1$ the evolution equations are

$$\begin{aligned}\frac{\mathrm{d}}{\mathrm{d}t}P(m) &= -(1+\omega)(1+s)P(m) + \omega P(m+1) + \omega s P(m-1) + \sum_{k=1}^{m} P(m-k)P(k)\\ \frac{\mathrm{d}}{\mathrm{d}t}P(0) &= -(1+\omega)sP(0) + \omega P(1) + s,\end{aligned} \tag{5.40}$$

for $m \geq 1$.

Theorem 5.10 (Majumdar et al. [59])**.** *The moment generating function of the equilibrium distribution is given by*

$$G_{eq}(z) = \frac{\omega + 2s + \omega s}{2} - \frac{\omega}{2z} - \frac{\omega s z}{2} + \omega s\cdot\frac{1-z}{2z}\sqrt{(z_1 - z)(z_2 - z)}, \tag{5.41}$$

where

$$z_1 = \frac{\omega + 2 - \sqrt{\omega+1}}{\omega s}, \qquad z_2 = \frac{\omega + 2 + \sqrt{\omega+1}}{\omega s}. \tag{5.42}$$

In particular, there is a subcritical phase $z_1 > 1$ *where*

$$P_{eq}(m) = \theta(z_1^{-m} m^{-3/2}) \tag{5.43}$$

and a critical phase $z_1 = 1$ *where*

$$P_{eq}(m) = \theta(m^{-5/2}). \tag{5.44}$$

Proof. By summing up, we find that the generating function of the equilibrium distribution satisfies the following equation

$$0 = -(1+\omega)(1+s)G_{eq} + \frac{\omega}{z}G_{eq} - \omega P_{eq}(1) + \omega s z(G_{eq} + P_{eq}(0)) + G_{eq}^2 + (1-s)G_{eq}$$
$$0 = -(1+\omega)s(1-s) + \omega P_{eq}(1) + s.$$

Hence, G_{eq} satisfies the equation

$$0 = G_{eq}^2 + \left[-(1+\omega)(1+s) + \frac{\omega}{z} + \omega s z\right] G_{eq} + \left[-(1+\omega)s(1-s) + s + \omega s z(1-s)\right].$$

In particular, equation (5.41) holds. When $z_1 > 1$, using Theorem 5.6, when m goes to infinity we have

$$\begin{aligned} P_{eq}(m) &= [z^m]\, G_{eq}(z) \sim [z^m]\, \omega s \cdot \frac{1-z}{2z}\sqrt{(z_1 - z)(z_2 - z)} \\ &= \frac{[z^{m+1}] - [z^m]}{2}\left(\omega s\sqrt{z_1 z_2 - z_1 z}\cdot\sqrt{1 - z/z_1}\right) \\ &= \frac{z_1^{-(m+1)}[z^{m+1}] - z_1^{-m}[z^m]}{2}\left(\omega s\sqrt{z_1(z_2 - z_1 z)}\cdot\sqrt{1-z}\right) \\ &\sim \frac{\omega s(1-z_1)\sqrt{z_1 z_2 - z_1^2}}{\Gamma(-1/2)}\cdot z_1^{-m} m^{-3/2} \sim \omega s(z_1 - 1)\sqrt{\frac{z_1 z_2 - z_1^2}{\pi}} z_1^{-m} m^{-3/2}. \end{aligned}$$

In particular, equation (5.43) is verified. Similarly, when $z_1 = 1$ we can prove equation (5.44)

$$\begin{aligned} P_{eq}(m) &\sim [z^m]\, \omega s \cdot \frac{(1-z)^{3/2}}{2z}\cdot\sqrt{z_2 - z} \\ &\sim \omega s \cdot (1-z)^{3/2}\cdot\sqrt{z_2 - z} \sim \frac{\omega s\sqrt{z_2 - 1}}{\Gamma(5/2)}\cdot m^{-5/2} \sim \frac{4\omega s}{3}\sqrt{\frac{z_2 - 1}{\pi}} m^{-5/2}. \end{aligned}$$

□

5.4. Mass distribution fitted curves

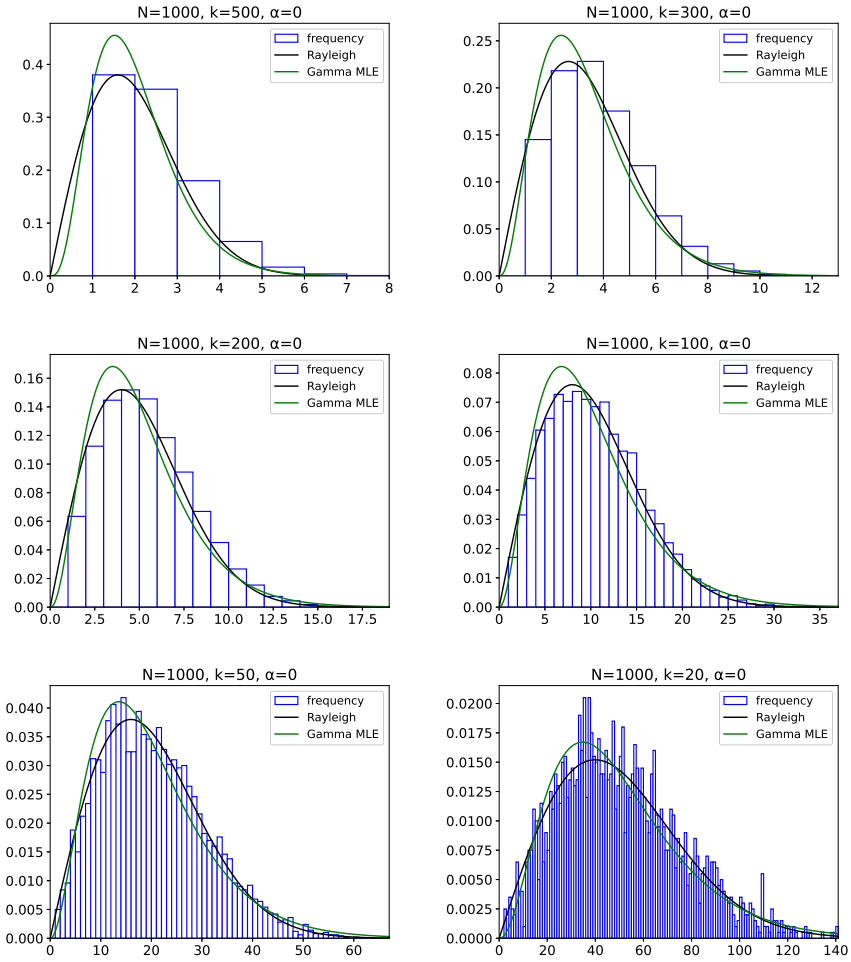

Figure 5.5: Mass distribution evolution ($N = 1000$, $\alpha = 0$)

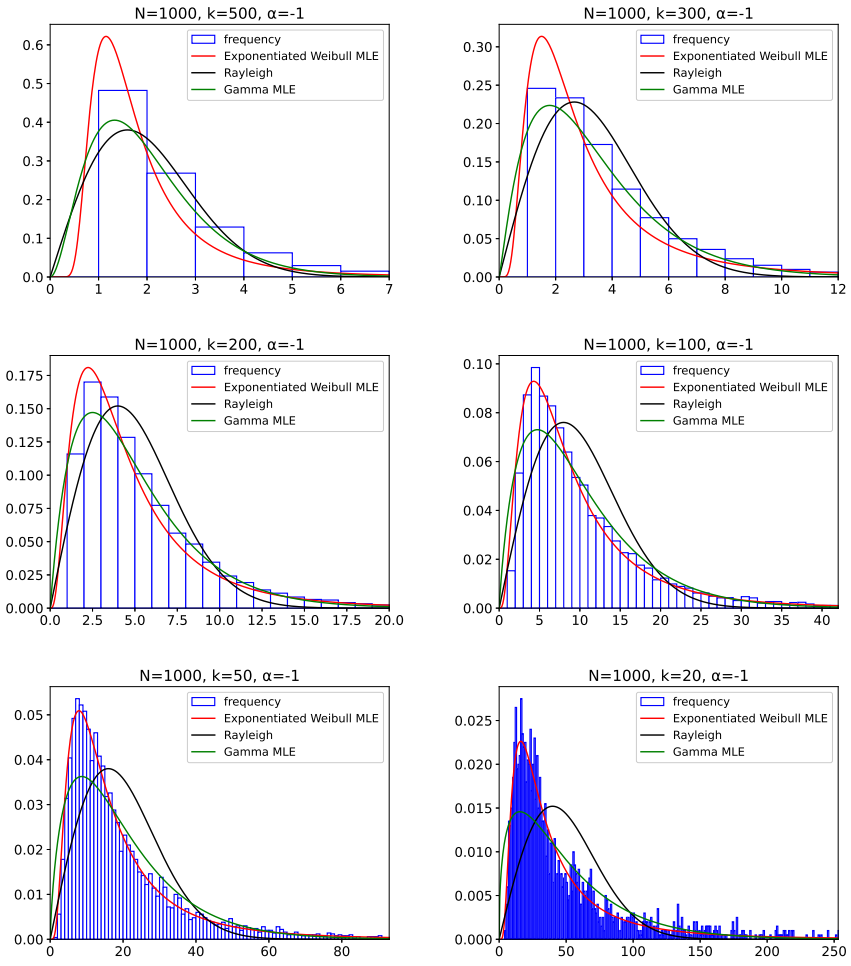

Figure 5.6: Mass distribution evolution ($N = 1000$, $\alpha = -1$)

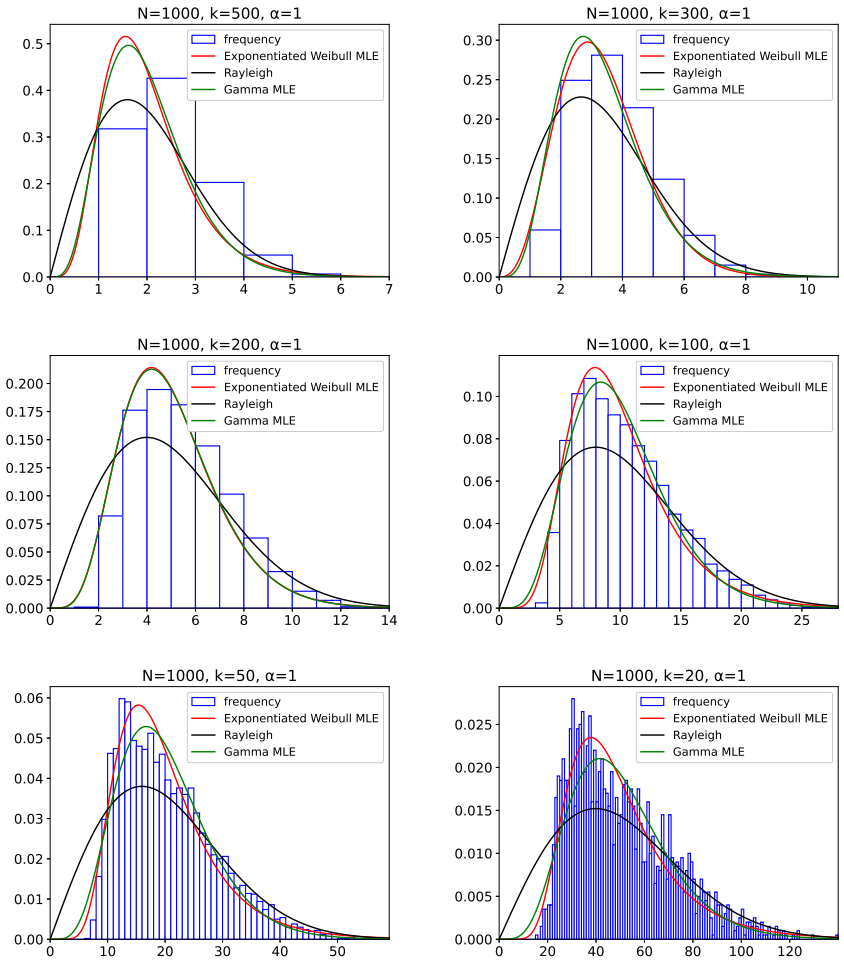

Figure 5.7: Mass distribution evolution ($N = 1000$, $\alpha = 1$)

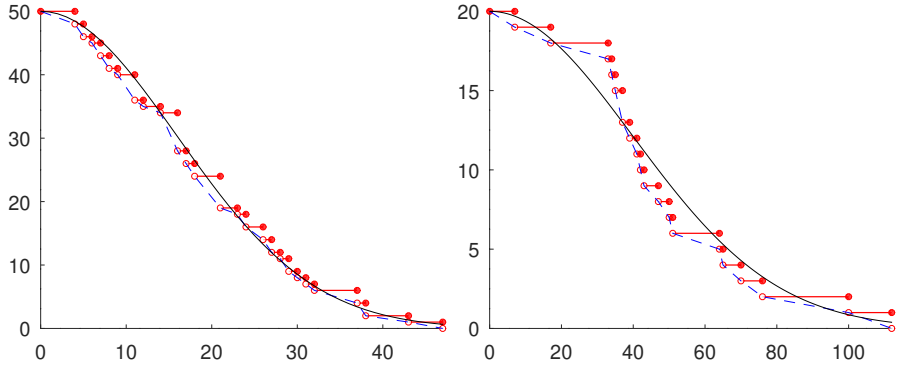

Figure 5.8: Young diagram for a single instance $N = 1000$, $\alpha = 0$, $k = 50$ (left), $k = 20$ (right), compared to Rayleigh (black curve)

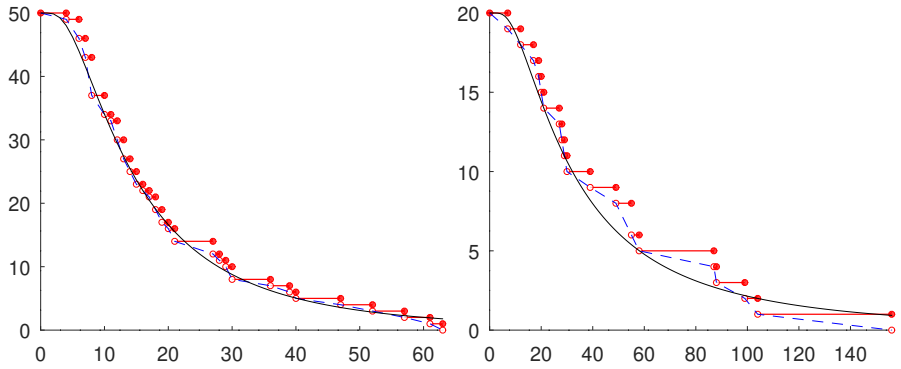

Figure 5.9: Young diagram for a single instance $N = 1000$, $\alpha = -1$, $k = 50$ (left), $k = 20$ (right), compared to exponentiated Weibull (black curve)

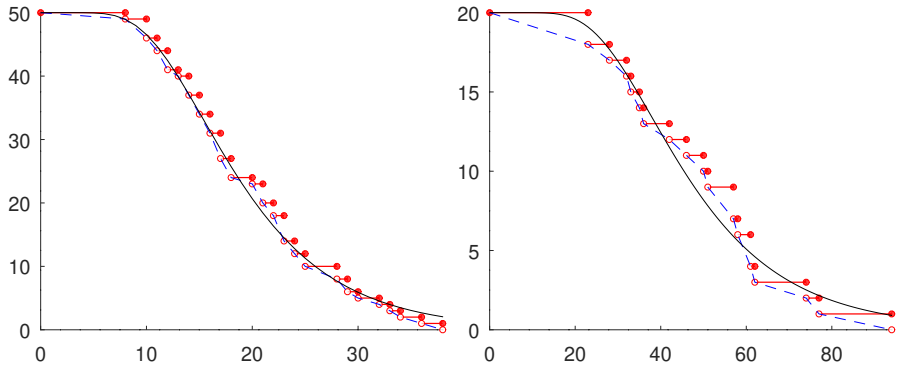

Figure 5.10: Young diagram for a single instance $N = 1000$, $\alpha = 1$, $k = 50$ (left), $k = 20$ (right), compared to exponentiated Weibull (black curve)

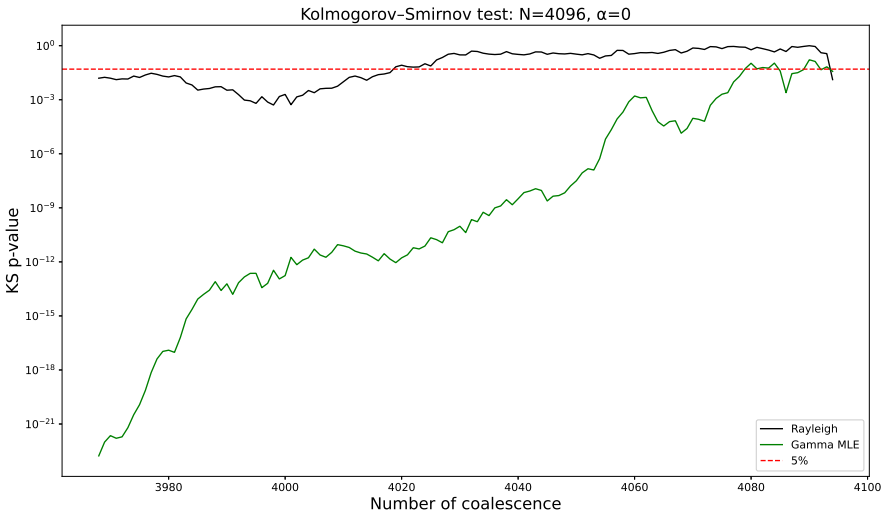

Figure 5.11: Kolmogorov–Smirnov test ($N = 4096$, $\alpha = 0$)

Chapter 6

Conclusion and future work

6.1. Summary of the results

6.1.1. Chapter 2

We examined the Boltzmann distribution $\mathsf{P}_{\boldsymbol{z}}$ under Assumption 2.1. The expected values of the pair (N_λ, M_λ) are linked to $\boldsymbol{z}$ as established in Theorem 2.21. Their variance is determined by Theorem 2.24. Subsequent sections of this chapter address two distinct cases.

- **Constant $\langle M \rangle$:** Theorem 2.26 states that the asymptotic distribution for the length is Poisson, while for the weight it is compound gamma. This theorem is crucial for establishing the cumulative cardinality formula stated in Theorem 2.34. Additionally, Theorem 2.31 is a variation of Theorem 2.26 when the largest part is bounded. Theorem 2.35 provides the limit distribution for both minimal and maximal parts. It shows, in particular, that asymptotically, all parts scale identically.

- **Large $\langle M \rangle$:** Theorem 2.26 evolves into a Gaussian limit, as specified in Theorem 2.40, and a law of large numbers given in Corollary 2.40.1. Theorem 2.35 turns into Theorem 2.48, which implies that that parts no-longer scale identically. Additionally, the Young diagram assumes a uniform scaling limit, described in Theorem 2.44. Fluctuations around this limit shape are quantified and shown to be Gaussian, as detailed in Theorem 2.45.

6.1.2. Chapter 3

- **Free sampling:** Algorithm 1 performs a sampling from the distribution $\mathsf{P}_{\boldsymbol{z}}$ with a truncation of the part source. This approach allows us to reduce the sampling to a finite sequence of independent Bernoulli trials for the

multiplicities. Theorems 2.35 and 2.48 provide guidelines for selecting an appropriate truncation threshold, ensuring that the approximation of P_z is as faithful as required. The algorithm has been implemented and subjected to testing; the observations we gathered align with the theorems outlined in Chapter 2, as demonstrated in Figure 3.1.

- **Rejection and gap detection:** Algorithm 1 is complemented by a rejection sampling scheme, detailed in Algorithm 2, which aims targets of the form $\{\lambda : M_\lambda = m \text{ and } n \leq N_\lambda \leq \theta n\}$ (with $\theta \leq 1$). Generally, there is no guarantee of a non-empty target, even when n approaches infinity. Therefore, it is necessary to set a limit, denoted as t^*, for the number of sampling attempts. Section 3.2.2 outlines how to select the limit t^*, ensuring that non-empty targets are reached with a given confidence level, while also avoiding unnecessary attempts when the target is empty. While this task is a necessity for rejection sampling, it can be also be leveraged as a feature to explore partitionability. A proof of this concept is provided in Section 3.3. We also argue Boltzmann sampling can be used as an experimental tool to estimate individual terms of the counting sequence, contrasting with the previously derived cumulative formula. The observations reported in Figure 3.4 suggest the presence of a pattern in the fluctuation of the counting sequence.

6.1.3. Chapter 4

Section 4.2 outlines the key principles for deriving limit shape theorems in partition models constructed as per Section 4.1. This is achieved for the Rayleigh distribution, which, unlike in [14], involves only one parameter and does not necessitate distinguishing between multiple asymptotic regimes. Here we allow the length to be random, provided it is independent of the parts and satisfy the "bumpiness" Assumption 4.1. The rescaled Young diagram is shown to converge to the complementary cumulative distribution of the Rayleigh distribution. When the length is deterministic, the fluctuations of the Young diagram are shown to be Gaussian.

Although the model in Section 4.1 does not inherently incorporate restrictions on multiplicities, such restrictions can be applied a posteriori through projection. In Section 4.3, we examine how the frequency distribution is transformed under this projection. In particular, this link can be used to provide an alternative to Algorithm 1.

6.1.4. Chapter 5

Section 5.1 proposes an extension of a previously studied model of aggregation and fragmentation. This chapter presents a series of preliminary results in particular cases of this model. In Section 5.2 we focus on a dynamic that is purely driven by the diffusion and aggregation of massive particles on a cycle. Our study involves the determination of aggregation times, the analysis of the second order moments and of the distribution of mass between the particles at each aggregation time with a combination of computer simulations (for which the design is presented in Section 5.2.1) and analytical methods. In Section 5.3 we study the equilibrium in a mean-field setting.

- **Pure aggregation on a cycle**
  - **Fixed diffusion rate:** Times of encounter between particles are given by equation (5.18). The equation for the second order moments is solved by Proposition 5.3. Both the distribution of mass and the Young diagram at late stopping times exhibits a Rayleigh limit shape as shown in Figures 5.5 and 5.8. It is further confirmed by goodness of fit tests reported in Table 5.1 and Figure 5.11. This is consistent with a result of Majumdar, yet it also indicates that this result might be improved.
  - **Linear dependence:** Times of encounter between particles are given by Equation (5.27). The results reported in Figures 5.6 and 5.9 suggest that the exponentiated Weibull distribution is the limit shape. The tests reported in Table 5.2, are not sufficient to be conclusive and indicate that further simulations on bigger systems should be performed.
  - **Inverse dependence:** No analytical results have been obtained and no distribution models have provided a good fit. The simulated coalescence times appear to be coherent when compared to the other cases, as shown in Figure 5.2.
- **Equilibrium in mean-field**
  - **No diffusion and chipping rate independent of the mass:** Theorem 5.7 shows that the equilibrium distribution is geometric.
  - **No diffusion and chipping rate proportional to the mass:** Theorem 5.9 shows that the equilibrium distribution is the Poisson law.
  - **Diffusion and chipping rates independent of the mass:** The solution of Majumdar is stated in Theorem 5.10, we re-derived it by using the radius of convergence transfer theorem.

6.2. Extension to real powers

In this section we propose two ways to extend $\mathsf{P}_{\boldsymbol{z}}$ to non integers q while maintaining a class of integer partitions. To do so, we propose to round down the q-th powers. The source of the parts will thus be given by the image of the function:

$$\begin{aligned} n &\mapsto \lfloor n^q \rfloor \\ \mathbb{N} &\to \mathbb{N} \end{aligned}$$

Definition 6.1. We define the *degeneracy*

$$g_\ell = \#\{n \in \mathbb{N} \colon \lfloor n^q \rfloor = \ell\}, \qquad \ell \in \mathbb{N}, \tag{6.1}$$

as the number of ways of producing each part. We remark that if $q \geq 1$ the degeneracy is 0 or 1, this case essentially coincides with what was done earlier. However, if $q < 1$, we have $g(\ell) \geq 1$ (it is even going to infinity). We will focus on this case for the rest of the section.

Lemma 6.1. *For $q \leq 1$, when ℓ goes to infinity,*

$$g_\ell = \lceil (\ell+1)^{1/q} \rceil - \lceil \ell^{1/q} \rceil, \tag{6.2}$$

in particular,

$$g_\ell \sim \frac{\ell^{1/q-1}}{q}. \tag{6.3}$$

Extension 6.1. We consider $\mathsf{P}_{\boldsymbol{z}}$ as the Boltzmann distribution over the partitions with multiplicity ν_ℓ smaller than g_ℓ for all natural ℓ. Formally it is the structure specified by

$$\prod_{\ell \in \mathbb{N}} Seq_{\leq g_\ell}(\{\ell\}), \qquad Seq_{\leq g_\ell}(\{\ell\}) := \{\varnothing, (\ell), (\ell,\ell), \cdots\}. \tag{6.4}$$

Lemma 6.2. *The Boltzmann distribution for Extension 6.1 has mutually independent multiplicities with distribution,*

$$\mathsf{P}_{\boldsymbol{z}}(\nu_\ell = k) = \frac{z_1^{k\ell} z_2^k}{F_\ell}, \qquad F_\ell = \frac{1 - (z_1^\ell z_2)^{g_\ell+1}}{1 - z_1^\ell z_2}. \tag{6.5}$$

In particular the expectation of the multiplicities verifies,

$$\mathsf{E}_{\boldsymbol{z}}(\nu_\ell) = z_1^\ell z_2 \, (1 + O(z_2^2)). \tag{6.6}$$

Proof. The law given by the equation (6.5) is an immediate consequence of the specification. Otherwise we can easily check that the law given the equation (6.5) coincides with the Boltzmann distribution,

$$\prod_{l=1}^{\infty} \frac{z_1^{\nu_\ell \ell} z_2^{\nu_\ell}}{F_\ell} = \frac{z_1^{N(\lambda)} z_2^{M(\lambda)}}{\prod_{\ell=1}^{\infty} F_\ell} = \mathsf{P}_{\boldsymbol{z}}$$

The estimation of the expectation is straightforward,

$$\mathsf{E}_{\boldsymbol{z}}(\nu_\ell) = \frac{1 - z_1^\ell z_2}{1 - (z_1^\ell z_2)^{g_\ell}} \sum_{k=1}^{g_\ell} k (z_1^\ell z_2)^k$$

where

$$\frac{1}{1 - (z_1^\ell z_2)^{g_\ell + 1}} = 1 + O(z_2^{g_\ell + 1}),$$

and

$$\begin{aligned} \sum_{k=1}^{g_\ell} k (z_1^\ell z_2)^k &= z_1^\ell z_2 \ \frac{\partial}{\partial (z_1^\ell z_2)} \sum_{k=1}^{g_\ell} (z_1^\ell z_2)^k \\ &= z_1^\ell z_2 \ \frac{1 - (g_\ell + 1)(z_1^\ell z_2)^{g_\ell} + g_\ell (z_1^\ell z_2)^{g_\ell + 1}}{(1 - z_1^\ell z_2)^2} = z_1^\ell z_2 \ (1 + O(z_2)), \end{aligned}$$

thus we can conclude,

$$\begin{aligned} \mathsf{E}_{\boldsymbol{z}}(\nu_\ell) &= (1 - z_1^\ell z_2) \cdot (1 + O(z_2^{g_\ell + 1})) \cdot z_1^\ell z_2 \ (1 + O(z_2)) \\ &= z_1^\ell z_2 \ (1 + O(z_2^2)) = z_1^\ell z_2 \ (1 + O(z_2^2)). \end{aligned}$$

□

Extension 6.2. We define the degenerate parts given by the structure

$$\lfloor N^q \rfloor := \bigcup_{\ell=1}^{\infty} \biguplus_{k=1}^{g_\ell} \{\ell\} \tag{6.7}$$

We consider the *state space*

$$S := PSet(\lfloor \mathbb{N}^q \rfloor). \tag{6.8}$$

An element of S can be represented as a sequence of multiplicities for each state

$$(\nu^S_{(1,\epsilon_1)}, \nu^S_{(1,\epsilon_2)}, \dots, \nu^S_{(1,\epsilon_{g_1})}, \nu^S_{(2,\epsilon_1)}, \nu^S_{(2,\epsilon_2)}, \dots, \nu^S_{(2,\epsilon_{g_2})}, \dots), \tag{6.9}$$

where the ϵ_k are distinct elements such that $N(\epsilon_k) = M(\epsilon_k) = 0$.

In order to obtain a distribution over Λ^q, we consider the pushforward of the Boltzmann distribution over S^q by the transformation:

$$\begin{aligned} T\colon S^q &\to \Lambda^q \\ \nu^S &\mapsto \nu = \left(\sum_{k=1}^{g_1} \nu^S_{(1,\epsilon_k)}, \sum_{k=1}^{g_2} \nu^S_{(2,\epsilon_k)}, \cdots \right). \end{aligned}$$

Extension 6.2 is akin to the notion of degenerate states in physics contrary to Extension 6.1 it does not retain the property conditional uniformity of the Boltzmann distribution.

Lemma 6.3. *The distribution given in Extension 6.2 has mutually independent multiplicities with Binomial distribution,*

$$\mathsf{P}_{\boldsymbol{z}}(\nu_\ell = k) = \binom{g_\ell}{k} p_\ell^k (1-p_\ell)^{g_\ell - k}, \qquad k \in [\![0, g_\ell]\!], \qquad p_\ell = \frac{z_1^\ell z_2}{1 + z_1^\ell z_2}. \tag{6.10}$$

6.3. Occupancy models

- **Relaxing the independence of the length:** In view of the Wald identity, we should be able to relax the condition of M being independent of the X^i and instead take a stopping time.

- **Higher dimension:** The production of a plane partition from an occupancy model is straightforward and would be useful to fit bi-dimensional data. Let (X^k) be a sequence of independent identically distributed random variables with values in $\mathbb{N} \times \mathbb{N}$ and distribution $f := (f_{ij})$. Let M be a random variable. We define the indicators $X^k_{ij} := \mathbf{1}(X^k = (i,j))$ and a random plane partition with the following diagram

$$Y(x,y) := \sum_{i \geq x} \sum_{j \geq y} \sum_{k=1}^{M} X^k_{ij}, \qquad x, y \in \mathbb{R}^+. \tag{6.11}$$

  This is indeed the Young diagram of a plane partition as it is weakly decreasing. We remark that when f is separable (i.e. we can write $f_{ij} = f_i f_j$) the analysis in this setting is essentially identical to the one dimensional case, provided that the scaling factors are compatible. A natural extension of the separable case may consists in considering models with a "small" covariance.

- **Minimal difference partitions:** MDP(d) the class of partitions such that successive parts differ from one another by at least d. In particular MDP(1)

is the class of the strict partitions. Contrary to the strict partitions there is no canonical projection from the unrestricted partitions to MDP(d). An arbitrary choice is to apply the projection to the strict partitions first, then going through the parts in the increasing order and decimating parts until the minimal difference d is achieved. As we did for the strict partitions, it would be interesting to understand how such projection transforms the occupancy model. Clearly, by an argument of homogeneity, it cannot be used to reproduce the Boltzmann distribution over MDP(d). In order to do so, we should use a randomised decimation scheme.

6.4. Multispecies aggregation and fragmentation

For more generality, it is possible to consider models with multiple types of units of mass. It adds degrees of freedom, allowing to incorporate the interactions between masses of different types in addition to the interactions between masses of the same type. We have made preliminary simulation for a purely aggregating model on a cycle $S = \mathbb{Z}/n\mathbb{Z}$ with two types of mass (denoted as type A and type B). The configuration space is defined as

$$\Omega := \left\{ \mu = (\mu_x^A, \mu_x^B) \in (\mathbb{N}^2)_0^S \colon \sum\nolimits_{x\in S} \mu_x^A = \sum\nolimits_{x\in S} \mu_x^B = n \right\}. \tag{6.12}$$

The interactions are the diffusion of the whole mass of type A and the diffusion of the whole mass of type B from a site x to a site $x-1$. We made simulations for two configurations

1. when μ_x^A diffuses at rate μ_x^B and μ_x^B diffuses at rate μ_x^A (the simulation code is provided in D.5),
2. when μ_x^A diffuses at rate $(\mu_x^A)^2\mu_x^B$ and μ_x^B diffuses at rate μ_x^A.

In these cases the equilibrium state is not unique and is reached when no sites contain both types of mass. Simulation results are reported in Figure 6.1 and Figure 6.2.

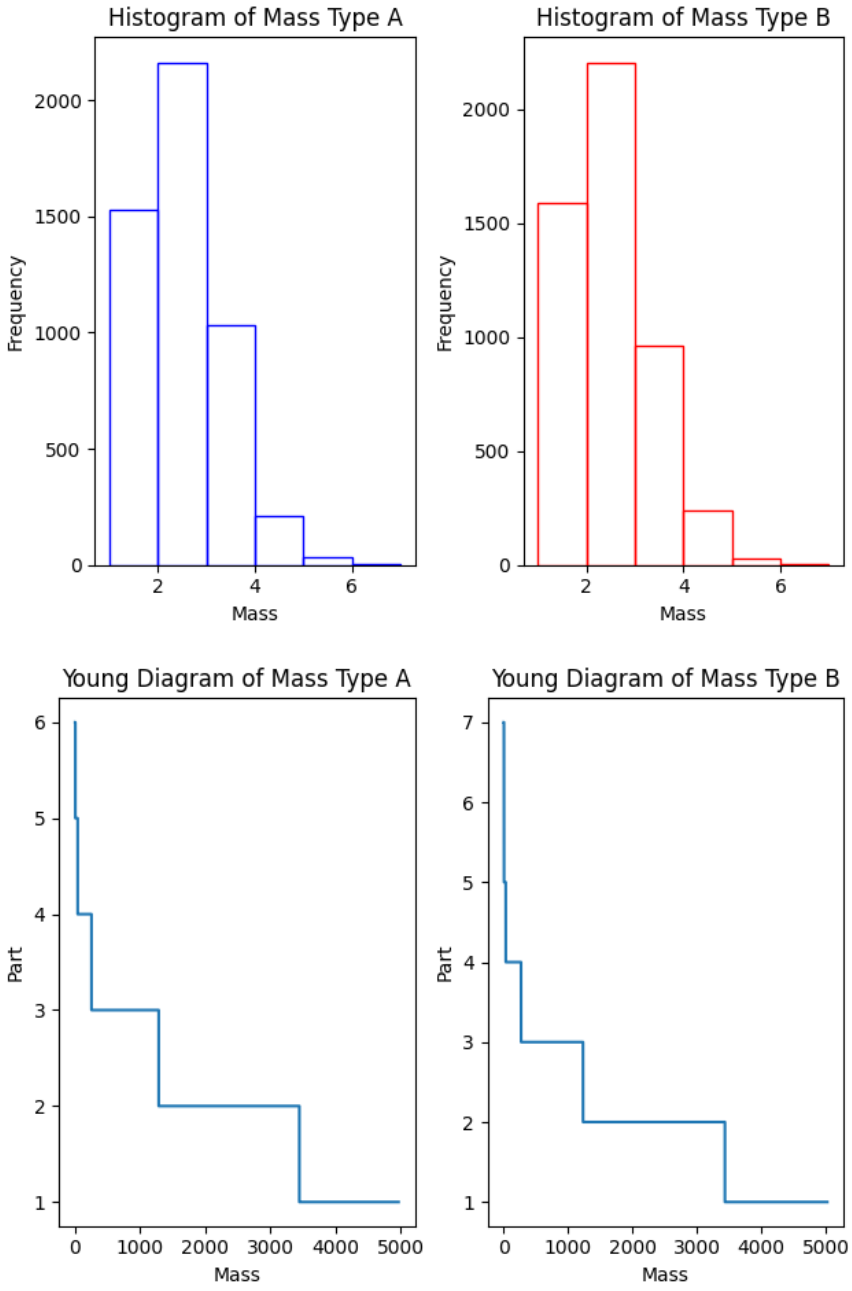

Figure 6.1: Equilibrium state ($n = 10^4$, configuration 1)

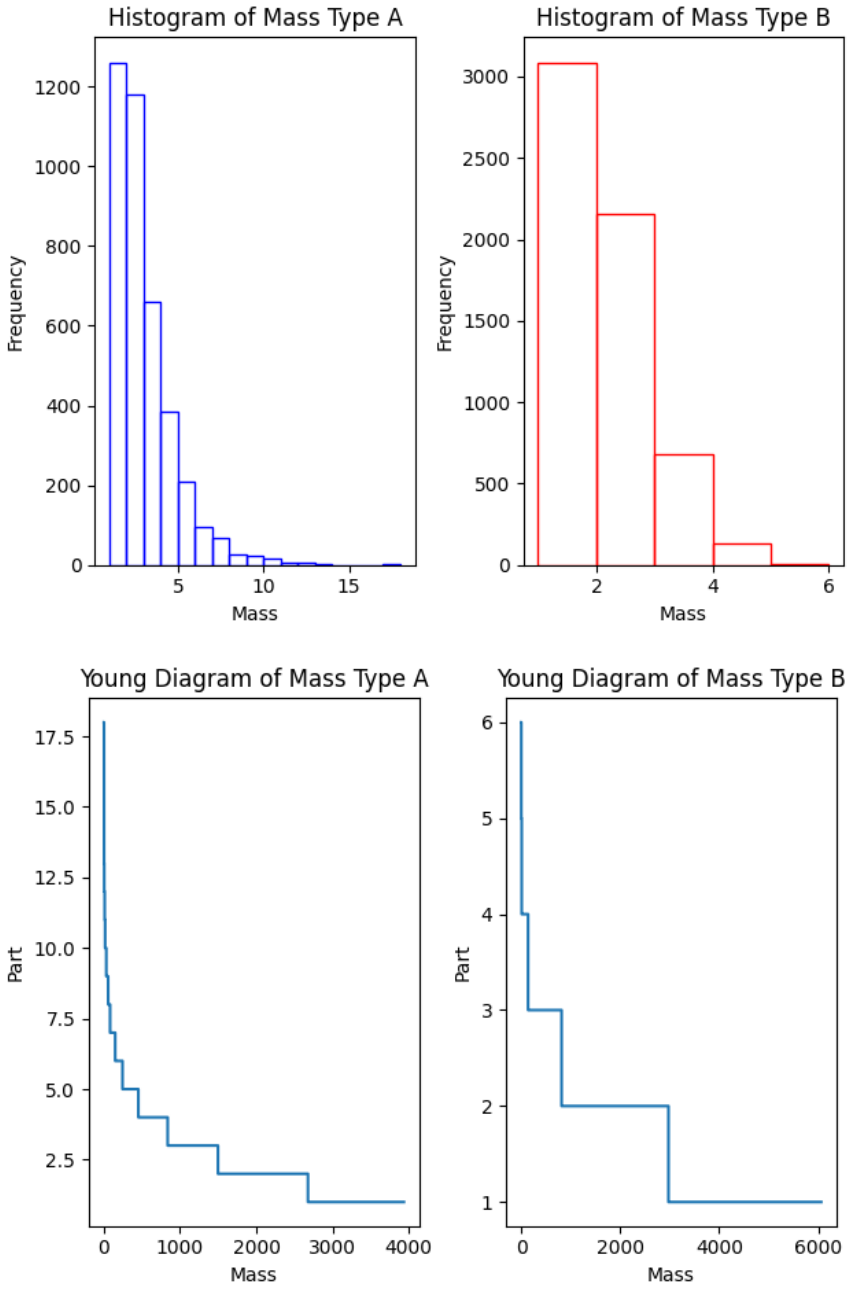

Figure 6.2: Equilibrium state ($n = 10^4$, configuration 2)

Appendix A

General perspective on partitions

A.1. Asymptotic combinatorics

The study of integer partitions is a classical area of mathematics, dating back, a least, to Euler, Sylvester, MacMahon, Hardy and Ramanujan. It is a source of many problems and results (see the monograph by Andrews [2] for historical comments and further references). As they form a combinatorial structure, many significant results concern their enumeration, a famous example of such result being the Hardy–Ramanujan formula [41, Sec. 1.4, p. 79, and Sec. 1.7, pp. 84–85] with the principal term

$$p(n) \sim \frac{1}{4\sqrt{3}\,n} \exp\left(\pi\sqrt{\frac{2n}{3}}\right), \tag{A.1}$$

where $p(n)$ counts the number of partitions of n.

Partitions can also be enumerated under structural constraints. For instance parts can be restricted to a subset of $\mathbb{N}$ such as the perfect q-th powers for a given integer q [41, Sec. 7.3, p. 111],

$$p^{(q)}(n) \sim \frac{k_q\,\sqrt{q/(q+1)}}{(2\pi)^{(q+1)/2}\,n^{1/(q+1)-3/2}} \exp\left((q+1)\,k_q\,n^{1/(q+1)}\right). \tag{A.2}$$

where

$$k_q := \left\{\frac{1}{q}\,\Gamma\left(1+\frac{1}{q}\right)\zeta\left(1+\frac{1}{q}\right)\right\}^{q/(q+1)} \qquad (q \in \mathbb{N}). \tag{A.3}$$

There has been intensive research into additive representations of integers with q-power parts, starting with $q = 2$ (squares) and dating back to Hardy and Ramanujan [41] (see also [82, 90]). In connection with combinatorial enumeration, the class of (non-strict) integer partitions with a fixed number m of q-power parts

is featured in at least two classical problems, the *Waring problem* [42, 83] and the *Gauss circle problem* [40, Sec. F1, pp. 365–367], both originally considered for squares ($q = 2$) and with $m \leq 4$ or $m \leq 2$ parts, respectively. The Waring problem concerns q-power representability of *all positive integers*[1] using at most $g(q)$ parts, whereas the Gauss circle problem focuses on the cumulative cardinality of such representations (more precisely, on error bounds for the area/volume approximation). For instance, by virtue of the Lagrange theorem it is known that $g(2) = 4$, that is, any natural number can be written as a sum of at most 4 squares, while 3 squares may not be enough. Moreover, Legendre's theorem gives an exact description of integers that can be represented as a sum of 3 squares — these are numbers not congruent to 7 (mod 8); for example, for $23 = 7 \pmod 8$ the only representation is $9+9+4+1 = 23$. On the other hand, numbers not representable using exactly 4 positive squares are given by the sequence comprising eight odd numbers, 1, 3, 5, 9, 11, 17, 29, 41, and all numbers of the form $\ell \cdot 4^k$ with $k \in \mathbb{N}_0$ and $\ell \in \{2, 6, 14\}$. These two sequences overlap: for example, $16 + 1 + 1 + 1 = 9 + 9 + 1 = 19 = 3 \pmod 8$. Another famous result, now about sums with up to 2 squares, is the Landau theorem [51] stating that the fraction of numbers up to n having such a representation is asymptotically given by $Kn/\sqrt{\log n}$, where $K \doteq 0.764223653$ is the *Landau–Ramanujan constant*. In physics, this kind of constraint is relevant as the energy levels of a system are not necessarily evenly spaced.

Another kind of structural constraints consists in imposing the parts to be unequal. An asymptotic for the number of so-called *strict partition* was stated in [41] (and later on elaborated by Hua [45])[2]

$$\check{p}(n) \sim \frac{1}{4 \cdot 3^{1/4}\, n^{3/4}} \exp\left(\pi \sqrt{\frac{n}{3}}\right) \qquad . \tag{A.4}$$

Strict partitions and their generating function $\check{F}(z) = \prod_{n=0}^{\infty}(1 + z^x)$ were considered by Euler who noticed that $\check{p}(n)$ coincides with the number of partitions of n with odd parts, using a simple identity for the corresponding generating

[1] It is known that $g(q) \geq 2^q + \lfloor (3/2)^q \rfloor - 2$ for any $q \in \mathbb{N}$, and it is believed that in fact the equality is true — although exceptions may be possible in principle, no counter-examples have been found to date. While this version of the Waring problem (i.e., for all numbers $n \in \mathbb{N}$) is almost completely settled, the asymptotic version asking for the smallest number of parts, denoted $G(q)$, sufficient to partition any sufficiently large natural number into a sum of q-powers, remains largely open (clearly, $G(2) = 4$, and it is also known that $G(4) = 16$). See further details and references in [83].

[2] The leading term of the asymptotic expansion of $\check{p}(n)$ was given in [41, Sec. 7.1, p. 109] in terms of (the derivative of) the Bessel function $J_0(z)$, from which it is easy to derive an explicit formula (A.4) using the relation $J_0'(z) = -J_1(z)$ [66, 10.6.3, p. 222] and the asymptotics of $J_1(z)$ [66, 10.7.8, p. 223]. See more direct derivations in [48].

functions, $\check{F}(z) = F(z)/F(z^2)$, that is,

$$\prod_{n=0}^{\infty}(1+z^n) = \prod_{n=0}^{\infty}\frac{1-z^{2n}}{1-z^n} = \prod_{n=0}^{\infty}(1-z^n)^{-1}\left(\prod_{n=0}^{\infty}(1-z^{2n})^{-1}\right)^{-1}. \tag{A.5}$$

This identity has been made explicit via numerous bijections [67, Sec. 3].

A.2. Probabilistic approach

Two identical fermions cannot occupy a same state due to the *Pauli exclusion principle*. While bosons and fermions are the only two types of elementary particles in dimension 3 and above, intermediate particles known as *anyons* have been theoretically predicted to emerge in physical systems that are effectively confined to two dimensions and have been recently observed [63]. From the point of view of the theory of partitions, extension of models based *minimal difference partitions* may be viable to represent anyons systems [20, 15]. It is the class of partitions defined by the condition that successive parts differ from one another by at least a prescribed value (e.g. 0 for bosons, 1 for fermions).

A more recent boost of research in this area has been due to a statistical approach focusing on asymptotic properties of typical random partitions and other decomposable combinatorial structures of large size (see, e.g., [4, 5, 24, 84]). The words "typical" and "random" imply that partition ensembles of interest are endowed with suitable probability measures, such as the uniform distribution on the spaces of partitions of a given $n \in \mathbb{N}$ (so that all such partitions are assumed equally likely). Amongst the first results in this direction established in a seminal paper by Erdős and Lehner [26] is that the growth rate of the number of parts in the bulk of integer partitions of large n (i.e., in the sense of Law of Large Numbers) is given by $\pi^{-1}\sqrt{3n/2}\log n$. A snapshot of subsequent advances is documented, for example, in papers [27, 34, 47, 84] and references therein. This research culminated in the discovery of so-called *limit shapes* of partition ensembles, which describe a typical settlement of parts and their multiplicities within large partitions under appropriate scaling (see [84, 85, 70, 28, 13, 15, 87, 92]). The limit shapes have a natural geometric interpretation through the Young diagrams. Incidentally, Young diagrams make it self-evident (by flipping rows and columns, called *conjugation*) that the number of partitions of n with at most m parts is the same as the number of partitions of n with the largest part not exceeding m, which immediately implies that the aforementioned asymptotics for the typical number of parts also hold for the largest part [26]. For our purposes a shape is merely a curve given by a function $f : [0,\infty) \to [0,\infty)$ (hence the boundary of every Young diagram is a shape). In this context two shapes cannot

be identified if the area under their curve is different. More generally two shapes might be identified if they agree up to translation, scaling, rotation or even in cases where they are not embedded in the same space. The comparison of such shapes requires to introduce an adequate topology such as the one induced by the Gromov–Hausdorff distance.

The modern approach to the asymptotic analysis of random combinatorial structures is based on a suitable *randomisation* of the model parameters (collectively called *poissonisation*) and the subsequent *conditioning* (*de-poissonisation*) in order to return to the original (say, uniform) distribution with fixed parameters (see, e.g., [4, 5, 69, 84]). In the context of random integer partitions, this method was first successfully applied by Fristedt [34], leading to the probability measure on the space of partitions of *all integers* $n \in \mathbb{N}$ by assigning to each such partition a probability proportional to z^n, respectively, where $z \in (0, 1)$ is a free parameter. Under such a measure (commonly referred to as *Boltzmann distribution*), the multiplicities of candidate parts $j \in \mathbb{N}$, previously restricted by the partition target n (often called *weight*), become independent geometric random variables with success probability $1 - z^j$, respectively. Furthermore, conditioning on the partition weight to be equal to n restores the uniform distribution on the space of all partitions of that n. This holds for any value of z, but it is helpful to calibrate the randomised model by replicating the original macroscopic properties (such as the partition weight) in terms of expectation. Crucially, for the conditioning trick to work effectively, asymptotic information is needed about the probability of the condition, specialised here as a weighted sum of random multiplicities, thus taking a familiar form of a local limit theorem in probability theory, albeit somewhat peculiar since the number of terms in the sum is random but almost surely finite (see [34, 37, 13, 87, 33, 47]).

Similar ideas are known as "equivalence of ensembles" in statistical physics, where the probabilistic description of the particle system of interest (e.g., ideal gas) may vary subject to optional fixation of the total energy and/or the number of particles, leading accordingly to *micro-canonical*, *canonical* or *grand-canonical Gibbs distributions*[1]. The usual tool to establish such equivalence is via the Darwin–Fowler method involving a saddle-point asymptotic analysis of high-dimensional integrals (see [46]). As an alternative, Khinchin [49] advocated a systematic use of local limit theorems of probability theory in problems of statistical mechanics, which facilitates the analysis by invoking probabilistic insight and well-developed analytical tools.

In fact, connections with statistical physics go even deeper, whereby integer

[1] Cf. also [15], where the term "meso-canonical" was proposed as better suited to the space of integer partitions with a given weight and any length (interpreted as an assembly with fixed energy and an indefinite number of particles).

partitions serve as a model for the random partitioning of total energy (under a suitable choice of units) in a large assembly of indistinguishable particles. The Boltzmann distribution arising naturally as a thermodynamic equilibrium. An elementary derivation of the Boltzmann distribution based on Stirling formula and the method of Lagrange multipliers can be found in numerous statistical physics books (see e.g. [76, Chapter II] or [46, Sec. 4.3]).

Specific models of relevance include an ensemble of harmonic oscillators at high temperatures and ideal quantum gases, where discrete partition structures are particularly tailored to the energy quantization [6]. In this context, plain partitions are interpreted as *bosons* following the *Bose–Einstein statistics*, with no restriction on the energy level occupancy, while strict partitions model *fermions* under the *Fermi–Dirac statistics*. This analogy is quite productive — for instance, it offers an insightful combinatorial explanation of the *Bose–Einstein condensation*, manifested as a measurable excess of particles at the lowest (ground) energy level at temperatures close to the absolute zero [6, 86].

The notion of Boltzmann distribution can be extended to a variety of combinatorial structures provided that they can be endowed with a suitable *size function* and their generating function has a non-zero radius of convergence [24]. Using additional free parameters allows to control multiple combinatorial parameters [9, 86]. When the generating function has a null radius of convergence, typically in the case of *labelled structures* such as integer partitions, with the use of the exponential generating function, it is still possible to introduce a variant of the Boltzmann distribution [24, Sec. 4]. Multi-parametric versions may also be considered [85, 10]. This may be needed if we wish to control more than one macroscopic characteristic of a combinatorial object, such as the number of parts (length) in addition to the partition weight. Another reason may arise if we are dealing with a truly multi-dimensional structure, such as vector partitions, convex lattice polygonal lines, or digitally convex polyominoes [79, 85, 16, 18, 12]. In computer science, it is an effective tool to sample random instances of combinatorial objects — if required, with a given size, exact or approximate (which is achieved via rejection applied to the output of a free sampler, so as to implement the conditioning step), and with a uniform distribution of the output [24, 31, 12, 11].

Aside from Boltzmann models, alternative probability distributions on partition spaces are interest. The *Ewens sampling formula* [29, 50] mentioned earlier, has significant applications in population genetics and ecology. In group theory, the *Plancherel measure* arises by taking the uniform distribution over the partitions of a given number and keeping only the length of cycles.

Other classes of distributions are derived from infinite *occupancy models*, that is models where some "balls" are thrown independently into a series of "boxes" labelled by $j \in \mathbb{N}$ with a certain *frequency distribution* (f_j). One way to produce

a partition through such scheme consists in taking as parts the number of balls thrown into each box [36] thus producing a partition of the number of balls. Alternately, boxes can be interpreted as parts' multiplicities thus giving a flexible model where the frequency distribution can be inferred via some count data [65, 14]. Contrary to the Boltzmann models, in the latter model the independence is in the individual parts instead of the multiplicities. This does not allow a structural constraint of the multiplicities without applying a projection.

A.3. Stochastic processes

Partitions also occur in the context of stochastic processes. A practical example arises in modelling the growth of a two-dimensional crystal in a quadrant [81]. In this example, a process of growth is defined by adding successive blocks to a Young diagram. This process can be interpreted as a downward random walk on the *Young lattice*, obtained by representing the relation of inclusion between partitions via their Young diagram (see Figure 1.3).

Coalescence and fragmentation dynamics, that is, the evolution of the distribution of an extensive quantity over an ambient space naturally involve integer partitions. It is also possible to focus on *mean-field models*, where the ambient space can essentially be interpreted as a complete graph. A famous example of mathematical model of aggregation is the *Smoluchowski equation*, here below in the version with discrete masses

$$\frac{\mathrm{d}c_j}{\mathrm{d}t} = \underbrace{\frac{1}{2}\sum_{j'=1}^{j-1} K_{j',j-j'}c_{j'}c_{j-j'}}_{\text{formation of aggregates of mass } j} - \underbrace{c_j\sum_{j'=1}^{\infty} K_{j,j'}c_{j'}}_{\text{loss of aggregates of mass } j} .$$

This equation describes the evolution of a population of aggregates that can take masses $j \in \mathbb{N}$. (c_j) corresponds to the distribution of aggregates size and the *aggregation kernel* $K_{j,j'}$ is the rate of aggregations of two couples of aggregates of respective size j and j'. It is an instance of mean-field model. Such models are more tractable analytically than models on more complex ambient spaces, they however remain unsolved except for particular aggregation kernels (see [1, Table 2 p8] for examples of solved cases). While it is a deterministic model, it has a stochastic analog, the Marcus–Lushnikov process [60, 56]. In this Markov process the configuration space is the set of all partitions of a given number N (the total mass of the system) and a configuration represented by the multiplicities (ν_j) can undergo the aggregation of a couple of masses, say j and j', at rate $K_{jj'}\nu_j\nu_{j'}/N$. A review of mean-field aggregation is provided in [1]. The two models mentioned here are purely aggregating, thus their equilibrium behavior is trivial. If fragmentation is introduced it allows models with non-trivial equilibrium behaviour to

explore [25]. Moreover, it is possible to study the partitions that arise in spatial dependent models after "forgetting" the spatial information. It is what we have done in Section 5.2.

Appendix B

Elements of combinatorics and Boltzmann distributions

In Chapters 2 and 3 we focused on the Boltzmann distribution over a particular case of combinatorial structure with two parameters (the weight and the length). The purpose of this appendix is to provide a more general context by providing a succinct presentation of some of the key concepts of analytic combinatorics [32]. A key principle of analytic combinatorics is that one can describe a combinatorial structure with a symbolic language that can naturally be translated into an analytic language that allows to extract information about the structure (distribution of some parameters, counting sequence, shape ...). Similarly, one can interpret a specification via a probabilistic language using Boltzmann distributions. Our guiding principle for this section is to progressively produce more complex structures starting from elementary objects.

B.1. Combinatorial structures with one or two parameters

Definition B.1. A *(one-parameter) combinatorial structure* is a countable set $\mathcal{A}$ endowed with a *size function* $N\colon \mathcal{A} \to \mathbb{N}_0$ such that, for all n,

$$a_n := \#\{a \in \mathcal{A}\colon N(a) = n\} < \infty. \tag{B.1}$$

Depending on the context, N might also be called *weight*, *energy*, etc.

The *generating function* of the structure $(\mathcal{A}, N)$ is the power series defined by

$$A(z) := \sum_{a\in\mathcal{A}} z^{N(a)} = \sum_{n=0}^{\infty} a_n z^n, \tag{B.2}$$

where $a_n = \#\{a \in \mathcal{A} \colon N(a) = n\}$ is the *counting sequence*.

In order to specify a combinatorial structure, one can combine simpler structures, or provide a recursive definition, using elementary operations that we call *constructors*. We will give the most common constructors applied to two one-parameter combinatorial structures, $(\mathcal{A}, N_{\mathcal{A}})$ and $(\mathcal{B}, N_{\mathcal{B}})$. For convenience we may omit the index on the size function.

Definition B.2. In terms of sets, the *Cartesian product* $\mathcal{A} \times \mathcal{B}$ is defined as the set of all ordered pairs (a, b) for $a \in \mathcal{A}$ and $b \in \mathcal{B}$. We define $(\mathcal{A} \times \mathcal{B}, N)$ as a combinatorial structure with the *inherited size* function $N \colon A \times B \to \mathbb{N}_0$ by setting $N(a, b) := N(a) + N(b)$.

Remark B.1. The restriction of a combinatorial structure to a subset is a combinatorial structure. Complementarily, if the size function of two structures agree on their intersection then we have a structure on the union in the obvious way. In particular, if two structures are disjoint then the union has a corresponding structure.

Definition B.3. The *disjoint union* $\mathcal{A} \uplus \mathcal{B}$ is defined by introducing two distinct singleton combinatorial structures $(\{\epsilon_1\}, N = 0)$ and $(\{\epsilon_2\}, N = 0)$, and writing

$$\mathcal{A} \uplus \mathcal{B} := (\{\epsilon_1\} \times \mathcal{A}) \cup (\{\epsilon_2\} \times \mathcal{B}). \tag{B.3}$$

Remark B.2. Contrary to the union, this allows the repetitions if $\mathcal{A}$ and $\mathcal{B}$ intersect and it is a well defined structure even if the size functions don't coincide on the intersection.

Example B.1. The set of the natural numbers endowed with the identity as a size function can be produced by adding up ones recursively. Thus it can be specified recursively in the following way,

$$\mathbb{N} = \{1\} \uplus (\{1\} \times \mathbb{N}), \tag{B.4}$$

where $N(1) = 1$.

Definition B.4. If $\mathcal{A}$ has no elements of size 0 (in order to satisfy condition (B.1)), we can define the (finite) *sequences* $Seq(\mathcal{A})$ of elements of $\mathcal{A}$,

$$Seq(\mathcal{A}) := \biguplus_{n=0}^{\infty} \mathcal{A}^n \text{ where } \mathcal{A}^n = \underbrace{\mathcal{A} \times \cdots \times \mathcal{A}}_{n \text{ times}}. \tag{B.5}$$

and $\mathcal{A}^0 = \{\epsilon\}$ with $N(\epsilon) = 0$.

Example B.2. The non-negative integers can be specified as follows:

$$\mathbb{N}_0 = Seq(\{1\}), \tag{B.6}$$

using $N(1) = 1$ as in the previous example.

Definition B.5. The *multiset* $MSet(\mathcal{A})$ which is the set of the finite sequences of elements of $\mathcal{A}$ up to permutation. Since we do not consider the order, we can arbitrary regroup the identical elements, thus we can specify $MSet(\mathcal{A})$ with the previous constructors:

$$MSet(\mathcal{A}) := \prod_{a\in\mathcal{A}} Seq(\{a\}). \tag{B.7}$$

In other words assuming that $\mathcal{A} = \{a_1, a_2, a_3 \cdots\}$ is ordered:

$$MSet(\mathcal{A}) = Seq(\{a_1\}) \times Seq(\{a_2\}) \times Seq(\{a_3\}) \times \cdots .$$

It is a well defined combinatorial structure as each term $Seq(\{a_j\})$ contains the empty sequence.

Example B.3. The integer partitions:

$$\Lambda = MSet(\mathbb{N}). \tag{B.8}$$

Definition B.6. The *powerset* $PSet(\mathcal{A})$ that contains every finite subsets of $\mathcal{A}$ or equivalently every element of $MSet(\mathcal{A})$ with multiplicities restricted to $\{0, 1\}$:

$$PSet(\mathcal{A}) := \prod_{a\in\mathcal{A}} \{a\} \uplus \{\epsilon\}, \tag{B.9}$$

where we set $N(\epsilon) = 0$.

Example B.4. The strict partitions:

$$\check{\Lambda} = PSet(\mathbb{N}). \tag{B.10}$$

Lemma B.3. *The following table summarises the constructors defined previously and their interpretation in terms of generating functions.*

Table B.1: Correspondence between constructors and generating functions

Symbol	**Size function**	**Generating function**
$\mathcal{C} = \mathcal{A} \biguplus \mathcal{B}$	$N = N \cdot \mathbf{1}_{\mathcal{A}} + N \cdot \mathbf{1}_{\mathcal{B}}$	$C(z) = A(z) + B(z)$
$\mathcal{C} = \mathcal{A} \times \mathcal{B}$	$N(a, b) = N(a) + N(b)$	$C(z) = A(z) \cdot B(z)$
$\mathcal{C} = Seq(\mathcal{A})$	$N((a_i)_i) = \sum_i N(a_i)$	$C(z) = (1 - A(z))^{-1}$
$\mathcal{C} = MSet(\mathcal{A})$	$N((a_i)_i) = \sum_i N(a_i)$	$C(z) = \prod_{a\in\mathcal{A}}(1 - z^{N(a)})^{-1}$
$\mathcal{C} = PSet(\mathcal{A})$	$N((a_i)_i) = \sum_i N(a_i)$	$C(z) = \prod_{a\in\mathcal{A}}(1 + z^{N(a)})$

Proof.

- For the union and the Cartesian product the correspondence is immediate.
- For the Sequence, we just decompose $Seq(\mathcal{A})$ into every possible lengths. According to the correspondence for the Cartesian product the generating function of $\mathcal{A}^n$ is $A(z)^n$ thus we obtain a geometric sum,

$$C(z) = 1 + A(z) + A(z)^2 + \cdots = (1 - A(z))^{-1}. \tag{B.11}$$

- For the multiset and the powerset, it follows from the specifications (B.7) and (B.9) and the previous correspondences.

□

Definition B.7. If $(\mathcal{A}, N)$ is a combinatorial structure, a *combinatorial parameter* is a function $M\colon \mathcal{A} \to \mathbb{N}_0$. We define the generating function of the *two-parameter structure* $(\mathcal{A}, N, M)$

$$A(z_1, z_2) := \sum_{a\in\mathcal{A}} z_1^{N(a)} z_2^{M(a)} = \sum_{n=0}^{\infty}\sum_{m=0}^{\infty} a_{n,m} z_1^n z_2^m. \tag{B.12}$$

Example B.5. Λ or $\check{\Lambda}$ with the size and the length inherited from $N(\ell) = \ell$ and $M(\ell) = 1$ for $\ell \in \mathbb{N}$.

B.2. Boltzmann distributions

In this section we assume that $(\mathcal{A}, N, M)$ is a two parameters combinatorial structure, where the corresponding generating function $A(z_1, z_2)$ has a non-zero convergence radius. For convenience we will write $\boldsymbol{z} = (z_1, z_2)$.

Definition B.8. Suppose that $\boldsymbol{z} = (z_1, z_2)$ is a pair of positive parameters such that $A(\boldsymbol{z})$ is defined. We call the *Boltzmann distribution* over $\mathcal{A}$ with the parameters $\boldsymbol{z}$, the probability distribution defined by

$$\mathsf{P}_{\boldsymbol{z}}(a) = \frac{z_1^{N(a)} z_2^{M(a)}}{A(\boldsymbol{z})} \tag{B.13}$$

for all $a \in \mathcal{A}$.

Lemma B.4. *Let $\mathcal{S} \subset \mathcal{A}$, then the conditional distribution $\mathsf{P}_{\boldsymbol{z}}(\cdot|\mathcal{A})$ coincides with the Boltzmann distribution over $\mathcal{S}$.*

An interesting property of the Boltzmann distributions family is their stability under conditioning.

Proof. The conditional distribution is

$$\mathsf{P}_{\boldsymbol{z}}(a|\mathcal{S}) = \frac{\mathsf{P}_{\boldsymbol{z}}(a)}{\mathsf{P}_{\boldsymbol{z}}(\mathcal{S})} = \frac{z_1^{N(a)} z_2^{M(a)}}{A(\boldsymbol{z})} \times \frac{A(\boldsymbol{z})}{\sum_{a' \in \mathcal{S}} z_1^{N(a')} z_2^{M(a')}}.$$

By definition the generating function of $\mathcal{S}$ is $\sum_{a' \in \mathcal{S}} z_1^{N(a')} z_2^{M(a')}$, thus we can conclude. □

The following lemma is fundamental if we want to use Boltzmann distributions as an enumeration tool or for the simulation of uniform distributions.

Lemma B.5. *Let n, m be such that $a_{n,m} \neq 0$. For all valid choice of parameters, the corresponding Boltzmann distribution is conditionally uniform,*

$$\mathsf{P}_{\boldsymbol{z}}(a|N(a) = n, M(a) = m) = \frac{1}{a_{n,m}}. \tag{B.14}$$

In particular

$$a_{n,m} = \frac{A(\boldsymbol{z})\, \mathsf{P}_{\boldsymbol{z}}(N(a) = n, M(a) = m)}{z_1^n z_2^m}. \tag{B.15}$$

Lemma B.6. *The following table is an interpretation of the elementary constructors in terms of the Boltzmann distribution*

Table B.2: Correspondence between constructors and Boltzmann distribution

Symbol	**Boltzmann**
$\mathcal{C} = \mathcal{A} \biguplus \mathcal{B}$	Bernoulli: $\mathsf{P}^{\mathcal{C}}_{\boldsymbol{z}}(\mathcal{A}) = A(\boldsymbol{z})/(A(\boldsymbol{z}) + B(\boldsymbol{z}))$
$\mathcal{C} = \mathcal{A} \times \mathcal{B}$	Product: $\mathsf{P}^{\mathcal{C}}_{\boldsymbol{z}}(a, b) = \mathsf{P}^{\mathcal{A}}_{\boldsymbol{z}}(a) \cdot \mathsf{P}^{\mathcal{B}}_{\boldsymbol{z}}(b)$
$\mathcal{C} = Seq(A)$	Geometric: $\mathsf{P}_{\boldsymbol{z}}(\mathcal{A}^d) = A(\boldsymbol{z})^d(1 - A(\boldsymbol{z}))$

In particular, for the multisets and the powersets, the multiplicities are independent and given by:

- $\mathcal{C} = MSet(\mathcal{A})$*:*

$$\mathsf{P}_{\boldsymbol{z}}(\nu_a = k) = z_1^{kN(a)} z_2^{kM(a)} (1 - z_1^{N(a)} z_2^{M(a)}). \tag{B.16}$$

- $\mathcal{C} = PSet(\mathcal{A})$:

$$\mathsf{P}_{\boldsymbol{z}}(\nu_a = 1) = \frac{z_1^{N(a)} z_2^{M(a)}}{1 + z_1^{N(a)} z_2^{M(a)}}. \tag{B.17}$$

Proof. It is an immediate consequence of the correspondences given in Table B.1. □

In order to use the Boltzmann distributions, we need to be able to select $\boldsymbol{z}$ in order to make the the weight and the length "close" to values $\langle N \rangle$ and $\langle M \rangle$ prescribed by the user. We pursue the approach (see, e.g., [13], [34], [87] [88]) based on making the expected values of N and M consistent with $\langle N \rangle$ and $\langle M \rangle$, respectively:

$$\mathsf{E}_{\boldsymbol{z}}(N) = \langle N \rangle\,, \qquad \mathsf{E}_{\boldsymbol{z}}(M) = \langle M \rangle\,. \tag{B.18}$$

The following lemma, along with its corollary, justifies the use of hyper-parameters $\langle N \rangle$, and $\langle M \rangle$. It also gives information about the dispersion around these values.

Proposition B.7. *The moments of order one and two of the Boltzmann distribution over $\mathcal{A}$ are given by*

$$\begin{pmatrix} \mathsf{E}_{\boldsymbol{z}}(N) \\ \mathsf{E}_{\boldsymbol{z}}(M) \end{pmatrix} = \begin{pmatrix} z_1 & 0 \\ 0 & z_2 \end{pmatrix} \nabla\big(\log A(\boldsymbol{z})\big), \tag{B.19}$$

$$\boldsymbol{K}(\boldsymbol{z}) := \begin{pmatrix} \mathsf{Var}_{\boldsymbol{z}}(N) & \mathsf{Cov}_{\boldsymbol{z}}(N,M) \\ \mathsf{Cov}_{\boldsymbol{z}}(N,M) & \mathsf{Var}_{\boldsymbol{z}}(M) \end{pmatrix} = \begin{pmatrix} z_1 & 0 \\ 0 & z_2 \end{pmatrix} \nabla\big(\mathsf{E}_{\boldsymbol{z}}(N), \mathsf{E}_{\boldsymbol{z}}(M)\big). \tag{B.20}$$

Proof. We just prove the first row of equation (B.19), the rest of the proof is similar

$$\begin{aligned} z_1\, \partial_{z_1}(\log A) &= \sum_{n=0}^{\infty} \sum_{m=0}^{\infty} n a_{n,m} z_1^n z_2^m = \sum_{a \in \mathcal{A}} N(a) \cdot \frac{z_1^{N(a)} z_2^{M(a)}}{A(\boldsymbol{z})} = \sum_{a \in \mathcal{A}} N(a)\, \mathsf{P}_{\boldsymbol{z}}(a) \\ &= \mathsf{E}_{\boldsymbol{z}}(N). \end{aligned}$$

□

Corollary B.7.1. *Any system of equations in variables $\boldsymbol{z} = (z_1, z_2)$ of the form (B.18) has at most one solution if and only if* $\det \boldsymbol{K} > 0$.

In particular it means that M shouldn't be taken proportional to N.

Let us give a short example to illustrate how we can construct the Boltzmann distribution and use it in an asymptotic regime.

Example B.6. We take $\mathcal{A}$ as the class of the unary-binary trees, with the size function N counts the number of internal nodes and the parameter M counts the number of unary nodes.

The class $\mathcal{A}$ can be specified in the following way:

$$\mathcal{A} = \underbrace{\bullet}_{\text{single node}} \biguplus \underbrace{(\bullet \times \mathcal{A})}_{\text{unary root}} \biguplus \underbrace{(\mathcal{A} \times \bullet \times \mathcal{A})}_{\text{binary root}}. \tag{B.21}$$

For convenience we will denote by $\mathcal{U}$ the subclass of elements that have a unary root and by $\mathcal{B}$ the subclass of elements that have a binary root. The Boltzmann distribution can be interpreted as a Galton–Watson tree with reproduction laws given by $\mathsf{P}_{\boldsymbol{z}}(\bullet)$, $\mathsf{P}_{\boldsymbol{z}}(\mathcal{U})$, and $\mathsf{P}_{\boldsymbol{z}}(\mathcal{B})$.

The parameters are defined through the following relations:

$$\begin{aligned}
\bullet &: \quad N(\bullet) = 0, \quad M(\bullet) = 0 \\
\mathcal{U} &: \quad N(\bullet, A) = 1 + N(A), \quad M(\bullet, A) = 1 + M(A) \\
\mathcal{B} &: \quad N(A_1, \bullet, A_2) = 1 + N(A_1) + N(A_2), \quad M(A_1, \bullet, A_2) = M(A_1) + M(A_2).
\end{aligned}$$

The symbolic specification (B.21) can be immediately translated into an equation for the generating function:

$$A(\boldsymbol{z}) = 1 + z_1 z_2 A(\boldsymbol{z}) + z_1 A(\boldsymbol{z})^2.$$

This is a quadratic equation for $A(\boldsymbol{z})$, which solves to

$$A(\boldsymbol{z}) = \frac{(1 - z_1 z_2) - \sqrt{(1 - z_1 z_2)^2 - 4 z_1}}{2 z_1}.$$

The root is determined uniquely by noting that $\lim_{\boldsymbol{z} \to \mathbf{0}} A(\boldsymbol{z}) = 1$. In virtue of the law of total expectation, the expected values of N and M satisfy the relations

$$\begin{aligned}
\mathsf{E}_{\boldsymbol{z}}(N) &= \mathsf{P}_{\boldsymbol{z}}(\mathcal{U}) \cdot (1 + \mathsf{E}_{\boldsymbol{z}}(N)) + \mathsf{P}_{\boldsymbol{z}}(\mathcal{B}) \cdot (1 + 2\,\mathsf{E}_{\boldsymbol{z}}(N)), \\
\mathsf{E}_{\boldsymbol{z}}(M) &= \mathsf{P}_{\boldsymbol{z}}(\mathcal{U}) \cdot (1 + \mathsf{E}_{\boldsymbol{z}}(M)) + \mathsf{P}_{\boldsymbol{z}}(\mathcal{B}) \cdot 2\,\mathsf{E}_{\boldsymbol{z}}(M).
\end{aligned} \tag{B.22}$$

If we assume the calibration equations (B.18) and substitute the probabilities $\mathsf{P}_{\boldsymbol{z}}(\mathcal{U}) = z_1 z_2$ and $\mathsf{P}_{\boldsymbol{z}}(\mathcal{B}) = z_1 A(\boldsymbol{z})$, then the equations (B.22) specialise to

$$\begin{aligned}
\langle N \rangle &= z_1 z_2 (1 + \langle N \rangle) + z_1 A(\boldsymbol{z}) \cdot (1 + 2\,\langle N \rangle), \\
\langle M \rangle &= z_1 z_2 (1 + \langle M \rangle) + 2 z_1 A(\boldsymbol{z})\,\langle M \rangle\,.
\end{aligned}$$

Setting $\langle N \rangle = n$ and $\langle M \rangle = m$, the calibration equations are solved exactly,

$$\begin{aligned}
z_1 &= \frac{n^2 - 2mn + n + m^2 - m}{4n^2 - 4mn + 4n + m^2 + 1}, \\
z_2 &= \frac{2mn - m^2 + m}{n^2 - 2mn + n + m^2 - m}.
\end{aligned}$$

Appendix C

Boltzmann sampling

C.1. Elementary principles

A *Boltzmann sampler* for a combinatorial structure $(\mathcal{A}, N, M)$ (as in Definition B.7) is an algorithmic realisation of the Boltzmann distribution for a parameter $\boldsymbol{z}$ given by the user. Boltzmann samplers are often integrated in a *rejection loop* that repeats the sampler until the value of (N, M) of the last sampled object belong the a prescribed set that we call the *target*. If this set contains only one point, we say that the rejection scheme is *exact*, otherwise we say that it is *approximate*. The rejected loop is usually preceded by a calibration of $\boldsymbol{z}$ in order to minimise the number of failed iterations. Some pre-computations may also be useful if their result will be reused at every iterations (e.g. generating function).

As we have seen in the first chapter, the Bernoulli and the geometric distributions play an important role in the interpretation of Boltzmann distributions. So for the rest of the chapter we will assume that we have the following primitives:

- $\texttt{Ber}(p)$ generates a 1 with probability p and a 0 with probability $1-p$
- $\texttt{Geom}(p)$ generates $k \in [\![0, \infty]\!]$ with probability $(1-p)^k p$.

We will also assume that those operations can produce perfectly random output in a bounded time.

Of course, the complexity is crucial in order to determine if a particular sampling scheme is relevant. Here, we will only consider the time complexity assuming that every elementary operations (arithmetic, logic, `Ber` and `Geom`) cost one unit of time. This is a random variable for which we will analyse the expectation. We decompose it in the following way:

$$T = P + S \cdot R, \tag{C.1}$$

where T is the time complexity, P is the complexity of the pre-computations (which will be negligible), S is the complexity of the sampler and R is the number of rejections. Those quantities are random variables for which the law depend on the inputs. Another measure of the efficacy of a sampling algorithm, that we do not consider here, is its costs in terms of random bits since this will ultimately affect the bias of the sampler.

Example C.1. Let $\mathcal{A}$ the set of the Bernoulli processes:

$$\mathcal{A} = \{0,1\} \uplus \{0,1\} \times \mathcal{A} \tag{C.2}$$

where N counts the number of attempts (i.e. $N(0) = N(1) = 1$) and M counts the number of successful attempts ($M(0) = 0$ and $M(1) = 1$). The generating function of $\mathcal{A}$ verifies the following equation:

$$A = \underbrace{z_1 + z_1 z_2}_{\{0,1\}} + \underbrace{(z_1 + z_1 z_2)A}_{\{0,1\}\times\mathcal{A}} \tag{C.3}$$

so we have:

$$A = \frac{z_1(1+z_2)}{1 - z_1(1+z_2)}. \tag{C.4}$$

We have the Boltzmann sampler here below (Figure 4):

Algorithm 4: $\Gamma_{\mathcal{A}}(\boldsymbol{z})$

```
b ← Ber(z_1(1 + z_2)/A)
if b = 1 then
    b ← Ber((1 + z_2)^{-1})
    if b = 1 then
        return 0
    end
    return 1
end
b ← Ber((1 + z_2)^{-1})
if b = 1 then
    return (0, Γ_A(z))
end
return (1, Γ_A(z))
```

Figure C.1: Boltzmann sampler for Bernoulli processes

The complexity of this algorithm is a random variable that is asymptotically proportional to N, which follows a geometric law (starting from 1) with success

rate $\mathsf{P}_{\boldsymbol{z}}[\{0,1\}] = 1 - z_1(1+z_2)$. In particular the expected length of the process is:

$$\mathsf{E}_{\boldsymbol{z}}[N] = \frac{1}{1 - z_1(1+z_2)},$$

setting the hyperparameters $\langle N \rangle$ and $\langle M \rangle$ as usual, this gives a more convenient expression for the generating function and the probability of termination:

$$A = \langle N \rangle - 1, \qquad \mathsf{P}_{\boldsymbol{z}}[\{0,1\}] = \frac{1}{\langle N \rangle}$$

In order to solve the calibration equations we also need to evaluate the expected value of M. This can be done by using the recursive specification:

$$\begin{aligned}
& \langle M \rangle = \mathsf{P}_{\boldsymbol{z}}[(1)] + \mathsf{P}_{\boldsymbol{z}}[(0,\mathcal{A})] \cdot \langle M \rangle + \mathsf{P}_{\boldsymbol{z}}[(1,\mathcal{A})] \cdot [1 + \langle M \rangle] \\
\Leftrightarrow\ & \langle M \rangle = \frac{z_1 z_2}{A} + z_1 \cdot \langle M \rangle + z_1 z_2 \cdot [1 + \langle M \rangle] \\
\Leftrightarrow\ & \frac{\langle M \rangle}{\langle N \rangle} = z_1 z_2 \cdot \frac{\langle N \rangle}{\langle N \rangle - 1} \Leftrightarrow z_1 z_2 = \frac{\langle N \rangle \langle M \rangle - \langle M \rangle}{\langle N \rangle^2}.
\end{aligned}$$

Thus the parameters are given by:

$$z_1 = 1 - \frac{\langle N \rangle \langle M \rangle + \langle N \rangle - \langle M \rangle}{\langle N \rangle^2}, \qquad z_2 = \frac{\langle M \rangle}{\langle N \rangle - \langle M \rangle} \cdot \frac{\langle N \rangle - 1}{\langle N \rangle + 1}.$$

Of course we can also provide a calibrated uniform/exact sampler. We shall remark that it only requires to have $m \leq n$ to end almost surely, in some cases the target may be empty and we may either prefer to have an approximate sampler or to set a time limit.

Let us evaluate evaluate the success rate of an exact rejection procedure i.e. the probability to have $N = n$ and $M = m$:

$$\mathsf{P}_{\boldsymbol{z}}[N = n, M = m] = \mathsf{P}_{\boldsymbol{z}}[M = m | N = n] \cdot \mathsf{P}_{\boldsymbol{z}}[N = n]$$

As in Example B.6 we consider that $\langle N \rangle \to \infty$ and $\langle M \rangle = c \langle N \rangle$ for $c \in (0,1)$. Every time a bit is added, whether it is the ending bit or not, it is 0 with probability $(1+z_1)^{-1}$ and 1 with probability $z_2(1+z_2)^{-1} \sim c$ so the distribution of M conditionally on having $N = n$ is approximately Binomial(n, c). In particular we can estimate the success rate:

$$\mathsf{P}_{\boldsymbol{z}}[N = n, M = m] = \mathsf{P}_{\boldsymbol{z}}[N = n, M = m] \sim \frac{n^{-3/2}}{\sqrt{2\pi c(1-c)}}$$

so the order of complexity of the exact sampling procedure is $O(n^{5/2})$.

Remark C.1. It is just a toy example which is not a particularly efficient. For instance if we want to make exact sampling we can just set the length and set each bit to 1 with probability $z_2(1+z_2)^{-1}$ until we reach the required number of 1, then we fill the rest of the sequence with 0 and to avoid bias we compute the probability that the remaining bits are 0. This would give a complexity of $O(n^{3/2})$ as there will be no rejection for the length of the process.

C.2. Sampler for multisets and powersets

As we saw in Lemma B.6 a simple way to describe the Boltzmann distribution over $MSet(\mathcal{A})$ is to observe that the multiplicities of each elements of $\mathcal{A}$ are independent and geometric. Thus we deduce a (theoretical) sampling algorithm that consists in a loop that generates all the multiplicities. Such algorithm only terminates if the structure $\mathcal{A}$ is finite. In this case its complexity is deterministic and proportional to the number of elements of $\mathcal{A}$. Of course in general $\mathcal{A}$ may be infinite, in which case there are at least two approaches to ensure the termination of the algorithm. One approach consists in truncating the structure $\mathcal{A}$ and to not sample multiplicities that are likely to be zero. Unless it is included in a rejection scheme, this approach is necessarily biased and requires reliable estimates. Another approach consists in using an alternative specification. It is detailed in [31] and [71] in the context of structures with a single parameter. It can be adapted with limited efforts to structures that include multiple parameters. These references also provide a procedure to sample powersets, alternately Theorem 4.9 can be used. Any of these procedure, apart from the one based on a truncation, require an *oracle* to estimate the generating function.

Appendix D

Code

D.1. Young diagram visualisation

```
function young_plot(lambda)
  lambda = flip(sort(lambda));
  m = length(lambda); %height of the diagram (total number of
      parts)
  L = max(lambda);  %length of the diagram (maximal parts)
  Y = zeros(1,L); %y coordinates of the upper bound
  X = zeros(1,L); %x coordinates of the upper bound

  hold on;

%draw the boxes
  for(i=1:m)
    for(j=1:lambda(i))
      rectangle("position", [j-1, i-1, 1, 1], "FaceColor", [0.9,
          0.9, 0.9]);
    endfor
  endfor

%draw the upper bound
  for(i=1:L)
    Y(i) = cumsum(lambda>i-1)(m);
    X(i) = i-1;
  endfor

  for(i=1:L)
    line([X(i),X(i)+1], [Y(i),Y(i)], "linewidth", 1, "color", "r
        ");
  endfor

  line([X(L)+1, X(L)+2], [0,0], "linewidth", 1, "color", "r");

```

```
29   plot(lambda(1),0, 'o', 'markersize', 5, 'markeredgecolor', 'r',
         'markerfacecolor', 'w');
30   for(i=2:L)
31     if(Y(i-1)>Y(i))
32       plot(X(i),Y(i), 'o', 'markersize', 5, 'markeredgecolor', 'r
             ', 'markerfacecolor', 'w');
33     endif
34   endfor
35
36   plot(lambda(1),1, 'o', 'markersize', 5, 'markeredgecolor', 'r',
         'markerfacecolor', 'r');
37   for(i=1:L-1)
38     if(Y(i+1)<Y(i))
39       plot(X(i)+1,Y(i), 'o', 'markersize', 5, 'markeredgecolor',
             'r', 'markerfacecolor', 'r');
40     endif
41   endfor
42
43   plot(0,m, 'o', 'markersize', 5, 'markeredgecolor', 'r', '
        markerfacecolor', 'r');
44
45 %set the axis at the right scale
46   set(gca, "fontsize", 14)
47   axis("equal", [0,lambda(1)+0.5,0,m+0.5]);
48
49 %save the picture in the eps format
50   print -color -depsc young.eps
51 endfunction
```

D.2. Free sampler benchmark

```
1  #include <stdlib.h>
2  #include <stdio.h>
3  #include <math.h>
4  #include <time.h>
5
6  typedef struct partition
7  {
8      int n;
9      int m;
10     int* parts;
11 } partition;
12
13 int ber(double);
14 void freesampler(int, double, double, int, partition*);
15
16 int main()
```

```
{
    clock_t start = clock();

    partition lambda;
    int p = 2;
    int L = 100000 * (1.1);
    double n = 100000;
    double m = 5;
    srand(time(NULL));

    double nmoy = 0.;
    double mmoy = 0.;

    int nsamples = 10000;
    int nsamples_free = 0;
    int i;
    for (i = 0; i < nsamples; i++)
    {
        nsamples_free += 1;
        freesampler(p, n, m, L, &lambda);
        nmoy += lambda.n;
        mmoy += lambda.m;
        free(lambda.parts);
        while (lambda.m != 5)
        {
            nsamples_free += 1;
            freesampler(p, n, m, L, &lambda);
            nmoy += lambda.n;
            mmoy += lambda.m;
            free(lambda.parts);
        }
    }

    printf("Mean execution time : %f ms\n", (double)(clock() -
       start) / (CLOCKS_PER_SEC*(nsamples/1000)));
    printf("average size : %f\n", nmoy / nsamples_free);
    printf("average length : %f\n", mmoy / nsamples_free);
    printf("mean number of attempts : %f\n", (double)
       nsamples_free / nsamples);


    return EXIT_SUCCESS;
}

int ber(double p)
{
    return (double)rand() / RAND_MAX <= p;
}

```

```
64 void freesampler(int p, double n, double m, int L, partition*
       lambda)
65 {
66     double z1, z2, gamma, q;
67     int jmax, j, N, M, l;
68     gamma = m / (p * n);
69     z1 = exp(-gamma);
70     z2 = (double)p * m * pow(gamma, 1. / (double)p) / tgamma(1. /
           (double)p);
71
72     jmax = (int)floor(pow(L, 1. / (double)p));
73
74     N = 0;
75     M = 0;
76     lambda->parts = (int*)malloc(sizeof(int));
77
78     for (j = 1; j <= jmax; j++)
79     {
80         q = 1;
81         q = pow(z1, pow((double)j, (double)p));
82         q = q * z2 / (1. + q * z2);
83         if (ber(q))
84         {
85             l = round(pow((double)j, (double)p));
86             N = N + l;
87             M++;
88             lambda->parts = (int*)realloc(lambda->parts, M *
                   sizeof(int));
89             lambda->parts[M - 1] = l;
90         }
91     }
92     lambda->m = M;
93     lambda->n = N;
94 }
```

D.3. Density test

```
1 """
2 Title: Partition test density
3
4 Purpose: Given four integers L, l, m and q, a float delta in
5 (0,1), this program tests with significance level delta which
6 integers from l to L can be represented as strict partitions into
7 m integers raised to the power q.
8
9 The program realises for each integer n from L down to l parallel
10 independent random realisations of a sampler that has a success
```

```
rate bounded below by the Boltzmann distribution.
"""

import multiprocessing as mp
import random
import numpy as np
from math import gamma, factorial, exp, log, floor
import time

#Sample strict partitions into m parts which are q-th powers
smaller than L.
#z1 and z2 are calibration parameters for the sampler
def worker_sampler(q,L,n,m,z1,z2):
    part=[]
    N=0
    M=0
    j=1
    l=1
    while M<m and l<=n-N and l<=L:
        Z=(z1**l)*z2
        p=Z/(1+Z)
        if np.random.binomial(1, p):
            part.append(l)
            N=N+l
            M=M+1
        j=j+1
        l=j**q
    return part,N,M

#Iterates the sampler
def worker_test(name,q,L,n,m,max_attempt,z1,z2,stop_flag):
    nb_attempts=0
    N=0
    M=0
    representable_test_worker = [0]*L
    while (N!=n or M !=m) and (nb_attempts<max_attempt) and not
       stop_flag.value:
        part,N,M=worker_sampler(q,L,n,m,z1,z2)
        nb_attempts=nb_attempts+1
        if M==m:
            representable_test_worker[N-1]=1
        if N==n and M==m:
            stop_flag.value=True
    return representable_test_worker

#Helper function to unpack arguments and call worker_test
def worker_helper(args):
    return worker_test(*args)

```

```
#Compute the maximal number of attempts per worker
def max_attempt_comp(q,n,m,delta, nworkers):
    a=m/q
    return floor(-n*((exp(1)/a)**a)*(gamma(a)*log(delta))*
       factorial(m)/((m**m)*exp(-m)*nworkers))

#Calibrate z1 and z2
def calibration(q,n,m):
    kappa=(m**(q+1))/n
    z1=np.exp(-m/(q*n))
    z2=(kappa**(1/q))/((q**(1/q))*gamma(1+1/q))
    return z1,z2

#Combine list of representability results obtained by the workers
def combine_workers(representable_test_workers):
    combined_list = [int(any(elements)) for elements in zip(*
       representable_test_workers)]
    return combined_list

#Combine two lists of representability results
def combine_lists(list1, list2):
    combined_list = [max(x, y) for x, y in zip(list1, list2)]
    return combined_list

#Print the list of reprentable numbers that have been obtained
def print_representable(representable_test):
    print("The following numbers are representable:")
    indices = []
    for index, value in enumerate(representable_test):
        if value == 1:
            indices.append(str(index + 1))
    print(", ".join(indices))
    print(f"This list contains {len(indices)} elements")

#Test if n is representable
def single_n_test(q,L,n,m,delta):
    # Compute the number of workers
    nworkers = mp.cpu_count()-1
    # Compute the maximal number of attempts per worker
    max_attempt = max_attempt_comp(q,n,m,delta,nworkers)
    # Calibrate the parameters
    z1,z2=calibration(q,n,m)
    # Create a manager to manage shared variables
    manager = mp.Manager()
    # Create a shared stop flag variable
    stop_flag = manager.Value('i', False)
    # Create a pool of worker processes
    pool = mp.Pool()
    # Use imap_unordered with the helper function
```

```
106     representable_test_workers=pool.imap_unordered(worker_helper,
            [(name,q,L,n,m,max_attempt,z1,z2,stop_flag) for name in
        range(nworkers)])
107     # Close the pool to prevent any new tasks
108     pool.close()
109     # Wait for all worker processes to complete
110     pool.join()
111     # Combine the results of the workers
112     representable_test = combine_workers(
            representable_test_workers)
113     return representable_test
114 
115 #Test representability from L down to l
116 def multiple_test(q,L,l,m,delta):
117     representable_test = [0]*L
118     print("Coarse test")
119     for n in range(L, l-1, -1):
120         if not representable_test[n-1]:
121             print("Test the number", n)
122             representable_test=combine_lists(representable_test,
                    single_n_test(q,L,n,m,delta))
123     return representable_test
124 
125 
126 if __name__ == '__main__':
127     # Inputs of the programs
128     while True:
129         L = int(input("Enter a weight upper limit L: "))
130         l = int(input("Enter a weight lower limit l: "))
131         m = int(input("Enter a target length m: "))
132         q = int(input("Enter a power q: "))
133         delta = float(input("Enter significance level delta of
                single test (may be taken close to 1 if L-l is large):
                "))
134 
135         if m > 0 and q > 0 and 0 < delta < 1 and L>0 and l>0:
136             print("Input values are valid.")
137             break
138         else:
139             print("Invalid input. Please make sure n, m, q and L
                    are positive integers, and delta is a float
                    between 0 and 1.")
140 
141     # Starts the timer
142     start_time = time.time()
143     representable_test=multiple_test(q,L,l,m,delta)
144 
145     #print the representable numbers obtained
146     print_representable(representable_test)
```

```
    # End the timer
    end_time = time.time()
    # Calculate the elapsed time
    execution_time = end_time - start_time
    # Print the execution time
    print("Execution time: ", execution_time, "seconds")
```

D.4. Aggregation simulator

```
#define _CRT_SECURE_NO_WARNINGS
#include <stdio.h>
#include <stdlib.h>
#include <math.h>
#include <time.h>
#define PI 3.14159265359

typedef struct
{
  int* sites;
  int* masses;
  int nb_part;
} occupation_s;

typedef struct
{
  occupation_s occupation;
  int N;
  float rate;
  float alpha;
  float second_moment;
} config_s;

int mod(int, int);
float exp_clock(float);
float unif_rand(float, float);
void init_config(config_s*, int, float);
void update_config(config_s*);
void simulation(int, float, FILE*, FILE*);

/*reordering functions*/
/*the particles are relabelled by decreasing mass after each
   coalescence event*/
void quicksort(occupation_s*, int, int);
int partition(occupation_s*, int, int);
void swap(occupation_s*, int, int);

void print_part(occupation_s*, int, int);
```

```
38 void print_part_file(occupation_s*, int, int, FILE*);
39
40 int main()
41 {
42   int N = 1024;
43   float alpha = 0;
44   float res = 0;
45   FILE* file = fopen("sim_time.csv", "w");
46   FILE* file2 = fopen("sim_part.csv", "w");
47
48   srand(time(NULL));
49   simulation(N, alpha, file, file2);
50   fclose(file);
51   fclose(file2);
52   return EXIT_SUCCESS;
53 }
54
55 int mod(int a, int b)
56 {
57   int c = a % b;
58
59   if (c >= 0)
60     return c;
61   else
62     return b + c;
63 }
64
65 float exp_clock(float rate)
66 {
67   return -log(1 - (rand() / (RAND_MAX + 1.0))) / rate;
68 }
69
70 float unif_rand(float m, float M)
71 {
72   return rand() / (RAND_MAX + 1.) * (M - m) + m;
73 }
74
75 void init_config(config_s* config, int N, float alpha)
76 {
77   int i;
78   config->second_moment = N;
79   config->N = N;
80   config->rate = N;
81   config->alpha = alpha;
82   config->occupation.sites = (int*)malloc(N * sizeof(int));
83   config->occupation.masses = (int*)malloc(N * sizeof(int));
84   config->occupation.nb_part = N;
85
86   for (i = 0; i < N; i++)
```

```
87    {
88      config->occupation.sites[i] = i;
89      config->occupation.masses[i] = 1;
90    }
91  }
92
93  void update_config(config_s* config)
94  {
95    int i = -1;
96    float s = 0;
97    float u = unif_rand(0, config->rate);
98    int location_move = -1;
99
100   /*choice of the particle that moves (we specify the location in
          the table of the occupied sites)*/
101   while (location_move == -1)
102   {
103     i++;
104     s += 1. / powf(config->occupation.masses[i], config->alpha);
105     if (u <= s || i >= config->occupation.nb_part - 1)
106       location_move = i;
107   }
108
109   /*if the particle moves to an occupied site, we need to shorten
          the array of the occupied sites*/
110   {
111     if (location_move > 0)
112     {
113       config->second_moment -= powf(config->occupation.masses[
              location_move], 2) + powf(config->occupation.masses[mod(
              location_move - 1, config->occupation.nb_part)], 2);
114       config->second_moment += powf(config->occupation.masses[
              location_move] + config->occupation.masses[mod(
              location_move - 1, config->occupation.nb_part)], 2);
115
116       config->rate -= 1. / powf(config->occupation.masses[
              location_move], config->alpha) + 1. / powf(config->
              occupation.masses[mod(location_move - 1, config->
              occupation.nb_part)], config->alpha);
117       config->rate += 1. / powf(config->occupation.masses[
              location_move] + config->occupation.masses[mod(
              location_move - 1, config->occupation.nb_part)], config
              ->alpha);
118       config->occupation.masses[(location_move - 1) % config->
              occupation.nb_part] += config->occupation.masses[
              location_move];
119       config->occupation.nb_part--;
120
121       for (i = location_move; i < config->occupation.nb_part; i
```

```
        ++)
122     {
123       config->occupation.masses[i] = config->occupation.masses[
            i + 1];
124       config->occupation.sites[i] = config->occupation.sites[i
            + 1];
125     }
126   }
127   else
128   {
129     config->second_moment -= powf(config->occupation.masses[0],
          2) + powf(config->occupation.masses[config->occupation.
          nb_part - 1], 2);
130     config->second_moment += powf(config->occupation.masses[0]
          + config->occupation.masses[config->occupation.nb_part -
          1], 2);
131
132     config->rate -= 1. / powf(config->occupation.masses[0],
          config->alpha) + 1. / powf(config->occupation.masses[
          config->occupation.nb_part - 1], config->alpha);
133     config->rate += 1. / powf(config->occupation.masses[0] +
          config->occupation.masses[config->occupation.nb_part -
          1], config->alpha);
134     config->occupation.masses[config->occupation.nb_part - 1]
          += config->occupation.masses[0];
135     config->occupation.nb_part--;
136     for (i = 0; i < config->occupation.nb_part; i++)
137     {
138       config->occupation.masses[i] = config->occupation.masses[
            i + 1];
139       config->occupation.sites[i] = config->occupation.sites[i
            + 1];
140     }
141   }
142 }
143 else
144   config->occupation.sites[location_move] = mod(config->
        occupation.sites[location_move] - 1, config->N);
145 }
146
147 void simulation(int N, float alpha, FILE* file, FILE* file2)
148 {
149   clock_t start = clock();
150   //  FILE* file = fopen("sim.csv", "w");
151
152   int i;
153   int j = 0;
154   int k = 0;
155   int l;
```

```
156   float t = 0, t_cumul = 0;
157   config_s config;
158
159   config_s config_ordered;
160
161   int nb_part_prev = N;
162
163   init_config(&config, N, alpha);
164   init_config(&config_ordered, N, alpha);
165
166   while (config.occupation.nb_part > 1)
167   {
168     t = exp_clock(config.rate);
169     t_cumul += t;
170     j++;
171     update_config(&config);
172     if (config.occupation.nb_part > 1)
173     {
174       if (config.occupation.nb_part < nb_part_prev)
175       {
176         k++;
177         printf("coalescence %d    ", k);
178         printf("rate = %f\n", config.rate);
179
180         for (l = 0; l < config.occupation.nb_part; l++)
181         {
182           config_ordered.occupation.masses[l] = config.occupation
                .masses[l];
183           config_ordered.occupation.sites[l] = config.occupation.
                sites[l];
184         }
185
186         print_part_file(&config_ordered.occupation, config.
              occupation.nb_part, N, file2);
187         fprintf(file, "%f, %f\n", t_cumul, config.second_moment);
188         nb_part_prev = config.occupation.nb_part;
189       }
190     }
191     else
192       fprintf(file, "%f, %f\n", t_cumul, config.second_moment);
193   }
194 }
195
196 //quicksort with last element as the pivot
197 void swap(occupation_s* T, int a, int b)
198 {
199   int temp = T->masses[a];
200   T->masses[a] = T->masses[b];
201   T->masses[b] = temp;
```

```
202   temp = T->sites[a];
203   T->sites[a] = T->sites[b];
204   T->sites[b] = temp;
205 }
206
207 int partition(occupation_s* T, int l, int u)
208 {
209   int i;
210   int j = l;
211
212   for (i = l; i < u; i++)
213   {
214     if (T->masses[i] >= T->masses[u])
215     {
216       swap(T, i, j);
217       j++;
218     }
219
220   }
221   swap(T, j, u);
222   return j;
223 }
224
225 void quicksort(occupation_s* T, int l, int u)
226 {
227   if (l < u)
228   {
229     int m = partition(T, l, u);
230     quicksort(T, l, m - 1);
231     quicksort(T, m + 1, u);
232   }
233 }
234
235 void print_part(occupation_s* T, int N, int Nmax)
236 {
237   int i;
238   quicksort(T, 0, N - 1);
239
240   for (i = 0; i < N; i++)
241     printf("%d", T->masses[i]);
242
243   for (i = N; i < Nmax; i++)
244   {
245     printf("0");
246     if (i < Nmax - 1)
247       printf(",");
248   }
249
250   printf("\n");
```

```
}

void print_part_file(occupation_s* T, int N, int Nmax, FILE* data
    )
{
  int i;
  quicksort(T, 0, N - 1);

  for (i = 0; i < N; i++)
    fprintf(data, "%d,", T->masses[i]);

  fprintf(data, "\n");
}
```

D.5. Multispecies Aggregation simulator

```
import numpy as np
import matplotlib.pyplot as plt

# m_A(x) diffuses to x-1
def diffuseA(x, m):
    target = x - 1 if x > 0 else len(m) - 1
    m[target, 0] += m[x, 0]
    m[x, 0] = 0

# m_B(x) diffuses to x-1
def diffuseB(x, m):
    target = x - 1 if x > 0 else len(m) - 1
    m[target, 1] += m[x, 1]
    m[x, 1] = 0

#
def sum_of_rates(m):
    return np.sum(m[:, 0]) + np.sum(m[:, 1])

def calculate_dt(rates_sum):
    u = np.random.uniform(0, 1)
    dt = -np.log(u) / rates_sum
    return dt

# Selection of the transition
def choose_reaction(m, rates_sum):
    u = np.random.uniform(0, 1)
    cumulative_prob = 0.0

    for x in range(len(m)):
        prob_A = m[x, 1] / rates_sum
```

```
32          prob_B = m[x, 0] / rates_sum
33
34          cumulative_prob += prob_A
35          if u < cumulative_prob:
36              return 'diffuseA', x
37
38          cumulative_prob += prob_B
39          if u < cumulative_prob:
40              return 'diffuseB', x
41
42  def is_frozen(m):
43      for m_A, m_B in m:
44          if m_A > 0 and m_B > 0:
45              return False
46      return True
47
48  def plot_distribution(m):
49      plt.figure()
50      # Extract the masses of type A and B
51      mass_A = m[:, 0]
52      mass_B = m[:, 1]
53      # Create the x-axis labels
54      x = range(len(m))
55      # Plot mass type A
56      plt.plot(x, mass_A, label='Type A', marker='o', linestyle='
            None')
57      # Plot mass type B
58      plt.plot(x, mass_B, label='Type B', marker='x', linestyle='
            None')
59      # Add labels and title
60      plt.xlabel('Site')
61      plt.ylabel('Mass')
62      plt.title('Distribution of Mass Types A and B')
63      plt.legend()
64      plt.show()
65
66  def plot_histogram(m):
67      plt.figure()
68
69      mass_A = m[:, 0]
70      mass_B = m[:, 1]
71
72      # Filter out zeros
73      mass_A = m[:, 0][m[:, 0] > 0]
74      mass_B = m[:, 1][m[:, 1] > 0]
75
76      plt.subplot(1, 2, 1)
77      plt.hist(mass_A, bins=20, label='Type A', edgecolor='b',
            facecolor='none')
```

```
78      plt.title('Histogram of Mass Type A')
79      plt.xlabel('Mass')
80      plt.ylabel('Frequency')
81
82      plt.subplot(1, 2, 2)
83      plt.hist(mass_B, bins=20, label='Type B', edgecolor='r',
            facecolor='none')
84      plt.title('Histogram of Mass Type B')
85      plt.xlabel('Mass')
86      plt.ylabel('Frequency')
87
88      plt.tight_layout()
89      plt.show()
90
91  def plot_young(m):
92      plt.figure()
93
94      mass_A = np.sort(m[:, 0][m[:, 0] > 0])[::-1]
95      mass_B = np.sort(m[:, 1][m[:, 1] > 0])[::-1]
96
97      plt.subplot(1, 2, 1)
98      plt.step(range(len(mass_A)), mass_A, where='post')
99      plt.title('Young Diagram of Mass Type A')
100     plt.ylabel('Part')
101     plt.xlabel('Mass')
102
103     plt.subplot(1, 2, 2)
104     plt.step(range(len(mass_B)), mass_B, where='post')
105     plt.title('Young Diagram of Mass Type B')
106     plt.ylabel('Part')
107     plt.xlabel('Mass')
108
109     plt.tight_layout()
110     plt.show()
111
112 N = int(input("Enter the number of sites: "))
113 m = np.ones((N, 2), dtype=int)
114 t = 0
115 iteration = 0
116
117 while not (is_frozen(m)):
118     # Calculate the sum of rates
119     rates_sum = sum_of_rates(m)
120     # Calculate the time to the next event
121     dt = calculate_dt(rates_sum)
122     t = t+dt
123     # Choose the reaction and the site where it occurs
124     reaction, x = choose_reaction(m, rates_sum)
125     # Perform the chosen reaction
```

```
126     if reaction == 'diffuseA':
127         diffuseA(x, m)
128     elif reaction == 'diffuseB':
129         diffuseB(x, m)
130     iteration += 1
131 
132 plot_distribution(m)
133 plot_histogram(m)
134 plot_young(m)
```

Bibliography

[1] D. J. Aldous. Deterministic and stochastic models for coalescence (aggregation and coagulation): A review of the mean-field theory for probabilists. *Bernoulli*, 5(1):3–48, 1999. doi:10.2307/3318611. 144

[2] G. E. Andrews. *The Theory of Partitions*, volume 2 of *Encyclopedia of Mathematics and its Applications*. Addison-Wesley, Reading, MA, 1976. 48, 139

[3] W. Appel. *Probabilités pour les Non-Probabilistes*. H&K, 2015. 33

[4] R. Arratia, A. D. Barbour, and S. Tavaré. *Logarithmic Combinatorial Structures: A Probabilistic Approach*. EMS Monographs in Mathematics. European Mathematical Society, Zürich, 2003. doi:10.4171/000. 141, 142

[5] R. Arratia and S. Tavare. Independent process approximations for random combinatorial structures. *Advances in Mathematics*, 104(1):90–154, 1994. doi:10.1006/aima.1994.1022. 141, 142

[6] F.C. Auluck and D.S. Kothari. Statistical mechanics and the partitions of numbers. *Mathematical Proceedings of the Cambridge Philosophical Society*, 42(3):272–277, 1946. doi:10.1017/S0305004100023033. 1, 143

[7] A. D. Barbour and P. Hall. On the rate of Poisson convergence. *Mathematical Proceedings of the Cambridge Philosophical Society*, 95(3):473–480, 1984. doi:10.1017/S0305004100061806. 78

[8] A. D. Barbour, L. Holst, and S. Janson. *Poisson Approximation*, volume 2 of *Oxford Studies in Probability*. Clarendon Press, Oxford, 1992. 40

[9] M. Bendkowski, O. Bodini, and S. Dovgal. Polynomial tuning of multiparametric combinatorial samplers. In *Proceedings of the Meeting on Analytic Algorithmics and Combinatorics (ANALCO)*, pages 92–106, 2018. doi:10.1137/1.9781611975062.9. 143

[10] M. Bendkowski, O. Bodini, and S. Dovgal. Tuning as convex optimisation: a polynomial tuner for multi-parametric combinatorial samplers. *Combinatorics, Probability and Computing*, 31(5):765–811, 2022. doi:10.1017/S0963548321000547. 27, 63, 65, 67, 143

[11] M. Bernstein, M. Fahrbach, and D. Randall. Analyzing Boltzmann samplers for Bose–Einstein condensates with Dirichlet generating functions. In *Proceedings of the Meeting on Analytic Algorithmics and Combinatorics (ANALCO)*, pages 107–117, 2018. doi:10.1137/1.9781611975062.10. 10, 27, 143

[12] O. Bodini, P. Duchon, A. Jacquot, and L. Mutafchiev. Asymptotic analysis and random sampling of digitally convex polyominoes. In *Discrete Geometry for Computer Imagery*, pages 95–106. Springer, Berlin–Heidelberg, 2013. doi:10.1007/978-3-642-37067-0_9. 143

[13] L. V. Bogachev. Unified derivation of the limit shape for multiplicative ensembles of random integer partitions with equiweighted parts. *Random Structures and Algorithms*, 47(2):227–266, 2015. doi:10.1002/rsa.20540. 24, 141, 142, 152

[14] L. V. Bogachev, R. Nuermaimaiti, and J. Voss. Limit shape of the generalized inverse Gaussian-Poisson distribution, Preprint, 2023. doi:10.48550/arXiv.2303.08139. 7, 8, 10, 93, 98, 130, 144

[15] L. V. Bogachev and Yu. V. Yakubovich. Limit shape of minimal difference partitions and fractional statistics. *Communications in Mathematical Physics*, 373(3):1085–1131, 2020. doi:10.1214/10-AOP607. 141, 142

[16] L. V. Bogachev and S. M. Zarbaliev. Universality of the limit shape of convex lattice polygonal lines. *The Annals of Probability*, 39(6):2271–2317, 2011. doi:10.1214/10-AOP607. 143

[17] N. M. Bogoliubov and C. Malyshev. Zero range process and multidimensional random walks. *Symmetry, Integrability and Geometry: Methods and Applications*, 13(056), 2017. doi:10.3842/SIGMA.2017.056. 105

[18] J. Bureaux and N. Enriquez. Asymptotics of convex lattice polygonal lines with a constrained number of vertices. *Israel Journal of Mathematics*, 222:515–549, 2017. doi:10.1007/s11856-017-1599-3. 143

[19] A. Comtet, P. Leboeuf, and S. N. Majumdar. Level density of a Bose gas and extreme value statistics. *Physical Review Letters*, 98(7), 070404, 2007. doi:10.1103/PhysRevLett.98.070404. 13

[20] A. Comtet, S. N. Majumdar, S. Ouvry, and S. Sabhapandit. Integer partitions and exclusion statistics: limit shapes and the largest parts of young diagrams. *Journal of Statistical Mechanics: Theory and Experiment*, 2007(10), P10001, 2007. doi:10.1088/1742-5468/2007/10/P10001. 141

[21] J. T. Cox. Coalescing random walks and voter model consensus times on the torus in $\mathbb{Z}^d$. *The Annals of Probability*, 14(4):1333–1366, 1989. 105

[22] H. Cramér. *Mathematical Methods of Statistics*, volume 9 of *Princeton Mathematical Series*. Princeton University Press, Princeton, NJ, 1999. URL: http://www.jstor.org/stable/j.ctt1bpm9r4. 30

[23] N. Enriquez D. Beltoft, C. Boutillier. Random young diagrams in a rectangular box. *Moscow Mathematical Journal*, 12(4). URL: https://hal.science/hal-00508535. 59

[24] P. Duchon, P. Flajolet, G. Louchard, and G. Schaeffer. Boltzmann samplers for the random generation of combinatorial structures. *Combinatorics, Probability and Computing*, 13(4-5):577–625, 2004. doi:10.1017/S0963548304006315. 8, 10, 27, 63, 67, 74, 141, 143

[25] R. Durrett, B. L. Granovsky, and S. Gueron. The equilibrium behavior of reversible coagulation-fragmentation processes. *Journal of Theoretical Probability*, 12:447–474, 1999. doi:10.1023/A:1021682212351. 145

[26] P. Erdös and J. Lehner. The distribution of the number of summands in the partitions of a positive integer. *Duke Mathematical Journal*, 8(2):335–345, 1941. doi:10.1215/S0012-7094-41-00826-8. 3, 5, 13, 18, 35, 48, 141

[27] P. Erdös and P. Turán. On some general problems in the theory of partitions, I. *Acta Arithmetica*, 18(1):53–62, 1971. doi:10.4064/aa-18-1-53-62. 141

[28] M. M. Erlihson and B. L. Granovsky. Limit shapes of Gibbs distributions on the set of integer partitions: The expansive case. *Annales de l'Institut Henri Poincaré – Probabilités et Statistiques*, 44(5):915–945, 2008. doi:10.1214/07-AIHP129. 141

[29] W. J. Ewens. The sampling theory of selectively neutral alleles. *Theoretical Population Biology*, 3(1):87–112, 1972. doi:10.1016/0040-5809(72)90035-4. 1, 143

[30] W. Feller. *An Introduction to Probability Theory and Its Applications, Volume II*. Wiley Series in Probability and Mathematical Statistics. Wiley, New York, 2nd edition, 1971. 42, 52

[31] P. Flajolet, E. Fusy, and C. Pivoteau. Boltzmann sampling of unlabelled structures. In *Proceedings of the Workshop on Analytic Algorithmics and Combinatorics (ANALCO)*, pages 201–211. SIAM, 2007. doi:10.1137/1.9781611972979.5. 8, 10, 67, 143, 158

[32] P. Flajolet and R. Sedgewick. *Analytic Combinatorics*. Cambridge University Press, Cambridge, 2009. doi:10.1017/CBO9780511801655. 8, 147

[33] G. Freiman, A. M. Vershik, and Yu. V. Yakubovich. A local limit theorem for random strict partitions. *Theory of Probability and Its Applications*, 44(3):453–468, 2000. doi:10.1137/S0040585X97977719. 13, 59, 142

[34] B. Fristedt. The structure of random partitions of large integers. *Transactions of the American Mathematical Society*, 337:703–735, 1993. doi:10.1090/S0002-9947-1993-1094553-1. 24, 141, 142, 152

[35] W. Fulton. *Young Tableaux: With Applications to Representation Theory and Geometry*, volume 35 of *London Mathematical Society Student Texts*. Cambridge University Press, Cambridge, 1997. doi:10.1017/CBO9780511626241. 1

[36] A. Gnedin, B. Hansen, and J. Pitman. Notes on the occupancy problem with infinitely many boxes: General asymptotics and power laws. *Probability Surveys*, 4:146–171, 2007. doi:10.1214/07-PS092. 7, 93, 144

[37] W. M. Y. Goh and P. Hitczenko. Random partitions with restricted part sizes. *Random Structures and Algorithms*, 32:440–462, 2008. doi:10.1002/rsa.20191. 142

[38] M. J. C. Gover. The eigenproblem of a tridiagonal 2-Toeplitz matrix. *Linear Algebra and its Applications*, 197-198:63–78, 1994. doi:10.1016/0024-3795(94)90481-2. 117

[39] P. De Gregorio and L. Rondoni. Microcanonical entropy, partitions of a natural number into squares and the Bose–Einstein gas in a box. *Entropy*, 20(9), 645, 2018. doi:10.3390/e20090645. 13

[40] R. K. Guy. *Unsolved Problems in Number Theory*, volume 1 of *Problem Books in Mathematics*. Springer, New York, 2013. doi:10.1007/978-0-387-26677-0. 140

[41] G. H. Hardy and S. Ramanujan. Asymptotic formulaæ in combinatory analysis. *Proceedings of the London Mathematical Society*, s2-17(1):75–115, 1918. doi:10.1112/plms/s2-17.1.75. 3, 48, 139, 140

[42] G. H. Hardy and E. M. Wright. *An Introduction to the Theory of Numbers*. Oxford Mathematics. Oxford University Press, 6th edition, 2008. URL: https://global.oup.com/ukhe/product/an-introduction-to-the-theory-of-numbers-9780199219865. 140

[43] C. B. Haselgrove and H. N. V. Temperley. Asymptotic formulae in the theory of partitions. *Mathematical Proceedings of the Cambridge Philosophical Society*, 50(2):225–241, 1954. doi:10.1017/S0305004100029273. 3

[44] R. A. Horn and C. R. Johnson. *Matrix Analysis*. Cambridge University Press, Cambridge, 2013. 75

[45] L.-K. Hua. On the number of partitions of a number into unequal parts. *Transactions of the American Mathematical Society*, 51(1):194–201, 1942. doi:10.2307/1989985. 13, 140

[46] K. Huang. *Statistical Mechanics*. Wiley, New York, 2nd edition, 1987. 142, 143

[47] H.-K. Hwang. Limit theorems for the number of summands in integer partitions. *Journal of Combinatorial Theory, Series A*, 96(1):89–126, 2001. doi:10.1006/jcta.2000.3170. 141, 142

[48] A. E. Ingham. A Tauberian theorem for partitions. *Annals of Mathematics*, 42(5):1075–1090, 1941. doi:10.2307/1970462. 3, 140

[49] A. I. Khinchin. *Mathematical Foundations of Statistical Mechanics*. Dover Books on Mathematics. Dover Publications, 1949. 142

[50] J. F. C. Kingman. Random partitions in population genetics. *Proceedings of the Royal Society of London, Series A*, 361(1704):1–20, 1978. doi:10.1098/rspa.1978.0089. 143

[51] E. Landau. Über die Einteilung der positiven, ganzen Zahlen in vier Klassen nach der Mindestzahl der zu ihrer additiven Zusammensetzung erforderlichen Quadrate. (German) [On the division of positive integers into four classes according to the minimum number of squares required for their additive composition]. *Archiv der Mathematik und Physik*, 13:305–312, 1908. URL: https://ia600309.us.archive.org/31/items/archivdermathem37unkngoog/archivdermathem37unkngoog.pdf. 91, 140

[52] D. V. Lee. The asymptotic distribution of the number of summands in unrestricted Λ-partitions. *Acta Arithmetica*, 65(1):29–43, 1993. doi:10.4064/aa-65-1-29-43. 3

[53] P. LeVan and D. Prier. Improved bounds on the anti-waring number. *Journal of Integer Sequences*, 20(Article 17.8.7), 2017. URL: https://cs.uwaterloo.ca/journals/JIS//VOL20/Prier/prier3.html. 4

[54] T. M. Liggett. *Interacting Particle Systems*. Classics in Mathematics. Springer, Berlin, Heidelberg, 2006. doi:10.1007/b138374. 107

[55] M. S. Longuet-Higgins. On the statistical distribution of the heights of sea waves. *Journal of Marine Research*, XI(3), 1953. 113

[56] A. Lushnikov. Some new aspects of coagulation theory. *Izvestiya, Atmospheric and Oceanic Physics*, 14, 01 1978. 144

[57] S. N. Majumdar and D. A. Huse. Growth of long-range correlations after a quench in phase-ordering systems. *Physical Review E*, 52(1):270–284, 1995. doi:10.1103/PhysRevE.52.270. 6, 10, 11, 107

[58] S. N. Majumdar, S. Krishnamurthy, and M. Barmar. Nonequilibrium phase transitions in models of aggregation, adsorption, and dissociation. *Physical Review Letters*, 81(17):3691–3694, 1998. doi:10.1103/PhysRevLett.81.3691. 6, 10, 105

[59] S. N. Majumdar, S. Krishnamurthy, and M. Barmar. Nonequilibrium phase transition in a model of diffusion, aggregation, and fragmentation. *Journal of Statistical Physics*, 99:1–29, 2000. doi:10.1023/A:1018632005018. 6, 10, 11, 105, 121

[60] A. H. Marcus. Stochastic coalescence. *Technometrics*, 10(1):133–143, 1968. doi:10.2307/1266230. 144

[61] G. Meinardus. Asymptotische aussagen über partitionen. (german) [asymptotic statements about partitions]. *Mathematische Zeitschrift*, 1953. doi:10.1007/BF01180268. 3

[62] G. L. Miller. Riemann's hypothesis and tests for primality. *Journal of Computer and System Sciences*, 13(3):300–317, 1976. doi:10.1016/S0022-0000(76)80043-8. 89

[63] J. Nakamura, S. Liang, G. Gardner, and M. Manfra. Direct observation of anyonic braiding statistics. *Nature Physics*, 16(9):931–936, 2020. doi:10.1038/s41567-020-1019-1. 141

[64] S. Y. Novak. Poisson approximation. *Probability Surveys*, 16:228–276, 2019. doi:10.1214/18-PS318. 40

[65] R. Nuermaimaiti, L. V. Bogachev, and J. Voss. A generalized power law model of citations. In W. Glänzel, S. Heeffer, P.-S. Chi, and R. Rousseau, editors, *18th International Conference on Scientometrics & Informetrics, ISSI 2021 (12–15 July 2021, KU Leuven, Belgium)*, pages 843–848. ISSI, Leuven, 2021. URL: https://kuleuven.app.box.com/s/kdhn54ndlmwtil3s4aaxmotl9fv9s329. 1, 7, 144

[66] F. W. J. Olver, D. W. Lozier, R. F. Boisvert, and C. W. Clark (Editors). *NIST Handbook of Mathematical Functions*. National Institute of Standards and Technology, U.S. Department of Commerce; Cambridge University Press, Cambridge, 2010. URL: https://www.cambridge.org/catalogue/catalogue.asp?isbn=9780521192255. 31, 33, 140

[67] I. Pak. Partition bijections, a survey. *The Ramanujan Journal*, 12:5–75, 2006. doi:10.1007/s11139-006-9576-1. 141

[68] J. C. Peyen, L. V. Bogachev, and P. P. Martin. Boltzmann distribution on "short" integer partitions with power parts: Limit laws and sampling. 2023. arXiv:2303.16960. 9

[69] J. Pitman. *Combinatorial Stochastic Processes (Ecole d'Eté de Probabilités de Saint-Flour XXXII – 2002)*, volume 1875 of *Lecture Notes in Mathematics*. Springer, Berlin, 2006. doi:10.1007/b11601500. 142

[70] B. Pittel. On a likely shape of the random Ferrers diagram. *Advances in Applied Mathematics*, 18(4):432–488, 1997. doi:10.1006/aama.1996.0523. 18, 141

[71] C. Pivoteau. *Génération aléatoire de structures combinatoires: méthode de Boltzmann effective (French) [Random generation of combinatorial structures: an effective Boltzmann method]*. PhD thesis, Laboratoire d'Informatique de Paris VI, 2008. URL: http://igm.univ-mlv.fr/~pivoteau/these.pdf. 10, 158

[72] J. Polcari. An informative interpretation of decision theory: The information theoretic basis for signal-to-noise ratio and log likelihood ratio. *IEEE Access*, 1:509–522, 2013. doi:10.1109/ACCESS.2013.2277930. 75

[73] M. O. Rabin. Probabilistic algorithm for testing primality. *Journal of Number Theory*, 12(1):128–138, 1980. doi:10.1016/0022-314X(80)90084-0. 89

[74] S. I. Resnick. *Extreme Values, Regular Variation, and Point Processes*, volume 4 of *Applied Probability: a series of the Applied Probability Trust*. Springer, New York, 1987. doi:10.1007/978-0-387-75953-1. 33

[75] J. Roccia and P. Leboeuf. Level density of a Fermi gas and integer partitions: A Gumbel-like finite-size correction. *Physical Review C*, 81(4), 044301, 2010. doi:10.1103/PhysRevC.81.044301. 13

[76] E. Schrödinger. *Statistical Thermodynamics*. Dover Books on Physics. Dover Publications, New York, 1989; reprinted from a 1952 edition by Cambridge University Press. 143

[77] R. Sedgewick and P. Flajolet. *Introduction to the Analysis of Algorithms*. Addison-Wesley, Upper Saddle River, NJ, 2nd edition, 2013. 119

[78] A. N. Shiryaev. *Probability*, volume 95 of *Graduate Texts in Mathematics*. Springer, New York, 2nd edition, 1996. doi:10.1007/978-1-4757-2539-1. 22, 46, 94

[79] Y. G. Sinai. A probabilistic approach to the analysis of the statistics of convex polygonal lines. *Functional Analysis and Its Applications*, 28:41–48, 1994. doi:10.1007/BF01076497. 143

[80] R. Solovay and V. Strassen. A fast Monte-Carlo test for primality. *SIAM Journal on Computing*, 6(1):84–85, 1977. doi:10.1137/0206006. 89

[81] H. N. V. Temperley. Statistical mechanics and the partition of numbers II: The form of crystal surfaces. *Mathematical Proceedings of the Cambridge Philosophical Society*, 48(4):683–697, 1952. doi:10.1017/S0305004100076453. 4, 5, 18, 144

[82] R. C. Vaughan. Squares: Additive questions and partitions. *International Journal of Number Theory*, 11(5):1367–1409, 2015. doi:10.1142/S1793042115400096. 139

[83] R. C. Vaughan and T. D. Wooley. Waring's problem: A survey. In M. A. Bennett, B. C. Berndt, N. Boston, H. G. Diamond, A. J. Hildebrand, and W. Philipp, editors, *Number Theory for the Millennium, Volume III*, pages 301–340. A. K. Peters, Natick, MA, 2002. 4, 77, 140

[84] A. M. Vershik. Asymptotic combinatorics and algebraic analysis. In S. D. Chatterji, editor, *Proceedings of the International Congress of Mathematicians (August 3–11, 1994 Zürich, Switzerland)*, pages 1384–1394. Birkhäuser, Basel, 1994. doi:10.1007/978-3-0348-9078-6_133. 18, 141, 142

[85] A. M. Vershik. Statistical mechanics of combinatorial partitions, and their limit shapes. *Functional Analysis and Its Applications*, 30:90–105, 1996. doi:10.1007/BF02509449. 4, 13, 18, 141, 143

[86] A. M. Vershik. Limit distribution of the energy of a quantum ideal gas from the viewpoint of the theory of partitions of natural numbers. *Russian Mathematical Surveys*, 52(2):379–386, 1997. doi:10.1070/RM1997v052n02ABEH001782. 73, 143

[87] A. M. Vershik and Yu. V. Yakubovich. The limit shape and fluctuations of random partitions of naturals with fixed number of summands. *Moscow Mathematical Journal*, 1:457–468, 2001. URL: http://www.mathjournals.org/mmj/vol1-3-2001/abst1-3-2001.html#vershik_abstract. 24, 141, 142, 152

[88] A. M. Vershik and Yu. V. Yakubovich. Fluctuation of maximal particle energy of quantum ideal gas and random partitions. *Communications in Mathematical Physics*, 261:759–769, 2005. doi:10.1007/s00220-005-1434-2. 13, 24, 152

[89] E. T. Whittaker and G. N. Watson. *A Course of Modern Analysis*. Cambridge Mathematical Library. Cambridge University Press, Cambridge, 4th edition, 1996. doi:10.1017/CBO9780511608759. 52

[90] E. M. Wright. Asymptotic partition formulae. III. Partitions into k-th powers. *Acta Mathematica*, 63:143–191, 1934. doi:10.1007/BF02547353. 3, 13, 139

[91] E. M. Wright. The asymptotic expansion of the generalized Bessel function. *Proceedings of the London Mathematical Society*, s2-38(1):257–270, 1935. doi:10.1112/plms/s2-38.1.257. 43

[92] Yu. Yakubovich. Ergodicity of multiplicative statistics. *Journal of Combinatorial Theory, Series A*, 119(6):1250–1279, 2012. doi:10.1016/j.jcta.2012.03.002. 141

[93] J. Yeh. *Martingales and Stochastic Analysis*. Series on Multivariate Analysis. World Scientific, Singapore, 1995. doi:10.1142/2948. 56, 98

[94] A. Yong. A critique of Hirsch's citation index: a combinatorial Fermi problem. *Notices of the American Mathematical Society*, 61(9):1040–1051, 2014. doi:10.1090/noti1164. 1